

UNIVERSIDADE DE LISBOA

Faculdade de Medicina



**Unraveling the Molecular Mechanisms Underlying  
Alpha-Synuclein Oligomerization and Cytotoxicity**

Susana Alexandra de Barros Gonçalves

Orientador: Professor Doutor Tiago Fleming de Oliveira Outeiro

Tese especialmente elaborada para obtenção do grau de Doutoramento em  
Ciências Biomédicas, Especialidade em Neurociências

2017



UNIVERSIDADE DE LISBOA  
Faculdade de Medicina



# Unraveling the Molecular Mechanisms Underlying Alpha-Synuclein Oligomerization and Cytotoxicity

Susana Alexandra de Barros Gonçalves

Orientador: Professor Doutor Tiago Fleming de Oliveira Outeiro

Tese especialmente elaborada para obtenção do grau de Doutoramento em Ciências Biomédicas,  
Especialidade em Neurociências

## Júri

**Presidente:** Professor Doutor José Luís Bliebernick Ducla Soares, Professor Catedrático em regime de *tenure* e Vice-Presidente do Conselho Científico da Faculdade de Medicina da Universidade de Lisboa.

## Vogais:

- Doutor Duarte Custal Ferreira Barral, Professor Auxiliar Convidado da Faculdade de Ciências Médicas da Universidade Nova de Lisboa;
- Doutora Patrícia Espinheira Sá Maciel, Professora Associada do Instituto de Investigação em Ciências da Vida e Saúde da Universidade do Minho;
- Doutora Luísa Maria Vaqueiro Lopes, Investigadora e *Group Leader* do Instituto de Medicina Molecular, unidade de investigação associada à Faculdade de Medicina da Universidade de Lisboa;
- Doutora Ana Maria Ferreira de Sousa Sebastião, Professora Catedrática da Faculdade de Medicina da Universidade de Lisboa;
- Doutor Joaquim José Coutinho Ferreira, Professor Associado Convidado da Faculdade de Medicina da Universidade de Lisboa;
- Doutor Tiago Fleming de Oliveira Outeiro, Professor Associado Convidado da Faculdade de Medicina da Universidade de Lisboa (orientador).

**Instituições Financiadoras:** Axa Research Fund e Fundação para a Ciência e Tecnologia (SFRH/BD/79337/2011)

2017



O trabalho experimental relatado nesta tese foi realizado na Unidade de Neurociências Celular e Molecular, Instituto de Medicina Molecular, Faculdade de Medicina de Lisboa, Universidade de Lisboa.

As opiniões expressas nesta publicação são da exclusiva responsabilidade da autora.

**A impressão desta tese foi aprovada pelo Conselho Científico da Faculdade de Medicina de Lisboa em reunião de 23 de Novembro de 2016.**



Aos meus pais.

*“Como é fascinante escrever para saber o que é. (...) Mas o que se sabe é frágil e há que procurá-lo até à eternidade. Porque o que se encontra é ainda a procura, o além de todo o aquém. E é porque nunca se encontra, que a arte continua.”*

Vergílio Ferreira, in “Pensar”.





# Table of Contents

Table of Contents .....	I
Acknowledgments .....	III
Preface .....	V
Publications .....	V
Communications in Scientific Meetings .....	VI
Abstract .....	IX
Resumo.....	XIII
List of Abbreviations.....	XVII
I.    Introduction .....	21
1 Protein Misfolding Diseases .....	23
1.1 Loss of Neuronal Proteostasis and Neurodegeneration .....	25
1.2 Synucleinopathies .....	26
2 The Role of Alpha-Synuclein in Health and Disease .....	37
2.1 Structure and Function of Alpha-Synuclein .....	37
2.2 Genetic Association Between Alpha-Synuclein and Parkinson’s Disease .....	40
2.3 Alpha-Synuclein post-Translational Modifications .....	41
2.4 Alpha-Synuclein Aggregation and Cellular Dysfunction.....	46
2.5 Alpha-Synuclein and Neuronal Trafficking.....	47
2.6 Intercellular Propagation of Pathologic Alpha-Synuclein .....	50
2.7 Cellular Models of Alpha-Synuclein Oligomerization and Aggregation .....	54
II.    Aims.....	63
III.   Results .....	67
Author Contributions.....	69
A. Alpha-Synuclein Subcellular Dynamics in Living Cells .....	71
3.1. Assessing the Subcellular Dynamics of Alpha-Synuclein using Photoactivation Microscopy .....	71
B. Insights into the Mechanisms of Alpha-Synuclein Oligomerization and Aggregation.....	91
3.2. The Small GTPase Rab11 co-Localizes with Alpha-Synuclein in Intracellular Inclusions and Modulates its Aggregation, Secretion and Toxicity .....	91
3.3. shRNA-Based Screen Identifies Endocytic Recycling Pathway Components that Act as Genetic Modifiers of Alpha-Synuclein Aggregation, Secretion and Toxicity .....	117

3.4 Antibodies Against Alpha-Synuclein Reduce Oligomerization in Living Cells .....	145
IV. Conclusions and Future Directions.....	161
V. Annexes .....	171
5.1. Assessing the Subcellular Dynamics of Alpha-Synuclein using Photoactivation Microscopy .....	173
5.2. shRNA-Based Screen Identifies Endocytic Recycling Pathway Components that Act as Genetic Modifiers of Alpha-Synuclein Aggregation, Secretion and Toxicity .....	181
VI. References.....	211

## Acknowledgments

Besides answering questions, our duty as thinkers is to renew the right questions to answer. Thus, a PhD never ends; in fact it is the beginning of knowledge consolidation and an unfinished search of deeper understanding.

I am a privileged person as I am walking through this pathway surrounded with special, unique and transcendent people around me, to whom I am deeply grateful:

O meu reconhecido agradecimento ao Prof. Dr. Tiago Fleming Outeiro. Este doutoramento não seria uma realidade sem ele. Para além das capacidades de excelência que detém, exerceu uma mentoria excepcional que me permitiu cimentar as minhas capacidades de pensar, interpretar e trabalhar. No entanto, a humildade e transparência são as capacidades que mais me orgulho de ter desenvolvido com ele. Manter-se-á a honra que sinto de poder ter estado no laboratório de Lisboa desde o início. Considero que tive toda a liberdade de movimentos e apoio necessários a toda a minha investigação.

Agradeço também a todas as pessoas do laboratório e do Instituto de Medicina Molecular com que me cruzei. De todos guardo actos, frases, interajuda, troca de ideias, ou simples gestos como sorrisos. No seu conjunto constroem uma entidade de Ciência sólida cuja excelência seria menor sem um desses elementos que fosse.

To Dr. Flav Giorgini for all the support and collaboration in this work.

Ao Dr. Duarte Barral por toda a disponibilidade em me ajudar e receber sempre que tive dúvidas e pela preciosa colaboração neste doutoramento.

Ao Dr. José Rino e António Temudo pela formação contínua em *Bioimaging*, e pela assistência sempre prontamente prestada nas minhas longas sessões de microscopia.

Ao Dr. Pedro Daniel Simões, Dra. Catarina Ferreira Moita, Dra. Helena Raquel, e Dr. Luís Ferreira Moita, pela colaboração essencial na produção de vírus e na ajuda teórica sobre *screenings* de *RNAi*.

I am deeply grateful to my current supervisor, Dr. Matthew Hoare, for his support and ingenious mentorship.

Desejo expressar a minha sentida gratidão aos meus pais, Maria Mercedes e Ricardo, e à minha irmã, Paula. Pela ternura e protecção, pela confiança nas minhas escolhas; pelos exemplos de humildade, carácter, generosidade, trabalho árduo e dedicação como caminho único para o sucesso; pelo culto da simplicidade e genuinidade como a forma mais feliz de se viver.

Ao Pedro Matos Soares, pelos inúmeros momentos substanciais, medulares. Por tão peculiarmente ousar “Ser” e “estar” com uma inteligência ávida de sensações e estímulos. Pela sua ânsia interior de mais humanidade e altruísmo, que admiro. Agradeço também todos os momentos que partilhámos ao longo destes anos de amizade, em poesia, em dança, em silêncios que tão bem se decifram e tão cheios de significado; por ter sido essencial num processo de crescimento interior que me permitiu peneirar o que é importante cultivar e manter. Agradeço por fim, a partilha de opiniões sempre de forma justa, digna, e acima de tudo, evitando enviesamentos.

Ao António Bastos, pela descontraída amizade, e pelos abraços calorosos, templos de paz. Ao António Cavaleiro, por todos os estados de alma partilhados, pela alegria intrínseca e pela forma tão genuína de ser. Por caminhar comigo em todos os meus passos, e, acima de tudo, por me ouvir. Pela generosidade, que se impõe de forma dominante, e que revela alguém com um carisma muito forte, iluminado, que admiro e agradeço por ter como amigo.

To my dear friend Prof. Dr. Volker Sommer, for sharing his intelligent, bright reflections regarding humanity (and inhumanity), in the sense of its behavior, life and love. For being the most substantial, interesting, funny and complex person I have met in Cambridge. I am deeply grateful for the support and for sharing a life experience. That is awe-inspiring.

The financial support was given by AXA Research Fund and Fundação para a Ciência e Tecnologia (SFRH/BD/79337/2011).

## Preface

All the results here presented were reported in the following scientific meetings, journals and books:

### Publications

Goncalves, S. A., J. E. Matos and T. F. Outeiro (2010). "Zooming into protein oligomerization in neurodegeneration using BiFC." *Trends Biochem Sci* 35(11): 643-651.

Badiola, N., R. M. de Oliveira, F. Herrera, C. Guardia-Laguarta, S. A. Goncalves, M. Pera, M. Suarez-Calvet, J. Clarimon, T. F. Outeiro and A. Lleó (2011). "Tau enhances alpha-Synuclein aggregation and toxicity in cellular models of Synucleinopathy." *PLoS One* 6(10): e26609.

Nasstrom, T., Goncalves S., C. Sahlin, E. Nordstrom, V. Screpanti Sundquist, L. Lannfelt, J. Bergstrom, T. F. Outeiro and M. Ingelsson (2011). "Antibodies against alpha-Synuclein reduce oligomerization in living cells." *PLoS One* 6(10): e27230.

Gonçalves, S., H. Vicente Miranda and T. F. Outeiro (2012). *Novel molecular therapeutics in Parkinson's disease*. Human Molecular Therapeutics. R. R. David Whitehouse. UK, John Wiley & Sons. 1: 245-265.

Herrera, F., S. Goncalves and T. F. Outeiro (2012). "Imaging protein oligomerization in neurodegeneration using bimolecular fluorescence complementation." *Methods Enzymol* 506: 157-174.

Goncalves, S. and T. F. Outeiro (2013). "Assessing the subcellular dynamics of alpha-Synuclein using photoactivation microscopy." *Mol Neurobiol* 47(3): 1081-1092.

Basso, E., P. Antas, Z. Marijanovic, S. Goncalves, S. Tenreiro and T. F. Outeiro (2013). "PLK2 modulates alpha-Synuclein aggregation in yeast and mammalian cells." *Mol Neurobiol* 48(3): 854-862.

Chutna, O., S. Goncalves, A. Villar-Pique, P. Guerreiro, Z. Marijanovic, T. Mendes, J. Ramalho, E. Emmanouilidou, S. Ventura, J. Klucken, D. C. Barral, F. Giorgini, K. Vekrellis and T. F. Outeiro (2014). "The small GTPase Rab11 co-localizes with alpha-Synuclein in intracellular inclusions and modulates its aggregation, secretion and toxicity." *Hum Mol Genet*.

Goncalves, S. A., D. Macedo, H. Raquel, P. D. Simoes, F. Giorgini, J. S. Ramalho, D. C. Barral, L. Ferreira Moita and T. F. Outeiro (2016). "shRNA-based screen identifies endocytic recycling pathway components that act as genetic modifiers of alpha-Synuclein aggregation, secretion and toxicity." *PLoS Genet* **12**(4): e1005995.

Goncalves, S. A. and T. F. Outeiro (2016). "Traffic jams and the complex role of alpha-Synuclein aggregation in Parkinson's disease." *Small GTPases*: 1-7.

### **Communications in Scientific Meetings**

Gonçalves, S. and Outeiro T.F (2009), "Insights into Parkinson's disease pathophysiology". AXA Research Fund Meeting, Paris, invited oral communication.

Gonçalves, S. and Outeiro T.F (2009), "Novel insights into alpha-Synuclein intracellular dynamics". 11<sup>th</sup> Meeting of the Portuguese Society for Neurosciences, School of Health Sciences, University of Minho, Braga, Portugal, poster presentation.

Gonçalves, S. Moita, L.F. and Outeiro T.F (2009), "Dangerous attractions: modifying alpha-Synuclein dimerization in living cells". AXA Talent Day on Longevity and Long-Term Care meeting, AXA headquarters, Paris and III IMM PhD Student Meeting, Instituto de Medicina Molecular, Lisbon, Portugal, poster presentation.

Gonçalves, S. Moita, L.F. and Outeiro (2009), "Genetic modifiers of alpha-Synuclein oligomerization in living cells", Society for Neurosciences, Chicago, Illinois, EUA, poster presentation.

Gonçalves, S. Moita, L.F. and Outeiro (2010), “Genetic modifiers of alpha-Synuclein oligomerization in living cells”. EMBO Workshop Proteolysis and Neurodegeneration, Fundación Ramón Areces, Madrid, Spain, poster presentation.

Gonçalves, S. and Outeiro T.F (2010), “Monitoring alpha-Synuclein intracellular dynamics using photoactivation”. IV IMM PhD Student Meeting, Instituto de Medicina Molecular, Lisbon, Portugal, poster presentation.

Gonçalves, S. Moita, L.F. and Outeiro (2010), “Genetic modifiers of alpha-Synuclein oligomerization”, George-August University of Göttingen, invited oral communication.

Gonçalves, S. Moita, L.F. and Outeiro (2011), “Modifying alpha-Synuclein dimerization in living cells”. The 10<sup>th</sup> International Conference on Alzheimer’s & Parkinson’s Diseases, Barcelona, and 9<sup>th</sup> Göttingen Meeting of the German Neuroscience Society, Göttingen, poster presentation.

Gonçalves, S. Moita, L.F. and Outeiro (2011), “Modifying alpha-Synuclein dimerization in living cells”, AXA Talent Day on Longevity and Life Risks meeting, Paris, poster presentation.

Gonçalves, S. Moita, L.F. and Outeiro (2011), “Modifying alpha-Synuclein dimerization in living cells”, V IMM PhD Student Meeting, Instituto de Medicina Molecular, Lisbon, Portugal, oral presentation.

Gonçalves, S. and Outeiro T.F (2012), “Estudo dos mecanismos moleculares envolvidos na patologia da doença de Parkinson, AXA Portugal Meeting, Lisbon, Portugal, invited oral presentation:”.

Gonçalves, S. Barral D. C., Ramalho, J., Moita, L.F. and Outeiro (2013), “Elucidating the effect of modulators of alfa-Synuclein aggregation in vesicular trafficking”, XIII reunião da Sociedade Portuguesa de Neurociências, Luso, Portugal, oral and poster presentations.

Gonçalves, S. and Outeiro T.F (2014), “Neurodegenerative disorders and cognitive dysfunction”. III Congresso Internacional de Estudos do Envelhecimento Humano:

Envelhecer na Contemporaneidade. Universidade de Passo Fundo, Brasil, invited oral presentation.



## Abstract

Neurodegenerative disorders (NDs) are proteinopathies characterized by the accumulation of misfolded and aggregated proteins. Either through loss of normal protein function and the generation of abnormal protein interactions, the protein network deteriorates inside neurons and subsequently along the neuronal networks. Parkinson's disease (PD) is the second most frequent ND and is associated with the misfolding and aggregation of alpha-Synuclein (aSyn), a pre-synaptic protein whose function is still unclear. Importantly, aSyn dysregulation is also involved in other NDs, as Dementia with Lewy Bodies and Multiple System Atrophy, jointly referred to as Synucleinopathies. Thus, the study of aSyn became crucial for understanding the etiology of those pathologies. There is ample debate as to what the toxic species of aSyn are, although it has been postulated that misfolded oligomeric species of aSyn represent the toxic genus.

This thesis aimed to generate new insights into the role of aSyn in health and disease, at a molecular level. To visualize aSyn in the biological orchestra of the cell, we first studied its intracellular dynamics in a cellular model through photoactivation microscopy. Using photoactivatable green fluorescent protein as a reporter, we found that the availability of the aSyn amino-terminus modulates its shuttling into the nucleus. This finding has important implications regarding both the species of aSyn that enter the nucleus and also the function of the protein within that compartment. aSyn was recently suggested to exist naturally as a tetramer. Due to the nuclear pore size, only monomeric or dimeric forms of aSyn can enter the nucleus, and this has been related to a deleterious effect and neurotoxicity, due to transcription deregulation. Interestingly, intracellular dynamics of aSyn was finely modulated by the HSP70 chaperone, PD-associated mutations and by the phosphorylation state of the protein on S129 site. We found that the molecular chaperone HSP70 accelerates the entry of aSyn into the nuclear compartment. Also, A30P and A53T aSyn mutations increased the speed at which the protein moves between the nucleus and cytoplasm, respectively. Finally, specific kinases potentiate the shuttling of aSyn between nucleus and cytoplasm. Importantly, a mutant aSyn form that blocks S129 phosphorylation, S129A, results in the formation of cytoplasmic inclusions, suggesting

that phosphorylation modulates aggregation, and thus, alter the normal aSyn intracellular dynamics.

To better understand the aggregation process in disease, we focused on the initial steps of aSyn aggregation, thought to be the causative agents of pathology. We used cell-based models of Synucleinopathy to investigate the molecular mechanisms underlying aSyn oligomerization. In particular, we screened, in an unbiased manner, a subset of the human genome-wide collection of lentiviral RNA-interference constructs, targeting genes involved in signal transduction players, to identify modifiers of aSyn oligomerization, using the bimolecular fluorescence complementation assay (BiFC) as readout. Through this approach we identified 9 genetic modifiers of aSyn oligomerization. Interestingly, the hits we identified were functionally related, and associated with neuronal trafficking processes. We then characterized these hits with respect to their effects on aSyn aggregation, toxicity and protein levels. After this first level of general characterization, we further investigated the mechanism of action of the hits by assessing their effects on aSyn secretion, a central aspect in the spreading of aSyn pathology. aSyn is secreted under physiological conditions, via non-classical exocytosis, in association with exosomes, and possibly via other less conventional mechanisms. However, it was demonstrated that pathological and aggregated aSyn species can also be secreted, suggesting that aggregated and misfolded aSyn may be the key agent for propagation of aSyn pathology, possibly in a prion-like manner. Thus, in our study we selected four trafficking hits, based on the literature and on their relevance to secretory pathways. Ras-related Protein in Brain 8b (Rab8b), Rab11a, Rab13 and Synaptotagmin-Like Protein 5 were found to promote the clearance of aSyn inclusions and reduce aSyn toxicity. Moreover, we found that endocytic recycling and secretion of aSyn was enhanced upon expression of Rab11a or Rab13 in cells accumulating aSyn inclusions. Importantly, in cells with inclusions, the trafficking proteins co-localized with aSyn in inclusions. Altogether, our findings suggest specific trafficking steps may prove beneficial as targets for therapeutic intervention in Synucleinopathies, and should be further investigated in other models.

Here, we also studied the effects of monoclonal aSyn antibodies on the early stages of aggregation using the BiFC assay. Our results support passive immunization against Synucleinopathies by demonstrating that extracellular administration of monoclonal antibodies can inhibit early steps in the aggregation process of aSyn. As aSyn seems to

behave as a prion-like protein, immunization can be a mid-term strategy to delay the progression of Synucleinopathies.

The present study uncovered novel aspects about the intracellular dynamics of aSyn and allowed the identification of new genetic players involved in the aggregation, toxicity, secretion and immunization of aSyn, opening novel avenues towards the understanding of the molecular bases of Synucleinopathies.

**Key-words:** Alpha-Synuclein, Parkinson's Disease, Oligomerization, Aggregation.



## Resumo

As proteínas são os principais efectores biológicos na célula e regulam os processos vitais na mesma. Assim, a desregulação funcional daquelas em regiões específicas do cérebro pode culminar numa descontextualização espacial e temporal dos processos celulares. A acumulação destas proteínas disfuncionais pode, por sua vez, originar agregados de proteínas, que caracterizam as doenças neurodegenerativas (DNs).

A relação entre o *misfolding* de determinadas proteínas e a evolução para uma patologia cerebral não é totalmente compreendida. A função alterada de uma proteína neuronal pode culminar na formação de deposições proteicas no interior ou no exterior do neurónio, levando à perturbação dos mecanismos de síntese e transporte de moléculas, dos mecanismos de controlo de qualidade da célula e a uma perturbação na comunicação interneuronal. No seu conjunto, estas doenças designam-se também de doenças conformacionais, e representam grandes desafios para a Medicina actual, que tenta encontrar terapias apropriadas que minimizem o impacto da deposição de agregados proteicos nos neurónios. Em alguns casos, a deposição de agregados proteicos parece perturbar fisicamente o funcionamento de alguns grupos de células específicos e estender-se posteriormente para os respectivos tecidos e regiões adjacentes. Noutros casos, a ausência de proteína funcional, devido ao seu recrutamento para os agregados acumulados, resulta na falha de processos celulares cruciais. Segundo a hipótese amilóide, a agregação de proteínas numa estrutura fibrilar em DNs está relacionada com interacções proteicas aberrantes que culminam na disfunção neuronal e, em última instância, em neurodegeneração. Apesar de a célula possuir mecanismos de defesa e de reparação que o próprio organismo acciona contra essas proteínas tóxicas, as DNs surgem quando já nenhum mecanismo de defesa funciona na sua plenitude, e quando já há saturação dessas proteínas disfuncionais nos neurónios. Assim, no contexto das doenças neurodegenerativas, a hipótese amilóide postula que as proteínas podem ser convertidas, sob certas circunstâncias, em estruturas não nativas com propensão para a instabilidade. Nestas patologias, as proteínas podem apresentar estados conformacionais alternativos ou *misfolding* que podem estar associados a disfunção celular, mas os mecanismos exactos são apenas alusivos. Apesar dos componentes proteicos variarem, a formação de

inclusões nas DN partilham vias de formação comuns, como seja perda de função das proteínas envolvidas e formação de interações aberrantes. Assim, a comunicação entre as proteínas deteriora-se intraneuronalmente e, por conseguinte, entre neurónios. Perante este panorama, é essencial explicar a etiologia das DN ao nível bioquímico e molecular, para que haja impulso para o desenvolvimento de novas estratégias terapêuticas.

A doença de Parkinson (DP) é a segunda DN mais frequente e está associada ao *misfolding* e agregação de alfa-Sinucleína (do inglês *alpha-Synuclein*, aSyn), uma proteína neuronal cuja função não é totalmente conhecida. É de notar que a disfunção proteica de aSyn também foi relacionada posteriormente com outras DN, como sejam Demência com Corpos de Lewy e Atrofia Sistémica Múltipla, sendo no seu conjunto designadas de Sinucleinopatias. Assim, o estudo da aSyn tornou-se essencial para compreender a etiologia e o denominador comum daquelas doenças. Existe uma forte controvérsia relativamente à identificação das espécies tóxicas de aSyn; no entanto, as espécies oligoméricas e *misfolded* têm sido postuladas nos últimos anos como as mais tóxicas.

Apesar de a função da aSyn ser pouco clara, existem várias implicações fisiológicas propostas para a mesma, sendo uma das mais relevantes o seu envolvimento na plasticidade sináptica, na medida em que ratinhos *knockout* para a aSyn possuem défices de produção de vesículas celulares. Além disso, a aSyn parece actuar como um regulador negativo da neurotransmissão de dopamina. Outros estudos sugerem o envolvimento da aSyn no recrutamento de complexos necessários para o transporte entre o retículo endoplasmático e o complexo de Golgi e para a fusão vesicular com a membrana plasmática. Por outro lado, a disfunção de aSyn está associada a défices funcionais do proteossoma, aumento da produção de espécies de oxigénio reactivas e disfunção mitocondrial.

Assim, esta tese teve como principais objectivos entender a nível molecular e celular, a função da aSyn na normalidade e na patologia. Para tal, estudou-se a dinâmica intracelular da aSyn em modelos celulares, através de microscopia de fotoactivação. Assim, usando uma forma fotoactivável da proteína verde fluorescente como repórter da aSyn, verificou-se que a disponibilidade da sua extremidade amino-terminal determina a sua deslocação para o núcleo. Esta evidência tem importantes implicações no que se refere às espécies de aSyn que efectivamente entram no núcleo e à sua função no interior do mesmo. Se a recente hipótese que defende que a conformação natural de aSyn é um

tetrâmero está certa, deve-se considerar que apenas monómeros ou dímeros de aSyn podem entrar no núcleo, tendo em conta o tamanho descrito para o poro nuclear. Por outro lado, a presença de aSyn no núcleo está associada a neurotoxicidade, porque promove desregulação transcriptional. Curiosamente, verificamos que a dinâmica intracelular de aSyn é elegantemente modulada pela chaperone HSP70; a presença desta acelera a entrada de aSyn no compartimento nuclear. Para além disso, mutações associadas a DP e o estado de fosforilação da proteína no local S129 alteraram o comportamento dinâmico da aSyn na célula. Especificamente, as mutações A30P e A53T aumentaram a velocidade a qual a proteína se desloca para o núcleo e para o citoplasma, respectivamente. Por último, verificámos que certas cinases que fosforilam aSyn, também têm um efeito na dinâmica intracelular da mesma. O resultado mais claro acerca do efeito do estado de fosforilação na dinâmica da aSyn foi obtido com uma forma mutante que bloqueia a fosforilação no local S129, designada por S129A. A expressão desta forma mutante resultou na formação de inclusões citoplasmáticas, sugerindo que a fosforilação modula a agregação e assim, altera a dinâmica intracelular de aSyn.

Para melhor compreender o processo de agregação e a sua evolução num contexto patológico, estudou-se de seguida os passos iniciais de agregação de aSyn na célula. Segundo a hipótese amilóide, o início da patologia reside na formação de espécies diméricas e oligoméricas, diferentes da conformação nativa de aSyn. Assim, pensa-se que são estas espécies, que se acumulam de forma aberrante, as causadoras de toxicidade e de propagação da patologia. Para estudar os mecanismos moleculares por detrás da formação de espécies oligoméricas tóxicas, usaram-se modelos celulares de Sinucleinopatias. Em particular, efectuou-se um *screening* de interferência de RNA contra genes envolvidos em vias de transdução de sinalização na célula. O objectivo foi identificar de forma não enviesada, moduladores da oligomerização de aSyn, que foi monitorizada através do método de complementação biomolecular por fluorescência.

Nove moduladores genéticos da oligomerização de aSyn, funcionalmente relacionados e associados ao tráfego neuronal, foram identificados e validados. Assim, estes moduladores foram caracterizados no que diz respeito aos seus efeitos na agregação de aSyn, toxicidade e níveis proteicos. Após este primeiro nível de caracterização, investigou-se o mecanismo de acção destes moduladores a nível da secreção de aSyn, um paradigma central relativamente à progressão das Sinucleinopatias. A secreção de aSyn em

condições fisiológicas está descrita como ocorrendo por exocitose não-convencional, em associação com exossomas e possivelmente por outras vias menos convencionais. Contudo, está também demonstrado que as espécies patológicas e agregadas de aSyn podem ser secretadas, sugerindo-se que estas espécies podem ser um poderoso agente de propagação da patologia de aSyn, possivelmente à semelhança dos agentes priónicos. Assim, neste projecto, seleccionaram-se quatro moduladores de tráfego, com base na literatura e na sua relevância para as vias secretórias da célula: *Ras-related protein in Brain 8b* (Rab8b, Rab11a, Rab13 e *Synaptotagmin-Like Protein 5*. Estas proteínas, quando sobre-expressas, promoveram a remoção das inclusões proteicas de aSyn e reduziram a toxicidade celular associada a aSyn. Para além disso, verificou-se um aumento do uso da via endocítica e da secreção de aSyn quando Rab11a e Rab13 foram expressas num modelo de agregação de aSyn. Por fim, verificou-se que no mesmo modelo, aqueles quatro moduladores de tráfego co-localizaram com inclusões de aSyn.

Na sua totalidade, este trabalho sugere que certas vias específicas de tráfego celular são benéficas para a intervenção terapêutica a nível das Sinucleinopatias, e devem ser validadas noutros modelos.

Estudou-se também o efeito de anticorpos de aSyn em estados precoces de agregação da mesma, através de complementação biomolecular por fluorescência. Os resultados aqui descritos apoiam a imunização passiva contra Sinucleinopatias como sendo uma estratégia eficaz a médio prazo para atrasar o progresso de Sinucleinopatias.

O presente estudo põe a descoberto a dinâmica intracelular da aSyn, uma vez que a localização sub-celular dos muitos complexos proteicos que existem numa célula pode ajudar a desvendar as suas funções e mecanismos de acção que culminam na patologia de muitas DNS. Por outro lado, permitiu a identificação de novos moduladores genéticos que envolvem oligomerização, agregação, toxicidade, secreção e imunização de aSyn, contribuindo para o complemento do complexo esquema mecanístico que pode vir a explicar as bases moleculares das Sinucleinopatias.

**Palavras-chave:** Alfa-Sinucleína, Doença de Parkinson, Agregação, Oligomerização



## List of Abbreviations

<b>a<math>\beta</math></b>	Amyloid-beta peptide
<b>AcbA</b>	acyl-CoA binding protein
<b>AD</b>	Alzheimer's disease
<b>AGE</b>	Advanced glycation end-products
<b>ALS</b>	Amyotrophic Lateral Sclerosis
<b>aSyn</b>	alpha-Synuclein
<b>aSynT</b>	Truncated aSyn-GFP fusion protein
<b>ATP</b>	Adenosine triphosphate
<b>ATP6AP2</b>	ATP hydrolase 6 lysosomal accessory protein 2
<b>ATP13A2</b>	ATP hydrolase 13A2
<b>BAD</b>	Bcl-2-associated death protein
<b>Bax</b>	Bcl-2-associated X protein
<b>BBB</b>	Blood-brain barrier
<b>Bcl-2</b>	B-cell lymphoma 2
<b>BFA</b>	Brefeldin A
<b>BRET</b>	Bioluminescence resonance energy transfer
<b>bSyn</b>	beta-Synuclein
<b>bZIP</b>	basic leucine zipper
<b>C-terminal</b>	Carboxy-terminal
<b>CHIP</b>	Carboxyl terminus of Hsp70-interacting protein
<b>CI</b>	Confidence interval
<b>CK</b>	Casein kinase
<b>CM</b>	Conditioned media
<b>CMA</b>	Chaperone-mediated autophagy
<b>co-IP</b>	co-Immunoprecipitation
<b>COMT</b>	Catechol-O-methyltransferase
<b>CSF</b>	Cerebrospinal fluid
<b>DBS</b>	Deep brain stimulation
<b>DLB</b>	Dementia with Lewy bodies
<b>ENS</b>	Enteric nervous system
<b>ER</b>	Endoplasmic reticulum
<b>ERC</b>	Endosomal recycling compartment
<b>ERK</b>	Extracellular signal-regulated kinases
<b>FCS</b>	Fluorescence correlation spectroscopy
<b>FRET</b>	Fluorescence resonance energy transfer
<b>GBA</b>	Glucocerebrosidase
<b>GFP</b>	Green fluorescent protein
<b>GRK</b>	G-protein coupled receptor kinase
<b>gSyn</b>	gamma-Synuclein
<b>GTPase</b>	Guanosine triphosphate hydrolase
<b>h</b>	Hours

<b>HD</b>	Huntington's disease
<b>hGH</b>	human growth hormone
<b>HNE</b>	4-Hydroxynonenal
<b>Hsc70</b>	Heat shock cognate protein 70
<b>HSP</b>	Heat shock protein
<b>Htt</b>	Huntingtin
<b>L-DOPA</b>	L-3,4-Dihydroxyphenylalanine
<b>LAMP2</b>	Lysosomal associated membrane protein 2
<b>LB</b>	Lewy body
<b>LDH</b>	Lactate dehydrogenase
<b>LN</b>	Lewy neurite
<b>LRRK2</b>	Leucine-rich repeat kinase 2
<b>MAO-B</b>	Monoamine oxidase B
<b>MAPT</b>	Microtubule-associated protein Tau
<b>miRNA</b>	Micro RNA
<b>MPTP</b>	1-Methyl-4-phenyl1,2,3,6-tetrahydropyridine
<b>MSA</b>	Multiple system atrophy
<b>MVB</b>	Multivesicular body
<b>N-terminal</b>	Amino-terminal
<b>N2</b>	Notch2
<b>NAC</b>	non-Amyloid-beta component
<b>NADPH</b>	Nicotinamide adenine dinucleotide phosphate
<b>ND</b>	Neurodegenerative disorder
<b>NF-kB</b>	Nuclear factor kappa-light-chain-enhancer of activated B cells
<b>P25</b>	Tubulin polymerization-promoting protein
<b>P62</b>	Nucleosporin p62
<b>PA</b>	Photoactivation
<b>PAGFP</b>	Photoactivatable GFP
<b>PB</b>	Photobleaching
<b>PD</b>	Parkinson's disease
<b>PGC-1<math>\alpha</math></b>	Peroxisome proliferator-activated receptor gamma coactivator 1-alpha
<b>PINK1</b>	PTEN-induced putative kinase 1
<b>PLD2</b>	Phospholipase D2
<b>PMD</b>	Protein misfolding diseases
<b>PNS</b>	Peripheral nervous system
<b>PPAR</b>	Peroxisome proliferator-activated receptor
<b>PPI</b>	Protein protein interactions
<b>PTEN</b>	Phosphatase and tensin homolog
<b>PTM</b>	Post-translational modification
<b>RAB</b>	Ras-related proteins in brain
<b>RanBP2</b>	Ras-related nuclear binding protein 2
<b>RE</b>	Recycling endosome
<b>RNA</b>	Ribonucleic acid
<b>RNAi</b>	Ribonucleic acid interference
<b>ROS</b>	Reactive oxidative species

<b>S</b>	Seconds
<b>shRNA</b>	Short-hairpin RNA
<b>SIAH</b>	Seven in absentia homolog protein
<b>SNARE</b>	Soluble NSF attachment protein receptor
<b>SNCA</b>	Synuclein alpha gene
<b>SUMO</b>	Small Ubiquitin-like Modifier
<b>SUS</b>	Split ubiquitin system
<b>Tf</b>	Transferrin
<b>ThT</b>	Thioflavin-T
<b>UPS</b>	Ubiquitin-proteasome system
<b>v-ATPase</b>	Vesicular adenosine triphosphatase
<b>VPS35</b>	Vacuolar protein sorting 35
<b>Y2H</b>	Yeast two-hybrid system



# I. Introduction

---

**This chapter contains parts of the following publications:**

Gonçalves SA, Miranda HV Outeiro TF (2012), **Novel molecular therapeutics in Parkinson's disease. 1:** 245-265. *Molecular and Cellular Therapeutics*, First Edition, David Whitehouse and Ralph Rapley. John Wiley & Sons.

Gonçalves SA, Matos JE and Outeiro TF (2010), **Zooming into protein oligomerization in neurodegeneration using BiFC**, *Trends Biochem Sci* 35(11): 643-651.

Goncalves, S. A. and T. F. Outeiro (2016). **Traffic jams and the complex role of alpha-Synuclein aggregation in Parkinson's disease.** *Small GTPases*: 1-7.



## 1 Protein Misfolding Diseases

Cell viability depends on the maintenance of proteins integrity, which is directly dependent on the strict balance between protein synthesis, folding and degradation mechanisms. Protein folding and degradation are key quality control systems of the cell. The former is performed by molecular chaperones such as heat shock proteins (HSPs), and the later comprises the ubiquitin-proteasome and autophagy-lysosome pathways. Misfolded and damaged proteins can be targeted to the ubiquitin-proteasome system (UPS) to avoid accumulation and subsequent potentially toxic effects on cells, or can be processed by the autophagy-lysosome system (Figure 1A). The first is mainly involved in the nuclear/cytosolic protein degradation, and the latter in the clearance of cytosolic organelles and long-lived proteins. Three major types of autophagy are described (Figure 1B): Chaperone-mediated autophagy (CMA) selectively degrades proteins containing a pentapeptide motif (KFERQ) that is recognized by the heat shock cognate protein 70 (Hsc70); microautophagy implies the direct sequestration of cytoplasmic cargo by engulfment of the lysosomal membrane; finally, in macroautophagy, double-membrane vesicles termed autophagosomes are formed and sequester portions of cytosolic content or intact organelles (Juenemann & Reits 2012, Yang & Klionsky 2010) . Fine-tuned regulated macroautophagy is required for the survival of neurons, as lack of it leads to degeneration, but, if increased, it can turn into a cell death mechanism (Hara et al 2006, Komatsu et al 2006).

Although the native state of proteins is energetically favored, misfolding of proteins can arise when quality control systems fail their surveillance due to metabolic changes related to aging, cancer, stress conditions or genetic alterations (Hartl & Hayer-Hartl 2009). In those conditions, partially folded or misfolded proteins tend to aggregate and state for aberrant intra- or intermolecular interactions. Protein aggregation is driven by hydrophobic forces and can lead to the formation of amorphous or fibrillary structures. These highly ordered, cross-beta structures are called amyloid deposits and histopathologically define protein misfolding diseases (PMDs).

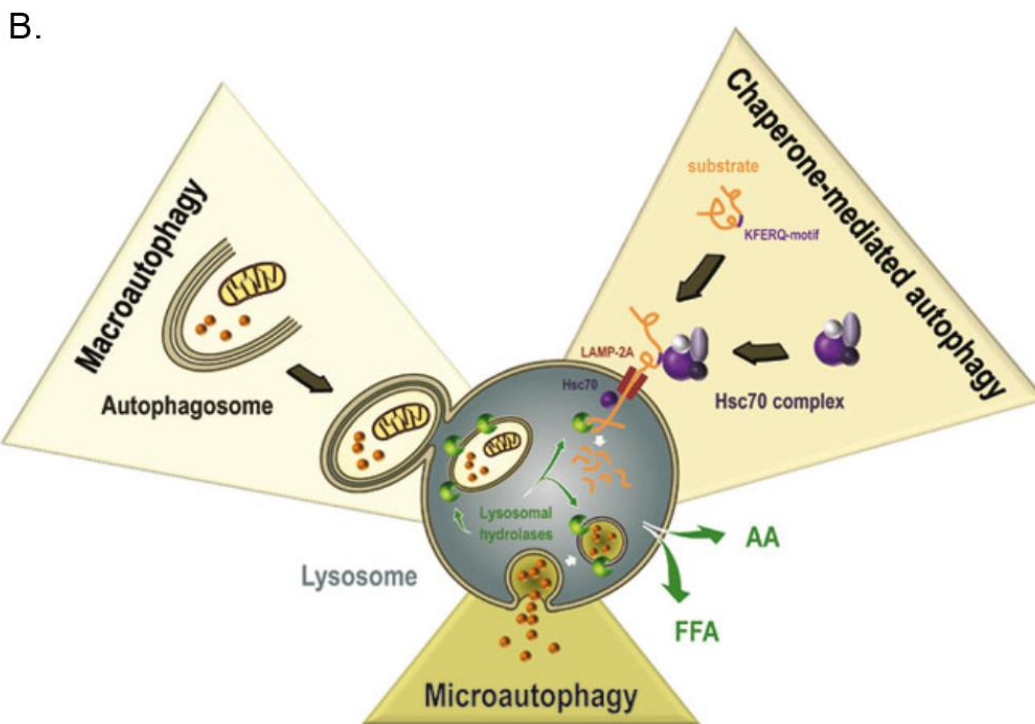
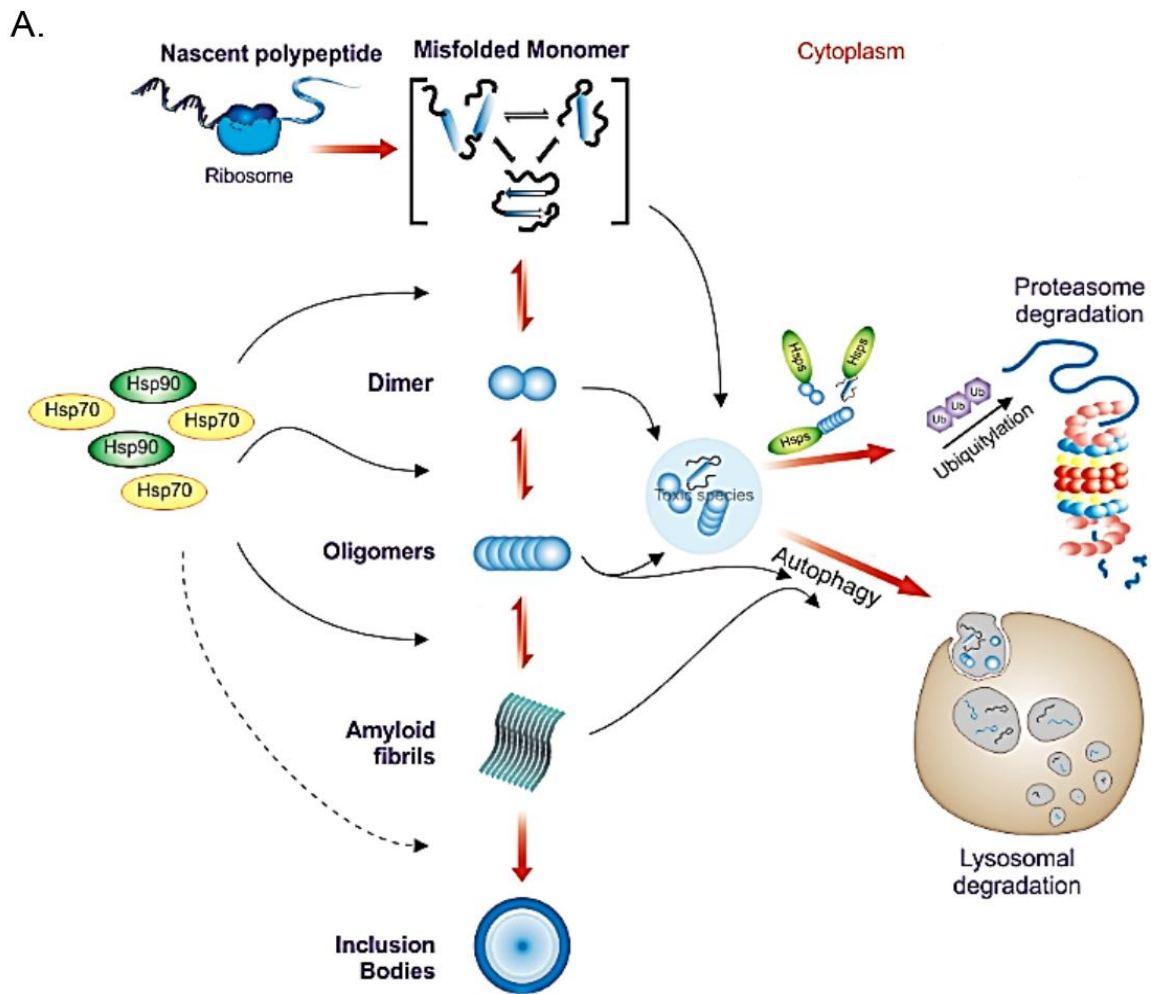




**Figure 1. The role of protein quality control systems in PMDs. A.** When destabilization of the native state of nascent proteins occurs, molecular chaperones are able to reverse it. In aging and disease, protein quality control systems are more prone to fail and proteins form amorphous aggregates, toxic oligomers or amyloid fibrils as a consequence of misfolding of the native states. Different HSPs can modulate the oligomerization state. In several diseases, Hsp70 and HSP90 are known to contribute to the correct folding of misfolded proteins, preventing the formation of aggregated forms. Oligomers are toxic soluble aggregated species that can occur as off-pathway intermediates of amyloid fibril formation. These may be either directly targeted by Hsp chaperones or they may also be directed for proteasomal degradation. Oligomeric and/or aggregated species that are not degraded by the proteasome may be processed by chaperone-mediated autophagy. **B.** Three different types of autophagy are represented: in macroautophagy, specialized vacuoles called autophagosomes are formed for cargo transportation. These vacuoles deliver proteins, lipids and organelles to the lysosome. Through Hsc70 complex, Chaperone-mediated autophagy recognizes proteins with KFERQ-like motif and targets them to lysosomal degradation. Finally, in microautophagy, cargo is directed engulfed by lysosomal membrane. AA: aminoacids, FFA: free fatty acids. Adapted from (Gonçalves et al 2012, Wirawan et al 2012).

## 1.1 Loss of Neuronal Proteostasis and Neurodegeneration

Neurons are long-lived post-mitotic cells and thus particularly susceptible in PMDs, as they are not able to dilute toxic proteins through cell division. Thus, they require fine-tuned quality control mechanisms when proteostasis is compromised. Autophagy-lysosome system is the ubiquitous and most well characterized mechanism to guarantee proteostasis in neurons. Notwithstanding, a specific “sort-and-degrade” mechanism has also been postulated (Wang et al 2013). Neuron-specific proteins, such as the regulator of membrane trafficking V0a1, the subunit a1 of V0-ATPase (a multi-subunit protein-complex that regulates endosomal to lysosomal pH), seems to be a neuron-specific health sustainer, as mutations in *v0a1* homolog in *Drosophila* cause neurodegeneration (Williamson et al 2010). Lysosomes, the terminal organelles on the endocytic pathway, digest macromolecules and make their components available to the cell as nutrients. Hydrolytic enzymes specific to a wide range of targets reside within the lysosome; these enzymes are activated by the highly acidic pH (Wang & Hiesinger 2012).

Similarly, mutations in the synaptic vesicle SNARE neuronal Synaptobrevin seems to cause cargo overload in neurons. SNAREs are the core regulation proteins in membrane fusion. Overall, the “sort and degrade” mechanism is active in parallel to ubiquitous endolysosomal and autophagosomal degradation and is essential for the normal neurotransmitter release (Haberman et al 2012).

The most prevalent PMDs in the brain are Alzheimer’s disease (AD), Parkinson’s disease (PD), Huntington’s disease (HD) and Amyotrophic Lateral Sclerosis (ALS). Clinically they result from the aggregation of different proteins in distinct neurons that can disrupt essential cellular functions. Aggregates can be extracellular, as plaques in AD, or intracellular, neurofibrillary tangles in AD or Lewy bodies in PD. The intracellular aggregates can be rapidly devastating to neurons as they can sequester essential cellular components as molecular chaperones or trafficking players. Moreover, they can promote oxidative stress, inhibit degradation systems and physically impair the release of neurotransmitters thus inhibiting the communication to the adjacent neurons (Gonçalves et al 2012).

It is not clear if fibrils are the toxic species in NDs, or if they arise from a defensive answer of cells aimed to protect themselves from toxic oligomeric species. Even if the mechanistic explanation of pathology in those disorders is variable, the common denominator among these NDs is the gain of toxic properties associated to misfolding. The aberrant conformation favors environmental stress which is aggravated by aging (associated with the decline in protein homeostasis capacity) and, in a long-term perspective, it promotes further protein accumulation and the potential self-propagation of aggregates to other neighboring neurons (Hartl et al 2011).

## **1.2 Synucleinopathies**

Synucleinopathies are neurodegenerative disorders (NDs) characterized by the abnormal neuronal accumulation of a small protein called alpha-Synuclein (aSyn). This protein is abundant in the central nervous system and its abnormal accumulation can occur in neurons, nerve fibers or glial cells. The major Synucleinopathies are PD, dementia with Lewy bodies (DLB) and multiple system atrophy (MSA) (Figure 2). AD and other neurodegenerative disorders related with iron accumulation in brain may also present

aSyn aggregation (Baba et al 1998, Irwin et al 2013, Spillantini et al 1997, Wakabayashi et al 1998).

Abnormal protein deposits were identified in brains from PD patients by Friedrich Lewy in the beginning of the twentieth century. However, only later aSyn was identified as the main component of Lewy bodies (LBs) (Lewy 1912, Spillantini et al 1997). Structurally, LBs are eosinophilic cytoplasmic large inclusions of 5-25 µm size composed of a halo of radial fibrils (Spillantini et al 1998b). The main component of LBs is phosphorylated (at S129), nitrated and also C-terminally truncated aSyn (Crowther et al 1998, Duda et al 2000, Fujiwara et al 2002, Giasson et al 2000, Spillantini et al 1997). However, the role of those post-translational modifications is not totally understood. In addition, molecular chaperones, proteasomal and lysosomal subunits were identified in LBs (Goedert et al 2013, Lowe et al 1988).

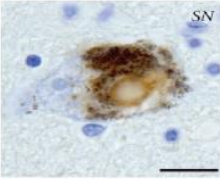
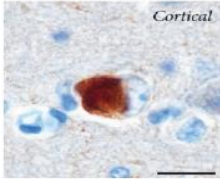
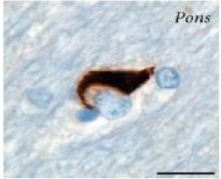
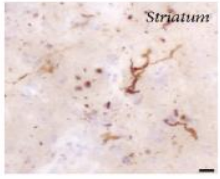
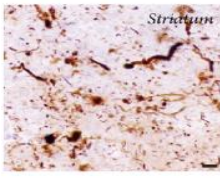
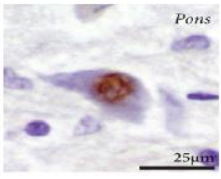
## **1.2.1 Parkinson's Disease**

### **1.2.1.1 Etiology and Pathophysiology of PD**

PD was first described in 1817 by James Parkinson as “the shaking palsy” and is the second most common neurodegenerative disease affecting 1% of the world population over the age of 60. About 90% of PD cases are sporadic, while only a small proportion of the cases are known to have dominantly or recessively inherited familial forms caused by several mutations in specific genes (de Lau & Breteler 2006, Parkinson 2002). In addition, environmental factors as the exposure to pesticides (as rotenone or paraquat), heavy metals (iron, manganese, copper, zinc) and brain injury may cause sporadic PD (Critchley 1957, de Lau & Breteler 2006).

The neuropathological hallmarks of PD comprise the loss of dopaminergic neurons in the *substantia nigra pars compacta* and the presence of intracellular proteinaceous inclusions in the surviving neurons mainly composed of aSyn (Damier et al 1999, Lewy 1912, Spillantini et al 1997). The lack of dopamine results in abnormal neurotransmission and thus prevents appropriate information transfer from motor command centers in the cerebral cortex (Aosaki et al 2010). This leads to different severity degrees of motor

symptoms, including muscle rigidity, resting tremor, bradykinesia and postural instability (Marsden 1982, Parkinson 2002, Wu et al 2015). Non motor signs are believed to manifest prior to motor disabilities, starting with difficulty in problem-solving, attention capacities and decision making (Pfeiffer 2016). Autonomic dysfunction is a common non-motor sign that may precede clinical PD, comprising orthostatic hypotension, constipation, insomnia, abnormalities in olfactory and visual perception, urinary dysfunctions and sweating abnormalities (Liepelt-Scarfone et al 2015). Later disease stages include neuropsychiatric symptoms as depression, anxiety, apathy, and casually, dementia (Gelb et al 1999, Kulisevsky et al 2008).

Clinical Aspects	Parkinson's disease	Dementia with Lewy bodies	Multiple system atrophy
Age of onset (years)	~ 60	~ 70s	~ 60
Duration (years)	~ 12	~ 5	~ 6
Motor signs	All	Some	All
L-dopa responsive	yes	Variable	No
<b>Non-motor signs</b>			
Autonomic	Late	Late	Early
Hallucinations	Late	Early	No
Olfactory dysfunction	Early	Early	No
Dementia	Late	Early	No
	NClIs	NClIs	GCIs
			
<b>Histopathology</b>	Neurites	Neurites	NNIs
			

**Figure 2. Clinical and histopathological hallmarks of the three main Synucleinopathies.** Dementia with Lewy bodies (DLB) has the oldest age of onset. Multiple system atrophy (MSA) has the earliest autonomic features. Histologically, Both PD and DLB are characterized by neuronal cytoplasmic inclusions (NClIs) and neurites, while MSA has glial cytoplasmic inclusions (GCIs) and neuronal intranuclear inclusions (NNIs). SN, *substantia nigra*. Images show aSyn immunoreactive structures counterstained with cresyl violet. Scale bars: 25  $\mu$ m. Adapted from (McCann et al 2014).

Histopathologically, surviving neurons often show protein inclusions, which develop as spindle-like Lewy neurites (LNs) (Braak et al 1994) or as globular LBs (Goedert et al 2013, Lewy 1912), both in sporadic and familial forms of PD (Spillantini et al 1997). As the disease progresses, aSyn aggregates can also be found in other areas of the brain as the olfactory bulb, neocortex and the limbic system (Braak et al 2003). Inclusions of aSyn can also occur in other regions of the central and peripheral nervous system as the enteric plexus of the gastrointestinal system (Dickson et al 2009).

#### **1.2.1.2 Familial PD Genes and their Convergent Role in Trafficking**

Counting for 5-10% of the total cases, inherited PD has been correlated to autosomal dominant or recessive genetic mutations. Multiple genes have been implicated in PD through linkage analysis, genome sequencing and genetic association and the majority features mutations in cellular trafficking proteins (Table 1). The discovery of mutated genes associated with PD was elucidative on the cellular pathways that upon dysfunction triggers to pathology, not only in familial but also in sporadic forms of PD. Consequently, three main interconnected cellular processes may trigger PD upon dysfunction: first, synaptic transmission (exocytosis and endocytosis), lysosome-mediated autophagy; and third, mitochondrial quality control and stress response (Figure 3) (Trinh & Farrer 2013). The most common autosomal dominant inherited cases of PD present mutations in SNCA and LRRK2 genes encoding for aSyn (and discussed below in section 2) and Leucine-rich repeat kinase 2, respectively (Polymeropoulos et al 1997, Zimprich et al 2004). LRRK2 is a guanosine triphosphate hydrolase (GTPase) and kinase with defined roles in neuronal transmission, arborization, endocytosis, autophagy and immunity. Several PD-associated mutations in LRRK2 were identified, presenting a clinical phenotype that resembles idiopathic PD (Cookson 2012). G2019S mutation in LRRK2 has been shown to interfere with chaperone-mediated autophagy in neurons, and to enhance co-localization of aSyn with Lysosomal Associated Membrane Protein 2 (LAMP2) (Orenstein et al 2013). Interestingly, genome-wide association findings suggest that LRRK2 variability confers both significant risk or protection against PD (Trinh & Farrer 2013). Besides, mutations in

Vacuolar protein sorting 35 (VPS35), which mediates retrograde transport of endosomes to trans-Golgi network, cause late-onset PD (Vilarino-Guell et al 2011b).

Autosomal recessive cases of PD contributes for less than 4% of PD and involve genes for Parkin (*PARK2*), DJ1 (*PARK7*) and Pten-induced kinase 1 (*PINK1*), between others (Abbas et al 1999, Bonifati et al 2003, Kitada et al 1998, Valente et al 2004). *PINK1* and *PARK2* encode proteins involved in mitophagy. Specifically, Parkin, an E3 ubiquitin ligase, was described to facilitate the degradation of damaged mitochondria. *PARK2* mutations are thought to result in insufficient protein clearance and subsequent protein accumulation and cellular damage (Kitada et al 1998). DJ1 is implicated in anti-oxidative stress responses, mainly through reactive oxidative species (ROS) scavenging (Ramsey & Giasson 2008). Mutations in the gene encoding for PINK1, a cytoplasmic but mitochondria-associated protein kinase, are thought to impair its kinase activity and contribute to disruption of mitochondrial trafficking, ROS formation, and protein aggregation (Liu et al 2009b, Valente et al 2004, Weihofen et al 2009). Moreover, mutant PINK1 is not able to translocate into the mitochondria, where it should stimulate mitophagy. Mutations in ATP13A2, a lysosomal ATPase, lead to impaired protein degradation (Park et al 2015, Ramirez et al 2006). Finally, mutations in ATP6AP2—a gene required for receptor-mediated endocytosis, membrane trafficking and lysosomal degradation—cause X- linked Parkinsonism (Korvatska et al 2013).

Recently, genome-wide studies have compelled the discovery of novel genes and polymorphisms associated with PD. One example is the established link between the genetic variability of microtubule-associated protein Tau (MAPT) loci and idiopathic PD. Tau is involved in microtubule stabilization, elongation and axonal transport (Lanktree et al 2011, Vandrovcova et al 2010). Moreover, carriers of a single Glucocerebrosidase (GBA) mutant allele have five times higher risk for PD. GBA is a housekeeping enzyme that helps to digest toxic molecules within lysosomes (Klein & Westenberger 2012). Remarkably all genetic forms present aSyn pathobiology with LBs, except for cases carrying *PARK2* and *LRRK2* mutations (Table 1 and Farrer et al 2001, van de Warrenburg et al 2001).

**Table 1. Known genetic loci linked to Parkinson's disease**

Locus	gene	Protein	Brain accumulat ion	Age at onset	Inheritance	Genetic alterations
<i>Loci implicated in late-onset Lewy body PD</i>						
<b>Park 1</b> <b>Park 4</b>	SNCA	aSyn	LBs	30-40s, fast progression	AD	Missense/gene dosage
<b>Park 3</b>	SPR	Sepiapterin reductase	LBs	60s	AD	DNA polymorphisms
<b>Park 5</b>	UCH-L1	Ubiquitin carboxy-terminal L1	LBs	50s	AD	Missense
<b>Park 8</b>	LRRK2	Leucine-rich repeat kinase 2	LBs, not in all cases	40s,	AD	Missense
<b>Park 10</b>	PARK10	?	unknown	50s	Risk factor	DNA polymorphisms
<b>Park 11</b>	GIGYF2	GRB10 interacting GYF protein 2	unknown	late	AD	Missense
<b>Park 12</b>	PARK12	ATP6AP2	Taupathy	juvenile and early onset	X-chromosome	Synonymous
<b>Park 13</b>	HTRA2	HtrA serine peptidase 2	unknown	50s	AD	Missense
<b>Park 16</b>	PARK16	?	unknown	?	Risk factor	DNA polymorphisms
<b>Park 17</b>	VPS35	Vacuolar protein sorting 35 Homolog	unknown	Late onset	AD	Missense
<b>Park 18</b>	EIG4G1	Eukaryotic translation initiation factor 4 gamma, 1	LBs	Late onset, mild	AD	Missense
<i>Juvenile and early-onset recessively inherited parkinsonism</i>						
<b>Park 2</b>	PARK2	Parkin	LBs, not in all cases	20s, slow progression	AR	Missense
<b>Park 6</b>	PINK1	Pten-induced kinase 1	unknown	30s	AR	Missense/truncating/dosage
<b>Park 7</b>	PARK7	DJ1	unknown	30s, slow progression	AR	Missense/truncating/dosage
<b>Park 9</b>	ATP13A2	ATPase type 13A2	Iron	Juvenile, atypical	AR	Truncating
<b>Park 14</b>	PLA2G6	Phospholipase A2, group VI	Iron	Juvenile, atypical	AR	Missense
<b>Park 15</b>	FBXO7	F-box protein 7	unknown	Juvenile	AR	Truncating
<b>Park 19</b>	DNAJC6	HSP40 Auxilin	unknown	Juvenile, atypical	AR	Splice site/Truncating

**Table 1. Known genetic loci linked to Parkinson's disease.** AD, autosomal dominant. AR, autosomal recessive. Table adapted from (Edvardson et al 2012, Quadri et al 2013, Trinh & Farrer 2013).

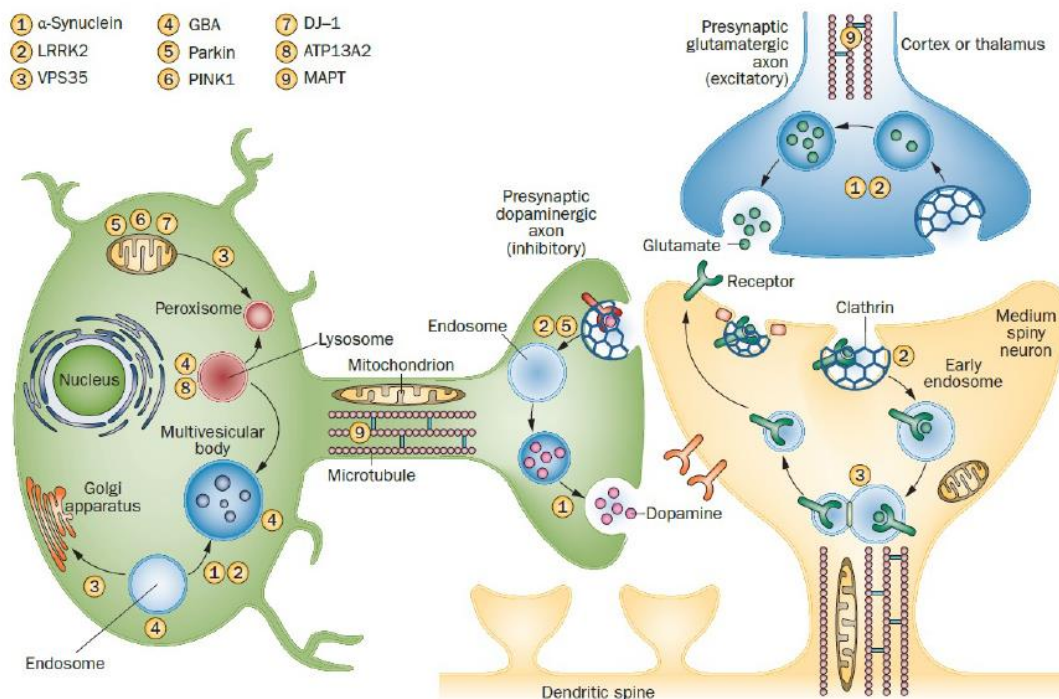


**Figure 3. Overview of cellular dysfunction and genes associated with PD.** A glutamatergic cortical neuron (blue), a dopaminergic *substantia nigra* neuron (green) and a dendritic spine of a medium spiny neuron (yellow) are represented. In presynaptic terminals, aSyn (1) promotes exocytosis and can play a part in endocytosis. Post-synaptically, LRRK2 (2) regulates the release of clathrin-coated endocytic vesicles through phosphorylation, neuronal polarity and arborization. LRRK2 also has roles in chaperone-mediated autophagy and microtubule stabilization. VPS35 (3) is an integral part of the retromer, a complex that mediates cargo endosomal-to-Golgi retrieval by forming a clathrin-independent carrier. Alternatively, cargoes may be destined for lysosomal degradation or exosome secretion. VPS35 mediates cargo recycling from endosomes to the Golgi apparatus or plasma membrane, and vesicle transport between mitochondria and peroxisomes. Lysosomal acid hydrolases, including GBA (4), also require the retromer for receptor recycling. Loss-of-function mutations in Parkin (5), PINK1 (6) and DJ1 (7) affect mitochondrial biogenesis and induction of autophagy. Parkin is involved in ubiquitination and proteasomal function, and PINK1 and Parkin are involved in mitochondrial maintenance. ATP13A2 (8) has a role in lysosome-mediated autophagy. MAPT (9) helps to regulate cargo trafficking and delivery, primarily in axons. Abbreviations: GBA, Glucocerebrosidase; LRRK2, Leucine-Rich Repeat Kinase 2; VPS35, Vacuolar Protein Sorting 35 (Trinh & Farrer 2013).



### 1.2.1.3 Current Therapies of PD

Most, if not all, currently available therapies for PD are just symptomatic. While they improve motor dysfunction symptoms, they do not modify disease progression nor prevent disease onset. These therapies include pharmacological modulation of the dopamine system, neurosurgery and physical therapy.

Since shortage of dopamine is one of the major deficits in the PD brain, current pharmacologic interventions are aimed either at replenishing dopamine levels in the brain or at modulating the dopamine system with specific agonists and antagonists. More specifically, the strategies are the immediate or controlled uptake of the stable dopamine precursor levodopa and the inhibition of monoamine oxidase B (MAO-B) or catechol-O-methyltransferase (COMT), which are enzymes that catabolize dopamine (Goetz et al 2005, Horstink et al 2006). Levodopa and dopamine agonists are the most widely used drugs, as they readily cross the blood-brain barrier (BBB) to exert their anti-Parkinsonian effects. However, long-term use of levodopa improves motor symptoms but does not slow disease progression and is associated with adverse effects such as motor fluctuations and dyskinesias (Fahn 2000, Olanow et al 2004). MAO-B inhibitors, such as Selegiline or Rasagiline, are thought to be neuroprotective as they can inhibit dopamine catabolism. COMT inhibitors also act on the dopamine pathway by inhibiting levodopa catabolism and by extending its half-life. For example, Tolcapone and Entacapone are effective in alleviating the motor impairments, but they are associated with hepatotoxicity (Williams et al 2010).

Peroxisome proliferator-activated receptors (PPARs) are also attractive targets to treat mitochondrial damage and oxidative stress associated with PD. They belong to a nuclear receptor superfamily involved in major biological processes such as inflammation, mitochondrial function, tissue differentiation, and lipid and glucose metabolism. Pioglitazone is a PPAR- $\gamma$  agonist which, when administered to mice before 1-methyl-4-phenyl-1,2,3,6-tetrahydropyridine (MPTP, a prodrug to the neurotoxin MPP<sup>+</sup> that causes symptoms of PD by destroying dopaminergic neurons in the *substantia nigra* of the brain) injection, prevents dopaminergic neuronal loss and glial cell activation, by inhibiting the conversion of MPTP into MPP<sup>+</sup>. Concordantly, in a rat model of PD, pioglitazone improved mitochondrial function, dopamine levels and neuroprotection. *In vitro* cell studies with

Rosiglitazone, another PPAR- $\gamma$  agonist, protected human neuroblastoma cells from acetaldehyde-induced ROS and apoptosis, through the induction of antioxidant enzymes. In *in vitro* models, ibuprofen and acetaminophen were also shown to impair neurotoxicity by binding to PPAR- $\gamma$  and PPAR- $\alpha$ . PPAR agonists are thus promising therapeutic targets, but further studies are needed to prove their safety and efficacy in PD patients. Moreover, although PD is a multifactorial disorder, the widespread involvement of PPAR in cell biology must be carefully regarded to avoid putative severe side effects (Chaturvedi & Beal 2008).

Surgical approaches such as deep brain stimulation (DBS) are presently used, where a neurostimulator delivers electric stimuli to targeted brain areas that are responsible for motor control. This strategy constitutes an alternative treatment in patients who meet specific criteria. A clinical trial comparing drug therapy with a combined drug therapy and DBS showed that patients of the latter group have an improved quality of life, regarding motor impairment and dyskinesias although this is only a symptomatic treatment (Lozano et al 2010).

PD is a progressive ND and treatment is only efficient for a limited stage of the disease (Tambasco et al 2012). In order to develop novel therapeutic strategies for PD it is crucial to gain a detailed understanding of the molecular mechanisms involved in the disease. Since aSyn-induced cytotoxicity seems to be mainly associated with its misfolding and aggregation, it is important to understand how cells respond to the accumulation of these protein species.

Notwithstanding, regular body exercising and healthy nutrition are associated with the delay of disease progression. Moreover, coffee consumption seems to reduce the risk of PD as caffeine is an inhibitor of adenosine A<sub>2</sub> receptors, that are responsible for decreased dopaminergic activity and inhibition of neuronal excitation. Thus, by inhibiting A<sub>2</sub> receptors, caffeine increases brain functions such cognition, learning, and memory and improves motor deficits in a mouse model of PD (Ribeiro & Sebastiao 2010). Resveratrol, a non-flavonoid polyphenol found in red wine and grapes also protects dopamine neurons through its antioxidant and anti-inflammatory properties. Resveratrol-mediated neuroprotection seems to act by inhibiting both lipopolysaccharide-induced neurotoxicity and microglia activation (Zhang et al 2010).

### **1.2.2 Dementia with Lewy bodies**

DLB is a ND characterized by dementia, cognitive impairment, visual hallucination and Parkinsonian motor symptoms. Patients with DLB also present LBs in midbrain but mainly in neocortical areas and brainstem. It is thought to account for up to 30% of dementia cases (Zaccai et al 2005). The most prominent difference between PD and DLB is that dementia can affect PD patients after more than one year with motor symptoms of parkinsonism while DLB patients suffer from it before or during the parkinsonism manifestation (Aarsland & Kurz 2010). Moreover, although most cases of DLB are sporadic, a genetic association is described whose profile overlaps with AD and PD ones. Thus, SNCA and LRKK2 mutations are found in DLB cases (Hyun et al 2013, Nervi et al 2011).

APOE  $\epsilon$ 4 allele is a strong risk factor for DLB, while APOE  $\epsilon$ 2 is protective. Moreover, mutations in GBA are a risk factor for DLB (Berge et al 2014, Bras et al 2014, Tsuang et al 2013).

The realization that patients with Parkinson's disease often develop cognitive deficits and dementia has led to extensive research efforts and new diagnostic criteria for PD and DLB. Improving diagnosis by developing new biomarkers, clarifying terminology and criteria, and determining protective and risk factors are crucial for an accurate diagnosis.

### **1.2.3 Multiple System Atrophy**

MSA is a sporadic progressive disease with mid-age onset. Clinically, patients can have a variable combination of autonomic and cognitive dysfunction, cerebellar ataxia or Parkinsonism. Histopathologically, MSA is characterized by the loss of neurons in the cerebellum, pons, basal ganglia and spinal cord. Genetic factors may play a role in the etiology of the disease, as SNCA variations were associated with MSA risk, as well as MAPT gene, encoding for Tau protein (Ross et al 2010, Vilarino-Guell et al 2011a). In addition, analysis of familial MSA has identified mutations in COQ2, a protein involved in the synthesis of coenzyme Q10 (Multiple-System Atrophy Research 2013). However, until now no gene was associated to MSA.

The neuropathological hallmark of MSA is the presence of filamentous glial cytoplasmic inclusions of aSyn, called glial cytoplasmic inclusions (GCIs) (Trojanowski et al 2007). Actually, this aspect is sufficient to diagnose the disease. Although aSyn is the main component of GCIs, other proteins as ubiquitin, Nucleosporin p62 (p62) and tubulin polymerization-promoting protein (TPPP or p25) are also found. GCIs are located surrounding the nucleus randomly arranged with packed filaments (Papp et al 1989). Interestingly, aSyn can also form glial nuclear inclusions (GNIs), or be aggregated in neurons (Papp & Lantos 1992). While the presence of aSyn in oligodendrocytes is still not well understood given the fact that those cells do not express aSyn mRNA, it was suggested that a neuron-to-oligodendrocyte transfer of aSyn may occur (Reyes et al 2014). GCIs are associated with myelin degeneration, microglia activation and ultimately to cell death. Once this happens, aSyn inclusions can be uptake by surrounding neurons and the process of inflammation and neuronal and oligodendrial dysfunction perpetuates to other brain regions (Brundin et al 2008, Streit et al 2004).

Patients with MSA usually do not respond well to dopamine replacement, probably because other populations than dopamine-producing cells are affected, including spiny neurons in the striatum (Sato et al 2007).

## 2 The Role of Alpha-Synuclein in Health and Disease

### 2.1 Structure and Function of Alpha-Synuclein

aSyn was first isolated from the fish *Torpedo californica*, being found in both synapses and nuclear envelope, whose predominant locations gave rise to the name “Synuclein” (Maroteaux et al 1988). In humans, it was first identified as being the non-amyloid-beta (a $\beta$ ) component (NAC) of AD amyloid precursor (Ueda et al 1993).

aSyn is part of the Synuclein family, which consists of aSyn, beta-Synuclein (bSyn) and gamma-Synuclein (gSyn) (Jakes et al 1994, Lavedan et al 1998). They are structurally similar to apolipoproteins and abundant in neuronal cytosol. The existence of three Synuclein isoforms may count to the modest phenotype of aSyn knockout mice. Concordantly, a triple Synuclein knockout mice show a substantial dopamine release *in vivo* not observed with the single knockouts (Anwar et al 2011).

Structurally, aSyn is a 140-amino acid protein with a molecular weight of 14.5 kDa, but a 112-amino acid splice variant has been identified in heart, skeletal muscle and pancreas (Ueda et al 1994). Being natively unfolded, aSyn acquires an alpha-helical secondary structure in the presence of phospholipids (Weinreb et al 1996). It contains three putative domains, a highly conserved amino-terminal (N-terminal), a hydrophobic NAC and an acidic carboxy-terminal (C-terminal) domain (Figure 4). The N-terminal amphipathic region is involved in lipid interaction, and it is where all PD-associated mutations are localized; the property of binding to phospholipids is promoted by an 11-mer of a seven imperfectly repeated hexamer, KTKEGV (George et al 1995); moreover, a putative mitochondrial target sequence exists within the first 32 aminoacids of the N-terminal of aSyn (Devi et al 2008). Interestingly, the PD-associated A30P mutation impairs association of aSyn with membranes, which supports a role for membrane binding by the N-terminus (Jo et al 2002). The hydrophobic NAC domain (residues 61-95) by itself can form amyloid fibrils and when exposed determines aggregation of aSyn (Giasson et al 2001, Yoshimoto et al 1995). Finally, the acidic C-terminal domain (residues 96-140) contains the binding sites for calcium and copper (residues 109-140), exhibits chaperone-

like functions and is subject to phosphorylation at serine and tyrosine residues (Goedert et al 2013, Hoyer et al 2004, Souza et al 2000b).

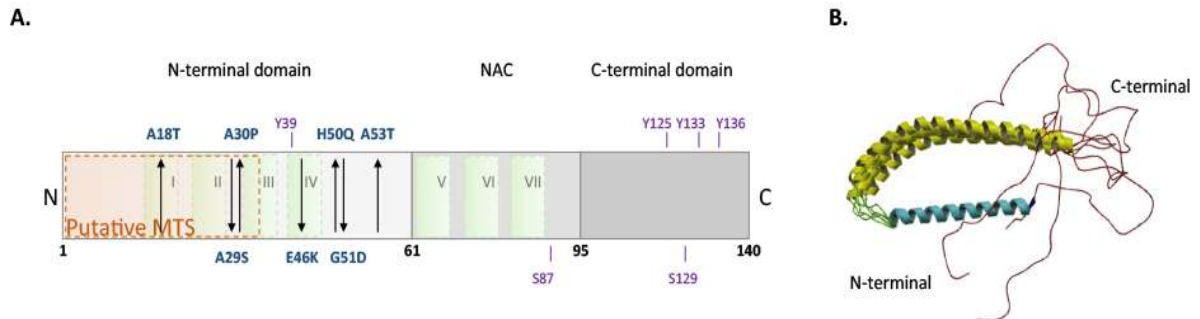


**Figure 4. Structure of aSyn.** **A.** The N-terminal domain contains all human missense mutations associated to familial PD (represented in blue). Although a typical mitochondrial targeting sequence is absent in aSyn, the first 32 aminoacids region is a putative mitochondrial-targeting signal (MTS, represented in orange) as its deletion abolishes aSyn entrance in mitochondria. The central hydrophobic core (NAC domain) promotes aggregation of the protein when exposed. I-VII (in green) represents KTKEGV repeats. The C-terminal domain (gray) is an acidic tail that contains phosphorylation and calcium binding sites. The phosphorylation sites described for aSyn are represented in purple. **B.** Structure of aSyn solved using nuclear magnetic and electron paramagnetic resonance. Adapted from (Emanuele & Chierregatti 2015, Hunn et al 2015).

aSyn is expressed predominantly in the brain, more abundantly in cell bodies during development and at nerve terminals in adulthood. It is also detected in cerebrospinal fluid, blood plasma, platelets and lymphocytes (Galvin et al 2001). At a cellular level, aSyn was initially found to occur in a pre-synaptic and nuclear localization in *Torpedo californica* (Maroteaux et al 1988). Further studies confirmed the presence of aSyn in the nucleus in mice, *Drosophila* and in different cell types (Goers et al 2003, McLean et al 2000, Seo et al 2002, Takahashi et al 2003). The physiological role of aSyn at the synapse has been extensively investigated but few studies have focused on its function within the nucleus.

Different physiological roles have been proposed for aSyn: 1) regulation of synaptic plasticity and neuronal differentiation. This arose from the fact that aSyn was found in the cell body of neuronal precursors in embryonic mice and humans, but in presynaptic

terminals in postnatal and adult cortex (Bayer et al 1999, Hsu et al 1998). In PC12 cells induced to neuronal differentiation, aSyn levels are substantially increased (Stefanis et al 2001). Also, aSyn is upregulated in phases of critical neuronal plasticity, both during song learning period in the case of a bird model, or in early postnatal rat brain, when synapse formation is crucial (George et al 1995, Petersen et al 1999). Probably, aSyn mediates synaptic plasticity through the inhibition of phospholipase D2 (PLD2). This was the first identified interactor of aSyn, which is involved in the hydrolysis of Phosphatidylcholine, a class of phospholipids abundant in biological membranes (Jenco et al 1998). 2) aSyn knockout mice presents normal behavior and no changes in the nervous system, although it has deficits in the dopamine system at *substantia nigra* (Abeliovich et al 2000). This suggests a role in the regulation of dopamine release, probably through regulation of dopamine vesicles. 3) aSyn was shown to be involved in the regulation of cell viability, as it was demonstrated its interaction with 14-3-3 chaperones, extracellular signal-regulated kinases (ERK), B-cell lymphoma 2 (Bcl-2)-associated death protein (BAD), a Bcl2 homologue that controls mitochondrial function, and protein kinase C (Ostrerova et al 1999). Consistent with this is the fact that overexpression of aSyn might lead to mitochondrial dysfunction in a hypothalamic neuronal cell line, leading to the generation of radical oxygen species. Actually, under basal conditions, aSyn interacts with mitochondria, but mitochondria isolated from PD patients presents a higher fraction of aSyn bound (Hsu et al 2000); 4) an important suggested function is the regulation of neurotransmitters exocytosis at the synapse, by interacting with Cysteine-string protein-alpha, which together chaperone SNARE complex assembly at the membrane interface. SNARE complex assists vesicles fusion with the membrane, after which they dissociate to an unfolded state (Chandra et al 2005).

Despite the neuroprotective role suggested to aSyn in a healthy state, misfolding, mutations or overexpression can promote neurodegeneration, cumulatively with age-related impairment of cell maintenance or environmental insults (Burre 2015).

The true physiological species of aSyn remains enigmatic. Originally, aSyn was described as a natively unfolded protein that may adopt a helical form in contact with membranes. Recent studies point out that aSyn exists *in vivo* as a tetramer. This was verified in human cell lines, red blood cells, mouse cortex and is corroborated by the existence of physiological tetramers in human cortex of 60 kDa, and, in minor quantity, of 80-100 kDa.

Such multimers are richer in alpha-helices than recombinant aSyn (Bartels et al 2011, Dettmer et al 2013, Luth et al 2015). They suggested aSyn monomers may be prone to aggregation and that stabilization of the tetramer may illuminate new strategies of therapy in pathology. The controversy arose when Burré and colleagues suggested that misfolded and boiled aSyn also migrate at 55 kDa on native-PAGE, supposedly because of the unstructured state of monomeric aSyn, and they contraposed by mass spectrometry that purified mouse brain aSyn has 16 kDa, consistent with a monomeric form of the protein (Fauvet et al 2012b). At this point, it remains possible that aSyn effectively adopts a physiological tetrameric state, where the presence of membranes is ubiquitous, but it can exist in its intrinsically disordered and unfolded form when a membrane interaction does not happen. Functionally, it is being established a pathway in which aSyn exists in different levels of folding. This pathway ranges from a natively unfold state in cytosol and membrane-bound physiological multimers that act to chaperone for instance SNARE-complex assembly (Burre et al 2010, Diao et al 2013).

## **2.2 Genetic Association Between Alpha-Synuclein and Parkinson's Disease**

The first link between aSyn dysfunction and PD was established in 1997 when A53T missense mutation in aSyn gene (SNCA) was shown to cause a dominant, inherited form of PD (Polymeropoulos et al 1997). On the same year, aSyn was identified as the main component of LBs and LNs (Spillantini et al 1997). Another linkage analysis studies have identified other PD-associated mutations (including A30P, E46K, H50G and G51D) (Appel-Cresswell et al 2013, Kruger et al 1998, Lesage et al 2013, Proukakis et al 2013, Zarranz et al 2004). A18T and A29S substitutions were also associated with Polish PD patients (Hoffman-Zacharska et al 2013). Moreover, duplications of SNCA were co-related with late-onset PD. Triplication of aSyn, rather than duplication, causes an exceptionally severe phenotype, with earlier onset, cognitive as well as motor severe impairments. (Chartier-Harlin et al 2004, Ross et al 2008, Singleton et al 2003). In these cases, aSyn was found in its wild-type form, predicting that a simple increase in the protein rather than a change in its properties is sufficient to pathology.



Additional functional variability in non-coding regions were associated with an eventual susceptibility to idiopathic PD. Specifically, single nucleotide polymorphisms (SNPs) in intron 4 or in the 3' untranslated region, or dinucleotide repeats in the 5' promoter of SNCA, were found in linkage association with the disease (Chiba-Falek et al 2003, Pals et al 2004, Rajput et al 2009, Sotiriou et al 2009, Winkler et al 2007).

## **2.3 Alpha-Synuclein post-Translational Modifications**

Post-translational modifications (PTMs) are known to modulate protein conformational changes and function (Figure 1). For example, the activation of some proteins depends on PTMs as phosphorylation or methylation, and their degradation is regulated by ubiquitylation. Thus, if the normal PTMs are altered, pathological conditions may arise. Therefore, it is of great importance to investigate the physiological role of PTMs of the major players in PD, namely aSyn.

The best well characterized PTM of aSyn is the phosphorylated S129 (Fujiwara et al 2002). Other described post-translational modifications of aSyn include oxidation, ubiquitylation, nitration, sumoylation, and glycation. However, the exact role of post-translational modifications in aSyn function in both physiological and pathological conditions remains to be unravel (Gonçalves et al 2012).

### **2.3.1 Phosphorylation**

Phosphorylation can affect protein conformational states, their fate, subcellular localization and can also precede or succeed further modifications in signaling pathways. Thus, phosphorylation is a complex mechanism that can affect the biological processes happening inside the cell in a dynamically regulated process (Salazar & Hofer 2009).

Approximately 90% of aSyn is phosphorylated in LB of PD patients, contrasting with only 4% of phosphorylated aSyn under physiological conditions *in vivo* (Anderson et al 2006, Fujiwara et al 2002). However, it is still unclear whether phosphorylation of this residue is either a trigger or a late event in aSyn oligomerization and whether modulating the activity of kinases/phosphatases can increase or decrease aSyn oligomerization and

toxicity. The studies using genetic mutants that attempt to mimic or block phosphorylated-S129 (S129D or S129E and S129A, respectively) associated phosphorylation with pathology, in *Drosophila melanogaster* and mice models (Chen & Feany 2005, Chen et al 2009, Freichel et al 2007, Salazar & Hofer 2009). Intriguingly, opposite results were obtained in different models, as yeast, rat and *Caenorhabditis elegans* (*C. elegans*) (Azeredo da Silveira et al 2009, Fiske et al 2011, Gorbatyuk et al 2008, Kuwahara et al 2008, Kuwahara et al 2012, Sancenon et al 2012). Similarly, the same controversy arises regarding the effect of phosphorylation on aSyn aggregation, both in cell and animal models. In fact some reports show a direct relationship (Arawaka et al 2006, Smith et al 2005, Wu et al 2011a) while others claim that unphosphorylated forms of aSyn increase aggregation (Azeredo da Silveira et al 2009, Tenreiro et al 2014). Those discrepancies might reflect the complex biological background involved in aSyn function; potentially, phosphorylation can be a secondary or a cumulative cause of aSyn pathology. This is concordant with a proposed model of inclusions occurring prior to phosphorylation and aggregated aSyn being a specific substrate for kinases but not phosphatases (Mbefo et al 2010, Waxman & Giasson 2011).

S87 and Y125 are now emerging as targets for phosphorylation, and demand further investigation. Similarly to S129, S87 studies lead to discrepant results: the most recent study points phosphorylated S87 being increased in Synucleinopathies rodent models and in human brains of ALS, DLB and MSA (Paleologou et al 2010) while previous studies claimed that phosphorylation on this residue was not detected in human brains or mouse models of Synucleinopathies (Anderson et al 2006, Fujiwara et al 2002). It was observed that Y125 phosphorylation decreases upon aging and is absent in the brains of patients with dementia with Lewy bodies (Chen et al 2009). In agreement, phosphorylation of Y125, Y133 and Y136 suppresses eosin-induced oligomerization (Negro et al 2002). However, it was also demonstrated that there is no differences in the levels of phosphorylated Y125 between PD brains and controls and further investigations may be needed to clarify the relationship between Y125 phosphorylation, aggregation and pathology of aSyn (Mahul-Mellier et al 2014). In the same study, Y39 was identified as a new phosphorylated residue in human brains but with no significant differences between PD and control brains. Notwithstanding, a new mechanistic clue arose from these reports

as the authors were able to relate Y39 and Y125 phosphorylation with aSyn clearance through proteasomic and autophagic pathways.

Several kinases were shown to phosphorylate aSyn at S129, as G-protein coupled receptor kinases (GRK1, GRK2, GRK5 and GRK6) (Inglis et al 2009, Krantz et al 1997, Pronin et al 2000, Sakamoto et al 2009), Casein kinases 1 and 2 (CK1, CK2) (Okochi et al 2000), polo-like kinases (PLKs) (Inglis et al 2009, Mbefo et al 2010) and LRKK2 (Qing et al 2009). The more well studied kinases in the context of PD are GRK5, which colocalizes with aSyn in LBs of PD patients (Arawaka et al 2006), and PLK2, which is correlated with increased levels of aSyn phosphorylation in disease (Basso et al 2013, Mbefo et al 2010).

The emerging objective is now to mechanistically explain the overall phospho-regulation of aSyn and to correlate the subsequent phosphorylation events between the kinases pool available and with disease.

### **2.3.2 Nitration and Nitrosylation**

In PD, nitrated aSyn was found in LBs. It was proposed that protein nitration/nitrosylation, the reaction between a nitro group and tyrosine or cysteine residues, may be one of the oxidative mechanisms responsible for the formation of di-tyrosine crosslinks which contribute for aSyn oligomerization (Giasson et al 2000, Hodara et al 2004, Souza et al 2000a). Moreover, soluble nitrated aSyn is not efficiently processed by proteases, leading to partial unfolding, accumulation and fibril formation. Interestingly, activated microglia is found to induce nitric oxide (NO)-dependent oxidative-stress in different cell types and consequently lead to nitration of aSyn that ultimately results in neurodegeneration (Hodara et al 2004).

### **2.3.3 Sumoylation**

aSyn can be modified by small ubiquitin-like modifiers (SUMO) in a process known as sumoylation. Sumoylated aSyn can be found in LBs suggesting that SUMO may act as a proteasome-mediated antagonist of aSyn degradation. Four different SUMO isoforms (SUMO-1 to SUMO-4) are expressed in humans. SUMO-4 is highly homologous to SUMO-3

and believed to be a SUMO-3 pseudogene (Bohren et al 2004, Su & Li 2002). SUMO recognizes a specific consensus motif, and polySUMO chains may be formed since SUMO2 and SUMO-3 contain this recognition motif (Rodriguez et al 2001, Tatham et al 2001). Parkin is an important player in sumoylation since it is shown to regulate the turnover of SUMO E3 ligase Ras-related nuclear binding protein 2 (RanBP2), ubiquitylating and promoting its proteasomal degradation (Um & Chung 2006). DJ1 is also a target for sumoylation in residue K130, and mutations in this residue block its correct sumoylation. Since DJ1 activity may rely on its correct sumoylation, dysregulation of the SUMO pathway may contribute to the degeneration of oxidative stress-sensitive neurons. Interestingly, the oxidation levels of the cell regulate DJ1 expression, whereas SUMO E1 and E2 activities are reversibly inhibited (Shinbo et al 2006). This suggests that a combination of sumoylation in Parkin and DJ1 pathways may play a role in PD pathogenesis.

### **2.3.4 Ubiquitylation**

There is an intense debate on whether ubiquitylation is a requirement for aSyn degradation by the UPS or whether it may enter the 20S proteasome system directly. Nonetheless, aSyn ubiquitylation occurs in specific lysine residues K6, K10, K12, K21 and K23 (Anderson et al 2006).

Interestingly, monoubiquitylation of aSyn by Seven in Absentia Homolog Protein (SIAH) increases the formation of aSyn inclusion bodies within dopaminergic neurons and enhances its toxicity (Rott et al 2008). These results suggest that monoubiquitylation may be a triggering event in aSyn aggregation.

Moreover, several mutations in genes associated with the ubiquitin-proteasome system are described as PD associated. Thus, ubiquitylation of aSyn may be a pathological event associated with the formation of LBs in a process that is modulated by different gene products, all of which might constitute targets for intervention.

### 2.3.5 Glycation

Other PTMs are known to occur in the cell, such as glycation, a spontaneous reaction between reducing sugars and free amino-groups. Since glycation agents such as methylglyoxal, a by-product of the glycolytic pathway, are known protein cross-linkers, glycation may contribute to the chemical crosslinking and proteolytic resistance of the protein deposits found in the LBs (Vicente Miranda & Outeiro 2010). This suggests that modulating the amounts of glycation agents in neurons also regulates the formation of inclusion bodies. One possible strategy to interfere with glycation involves the regulation of the enzymes responsible for the catabolism of glycation agents (mainly the glyoxalases and aldose reductase) (Maeta et al 2005). These enzymes are glutathione- or nicotinamide adenine dinucleotide phosphate (NADPH) -dependent, which are important compounds involved in the response to oxidative stress. Strategies aimed at increasing the levels of both glutathione and NADPH may be important to control oxidative stress and carbonyl stress, which may in turn prevent the aggregation of proteins such as aSyn. Interestingly, one aging-related event in PD is the decrease in glutathione levels (Thornalley 1998) contributing to an increase in the formation of advanced glycation end-products (AGE), the final products of glycation. Besides glutathione levels, the expression of glyoxalase I in normal individuals increases until the age of 55 and progressively declines with aging, contributing to AGE formation (Kuhla et al 2006). These species are specifically recognized by the receptors for AGE that trigger an inflammation and oxidative stress response via the Nuclear Factor kappa-light-chain-enhancer of activated B cells (NF- $\kappa$ B) induction and the formation of ROS. These receptors are highly expressed in PD patients when compared to age-matched controls, suggesting a role in the development and/or progression of the disease (Dalfo et al 2005). Interestingly, a synthetic derivative of vitamin B1, benfothiamine, was shown to prevent AGE formation in different models. In an Alzheimer's disease mouse model, this compound was shown to improve cognitive function and reduce a $\beta$  deposition and tau phosphorylation (Pan et al 2010).

## 2.4 Alpha-Synuclein Aggregation and Cellular Dysfunction

In the context of NDs, the “amyloid hypothesis” states that the aggregation of proteins into an ordered fibrillar structure is causally related to aberrant protein interactions that culminate in neuronal dysfunction and ultimately neurodegeneration (Hardy & Selkoe 2002). When proteins fail to adopt a proper and functional structure, and thus are not efficiently detected by molecular chaperones nor eliminated by the cellular degradation systems, they might undergo aberrant and harmful interactions (Bandopadhyay & de Belleruche 2009, Outeiro & Tetzlaff 2007). At this point, they can spontaneously form more stable and insoluble amyloid assemblies, which are rich in beta-sheet structures. More recently, smaller protein assemblies, known as oligomeric species, have entered the central stage (Outeiro et al 2008, Wong et al 2008). Available evidence suggests oligomers as either precursors for the formation of amyloid fibrils or off-pathway intermediates in the amyloidogenic cascade (Figure 1) (Ross & Poirier 2004, Taylor et al 2002).

aSyn also deposits in other NDs. Up to 60% of AD patients show LBs, but more restricted to amygdala (Uchikado et al 2006). The hyperphosphorylated microtubule-associated Tau (MAPT) is a major component of neurofibrillary tangles and plaque neurites in AD (Grundke-Iqbal et al 1986). The microtubule-binding domain of Tau was shown to bind to aSyn via its C-terminal. Consequently, only Tau that is not bound to microtubules interacts with aSyn. In addition, aSyn promotes the phosphorylation of Tau by protein kinase A, which impairs binding of Tau to microtubules. On the other side, N-terminal of aSyn binds to a $\beta$  and brain vesicles (Biernat et al 1993, Jensen et al 1999, Yoshimoto et al 1995). Synphilin-1 is another interacting partner of aSyn, whose function might be involved in vesicle transport or cytoskeletal function. Importantly, it is present in LBs of PD brains. *In vitro*, Synphilin-1 co-expression with aSyn promotes cytosolic eosinophilic inclusions that resemble LBs (Engelender et al 1999, McLean et al 2001, Wakabayashi et al 2000).

Similar to aSyn, bSyn and gSyn can deposit in both PD and DLB. Lack of studies and contradictory results did not consolidate yet the characterization regarding toxicity effects of bSyn and gSyn, still it is suggested that may cause degeneration (Ninkina et al 2009, Nishioka et al 2010). While bSyn has been suggested to ameliorate aSyn-induced toxicity through effects on its aggregation and expression (Fan et al 2006, Hashimoto et al

2001), other studies in cultured neurons reveal bSyn is as toxic as aSyn (Taschenberger et al 2013).

NDs with brain iron accumulation due to mutations in Pantothenate Kinase Type 2, involved in the Coenzyme A biosynthetic pathway, are also positive for aSyn, bSyn and gSyn in Lewy bodies, which can suggest that Synucleins are involved in transversal cellular pathways or they participate in the attempt to respond to injury (Galvin et al 2000).

## **2.5 Alpha-Synuclein and Neuronal Trafficking**

Trafficking processes govern the physiological homeostasis of neuronal cells in the brain, impacting on cell survival. Vesicular trafficking underlies the function of numerous essential cellular processes such as the export of newly synthesized proteins from the endoplasmic reticulum (ER) to the Golgi and to the cell surface; and the recycling, transportation and fusion of membrane receptors to lysosomal vesicles for degradation.

Thus, dysfunction of key intracellular trafficking processes may impact on normal neuronal function, especially in highly specialized cells such as dopaminergic neurons that appear to be particularly vulnerable in PD (Matsuda et al 2009). The burden imposed by trafficking processes in dopaminergic neurons might be larger than in other neuron types, as these neurons are estimated to establish 1-2.5 million synapses per neuron in the striatum, and present complex axonal arborisations (Hunn et al 2015). Indeed, defects in exocytosis, endocytosis, sorting and recycling of endosomal receptors at synaptic transmission sites have already been associated PD (Figure 5).

In PD, a consequence of vesicular transport impairment is the functional deficit of the nigrostriatal dopamine system. Dopamine, through a decrease of the vesicular neurotransmitter uptake, is stalled in the ER-Golgi compartments. This is associated with aSyn dysfunction in dopaminergic neurons, as transgenic human aSyn in rat and mouse models of PD attenuates the mobility, dispersion and the size of synaptic vesicle recycling pools (Nemani et al 2010, Scott & Roy 2012). In this case, Dopamine is rapidly oxidized to generate ROS, contributing for cell damage and death, an observation that is aggravated in transgenic mice expressing A30P, A53T and truncated forms of aSyn (Garcia-Reitböck et al 2010, Platt et al 2012, Taylor et al 2014).

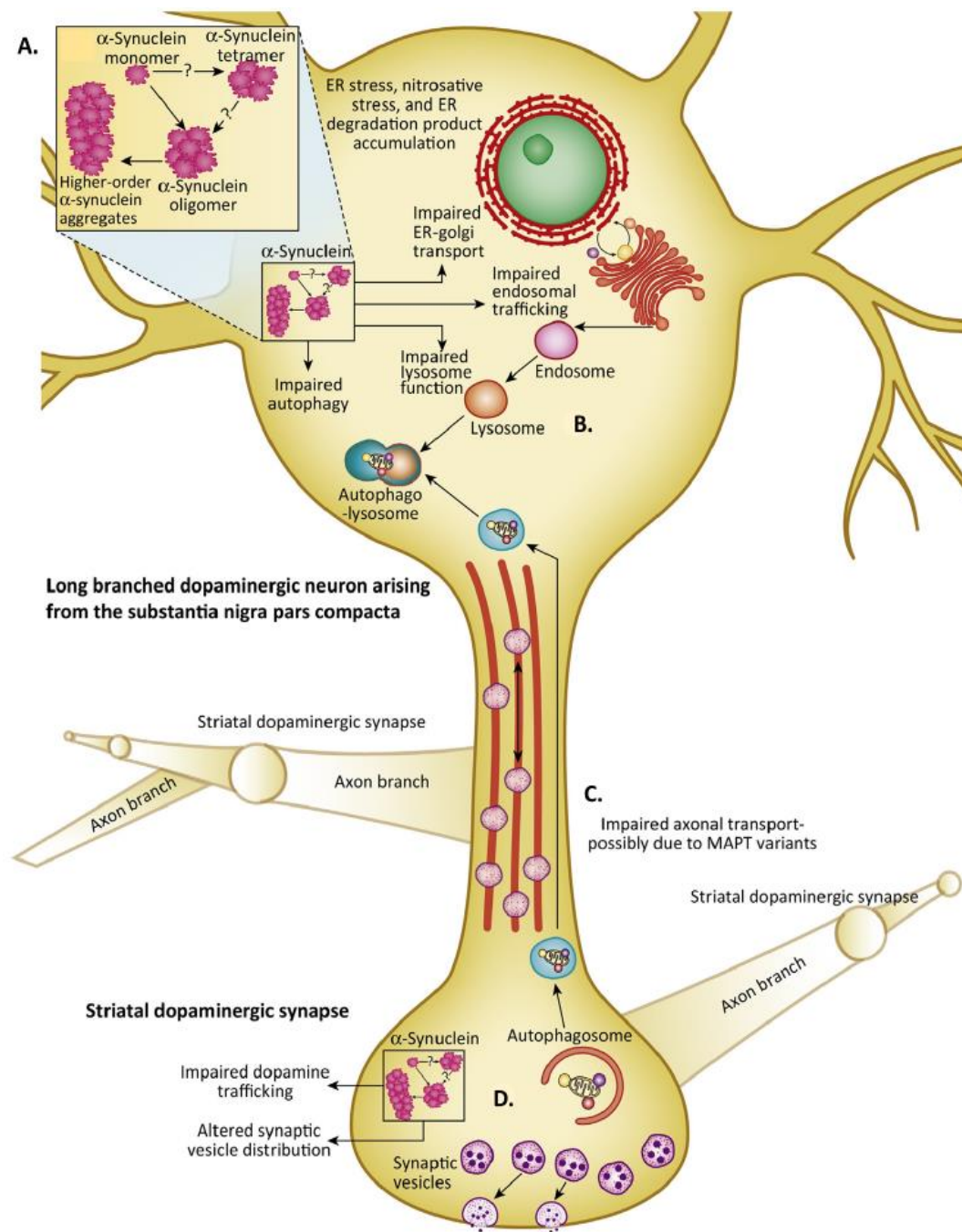


**Figure 5 Intracellular trafficking is impaired in PD.** **A.** The pathological and physiological species of aSyn remains unknown. However, increasing evidence suggests that oligomers and monomers are responsible for the deleterious effects in disease. **B.** aSyn impairs key events in the soma, such as endoplasmic reticulum–Golgi trafficking, endosomal trafficking, and autophagolysosome formation. **C.** Tau protein regulates microtubule stability, allowing efficient axonal transport. Variants in the gene for the MAPT protein confer PD susceptibility. Increased aSyn also impairs axonal transport. **D.** At the synapse, aSyn disturbs Dopamine and autophagosomes trafficking and synaptic vesicle distribution. Adapted from (Hunn et al 2015).



Actually, ER stress was pointed as the earliest aSyn-induced defect in a yeast PD model and was further confirmed in fly, rat and worm (Cooper et al 2006). Moreover, through an ribonucleic acid interference (RNAi) screen in a *C. elegans* model of PD, based on the expression of wild type-, A30P-, or A53T-aSyn, components of the endocytic pathway were identified to play an important role in the worm neurotoxicity, growth and movement coordination (Kuwahara et al 2008). This is supported by the observation that aSyn induced disruption of ER-to-Golgi trafficking occurs through direct interaction of aSyn and SNARE complexes (Thayanidhi et al 2010). Interestingly, aSyn is believed to assist the folding of SNARE proteins, involved in the fusion of vesicles, thereby modulating the release of synaptic neurotransmitters (Bonini & Giasson 2005).

Ras-related proteins in brain (Rab) GTPases are major players in those cellular processes. This highly conserved family of proteins is composed by more than 60 members in mammals (Zerial & McBride 2001). Overexpression of Rab1 in yeast, *C. elegans*, *D.melanogaster* and primary neuronal cultures, suppresses aSyn-induced toxicity (Cooper et al 2006). Moreover, different studies showed that dysregulation of Rab members as Rab3a (involved in exocytosis of synaptic vesicles), Rab5 (important for endocytosis), Rab7 (implicated in the formation and fusion of late endocytic structures with lysosomes) and Rab8 (involved in trans-Golgi transport), can be involved in aSyn pathology (Dalfo et al 2004b). In addition, Rab3b overexpression in rat can rescue the neurotoxicity of 6-hydroxydopamine, a neurotoxin that selectively kills dopaminergic and noradrenergic neurons (Chung et al 2009, Kuwahara et al 2008). Importantly, Rab7L1 has been shown to interact with LRRK2 and VPS35, and seems to play a role in endosomal–lysosomal trafficking (MacLeod et al 2013).

Rab proteins were also previously found to colocalize with aSyn inclusions in yeast cells, further supporting the possibility that aSyn, or other components of inclusions, might sequester Rab GTPases from their normal cellular functions. Also in yeast, it was found that deletion of Ypt6p, Ypt7p, and Ypt51p, homologues of mammalian Rab6, Rab7 and Rab5, respectively, that are involved in the endocytic pathway, increased aSyn aggregation (Soper et al 2011). Other studies also reported the interaction between a A30P mutant version of aSyn and Rab3a, Rab5 and Rab8, in transgenic mice (Dalfo et al 2004a, Dalfo et al 2004b).

It was not new that Rab proteins are linked to neuropathies; for instance, mutations in *RAB7* can cause Charcot-Marie-Tooth type 2B (Verhoeven et al 2003). In *LRRK2*-mediated PD, different steps of the endolysosomal pathway, regulated by Rab5 and Rab7, are impaired. *LRRK2* silencing causes impairment of Rab5-dependent synaptic vesicle endocytosis (Shin et al 2008). Moreover, *Lrrk2* seems to be a negative regulator of Rab7-mediated perinuclear clustering and localization of lysosomes, which is vital for multiple cellular functions, including autophagy (Dodson et al 2012).

Rab11a is also a recycling endosome (RE) regulator that has been related with aSyn pathology. Together with HSP90, it has been shown to associate with aggregated species of aSyn and to mediate the secretion of aSyn *in vitro* (Liu et al 2009a).

In a rat model of aSyn and in human tissue of brain with sporadic PD, it was demonstrated that there is a reduction in axonal transport proteins, as Kinesin, a protein to which Tau interacts (Chu et al 2012, Dixit et al 2008). This impaired axonal trafficking gains importance when for instance aSyn aggregates in the synapse need to retrogradely be cleaned through the autophagy-lysosome pathway (Maday et al 2012). Concordantly, in fly, aSyn and Tau co-localized in ubiquitin-positive aggregates and it was also associated with deficits in axonal transport and cytoskeleton (Roy & Jackson 2014).

Altogether, these findings suggest that aSyn aggregation can interfere with the cellular trafficking and, therefore, modulating vesicular trafficking function may constitute a valid therapeutic approach.

## **2.6 Intercellular Propagation of Pathologic Alpha-Synuclein**

As millions of copies of each protein are made during the lifetime of any cell, a random event can eventually occur shifting the conformation of a protein into a toxic configuration. Remarkably, the toxic configuration is often able to interact with other native copies of the same protein and catalyze their transition into the toxic state. The newly made toxic proteins repeat the cycle in a self-sustaining loop, amplifying the toxicity and thus leading to a catastrophic effect that eventually kills the cell or impairs its function. Because of this ability, they are known as prion-like proteins or prions. Thus, prions are misfolded forms of an endogenous protein that normally suffers

the conversion of alpha-helical to a beta-sheet rich structure. This shift propitiates infectivity, a property that enables refolding of native proteins into the prionic state.

Emerging evidence points that prion-like mechanisms of disease propagation exist in AD and PD, and possibly other disorders. In PD, this hypothesis is consistent with Braak's suggestion of pathology progression from the anterior olfactory bulb and lower brainstem into the dorsal motor nucleus of the vagus nerve, through midbrain and basal forebrain, eventually reaching the cortex (Figure 6). As this topographic sequence occurs following a non-random process, the severity of the clinical manifestations increase accordingly (Braak et al 2003). Supporting this line of thought, it is suggested that aSyn fibrils can act as seeds of surrounding monomeric aSyn. Moreover, A30P fibrils can induce assembly of WT-aSyn fibrils with the same conformational character as A30P fibrils (Wood et al 1999, Yonetani et al 2009). Importantly, LBs were found in foetal neural grafts in post-mortem PD brains 10 to 22 years after transplantation (Kordower et al 2008, Li et al 2008).

It is known that PD pathology also affects the peripheral nervous system (PNS), in particular the enteric nervous system (ENS). Indeed, Lewy pathology can be found both throughout the PNS as well in cases of asymptomatic incidental DLB (Beach et al 2010, Dickson et al 2009, Parkkinen et al 2005). Braak *et al* propose that PD pathology starts in the gastric system and precedes clinical Parkinsonism, affecting vulnerable neurons with a long and unmyelinated axon in CNS (Braak et al 2006, Braak & Del Tredici 2004).

The concept of intercellular propagation of aSyn has risen when this protein was found in cerebrospinal fluid (CSF) and blood plasma of both PD and normal cases, thus implicating that aSyn was being released by neurons in the extracellular space (Borghi et al 2000, El-Agnaf et al 2003). Although aSyn intercellular transition in PD is being well documented (Figure 7), the mechanism that leads to a general spreading in brain remains to be elucidated. Exocytosis of monomeric, oligomeric and aggregated forms of aSyn has been proven through exosomes *in vitro* (Danzer et al 2012, Emmanouilidou et al 2010, Lee et al 2005). Moreover, oligomeric and fibrillary aSyn enter neurons through conventional endocytosis, travel through endosomal pathway and eventually they can be degraded by lysosomes (Lee et al 2008). In rodents, it was also proved the spreading of aSyn pathology. In a first study, injection of synthetic aSyn into dorsal striatum of wild type mice led to the appearance of LBs in *substantia nigra* and motor deficits. Similarly, cultured dopaminergic neurons grafted into aSyn transgenic mice were also positive for

aSyn (Desplats et al 2009, Hansen et al 2011). These findings were not limited to neurons but were also shown in astrocytes where it triggers an inflammatory response (Lee et al 2010). Furthermore, it was demonstrated using a mouse model for a Synucleinopathy that inoculation of young asymptomatic mice with brain homogenates from old and symptomatic mice accelerated aggregation, promoted hyperphosphorylation of aSyn at S129 and decreased longevity. Importantly, this disease progression did not occur if inoculation was made in aSyn knockout animals, which suggests that endogenous aSyn is crucial for an effective transmission of pathology from an affected to an unaffected site, being consistent with a prion-like mechanism underlying the disease propagation (Mougenot et al 2012). Similarly, by striatal injection of fibrillary aSyn in mice, Lewy body pathology was monitored first in the injected area and later in ventral striatum, cortex and brainstem. Cell loss was rapidly noticeable in *substantia nigra* as characteristic in PD (Luk et al 2012).

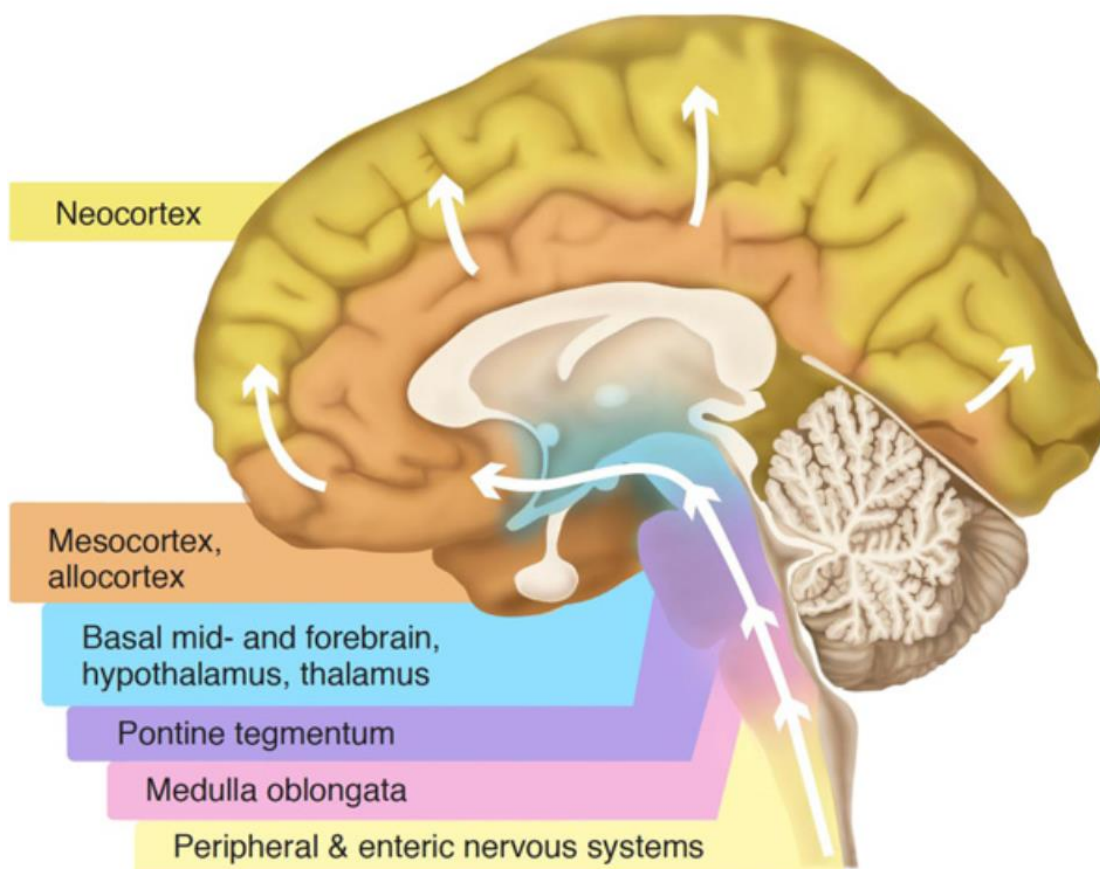


**Figure 6. Schematic of Parkinson’s disease progression as proposed by Braak and colleagues.** According to the Braak model, aSyn deposits in specific brain regions starting from the lower brainstem through susceptible regions of the midbrain (including *substantia nigra*) and forebrain (as amygdala) and into the cerebral cortex. It is hypothesized that the disease initiates in the periphery, gaining access to the CNS through retrograde transport along projection neurons from the gastrointestinal tract. Adapted from (Visanji et al 2013).

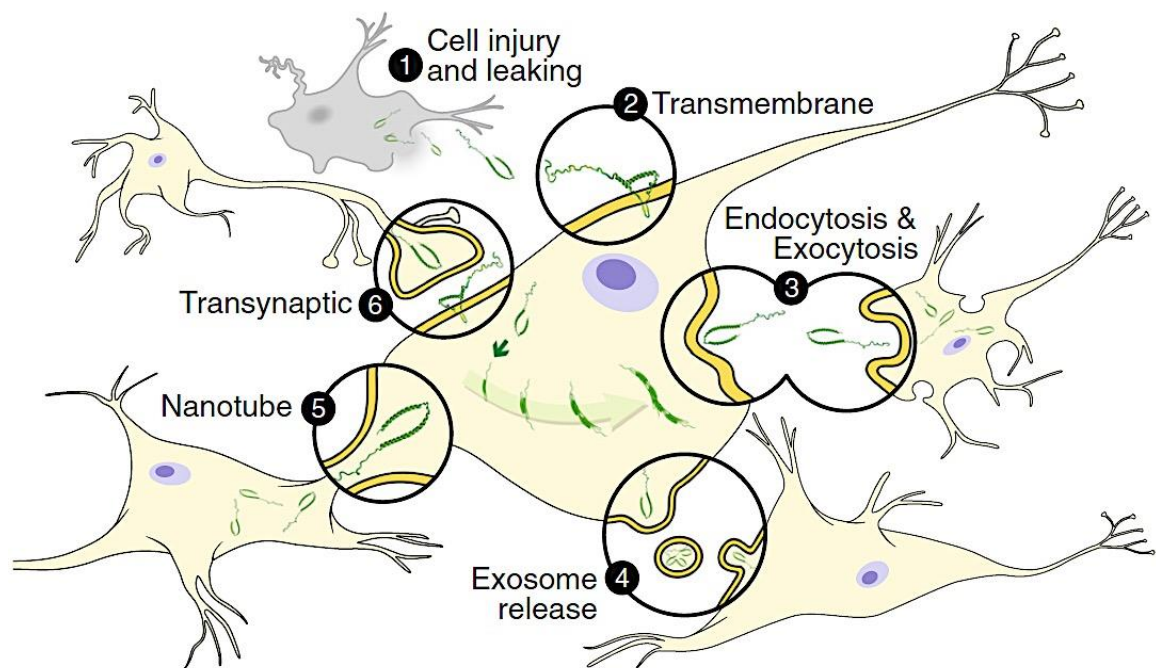


**Figure 7. Neuron-to-neuron transmission of aSyn.** aSyn can be released into the extracellular space via (1) leakage from injured cells. Extracellular aSyn is able to directly translocate the cell membrane and gain access to neighboring neurons (2), can be transmitted from cell-to-cell via conventional exocytosis and endocytosis (3) or can be packaged into exosomes which are released and taken up by surrounding cells (4). Tunneling nanotubes can form a direct connection between two cells potentially allowing aSyn to transfer freely from one cell to another (5). Finally, aSyn could be transmitted by direct synaptic contact (6). Adapted from (Visanji et al 2013).

## 2.7 Cellular Models of Alpha-Synuclein Oligomerization and Aggregation

In neurodegeneration, protein-protein interactions (PPIs), which lead to the formation of oligomeric species and amyloid-like protein aggregates, are thought to lie at the heart of cytotoxicity (Outeiro et al 2008, Wong et al 2008). Thus, animal and cellular models are necessary vehicles to study PD progression. Ideally, a live model with a complex nervous system where the key features of PD can be recapitulated could be a valuable tool to study the therapeutic solutions for the disease. However, mechanistic explanations of the disease are still lacking and thus, *in vitro* models than can mimic simple and few cellular pathways of disease etiology are in the edge of knowledge breakthroughs rather than *in vivo* models.

The formation of macroscopic proteinaceous inclusions has been reported in several models of NDs such as cell cultures, flies, worms, or mice (Feany & Bender 2000, Masliah & Hashimoto 2002). However, the detection and observation of oligomeric and prefibrillar species directly in living cells was only recently achieved (Chen et al 2006, Outeiro et al 2008).

We have witnessed the development of novel experimental approaches to directly detect PPIs. Traditional approaches such as co-immunoprecipitation (coIP) and co-purification, or even the recently developed protein microarrays, require the removal of proteins from their natural environment. The identification of PPIs is therefore performed under non-native conditions. Major limitations of these approaches include the possibility that the interaction observed does not reflect a physiological event and fail to provide information on the subcellular localization of the interactions. Methods that overcome this disadvantage, including functional analysis of compensatory mutations, imaging-based techniques or protein-fragment complementation assays (PCAs) have led to the identification of several PPIs (Remy & Michnick 2004). These methods have the advantage of allowing the various biological players to remain intact in the cellular environment.

Traditional imaging-based methods used to visualize interactions of protein complexes in cells include fluorescence- or bioluminescence- resonance energy transfer microscopy (FRET or BRET, respectively), fluorescence correlation spectroscopy (FCS) (Langowski

2008) and image correlation spectroscopy (Petersen et al 1993). FRET measures the distance between two interacting proteins *in vivo*, which are labeled with two different fluorophores. One of the proteins is labeled with a donor fluorophore that, upon excitation, transfers energy to the acceptor fluorophore that labels the second protein. The distance between the two interactors is calculated based on the difference between the lifetime of the two fluorophores. As the emission spectrum of the donor must overlap the excitation spectrum of the acceptor, this technique can identify interactions that occur within <10 nm (Rino et al 2009). FRET-based techniques enabled investigating the effect of mutations in the gene coding for the amyloid precursor protein (APP) on its interaction with Presenilin-1 (Herl et al 2009). These techniques were also used to characterize intra- and inter-molecular interactions of aSyn (Klucken et al 2006, Outeiro et al 2009).

FCS is a powerful bioimaging technique that measures fluctuations and diffusion rates of fluorescently-labeled molecules, using sophisticated theoretical analysis (Langowski 2008). These fluctuations are characteristic of particular physical interactions and aggregation patterns of the interacting partners. FCS has been used to investigate the formation of polyglutamine oligomers and amyloid-beta (a $\beta$ ) peptide aggregates (Funke et al 2007, Takahashi et al 2007). PCAs, such as the yeast two hybrid system (Y2H) (Fields & Song 1989) and the split ubiquitin system (SUS) (Johnsson & Varshavsky 1994), have also allowed the detection of transient PPIs in living cells. The Y2H system, in particular, led to several important discoveries in the field of NDs (Fombonne et al 2009, Greggio et al 2008). In both the Y2H and the SUS assays, PPIs activate reporter genes that will either enable growth on specific media or mediate a colorimetric reaction. Although the Y2H system requires the interactors to be localized in the nucleus, the derivative SUS technique affords the opportunity to investigate cytoplasmic or membrane-compartmentalized interactions. Nevertheless, these PCAs do not necessarily provide information regarding the normal subcellular localization of the interaction, which can only be achieved with imaging-based methods.

*In vitro* mammalian models of PD are multiple and complex to design as the expression of aSyn does not induce cytoplasmic inclusions or cytotoxicity *per se*. However, overexpressed aSyn can modulate toxicity, ROS production and the formation of cytoplasmic inclusions (Junn & Mouradian 2001, Xu et al 2002).

Along this work, we based our cell models in neuroglioma cells expressing aSyn oligomers and cytoplasmic inclusions. Bimolecular fluorescence complementation (BiFC) was used to directly visualize aSyn oligomerization in living cells, allowing to study the initial events leading to aggregates formation. Stabilization of aSyn oligomers via BiFC results in increased cytotoxicity, which can be rescued by Hsp70 in a process that reduces the formation of aSyn oligomers (Outeiro et al 2008).

Aggregates formation can instead be modeled co-expressing aSyn and Synphilin-1, an interactor of aSyn also found in LBs, which positively react for ThioflavinS staining (McLean et al 2001).

## **2.7.1 Bimolecular Fluorescence Complementation**

The BiFC assay was introduced in 2002 to investigate interactions between basic leucine zipper (bZIP) and Rel family transcription factors in their normal cellular environment, using the COS-1 cell line (Hu et al 2002). Since then, BiFC has been used successfully in different model organisms, including mammalian cell lines, plants, nematodes, yeast, and bacteria (Bracha-Drori et al 2004, Chen et al 2007). Importantly, this technique can also be used as a platform for genetic or chemical screens (Gehl et al 2009).

The development of the BiFC assay constituted a powerful technological advance; indeed, it allows the study of PPIs and their functional roles in the context of living cells (Chen et al 2006, Kerppola 2006, Outeiro et al 2008). This assay involves the fusion of two non-fluorescent fragments of a reporter protein to the proteins of interest. In the event of an interaction between two proteins of interest, the reporter fragments come together, fold into a quasi-native structure, and thereby reconstitute the activity of the reporter protein (Chen et al 2006, Kerppola 2006) (Figure 8).

### **2.7.1.1 Advantages and Disadvantages of BiFC**

The BiFC assay, through the formation of a fluorescent complex from non-fluorescent constituents, affords the possibility of overcoming some of the limitations of several techniques previously used for the study of PPIs. These limitations are most commonly



related to the size of protein complexes and the optical resolution of microscopes. There are two major advantages over the methods mentioned above: (i) it is unlikely that cellular conditions that are not related to protein–protein interactions cause changes in fluorescence intensity or lifetime, because the signal is generated uniquely upon complementation of two non-fluorescent fragments; and (ii) the fluorescent complexes can be directly visualized in living cells without the need for staining with exogenous molecules (Kerppola 2006).

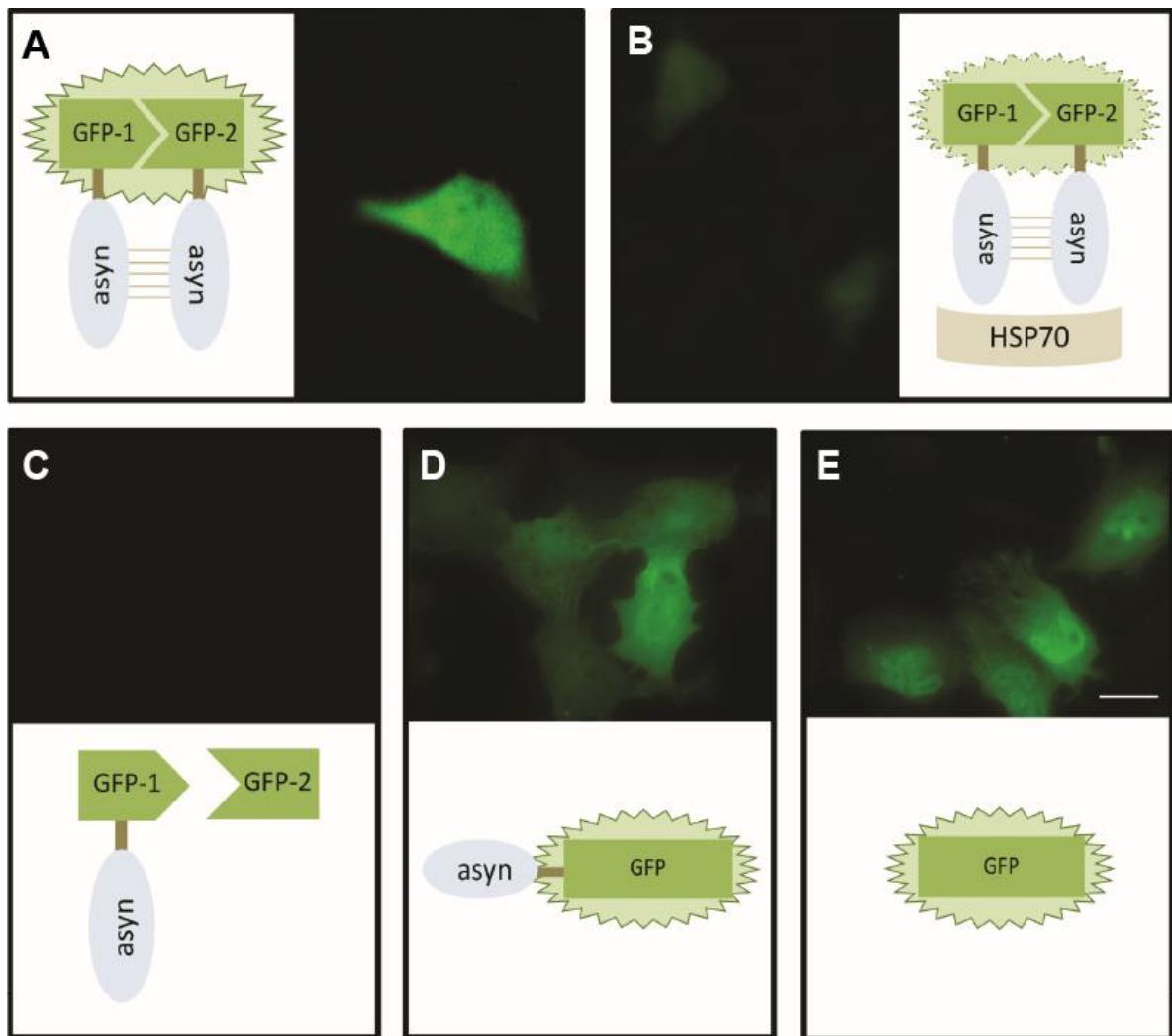


**Figure 8. HSP70 inhibits aSyn oligomerization in living cells.** **A.** Confocal microscopy showing aSyn dimers produced by BiFC; **B.** the presence of Hsp70 significantly reduces the fluorescence produced by the dimerization of aSyn. To emphasize the specificity of aSyn-aSyn interaction through BiFC, the negative control with one construct (**C.**) and the positive controls with the entire GFP (**D.** and **E.**) are shown. Scale bar: 20µm.

One limitation of BiFC is that it does not enable the direct identification of novel interacting partners because fluorescence complementation requires that the proteins are tagged with a fluorophore fragment. The generation of libraries similar to those available for Y2H screens, in which different cDNAs are fused to each of the fluorescent protein fragments, presents one possible way to overcome this limitation.

#### **2.7.1.2 Visualization of PPIs with BiFC – Reporter Proteins**

Several reporter proteins have already been successfully used for detection, including green fluorescent protein (GFP), cyan fluorescent protein (CFP), yellow fluorescent protein (YFP) and red fluorescent protein (RFP) (Chu et al 2009).

The first version of the BiFC assay used GFP and encompassed an initial incubation at 30°C. In some experimental settings, this might constitute a disadvantage. However, this disadvantage is now overcome with the development of a number of fluorescent proteins (FP) including Cerulean (CFP variant) (Rizzo et al 2004), Citrine (Griesbeck et al 2001), VENUS (Nagai et al 2002) (YFP variants) and mLumin (a far-red variant) (Chu et al 2009) whose improved biophysical properties enable the maturation of the fluorophore at 37°C. This is particularly important for studies in mammalian cells which typically prefer this later temperature and, therefore, for the study of neurodegeneration in mammalian models.

Multicolor BiFC was later developed to investigate both the dimerization selectivity of different members of the leucine zipper family, and the subcellular localization of such interactions (Hu & Kerppola 2003). Multicolor BiFC has been further applied to other areas such as neurobiology, where it is now giving its first steps. For instance, it has been used to study changes in A<sub>2A</sub> (adenosine) and D<sub>2</sub> (dopamine) heteromeric receptors formation upon drug stimulation (Vidi et al 2008).

#### **2.7.1.3 Application of BiFC in the Study of NDs**

One potential limitation of BiFC is the trapping of particular PPIs, because the reconstitution of the fluorophore by BiFC can lead to stabilization of the protein complex

(Kerppola 2006, Outeiro et al 2008, Tetzlaff et al 2008). This, together with the need for a maturation period, limits its usefulness for visualizing dynamic interaction changes. However, this disadvantage might actually turn out to be useful for some studies, because it allows the selective enrichment of dimeric/oligomeric species, thereby facilitating their study. In particular, for the study of NDs, the stabilization of certain PPIs could be extremely useful since it enables the study of species that might be transient, such as those generated in the protein aggregation process. BiFC, in contrast to other techniques, enables the visualization of small dimeric/oligomeric species in living cells without the need for antibody staining. However, it does not allow one to visually distinguish dimers from oligomers or another higher order species. In order to discern between species, BiFC can be coupled to other techniques such as FCS (Outeiro et al 2008, Tetzlaff et al 2008), sodium dodecyl sulfate (SDS)- or native-polyacrylamide gel electrophoresis (PAGE) (Anderie et al 2007, Chen et al 2006, Tetzlaff et al 2008). Immunoprecipitation (IP) (Chen et al 2006, Tetzlaff et al 2008), flow cytometry (Morell et al 2008), FRET (Shyu et al 2008) and BRET (Gandia et al 2008), when combined with BiFC, might provide insight into the dimeric/oligomeric state of the different protein species.

Thus, approaches, which use BiFC in combination with other complementary methodologies, hold a strong potential for unveiling phenomena, which would otherwise be difficult to investigate, such as oligomer composition in living cells. Indeed, BiFC was used to elucidate G protein-coupled adenosine receptor ( $A_{2A}$ ) stoichiometry; in the same study,  $A_{2A}$  oligomers, containing more than two promoters, were observed using BiFC coupled to BRET (Gandia et al 2008). In the field of NDs, where the formation of oligomeric complexes seems to play an important role in the pathological process, the BiFC assay constitutes a simple and easy-to-adapt tool to investigate the biochemical events involving the formation of those oligomeric species (Gandia et al 2008).

#### **2.7.1.4 BiFC in the study of Alzheimer's disease**

AD is the most common cause of dementia, and it continues to affect an increasing number of people due to aging of the human population. Patients suffer progressive and severe neuronal loss in the cerebral cortex and hippocampus (Gunther & Strittmatter 2010). The pathological hallmarks of AD are extracellular amyloid plaques mainly

composed of  $a\beta$  and neurofibrillary tangles, which are made primarily of hyperphosphorylated tau. The triggering signals and the molecular mechanisms that determine the formation of these two types of protein aggregates remain unclear because the majority of AD cases are sporadic and have no clear genetic determinant. In order to investigate the nature of the aggregates and to distinguish prefibrillar oligomers and fibrils, conformation-dependent antibodies have been developed (Kayed et al 2007). We posit that BiFC holds great potential for the study of the PPIs involved in the oligomerization and aggregation of these AD-associated proteins, affording the opportunity for direct visualization of PPIs in living cells. The  $a\beta$  precursor protein interacts with Notch2 (N2), a transmembrane receptor involved in neuronal function and embryonic and adult development (Oh et al 2005). The use of BiFC was crucial in determining the nature of the interaction between APP and N2. With this technique, not only were APP dimerization and APP–N2 heterodimerization visualized in living cells, but these interactions were shown to occur at the endoplasmic reticulum, Golgi, and plasma membrane (Chen et al 2006). Furthermore, the same group, using BiFC in Presenilin null fibroblasts, demonstrated that the APP–N2 interaction is Presenilin-independent (Oh et al 2010).

### **BiFC in the study of Parkinson's disease**

In order to unravel the molecular mechanisms involved in the formation of intermediary species that range from monomeric to aggregated forms of aSyn, BiFC has been used to visualize aSyn oligomers and to observe their modulation of other proteins (Figure 8) (Outeiro et al 2008). Another study applied BiFC to investigate the effect of carboxyl terminus of Hsp70-interacting protein (CHIP) on aSyn oligomerization; this study concluded that co-expression of aSyn with CHIP leads to a reduction in both aSyn oligomerization and toxicity (Outeiro et al 2008, Tetzlaff et al 2008). Due to its characteristics, BiFC is also used as readout to identify modifiers of aSyn oligomeric process, through the use of genetic screens (Goncalves et al 2016).

Multicolor BiFC has been used to investigate dopamine  $D_2$  and adenosine  $A_{2A}$  receptor oligomerization (Vidi et al 2008). G protein-coupled receptor oligomerization has been shown to be altered following long-term administration of drugs such as L-3,4-

dihydroxyphenylalanine (known as L-DOPA) which are used in the treatment of PD. This study identified a shift in the type of oligomers formed upon drug application:  $A_{2A}$ - $D_2$  heterodimers decreased in comparison to  $A_{2A}$  homodimers after stimulation by  $D_2$  agonists; the opposite effect was observed upon stimulation with  $D_2$  antagonists. Thus, it was suggested that long-term exposure to drugs might lead to an alteration of  $A_{2A}$ - $D_2$  receptor oligomerization.

### **2.7.2 An *in Vitro* Model of aSyn Aggregation**

McLean *et al* described a carboxy-terminally truncated aSyn-GFP fusion protein (aSynT) that altered the widespread subcellular distribution and solubility of aSyn by inducing the formation of cytoplasmic inclusions. These could be positively modulated by proteasome inhibitors and A53T mutation but negatively by A30P. Importantly, they have found that overexpression of Synphilin-1, an aSyn interacting protein also found in Lewy bodies, enhances and colocalizes with aSynT in discrete cytoplasmic inclusions (McLean *et al* 2001). Since then, this model is being largely used to induce aSyn aggregates spontaneously in cytoplasm (Chutna *et al* 2014b, Goncalves *et al* 2016, Smith *et al* 2005)(Figure 9).

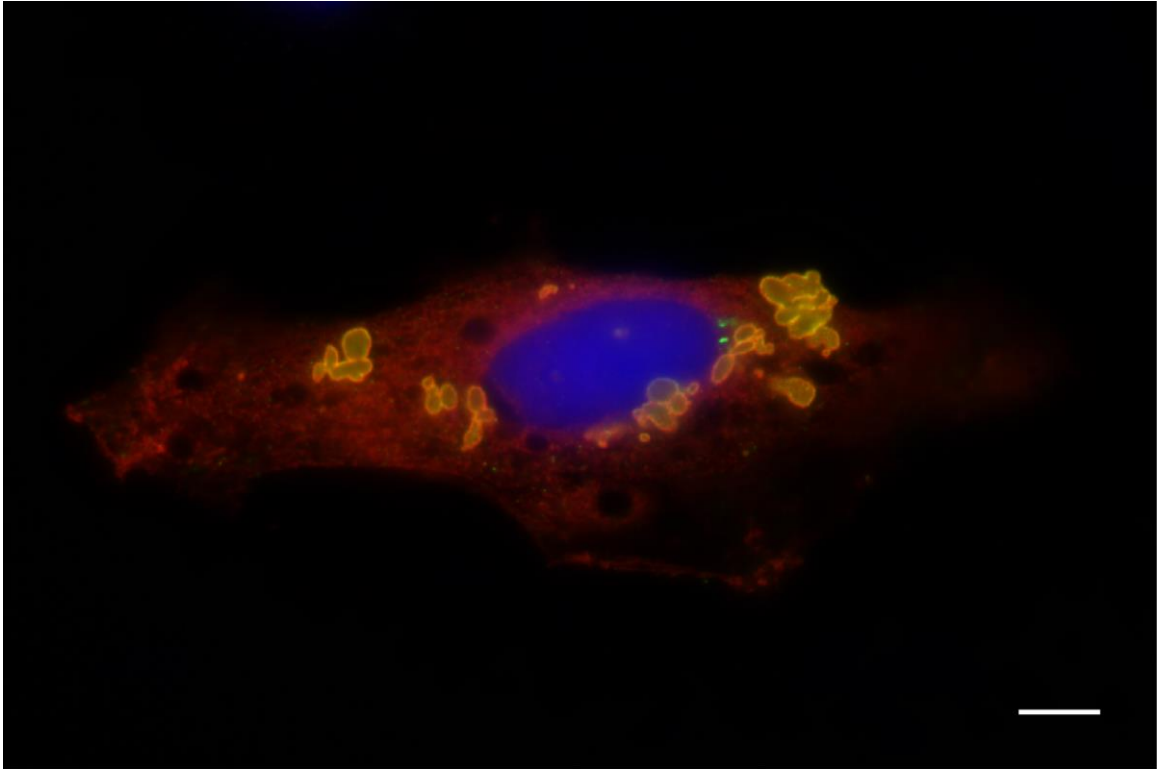


**Figure 9. A cellular model of aSyn aggregation.** Overexpression of carboxy-terminally truncated aSyn-GFP fusion protein and Synphilin-1 spontaneously form cytoplasmic inclusions in neuroglial cells. Co-transfected cells were detected by immunocytochemistry using anti-V5 antibody and a rhodamine-linked secondary antibody for Synphilin-1 (red) and Sc7012 primary and a fluorescein-linked secondary antibody for aSyn T (green). Scale bar 10  $\mu\text{m}$ .

## II. Aims

---





PD is a neurodegenerative condition associated with the misfolding and aggregation of aSyn, a neuronal protein whose function is not totally characterized. There is ample debate of what are the toxic species of aSyn that triggers to pathology, although it has been postulated that misfolded oligomeric aSyn are the most toxic species.

The work described here aimed to investigate the molecular mechanisms underlying aSyn pathogenesis, at its earlier stages. The molecular contextualization of aSyn early events of aggregation might guide us to a deeper and more assertive understanding of the role of aSyn in health and in disease conditions. Thus, the aims of this study were:

- A. To monitor and characterize the subcellular dynamics of aSyn between the nucleus and cytoplasm in living cells using photoactivation microscopy (Chapter III, section A).
  - I. By tracking the dynamics of aSyn-WT and PD-associated familial mutations, phosphorylated aSyn or aSyn in the presence of known interactors.
  
- B. To establish a cell model of aSyn oligomerization, based on bimolecular fluorescence complementation (BiFC), as readout for a lentiviral RNAi screen (Chapter III, section B).
  - I. Based on that, to identify genetic modulators of aSyn oligomerization and to further characterize them regarding aSyn subcellular localization, secretion and cytotoxicity;
  - II. To test the robustness of the identified genetic modulators on the context of aSyn aggregation, using a cell model of aSyn insoluble inclusions.



# III. Results

---

This chapter contains the total or parts of the following publications:

## A. Alpha-Synuclein Subcellular Dynamics in Living Cells

**3.1** Gonçalves, S. and T. F. Outeiro (2013). **Assessing the subcellular dynamics of alpha-Synuclein using photoactivation microscopy.** Mol Neurobiol 47(3): 1081-1092.

Basso, E., P. Antas, Z. Marijanovic, S. Gonçalves, S. Tenreiro and T. F. Outeiro (2013). **PLK2 modulates alpha-Synuclein aggregation in yeast and mammalian cells.** Mol Neurobiol 48(3): 854-862

## B. Insights into the mechanisms of alpha-Synuclein oligomerization and aggregation

**3.2** Chutna, O., S. Gonçalves, A. Villar-Pique, P. Guerreiro, Z. Marijanovic, T. Mendes, J. Ramalho, E. Emmanouilidou, S. Ventura, J. Klucken, D. C. Barral, F. Giorgini, K. Vekrellis and T. F. Outeiro (2014). **The small GTPase Rab11 co-localizes with alpha-Synuclein in intracellular inclusions and modulates its aggregation, secretion and toxicity.** Hum Mol Genet 23(25):6732-45.

**3.3** Gonçalves SA, Macedo D, Raquel H, Simões PD, Giorgini F, Ramalho JS, Barral DC, Ferreira Moita L and Outeiro TF (2016). **shRNA-Based screen identifies endocytic recycling pathway components that act as genetic modifiers of alpha-Synuclein aggregation, secretion and toxicity.** PLoS Genet. 28;12(4):e1005995.

**3.4** Nasstrom, T., Gonçalves S., C. Sahlin, E. Nordstrom, V. Screpanti Sundquist, L. Lannfelt, J. Bergstrom, T. F. Outeiro and M. Ingelsson (2011). **Antibodies against alpha-Synuclein reduce oligomerization in living cells.** PLoS One 6(10): e27230.



## Author Contributions

### A. Alpha-Synuclein Subcellular Dynamics in Living Cells

- 3.1.** Gonçalves, S. and T. F. Outeiro (2013). **Assessing the subcellular dynamics of alpha-Synuclein using photoactivation microscopy.** Mol Neurobiol 47(3): 1081-1092.

The author performed the experiments, analyzed the data and wrote the paper.

- Basso, E., P. Antas, Z. Marijanovic, S. Gonçalves, S. Tenreiro and T. F. Outeiro (2013). **PLK2 modulates alpha-Synuclein aggregation in yeast and mammalian cells.** Mol Neurobiol 48(3): 854-862

The author performed all the experiments and data analysis presented on figure 2 of the published paper, herein shown in Annex 5.1.6.

### B. Insights into the mechanisms of alpha-Synuclein oligomerization and aggregation

- 3.2** Chutna, O., S. Gonçalves, A. Villar-Pique, P. Guerreiro, Z. Marijanovic, T. Mendes, J. Ramalho, E. Emmanouilidou, S. Ventura, J. Klucken, D. C. Barral, F. Giorgini, K. Vekrellis and T. F. Outeiro (2014). **The small GTPase Rab11 co-localizes with alpha-Synuclein in intracellular inclusions and modulates its aggregation, secretion and toxicity.** Hum Mol Genet 23(25):6732-45.

The author performed the experiments and data analysis presented on figures 20 and 22 and reviewed the manuscript.

- 3.3** Gonçalves SA, Macedo D, Raquel H, Simões PD, Giorgini F, Ramalho JS, Barral DC, Ferreira Moita L and Outeiro TF (2016). **shRNA-Based screen identifies endocytic recycling pathway components that act as genetic modifiers of alpha-Synuclein aggregation, secretion and toxicity.** PLoS Genet. 28;12(4):e1005995.

The author performed the experiments, analyzed the data and wrote the paper.

**3.4** Nasstrom, T., Gonçalves S., C. Sahlin, E. Nordstrom, V. Screpanti Sundquist, L. Lannfelt, J. Bergstrom, T. F. Outeiro and M. Ingelsson (2011). **Antibodies against alpha-Synuclein reduce oligomerization in living cells**. PLoS One 6(10): e27230.

The author helped to analyse the data concerning the cell culture experiments on figures 30, 31, 32 and 33 and reviewed the manuscript.

## **A. Alpha-Synuclein Subcellular Dynamics in Living Cells**

### **3.1. Assessing the Subcellular Dynamics of Alpha-Synuclein using Photoactivation Microscopy**

#### **Abstract**

Alpha-Synuclein (aSyn) is implicated in Parkinson's disease and several other neurodegenerative disorders. To date, the function and intracellular dynamics of aSyn are still unclear. Here, we tracked the dynamics of aSyn using photoactivatable green fluorescent protein as a reporter. We found that the availability of the aSyn N-terminus modulates its shuttling into the nucleus. Interestingly, familial aSyn mutations altered the dynamics at which the protein distributes throughout the cell. Both the A30P and A53T aSyn mutations increase the speed at which the protein moves between the nucleus and cytoplasm, respectively. We also found that specific kinases potentiate the shuttling of aSyn between nucleus and cytoplasm. A mutant aSyn form that blocks S129 phosphorylation, S129A, results in the formation of cytoplasmic inclusions, suggesting that phosphorylation modulates aggregation in addition to modulating aSyn intracellular dynamics. Finally, we found that the molecular chaperone HSP70 accelerates the entry of aSyn into the nuclear compartment.

#### **Introduction**

Misfolded and aggregated alpha-Synuclein (aSyn) is the major component of intraneuronal inclusions known as Lewy bodies (LBs), the pathological hallmark of Parkinson's disease (PD) and other Synucleinopathies (Spillantini et al 1997). Despite the growing knowledge on aSyn, the normal function of the protein remains largely unclear. However, it is thought to play a role in synaptic function and plasticity, cell differentiation and vesicular trafficking (Crews et al 2008, Schneider et al 2007). The subcellular distribution of aSyn is also controversial and, although it is considered a pre-synaptic protein, it has also been found to be evenly distributed throughout the cells in different

cellular models and in mice (Goers et al 2003, Klucken et al 2006, Smith et al 2010, Unni et al 2010, Vivacqua et al 2011).

Although the majority of PD cases are idiopathic, three missense mutations in aSyn gene (A30P, E46K and A53T), restrained in the N-terminal domain, have been identified in rare, autosomal-dominant inherited forms of PD, as well as duplications and triplications of the aSyn-containing locus (Kruger et al 1998, Polymeropoulos et al 1997, Singleton et al 2003, Zarranz et al 2004). *In vitro* studies revealed that the A30P mutation blocks the membrane association and inhibits the synaptic localization of aSyn by destabilizing its first helical structure (Smith et al 2010, Ulmer & Bax 2005). Conversely, A53T and E46K mutations enhance the binding to phospholipids (Bodner et al 2010).

In the normal brain, 4% of aSyn is phosphorylated at serine 129 (S129), contrasting with 90% of aSyn that is found to be phosphorylated in LBs. This suggests that S129 phosphorylation might interfere with the oligomerization and aggregation process and contribute to the pathogenesis of PD (Anderson et al 2006, Fujiwara et al 2002). Among others, G protein-coupled receptor kinases (GRKs) and Polo-like kinases (PLKs) were found to phosphorylate the S129 residue of aSyn (Inglis et al 2009, Pronin et al 2000). Although it was proposed that S129 phosphorylation inhibits aSyn-induced regulation of tyrosine hydroxylase activity (Lou et al 2010), the exact role of this PTM in both physiological and pathological conditions remains unclear.

Other known modifiers of aSyn aggregation are molecular chaperones, such as HSP70, which modulates the misfolding, aggregation and toxicity of aSyn in different model systems (Auluck et al 2002, Dedmon et al 2005, Flower et al 2005, Klucken et al 2006, Klucken et al 2004). However, the mechanisms by which HSP70 suppresses aSyn toxicity are still unclear.

The new era of time-lapse bioimaging tools combined with GFP-derived fluorescent labels enables the characterization of protein kinetics in real time, providing invaluable insights into the molecular processes in which they are involved. Photoactivation (PA) microscopy is an emerging technique in the field of neuroscience (Roy et al 2012) in which a non-fluorescent molecule is converted into an activated and fluorescent state by the use of an intense and brief irradiation in a selected region of the cell. This process enables the direct tracking of a protein by photo-inducing fluorescence, instead of interfering with a steady state fluorescent signal, as photobleaching (PB) methods do. The newly activated



pool, obtained through the use of an ultraviolet laser, contrasts with a background of non-activated molecules, and can be followed within the cells as they reach their kinetics equilibrium (Lippincott-Schwartz et al 2003, Patterson & Lippincott-Schwartz 2002) (Figure 10A).

In order to further understand the biology of aSyn, we investigated the dynamics of aSyn between the nucleus and cytoplasm in living cells using PA microscopy (Figure 10B). We found that the N-terminal of aSyn wild-type (WT) determines its entry into the nuclear compartment. Moreover, aSyn shuttles between the nucleus and cytoplasm at rates which depend on mutations, phosphorylation state and on the presence of HSP70. Altogether, our novel approach provides novel insights into the biology of aSyn in living cells and may enable the development of novel strategies for therapeutic intervention in Synucleinopathies.

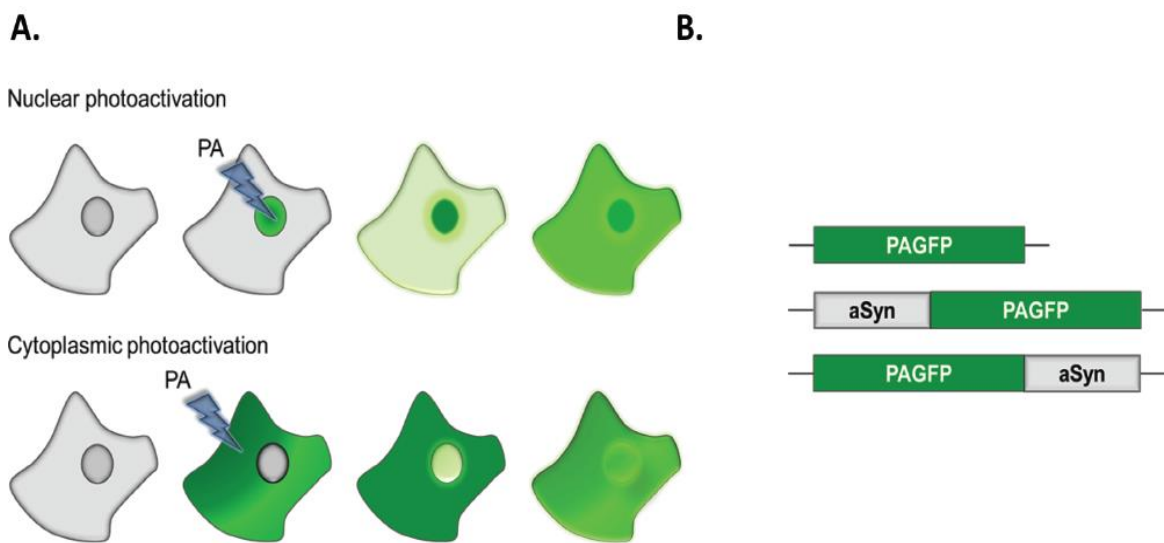


**Figure 10. Strategy for nuclear and cytoplasmic photoactivation of PAGFP-labeled proteins. A.** PAGFP displays negligible fluorescence in the spectral range where the activated fluorescence is detected. Upon photoactivation (PA) of a selected nuclear or cytoplasmic region with a 405 laser, PAGFP-labeled proteins become visible and the dynamics and fate of the activated molecules can be followed over time. **B.** PAGFP constructs used in this study. We used WT-, A30P-, E46K-, A53T- and S129A-aSyn variants.

## Results

### Blocking the N-terminal of aSyn modulates nuclear localization

To assess whether the subcellular localization of aSyn-WT is affected by appending different tags to either the N- or C-terminus, we performed immunocytochemistry analysis in cells expressing either untagged aSyn-WT or GFP-, Myc- or V5-tagged versions. Both tagged and non-tagged aSyn-WT were widely distributed throughout the cell, including the nucleus (Figure 11A-D). To further investigate the intracellular dynamics of aSyn-WT, we generated fusions with a photoactivatable green fluorescent protein (PAGFP) in order to follow the movement of a specific pool of aSyn over time at the N- or C-termini (aSyn-WT-PAGFP and PAGFP-aSyn-WT, respectively). H4 cells were transiently transfected with plasmids encoding aSyn-WT-PAGFP, PAGFP-aSyn-WT or PAGFP alone, as a control. As aSyn is widely distributed in the cell, we characterized the shuttling of aSyn between the nucleus and the cytoplasm. Reporter proteins were photoactivated in the nucleus or cytoplasm for 2 seconds (s) using a 405-nm laser, their cellular trafficking was monitored and the fluorescence intensities quantified. After PA, the PAGFP control was quickly detected in the cytoplasm or in the nucleus after nuclear or cytoplasmic PA, respectively, reaching equilibrium of PAGFP molecules between the two cellular compartments after 500 s. In contrast, we observed different trafficking behaviours for aSyn-WT-PAGFP and PAGFP-aSyn-WT (Figure 11E and Annex 5.1.1A; Videos S1, S2, S3, S4, S5 and S6, available online following doi: [10.1007/s12035-013-8406-x](https://doi.org/10.1007/s12035-013-8406-x)). WT-aSyn-PAGFP displayed different dynamics depending on the region where PA was performed. Upon cytoplasmic PA, aSyn-WT-PAGFP molecules entered into the nucleus and after 1,000 s were evenly distributed between the two subcellular compartments. Conversely, upon nuclear PA, aSyn-WT-PAGFP was maintained in this compartment for the remainder of the time analysed (1,000 s). In contrast with the behaviour observed for photoactivated aSyn-WT-PAGFP, PAGFP-aSyn-WT was not detected in the contiguous compartment to where the PA was performed and remained in the same subcellular region (Figure 11E and Annex 5.1.1A). Immunoblotting analysis of nuclear and cytoplasmic extracts from cells expressing either protein confirmed the predominant localization observed with microscopy (Annex 5.1.2A). To further validate the observations obtained using PA, we performed fluorescence recovery after PB (FRAP) experiments in H4 cells expressing aSyn-

WT-GFP, GFP-aSyn-WT or GFP alone. Upon PB of aSyn-WT-GFP in the nucleus, we found that the recovery of fluorescence in this compartment occurred after 500 s, while fluorescence was not significantly recovered in the cytoplasm after PB in this region. For GFP-aSyn-WT, PB in nucleus slightly recovered fluorescence of the reporter protein after 1,000 s (about 20% of recovery) while no cytoplasmic recovery was observed upon PB in this region (Figure 11F; Videos S7, S8, S9, S10, S11 and S12, available online following doi: [10.1007/s12035-013-8406-x](https://doi.org/10.1007/s12035-013-8406-x)).

Altogether, our novel PA and FRAP experiments show, for the first time, that the movement of aSyn between the nucleus and the cytoplasm depends on the availability of the N terminus of the protein.

### **PD-associated mutations alter the subcellular trafficking of aSyn**

Since we established a model to study aSyn intracellular dynamics, we next investigated whether PD familial mutations (A30P, E46K and A53T) in aSyn affected its trafficking in the cell (Figure 12). In comparison to the aSyn-WT-PAGFP, cytoplasmic aSyn-A30P- and aSyn-E46K-PAGFP are shuttled into the nucleus in half of the time (500 s) of the WT protein (at time points 500 s and 1,000 s after PA,  $p$  values between 0.0044 and  $<0.0001$ , respectively,  $\alpha=0.05$ ; Annex 5.1.3A). Because of this rapid movement into the nucleus, the fluorescence intensities in the cytoplasm and nucleus equalized earlier than in the control situation and remained in equilibrium for several minutes. In contrast to A30P and E46K mutants, aSyn-A53T-PAGFP remained in the compartment where the PA was performed, similarly to the WT protein.

In the fusions where PAGFP was on the N-terminus of aSyn, the behavior of A30P was similar to that of aSyn-WT. Additionally, upon cytoplasmic PA, there was a slight increase in molecules that remained on the nucleus ( $p$  value = 0.0185 at 1,000 s after nuclear or cytoplasmic PA,  $\alpha=0.05$ , Annex 5.1.3A and Figure 12A). In contrast, PAGFP-aSyn-E46K was translocated from the nucleus to the cytoplasm after nuclear PA ( $p$  value = 0.001 at 1,000 s after nuclear PA,  $\alpha=0.05$ , Annex 5.1.3A). The same occurred with PAGFP-aSyn-A53T, although at a more pronounced rate, since the fluorescence intensity was higher in the cytoplasm than in the nucleus, starting at 700 s after PA ( $p$  value = 0.0013 at 1,000 s after PA,  $\alpha=0.05$ , Annex 5.1.3A and Figure 12A). In order to investigate if the dynamics results were influenced by differences in the levels of WT and mutant aSyn, we performed

immunoblotting analysis. We verified that the levels of total aSyn did not differ between the WT and mutant forms of the protein (Figure 12B).

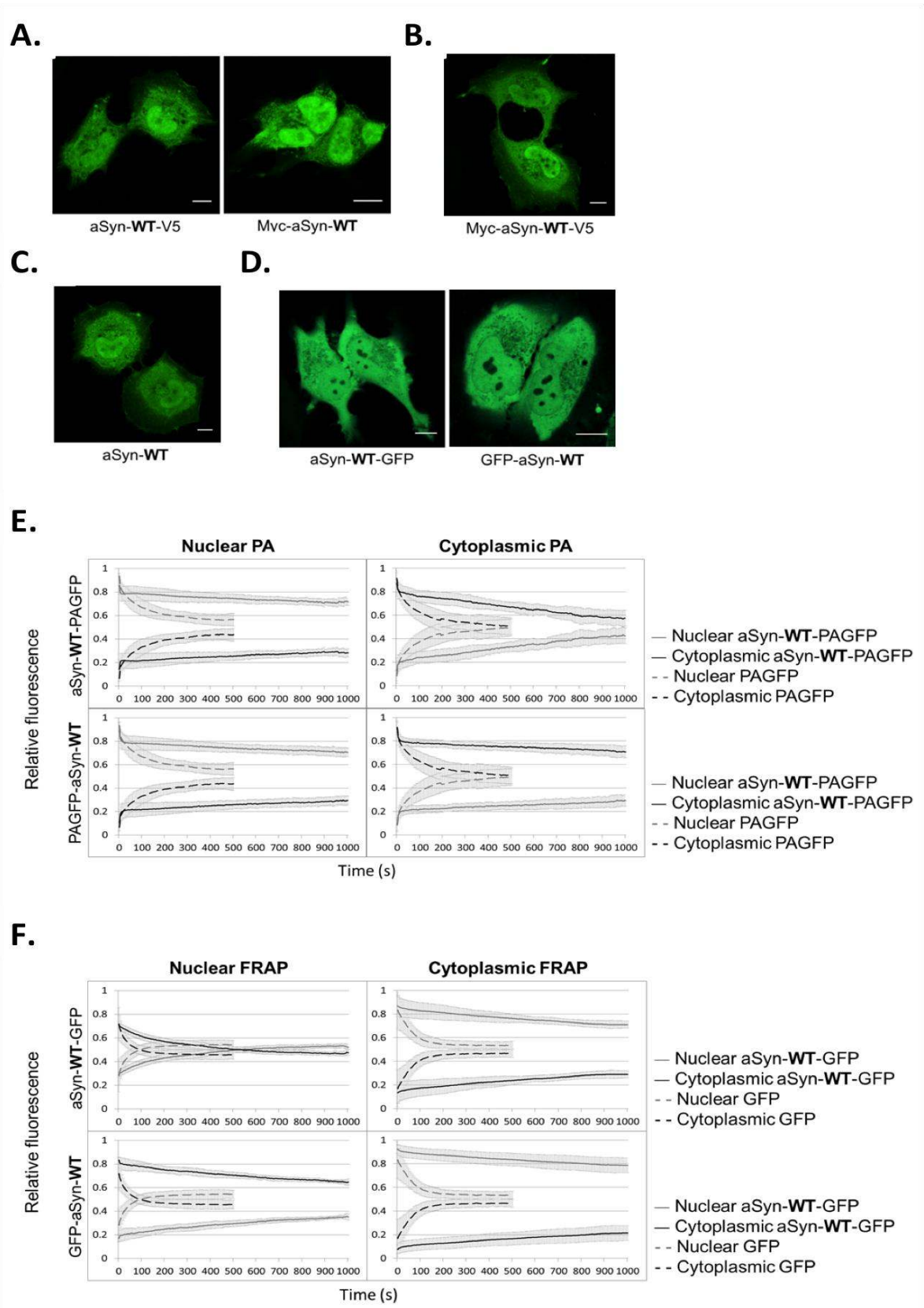


**Figure 11. Blocking the N-terminus of aSyn reduces its shuttling into the nucleus.** Immunofluorescence imaging of H4 cells showing the subcellular localization of transiently transfected aSyn (**A.**) N- and C-terminally tagged to Myc and V5, respectively, (**B.**) tagged on both terminals with Myc (N-terminal) and V5 (C-terminal) and (**C.**) untagged aSyn-WT. **D.** Live cell imaging of aSyn N- and C-terminally tagged to GFP. **E.** Measurements of fluorescence intensities over time in the nucleus (light grey line) and in the cytoplasm (dark grey line) of control PAGFP (dashed line) or fusion proteins of aSyn-WT with PAGFP (solid line). Values represent mean  $\pm$  standard deviation of up to 15 cells analyzed per condition. **F.** Measurements of fluorescence recovery after photobleaching over time in the nucleus (light grey line) and in the cytoplasm (dark grey line) of control GFP (dashed line) or fusion proteins of aSyn-WT with GFP (solid line). Scale bars: 10  $\mu$ m.

As expected, subcellular fractionation followed by immunoblotting analysis confirmed the presence of the protein in both cytoplasmic and nuclear compartments (Annex 5.1.2B). Altogether, these experiments show that A30P and E46K, but not the A53T mutation, promoted a faster shuttling of aSyn with a free N-terminus into the nucleus when compared to aSyn-WT. On the other hand, aSyn-A53T and aSyn-E46K with a free C-terminus, but not aSyn-A30P, were delayed in the cytoplasm.

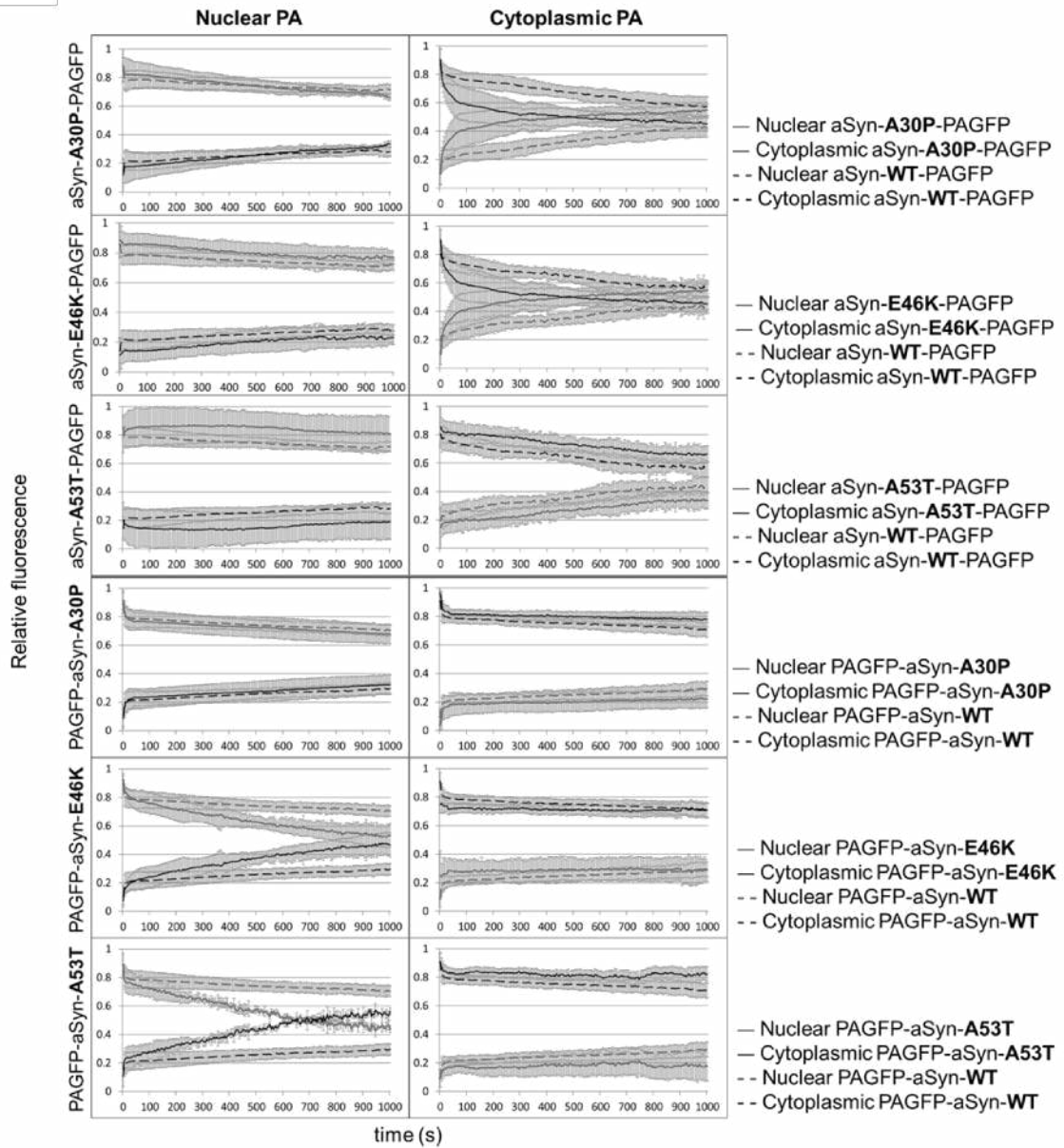
### **aSyn phosphorylation by GRK5 or PLK2 modulates its subcellular trafficking**

In order to assess the role of S129 aSyn phosphorylation on the intracellular dynamics of the protein, we co-expressed GRK2, GRK5, PLK2 or PLK3 kinases with aSyn-WT tagged with PAGFP on either its N- or C-terminal. The kinases tested did not significantly alter the dynamics of aSyn-WT-PAGFP. For aSyn-WT-PAGFP, co-expression with PLK2 did not alter the dynamics obtained in the absence of the kinase, but resulted in a more rapid progression towards the equilibrium fluorescence. The other kinases tested, GRK2, GRK5 and PLK3, did not induce significant differences (Annexes 5.1.3B and 5.1.4).

In contrast, stronger effects were observed for PAGFP-aSyn-WT. Overexpression of GRK2 did not affect the shuttling of aSyn-WT constructs between the nucleus and the cytoplasm as the values of fluorescence intensity were similar in the presence or absence of the kinase during the 1,000 s of imaging. Interestingly, GRK5 promoted the trafficking of PAGFP-aSyn-WT into the nucleus upon cytoplasmic PA, although the difference did not

reach statistical significance. Nuclear PA in cells overexpressing GRK5 did not significantly alter the dynamics of PAGFP-aSyn-WT (Figure 13A; Annex 5.1.3B).

**A.**



**B.**

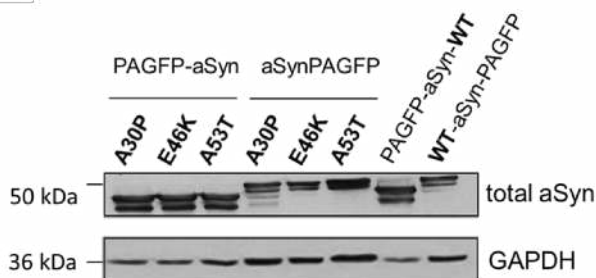


**Figure 12. Effect of aSyn mutations on its subcellular trafficking in living cells. A.** Fluorescence intensities after photoactivation in the nucleus (light grey line) and in the cytoplasm (dark grey line) of aSyn-A30P-, aSyn-E46K- and aSyn-A53T PAGFP-tagged proteins (solid line) over time. Fluorescence intensities of photoactivated control aSyn-WT PAGFP fusion proteins are shown in dashed line. Values represent mean  $\pm$  standard deviation of up to 15 cells analyzed per condition. **B.** Immunoblotting analysis of total aSyn levels in cells expressing WT- and mutant- aSyn reporter proteins.

Co-expression of PAGFP-aSyn-WT with PLK2 promoted its shuttling to the cytoplasm upon nuclear PA (similar nuclear and cytoplasmic fluorescence levels were reached 500 s after PA,  $p$  value=0.0141,  $\alpha$ =0.05, Annex 5.1.3B and Figure 13A). Upon cytoplasmic PA, PLK2 slightly accelerated the movement into the nucleus 500 s after PA (Annex 5.1.3B).

Co-expression of PAGFP-aSyn-WT with PLK3 promoted its shuttling to the cytoplasm upon nuclear PA but this movement was faster in the presence of PLK2. Although the difference was already significant 500 s after PA ( $p$  value=0.0198,  $\alpha$ =0.05, Annex 5.1.3B), at 1,000 s the levels of fluorescence were still higher in the nucleus than in the cytoplasm. Upon cytoplasmic PA, the presence of PLK3 did not alter the dynamics of PAGFP-aSyn-WT (Figure 13A; Annex 5.1.3B). We performed immunoblotting analysis to investigate if the results on the dynamics of aSyn were influenced by differences in expression in the presence and absence of the kinases tested. We verified that the levels of total aSyn were not altered in the presence of the kinases (Figure 13B). As expected, we also confirmed that the levels of aSyn phosphorylated at S129 were increased in the presence of both kinases (Annex 5.1.2C).

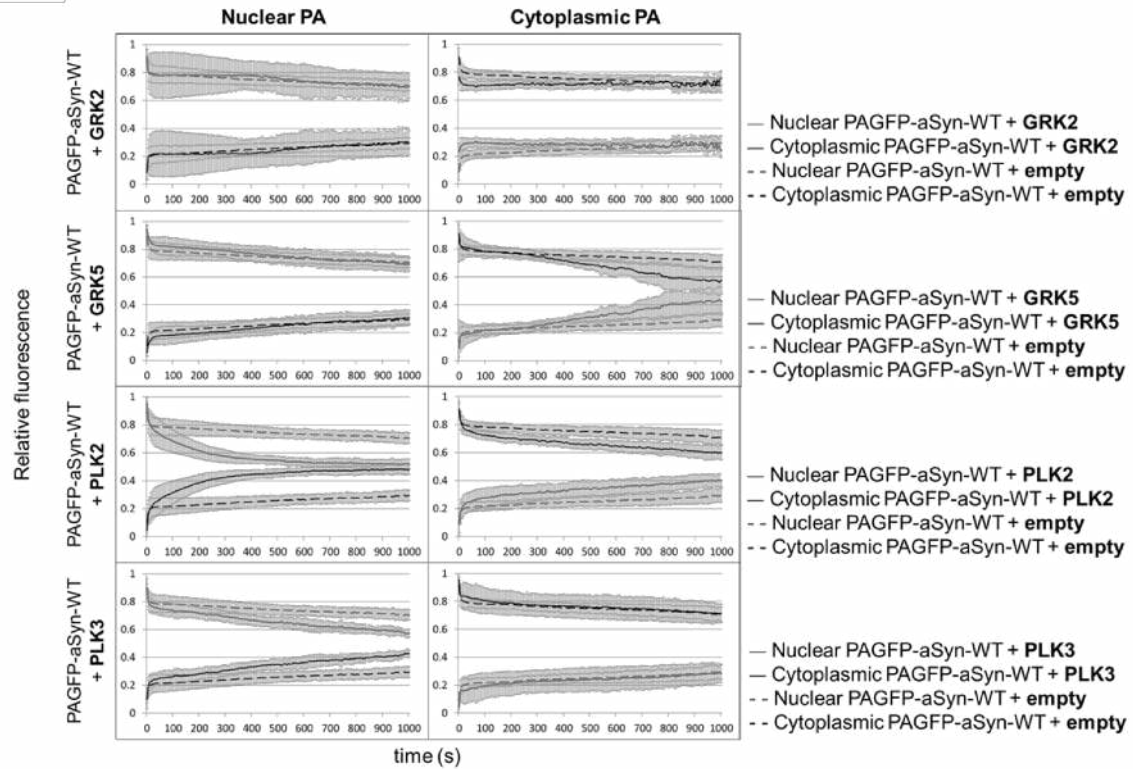
An important difference between GRK5 and PLKs was that the former induced a tendency of aSyn to traffic from the cytoplasm to the nucleus and the later had a strong effect in promoting the trafficking of aSyn from the nucleus to the cytoplasm.

Next, we tested the dynamics of S129A-aSyn, a phosphorylation-incompetent mutant, in order to further assess the effect of S129 phosphorylation in the trafficking of aSyn. No differences were observed on the dynamics of aSyn-S129A-PAGFP except for the existence of more photoactivated protein in the nucleus when compared to aSyn-WT immediately after nuclear PA (Annex 5.1.3A and 5.1.4D). However, PAGFP-aSyn-S129A

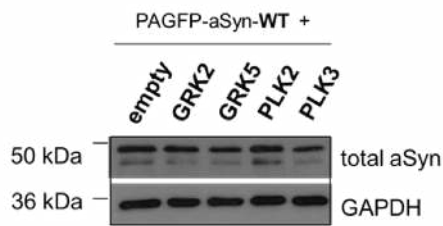


moved into the cytoplasm after 1,000 s of PA if PA was performed in the nucleus while the aSyn-WT did not. Moreover, PAGFP-aSyn-S129A remained in the cytoplasm if PA was performed in that compartment ( $p$  value = 0.0099,  $\alpha=0.05$ , Annex 5.1.3A and Figure 13C).

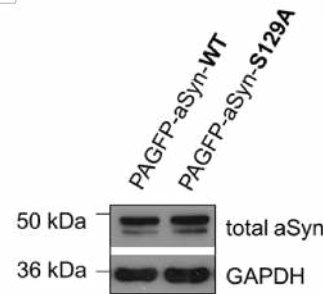
**A.**



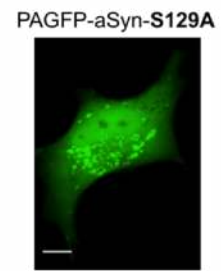
**B.**



**D.**



**E.**



**C.**

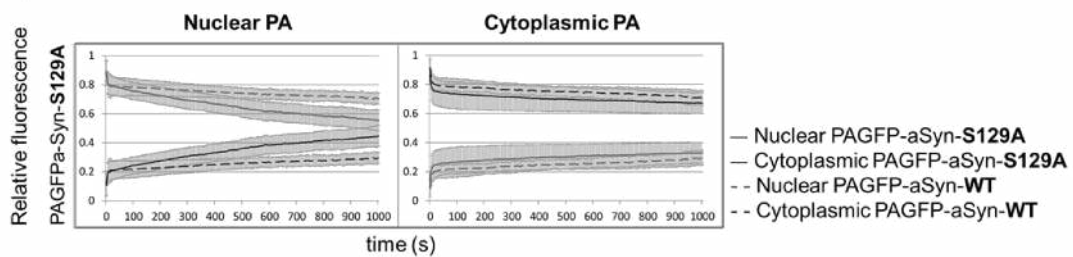




**Figure 13. Effect of S129 phosphorylation on the subcellular dynamics of aSyn.** **A.** Fluorescence intensities after photoactivation in the nucleus (light grey line) and in the cytoplasm (dark grey line) of PAGFP-aSyn-WT fusion protein co-expressed with GRK2, GRK5, PLK2 and PLK3 (solid line) or an empty vector (dashed lines) over time. Values represent mean  $\pm$  standard deviation of up to 15 cells analyzed per condition. **B.** Immunoblotting analysis of total aSyn levels in cells co-expressing aSyn-WT reporter proteins with the four tested kinases. **C.** Fluorescence intensities after photoactivation in the nucleus (light grey line) and in the cytoplasm (dark grey line) of PAGFP-aSyn-S129A fusion protein over time. Fluorescence intensities of photoactivated control (PAGFP-aSyn-WT) are shown in dashed lines. Values represent mean  $\pm$  standard deviation of up to 15 cells analyzed per condition. **D.** Immunoblotting analysis of total aSyn levels in cells expressing PAGFP-aSyn-WT or PAGFP-aSyn-S129A. **E.** Cytosolic inclusions in cells expressing PAGFP-aSyn-S129A. Images were taken 500 seconds after photoactivation in the nucleus in order to detect the cytosolic inclusions. Scale bar: 10  $\mu$ m.

These findings were in agreement with the fact that both aSyn-S129A fusion proteins were only marginally detected in the nuclear protein fraction, in contrast to aSyn-WT (Annexes 5.1.2A, 5.1.2D and 5.1.4E), although the total protein levels of aSyn-WT and aSyn-S129A were comparable (Figure 13D and Annex 5.1.4F).

Interestingly, we found that expression of either the N- or C-terminal S129A fusion proteins promoted the formation of cytosolic inclusions scattered around the nucleus (Figure 13E and Annex 5.1.4G).

### **HSP70 modifies the trafficking of aSyn**

HSP70 modulates the accumulation of oligomeric and aggregated forms of aSyn in different model systems. Thus, we next asked whether HSP70 could interfere with the subcellular dynamics of aSyn. HSP70 did not change the intracellular dynamics of aSyn-WT-PAGFP (Annex 5.1.3B and Figure 14A). Conversely, upon cytoplasmic PA, PAGFP-aSyn-WT was shuttled into the nucleus in the presence of HSP70 within 100 s after PA ( $p$  value  $< 0.0001$ ,  $\alpha=0.05$ , Annexes 5.1.1B, 5.1.3B and Figure 14A). Although the total levels of the protein were not altered in the presence of the chaperone (Figure 14B), the levels of aSyn were higher in the nucleus for both fusion proteins in this situation. Interestingly, HSP70 was present in the nuclear fraction only when aSyn was present (Annex 5.1.2E). Upon nuclear PA, the tendency was for the protein to move into the cytoplasm, but not as

quickly as in the former situation ( $p$  value at 100 s = 0.7836,  $p$  value at 1,000 s = 0.0014,  $\alpha=0.05$ , Annexes 5.1.1B, 5.1.3B and Figure 14A).

In summary, HSP70 increased the shuttling of PAGFP-aSyn-WT between the nucleus and cytoplasm.

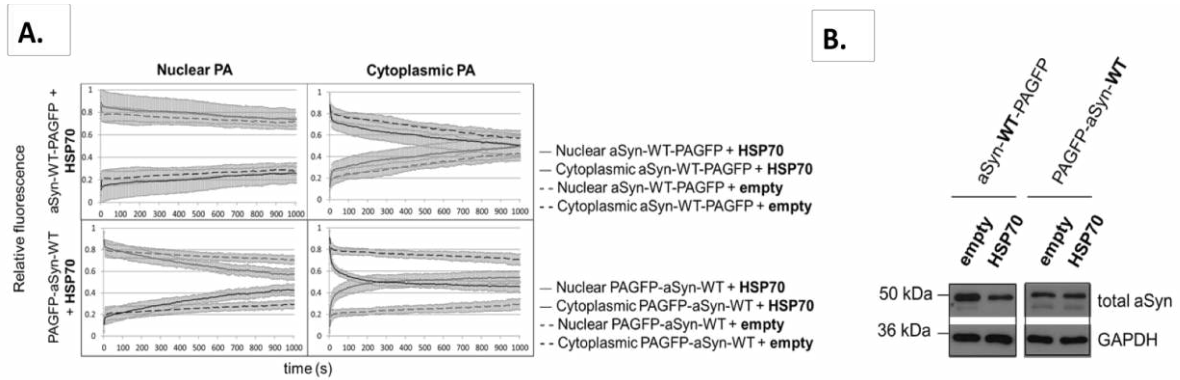


**Figure 14. Modulation of the dynamics of aSyn by HSP70.** **A.** Fluorescence intensities after photoactivation in the nucleus (light grey) and in the cytoplasm (dark grey) of aSyn-WT PAGFP fusion proteins co-expressed with HSP70 (solid line) over time. Fluorescence intensities of photoactivated control aSyn-WT reporters after co-transfection with an empty vector are shown in dashed lined. Values are mean  $\pm$  standard deviation of up to 15 cells analyzed per condition. **B.** Immunoblotting analysis of total aSyn levels in cells co-expressing aSyn with HSP70 or with an empty vector. Scale bar: 10  $\mu$ m.

## Discussion

Here, we investigated the intracellular dynamics of aSyn in living cells using photoactivatable GFP as a reporter. To control for putative effects of tagging aSyn in particular domains, we engineered fusions with PAGFP on either the N- or C-terminal of aSyn. We found that, although both aSyn fusion proteins were evenly spread throughout the cell, aSyn required a free N-terminus in order to move from the cytoplasm into the nucleus.

aSyn is evenly distributed throughout the cell in different *in vitro* models and in mice (Goers et al 2003, Klucken et al 2006, Smith et al 2010, Unni et al 2010, Vivacqua et al 2011). The N-terminus of aSyn seems to be important for membrane binding in various

model organisms, ranging from yeast to rats (Bodner et al 2010, Specht et al 2005, Vamvaca et al 2009, Yang et al 2010). Although the role of aSyn in the nucleus has not been defined, it is described to interact with histones, inhibiting acetylation and enhancing chromatin binding, and promoting neurotoxicity in cellular models, in mouse nigral neurons and in *Drosophila* (Goers et al 2003, Kontopoulos et al 2006, Siddiqui et al 2012).

We also investigated whether aSyn mutations, associated with familial forms of PD, altered the shuttling of aSyn between the nucleus and cytoplasm. We found that a) the A30P mutant is more prone to be located in the nucleus than the aSyn-WT; b) the E46K mutant loses the subcellular compartmentalization characteristic of the WT form; and c) the A53T mutation is more prone to be located in the cytoplasm than aSyn-WT.

Until recently, aSyn was thought to be an intrinsically unfolded protein (Bartels et al 2011, Wang et al 2011, Weinreb et al 1996). Nevertheless, it acquires two alpha-helical structures upon interaction with vesicles, contained in the residues 1-42 and from 45-98 (Chandra et al 2003, Perrin et al 2000, Ulmer et al 2005, Zhu & Fink 2003). *In vitro* studies showed that A30P disrupts membrane binding (Smith et al 2010, Ulmer & Bax 2005), perhaps being more available to shuttle into the nucleus. Thus, it is likely that the differences in dynamics between the aSyn familial forms are related with the location and effect of the mutation on the secondary structure of aSyn protein. In addition, aSyn seems to regulate actin bundling inside the cell, and the A30P mutant affects the structure and dynamics of the actin cytoskeleton, potentiating the formation of actin foci (Sousa et al 2009). Our results are also consistent with data showing that the A30P increases the nuclear localization of the protein (Kontopoulos et al 2006). A53T is described to promote the formation of cytosolic aggregates (Lashuel et al 2002, Smith et al 2010), which is compatible with its tendency to be localized in the cytoplasm when compared to aSyn-WT.

PTMs are known to modulate the intracellular fate of proteins, including their sub-cellular distribution. aSyn is thought to have several residues prone to phosphorylation: Y39, S87, Y125, S129, Y133 and Y136. S129 phosphorylation is the most studied, and little information exists on the kinases phosphorylating the other residues (Hejjaoui et al 2012, Oueslati et al 2012, Mahul-Mellier et al 2014). In LBs, the majority of aSyn is thought to be phosphorylated on S129, contrasting with almost no phosphorylation of this residue in

normal brain. However, the role of this PTM is still unclear and controversial. Phosphorylation of aSyn by GRKs inhibits its interaction with phospholipids (Okochi et al 2000). In *Drosophila*, co-expression of GRK2 with aSyn leads to S129 phosphorylation and enhanced aSyn neurotoxicity (Chen & Feany 2005). Moreover, the levels of specific PLKs are increased in brains of patients with Alzheimer's or LB disease (Mbefo et al 2010).

Here, we investigated whether a selected group of kinases, GRK2, GRK5, PLK2 and PLK3, modulated the dynamics of aSyn distribution in the cell. The kinases tested only affected the dynamics of aSyn with a free C-terminus, although both fusion proteins were phosphorylated in S129. This can be due to the fact that when the C-terminal of aSyn is free, the protein is more prone to phosphorylation at S129, resulting in a stronger effect in its intracellular dynamics. Overall, aSyn phosphorylation by GRKs or PLKs results in different dynamics of the protein. While GRK5 potentiates the nuclear localization of aSyn, PLKs modulate the shuttling of the protein between the nucleus and cytoplasm. In particular, PLK2 modulates the intracellular dynamics of PAGFP-aSyn-WT by increasing the movement from the nucleus to the cytoplasm at a higher rate than PLK3. These results are consistent with the fact PLK2 promotes aSyn inclusions in the same cell line (Annex 5.1.6) (Basso et al 2013). Since aSyn has more residues prone to phosphorylation, the different results obtained with GRK5 and PLKs might reflect different phosphorylation patterns in residues other than S129. Due to the limited availability of antibodies these studies are still not easy to perform but as novel tools become available one might be able to discriminate between the effects of phosphorylation in different residues.

Interestingly, we also observed that nuclear PAGFP-aSyn-S129A tends to move to the cytoplasm while cytoplasmic PAGFP-aSyn-S129A remains in this subcellular compartment. This tendency might at least partially explain the cytoplasmic inclusions detected in the cells expressing this mutant aSyn and suggest that the phosphorylation status on S129 is crucial for aggregation, in agreement with recent findings in yeast, in which S129A mutant potentiates the formation of aSyn foci (Fiske et al 2011).

GRKs and PLKs modulate the dynamics of aSyn in different ways and we did not find a consistent pattern that can explain the role of S129 phosphorylation on the distribution of aSyn. One possibility is that the effects of the kinases are also due to phosphorylation of other targets in addition to aSyn. Nevertheless, we verified that the phosphorylation status of aSyn on S129 was related with the aggregation state of the protein.

Molecular chaperones, such as HSP70, hold great potential as therapeutic targets due to their ability to reverse protein aggregation and to refold or promote degradation of misfolded proteins (Witt 2010). HSP70 was shown to inhibit formation of toxic pre-fibrillar forms of aSyn (Dedmon et al 2005) and to reduce its aggregation in aSyn transgenic mice (Klucken et al 2004). In flies, it was shown that co-expression of HSP70 with aSyn-WT suppresses the loss of dopaminergic neurons, and hence, the toxicity associated with aSyn-WT overexpression (Auluck et al 2002). A similar effect was observed in yeast and in mammalian cell models, suggesting that HSP70 inhibits aSyn toxicity by binding to the exposed hydrophobic NAC domain (non-a $\beta$  component of AD plaques; residues 61-95 of aSyn) and sequestering the protein (Flower et al 2005, Lee et al 2004b, Murray et al 2003, Zhou et al 2004b).

Here, we found that HSP70 boosted the shuttling of PAGFP-aSyn-WT to the adjacent compartment, suggesting it may assist aSyn to adopt a conformation that is more likely to cross the nuclear envelope. The selective effect with PAGFP-aSyn-WT and not with aSyn-WT-PAGFP suggests the interaction might take place through the C-terminus of aSyn, which is not blocked by PAGFP in this fusion protein.

In conclusion, we showed that PD-associated mutations in aSyn, S129 phosphorylation, and HSP70 exert different effects on aSyn trafficking within the cell (Annex 5.1.5; Figure 15). While additional studies will be important to clarify the relative contribution of each condition, our goal was to demonstrate the usefulness of PA microscopy for the study of aSyn dynamics in living cells, which is not possible to achieve with other types of approaches or with untagged protein.

Our data provide novel insights into the subcellular dynamics of aSyn by taking advantage of a powerful method for monitoring protein dynamics in living cells. A complete understanding of aSyn localization, intracellular dynamics and protein-protein interactions will be crucial for understanding the normal function of aSyn and may enable the development of novel strategies for intervention in PD and other Synucleinopathies.

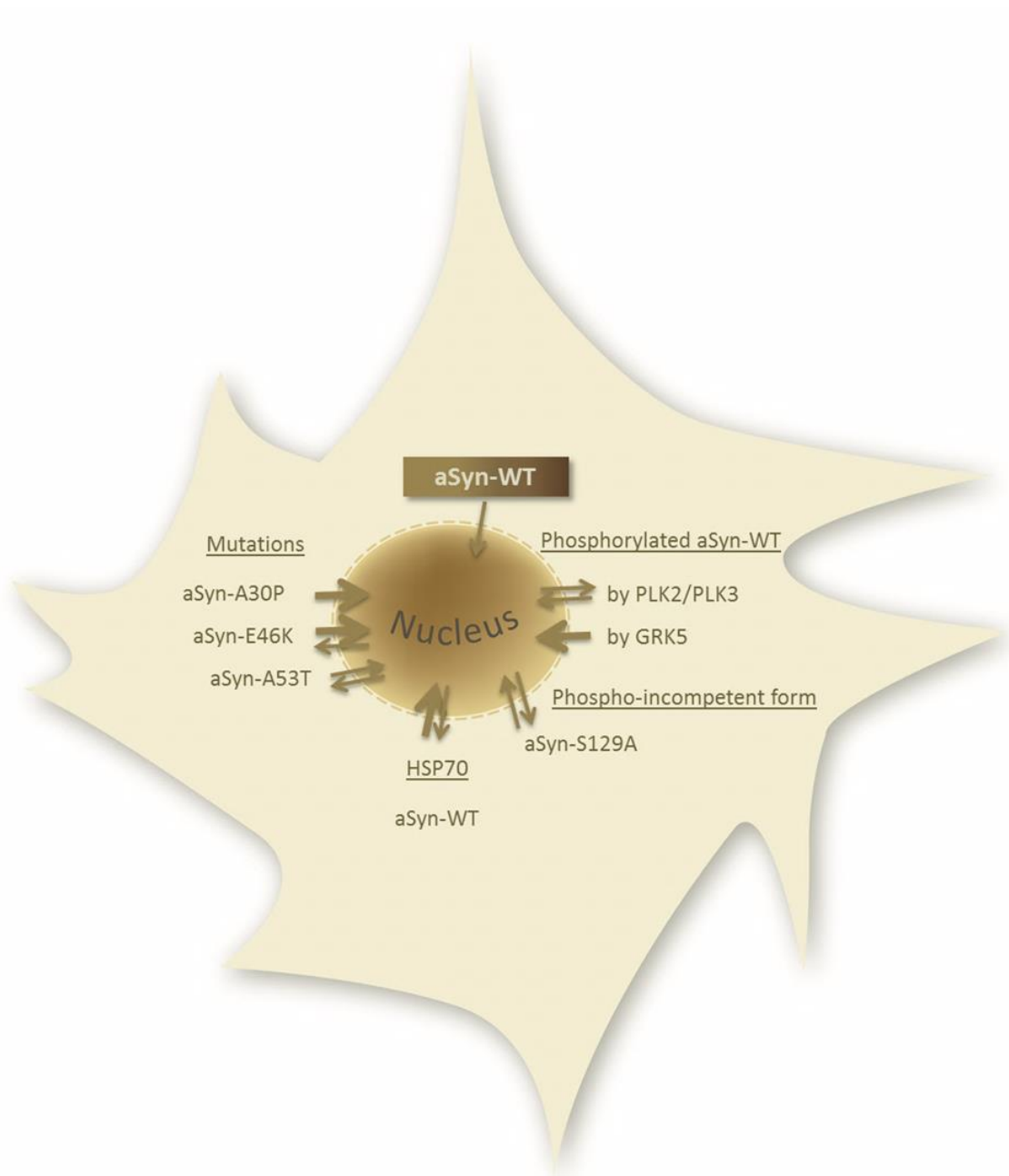


**Figure 15. Modifiers of aSyn intracellular dynamics.** aSyn-WT shuttles into the nucleus. This is enhanced (thicker arrow) by the presence of A30P mutation or GRK5 kinase, via phosphorylation of S129. The mutants A53T and S129A, or overexpression of PLK2 and PLK3 kinases, promote the bidirectional shuttling between the nuclear and the cytoplasmic compartments. E46K mutation and HSP70 chaperone instigate similar dynamics; however, they promote a faster shuttling into the nucleus (thicker arrow).

## Materials and Methods

### Plasmids and cloning procedures

aSyn-WT-PAGFP and PAGFP-aSyn-WT constructs were generated using aSyn-GC and GN-link-aSyn pcDNA3.1 vectors (Outeiro et al 2008), respectively, and verified by DNA sequencing.

In order to obtain PAGFP-aSyn-WT construct, PAGFP in C1 vector was amplified by PCR with primers 5'TAAGCTAGCATGGTGAGCAAGGGCGAGG3' (which contains a *NheI* restriction site) and 5'GGACTTAAGCTTGTACAGCTCGTCCATGCC3' (which contains a *AflIII* restriction site and eliminates the stop codon from PAGFP). PAGFP PCR product and GN-link-aSyn were digested with *NheI* and *AflIII* and ligated using T4 DNA ligase.

To obtain aSyn-WT-PAGFP, PAGFP in C1 vector was PCR amplified with the primers 5'GGGTCTAGACTATTACTTGTACAGCTCGTCCATGCC3' (which contains a *XhoI* restriction site and eliminates ATG site from PAGFP) and 5'GTATCTAGACTATTACTTGTACAGCTCGTCCATGCC3' (which contains a *XbaI* restriction site and the stop codon of PAGFP). PAGFP PCR product and aSyn-GC were digested with *XhoI/XbaI*, and ligated using T4 DNA ligase.

aSyn-A30P/E46K/A53T-PAGFP and PAGFP-aSyn-A30P/E46K/A53T constructs were generated using aSyn-WT-PAGFP and PAGFP-aSyn-WT plasmids as backbone. WT-aSyn was eliminated from aSyn-WT-PAGFP and PAGFP-aSyn-WT plasmids through *NheI/XhoI* and *AflIII/XhoI* sites, respectively. PD-associated aSyn mutant forms were obtained from aSyn-BiFC plasmids (Outeiro et al 2008) and were inserted in the PAGFP backbone vectors.

Mutant S129A, which mimics the constitutively unphosphorylated form of aSyn, was generated by site-directed mutagenesis from aSyn-WT constructs using primers 5'GAGGCTTATGAAATGCCTGCTGAGGAAGGGTATCAAG3' and 5'CTTGATACCCTTCCTCAGCAGGCATTTTCATAAGCCTC3' to obtain the S129A substitution.

All constructs were generated in the pcDNA3.1 vector and verified by DNA sequencing.

The constructs for human WT-untagged aSyn (pSI-aSyn-WT), C-terminally tagged aSyn (aSyn-WT-V5 and aSyn-WT-GFP), GFP-aSyn-WT and HSP70 were a kind gift of Dr. Bradley T. Hyman and were previously described (McLean et al 2001). Myc-aSyn-WT-V5 and Myc-aSyn-WT have been described previously (Outeiro et al 2009). PLK- and GRK-encoding

plasmids were a kind gift from Dr. Hilal Lashuel, Ecole polytechnique Federale de Lausanne, Switzerland.

### **Cell Culture, transfections and immunocytochemistry**

H4 human neuroglioma cells were maintained under standard conditions and passaged the day before transfection (Outeiro et al 2008). Transfections with aSyn, GFP and PAGFP constructs were performed using Fugene™ 6 reagent from Promega, according to the manufacturer's instructions. Immunocytochemistry experiments were performed as described previously for Myc-aSyn, aSyn-V5, Myc-aSyn-V5 and untagged aSyn constructs (Outeiro et al 2008). For PA experiments, cells were co-transfected with a mRFP in order to identify transfected cells. Cells were incubated for 48h before imaging.

### **Live Cell Imaging**

Cells were imaged using a Zeiss LSM510 META microscope with a ×63 1.4 NA oil immersion objective. aSyn-WT GFP-tagged was excited at 488 nm using an argon laser (5% transmission) and a 505- to 550-nm band pass filter. For PA experiments, cells transfected with PAGFP constructs were first identified through a 561-10 DPSS laser (1% transmission) to detect mRFP (561 nm) using a 575-nm long-pass filter, and photoactivated using a diode laser line at 405 nm (100% transmission) either in the cytoplasm or in the nucleus, using standard procedures for PA. PAGFP fluorescence emission was detected by excitation at 488 nm (5% transmission) using a 505- to 550-nm band nm band pass filter. About 500 images from each cell were taken with an interval of 2 s, and PA was performed after the second image; up to 15 cells per condition were analysed.

For FRAP experiments, cells transfected with GFP constructs were photobleached in the nucleus or in the cytoplasm using a diode laser line at 405 nm (100% transmission), using standard procedures for FRAP. Recovery fluorescence of GFP constructs was detected by excitation at 488 nm (5% transmission) using a 505- to 550-nm band nm band pass filter. About 500 images from each cell were taken per condition every two seconds, and FRAP was performed after the second image; 15 cells per condition were analysed.



## Image analysis

The dynamics of aSyn diffusion (after PA or FRAP) was followed by analysing time-lapse series of the PAGFP or GFP reporter protein by measuring the fluorescence intensity over time, in the nucleus and in the cytoplasm, using ImageJ LSM toolbox plugin and LSM Image browser.

For PA analysis, the normalized nuclear fluorescence (NF) was obtained as the following:

$$NF_{(t)} = \frac{[N_{(after\ PA)} - N_{(before\ PA)}]}{[(N+C_{(after\ PA)}) - (N+C_{(before\ PA)})]}$$

The normalized cytoplasmic fluorescence (FC) was obtained as the following:

$$CF_{(t)} = \frac{[C_{(after\ PA)} - C_{(before\ PA)}]}{[(N+C_{(after\ PA)}) - (N+C_{(before\ PA)})]}$$

For FRAP analysis, the normalized NF was obtained as the following:

$$NF_{(t)} = \frac{[N_{(after\ PB)}]}{[N+C_{(after\ PB)}]}$$

The normalized FC was obtained as the following:

$$NC_{(t)} = \frac{[C_{(after\ PB)}]}{[N+C_{(after\ PB)}]}$$

Where N and C refer to nucleus and cytoplasm, respectively.  $t=0$  s refers to the time lapse immediately after PA or PB. These normalizations correct the loss of fluorescence caused by imaging both in PA and in FRAP procedures.

## Statistical analysis

The numerical results are given as mean of NF or CF  $\pm$  standard deviation of up to 15 independent experiments.

The significance of the difference between the experimental and the control values of fluorescence was evaluated at three time points, 100, 500 and 1,000 s, in the nuclear compartment using 95% confidence intervals ( $\alpha=0.05$ ) through single comparisons by the two-tailed unpaired Student's *t* test followed by a Fisher's exact test to compare variances between the control and experimental groups.

## Immunoblot analysis

H4 total protein extracts were obtained 48-h post-transfection using standard procedures. Briefly, cells were washed twice in PBS and lysed in NP40 buffer (glycerol,

10%; HEPES, 20mM (pH7.9); KCl, 10mM; EDTA, 1 mM; NP40, 0.2 %; and DTT, 1mM) containing protease and phosphatase inhibitors cocktail (1 tablet/10ml; Roche Diagnostics). After centrifugation at 16,000xg for 20min at 4°C, supernatants were collected (cytoplasmic extract). The pellet was resuspended in NaCl buffer (glycerol, 20%; HEPES, 20mM (pH7.9); KCl, 10mM; EDTA, 1 mM; NaCl, 400mM; and DTT, 1mM) containing protease and phosphatase inhibitors cocktail tablets and then centrifuged again. After centrifugation, the supernatant corresponds to the nuclear extract. Protein concentration was determined using the BCA protein assay and 20 µg of protein lysates were resolved in 12% SDS-PAGE. Resolved proteins were transferred to nitrocellulose membranes. After quick washing in Tris-buffered saline and 0.1% Tween 20 (TBS-T), membranes were blocked in 5% non-fat dry milk in TBS for 1 hour (h) and then incubated with primary antibodies in 5% BSA in TBS overnight at 4°C. The primary antibodies used were mouse anti-aSyn, 1:1,000 (BD Transduction); mouse anti-GAPDH, 1:4,000 (Ambion); rabbit anti-HSP70, 1:1,000 (Assay Designs); and goat anti-LamininB C20, 1:500 (Santa Cruz Biotechnology). The membrane was then washed three times for 10 min each in TBS-T at room temperature and probed with ECL™ IgG horseradish peroxidase-conjugated (HRP) anti-mouse, anti-rabbit (GE Healthcare) or IgG HRP-conjugated anti-goat (Santa Cruz Biotechnology) secondary antibodies (1:10,000) for 1 h at room temperature. The membrane was then washed four times for 15 min each with TBS-T, and the signal was detected with an ECL chemiluminescence kit (Millipore Immobilon Western Chemiluminescent HRP Substrate).

### **Acknowledgements**

We are grateful to José Rino and António Temudo from the Bioimaging Unit, Instituto de Medicina Molecular, Lisbon, Portugal, for the valuable support with imaging optimization. This work was supported by Fundação para a Ciência e Tecnologia (PTDC/SAU-NEU/105215/2008). SG was supported by AXA Research Fund and by Fundação Ciência e Tecnologia (grant No. SFRH/BD/79337/2011). TFO was supported by an FP7 Marie Curie International Reintegration Grant (Neurofold) and by an EMBO Installation Grant.

## **B. Insights into the Mechanisms of Alpha-Synuclein Oligomerization and Aggregation**

### **3.2. The Small GTPase Rab11 co-Localizes with Alpha-Synuclein in Intracellular Inclusions and Modulates its Aggregation, Secretion and Toxicity**

#### **Abstract**

Alpha-Synuclein (aSyn) misfolding and aggregation are pathological features common to several neurodegenerative diseases, including Parkinson's disease (PD). Mounting evidence suggests that aSyn can be secreted and transferred from cell to cell, participating in the propagation and spreading of pathological events. Rab11, a small GTPase, is an important regulator in both endocytic and secretory pathways. Here, we show that Rab11 is involved in regulating aSyn secretion. Rab11 knockdown or overexpression of either Rab11a wild-type (Rab11a-WT) or Rab11a GDP-bound mutant (Rab11a-S25N) increased secretion of aSyn. Furthermore, we demonstrate that Rab11 interacts with aSyn and is present in intracellular inclusions together with aSyn. Moreover, Rab11 reduces aSyn aggregation and toxicity. Our results suggest that Rab11 is involved in modulating the processes of aSyn secretion and aggregation, both of which are important mechanisms in the progression of aSyn pathology in PD and other Synucleinopathies.

#### **Introduction**

Alpha-Synuclein (aSyn), a 140-amino-acid protein, is a key molecule involved in the pathophysiology of several neurodegenerative diseases, including Parkinson's disease (PD) and Dementia with Lewy bodies (DLB), collectively known as Synucleinopathies (Maroteaux et al 1988, Spillantini et al 1998a, Spillantini et al 1998b). Missense mutations

and multiplications of the SNCA gene encoding for aSyn are linked to familial forms of PD (Pacheco et al 2012). Furthermore, misfolded and aggregated aSyn is found in Lewy bodies (LB) and Lewy neurites (LN)—pathognomonic cytoplasmic inclusions characteristic of both PD and DLB (Spillantini et al 1998a). Although the mechanisms underpinning the pathophysiology of PD are not clearly understood, many studies indicate that aSyn aggregation is a critical event involved in this pathology (Marques & Outeiro 2012, Tyson et al 2015). aSyn is natively unfolded, but it acquires the  $\alpha$ -helical structure on its N-terminal region upon binding to membranes, both *in vitro* and *in vivo* (Bernis et al 2015, Davidson et al 1998, Smith et al 2010). Under pathological conditions, aSyn molecules associate to form oligomers that grow into protofibrils and, finally, form mature amyloid fibrillar structures. The identification of the cytotoxic aSyn species remains a subject of intense investigation. Nonetheless, there are several studies suggesting that oligomeric intermediates might constitute the most toxic aSyn species (Diogenes et al 2012, Karpinar et al 2009, Winner et al 2011).

While aSyn lacks an endoplasmic reticulum signal peptide and has therefore been considered a purely intracellular protein, recent studies have found that it can be actively secreted (Ebrahimi-Fakhari et al 2013, Ebrahimi-Fakhari et al 2012, Emmanouilidou et al 2010, Lee et al 2005). This is in agreement with the presence of aSyn in the cerebrospinal fluid and blood plasma of both PD patients and healthy subjects (Brundin et al 2010, El-Agnaf et al 2003). Notably, aSyn can be externalized via non-classical exocytosis and, in part, in association with exosomes (Emmanouilidou et al 2010). In enteric neurons, aSyn seems to follow a classical, ER-Golgi network-dependent pathway (Paillusson et al 2013). There is evidence that aSyn secretion is calcium-regulated and can be increased under conditions of cell stress (Jang et al 2010); however, the exact mechanisms regulating this process remain unclear.

aSyn pathology progresses from the lower brain stem through the midbrain to the cerebral cortex (Braak et al 2003), leading to the suggestion that a neurotropic pathogen may cause the spreading of LB and LN pathology during PD progression. This hypothesis is in agreement with clinical observations of aSyn pathology found in neuronal grafts in PD patients several years after transplantation (Li et al 2008). There is mounting evidence suggesting that aggregated aSyn is the key agent for propagation of PD pathology by a prion-like mechanism, where misfolded aSyn is released from a donor cell and is taken up

by a recipient cell where it seeds aggregation of endogenous aSyn (Danzer et al 2009, Desplats et al 2009, Hansen et al 2011). Additionally, extracellular aSyn is known to stimulate pro-inflammatory activity in microglia, which in turn can lead to a further increase in neurotoxicity and pathology progression (Croisier et al 2005, Hirsch et al 2005, McGeer et al 1988). Therefore, understanding the regulatory mechanisms involved in aSyn secretion might be highly relevant for therapy aimed at attenuating or halting the progression of PD pathology.

Rab11 is a member of the Rab small GTPase protein family, which plays critical roles in regulating transport, docking and fusion of vesicles with their target membranes (Esseltine & Ferguson 2013, Stenmark 2009). Rab11 associates with recycling endosomes, trans-Golgi membranes and secretory vesicles (Jung et al 2012, Ullrich et al 1996, Urbe et al 1993, Wilcke et al 2000). As is the case with Rab5, Rab11 is localized to synaptic vesicles in neuronal cells (Khvotchev et al 2003). Apart from a well-documented function in endosomal recycling, several studies indicate that Rab11 also plays a role in exocytic secretory pathways. It has been described to be involved in Ca<sup>2+</sup>-regulated and constitutive exocytosis (Khvotchev et al 2003), in insulin granule secretion (Sugawara et al 2009), in exosome release (Savina et al 2002) and in stretch-regulated exocytosis (Hasegawa et al 2011). These studies suggest that Rab11 is an important regulator in the crosstalk between endocytic and secretory pathways.

aSyn has recently been detected in endosomal compartments, co-localizing with Rab5a, Rab7 and Rab11a—markers of early, late and recycling endosomes, respectively (Hasegawa et al 2011). Notably, Rab11 regulates the secretion of aSyn from neurons, after internalization from the extracellular milieu, back to the extracellular space (Liu et al 2009a) and a portion of endogenous aSyn is trafficked via the recycling pathway regulated by Rab11 (Hasegawa et al 2011). Interestingly, recent work has found that Rab11 is neuroprotective in an *in vivo* model of Huntington's disease (HD), another neurodegenerative disease with pathological protein aggregation (Richards et al 2011, Steinert et al 2012). Rab11 was sequestered in LC3-positive amphisome-like structures in dendritic spines in the presence of mutant Huntingtin (Htt) aggregates, followed by impairment of Rab11-dependent endosomal recycling (Richards et al 2011). In addition, Rab11 overexpression rescued dendritic dysfunction, dystrophy and neurodegeneration caused by mutant Htt aggregation, providing a neuroprotective effect in a *Drosophila*

model of HD (Richards et al 2011, Steinert et al 2012). Moreover, Rab11 dysfunction was shown to slow trafficking of the neuronal glutamate transporter EAAC1 to the cell surface, causing oxidative stress and cell death in HD (Li et al 2010).

In the present study, we investigated the role of Rab11 in modulating aSyn secretion and aggregation. We found that Rab11 can regulate secretion of intracellular aSyn, and that Rab11 physically interacts with aSyn and co-localizes with aSyn in intracellular inclusions. Our results also suggest that Rab11 is involved in modulating aSyn aggregation. In total, our study provides molecular support for the protection afforded by Rab11 against aSyn-mediated behavioral and functional deficits in flies (Breda et al 2014), highlighting its potential as a therapeutic target in Synucleinopathies.

## Results

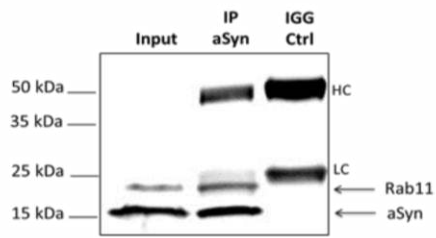
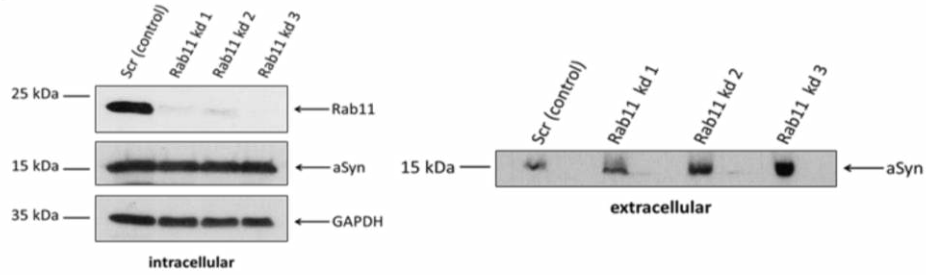
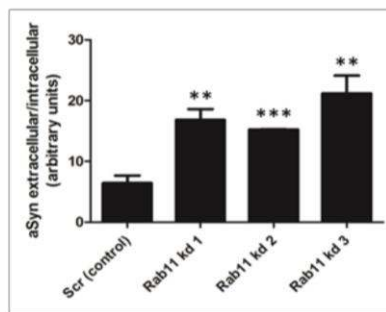
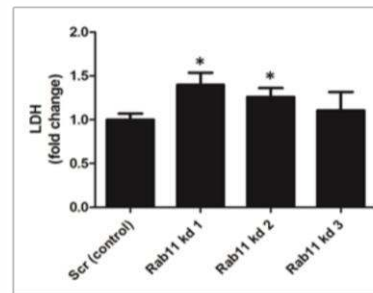
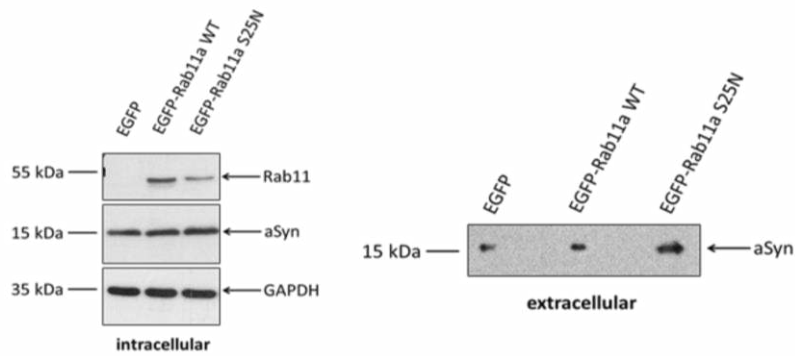
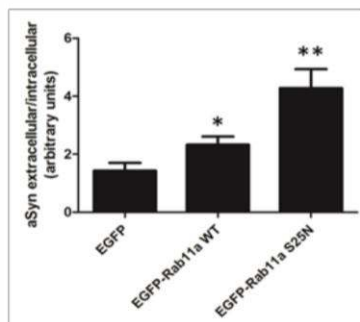
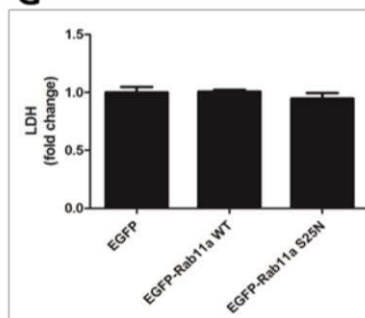
### **Rab11 interacts with aSyn *in vivo* and modulates aSyn secretion**

Co-localization of aSyn with Rab5a, Rab7 and Rab11a in endocytic compartments has recently been described in HEK293T and SH-SY5Y cells (Hasegawa et al 2011). In order to study if there is a direct interaction between Rab11 and aSyn *in vivo*, we performed a co-immunoprecipitation (co-IP) analysis of aSyn and Rab11 proteins from rat brain lysate. Following the immunoprecipitation of endogenous aSyn, endogenous Rab11 was detected using a Rab11-specific antibody (Figure 16A). This result suggests that these two proteins interact *in vivo* in addition to being present in the same subcellular compartment. Rab11 is an important regulator of various trafficking steps at the interface between endocytic and secretory pathways. Recently, it has been suggested that the endocytic pathway is involved in aSyn secretion (Emmanouilidou et al 2010, Hasegawa et al 2011). Thus, we next investigated whether Rab11 is involved in this process.

To determine whether Rab11 plays a role in aSyn secretion, we used SH-SY5Y cells expressing wild-type (WT) aSyn under control of the Tetracycline-off regulatory expression system (Emmanouilidou et al 2010, Vekrellis et al 2009). First, we knocked down Rab11 expression using three adenoviral vectors encoding for Rab11 miRNAs and measured the levels of intracellular as well as extracellular aSyn in the supernatant of the conditioned media (CM) by immunoblot analysis (Figure 16B). Rab11 knockdown led to a

parallel decrease in intracellular aSyn and an increase in levels of aSyn in the CM (Figure 16B and 16C). To assess whether this increase in extracellular aSyn was due to increased release of aSyn from dying cells, we measured the release of lactate dehydrogenase (LDH) into the CM as an indicator of cell-membrane permeability/dysfunction, which is typical of dying cells (Figure 16D). We found that Rab11 knockdown modestly increased LDH levels in the CM when compared with the control; however, this was not correlated to the increase in extracellular aSyn levels. Moreover, the construct for Rab11 knockdown leading to the highest aSyn extracellular levels displayed LDH levels comparable with control (kd 3, Figure. 16B and 16D). These data suggest that the increase in extracellular aSyn levels in Rab11 knockdown condition occurs due to an active secretory process.

Next, we investigated the effect of Rab11 on aSyn secretion by expressing EGFP-tagged wild-type Rab11a (Rab11a-WT), or the GDP-bound, dominant negative Rab11a mutant (Rab11a-S25N). While in the case of Rab11 knockdown, we decreased the total levels of endogenous Rab11, Rab11a-S25N altered the Rab11 function by introducing a GDP-bound Rab11a mutant that competes with the endogenous active Rab11 GTPase, therefore eliminating its activity. The levels of aSyn in the cell lysates, as well as in the 48 h—CM, were measured by immunoblot analysis (Figure 16E). In agreement with the results from Rab11 knockdown, the amount of externalized aSyn was significantly increased in the presence of Rab11a-S25N (Figure 16F), compared with the EGFP control. Interestingly, we also observed significantly higher levels of aSyn in the CM of Rab11a-WT expressing cells (Figure 16F). These results are consistent with previous findings showing increased secretion of overexpressed human growth hormone (hGH) in PC12 cells upon co-expression of Rab11a-WT or Rab11a-S25N, with Rab11a-WT having a moderate and Rab11a-S25N a more pronounced effect on hGH secretion (Khvotchev et al 2003). To further confirm that the increase in extracellular aSyn was not due to increased cell death, we performed LDH assays to assess its levels in the CM (Figure 16G). There was no significant difference in the LDH levels in the CM of the EGFP, EGFP-Rab11a-WT or EGFP-Rab11a-S25N transfected cells, indicating that the expression of Rab11a-WT or its dominant negative mutant form leads to increase in aSyn secretion due to an active process and not due to cell death.

**A****B****C****D****E****F****G**



**Figure 16. Rab11 interacts with endogenous aSyn *in vivo* and modulates aSyn secretion.** Rat brain lysate was analyzed for aSyn and Rab11 protein interaction by co-immunoprecipitation. **A.** Following the immunoprecipitation (IP) of endogenous aSyn, the co-IP with endogenous Rab11 is demonstrated with a Rab11-specific antibody. Highlighted are the unspecific signals from the heavy chain (HC) and light chain (LC) in the IGG control sample. Rab11 knockdown leads to increased secretion of aSyn into the CM. **B.** Representative immunoblot of cell lysate (intracellular) and CM (extracellular) of Rab11 knockdown SH-SY5Y cells overexpressing aSyn-WT is shown. **C.** Graphical representation of aSyn secretion (extracellular levels/intracellular levels normalized to GAPDH). **D.** LDH levels in the CM of Rab11 knockdown SH-SY5Y cells overexpressing aSyn-WT. **E and F.** Overexpression of Rab11a-WT and dominant negative mutant (Rab11a-S25N) leads to increased aSyn secretion. **G.** LDH levels in the CM of SH-SY5Y cells overexpressing aSyn WT transfected with EGFP, EGFP-Rab11a-WT or EGFP-Rab11a-S25N. All the data shown are representative of at least three independent experiments (mean  $\pm$  standard deviation, \* P, <0.05, \*\* P < 0.01, \*\*\* P < 0.001).

### **Rab11-mediated increases in aSyn secretion do not occur via the endocytic-recycling pathway**

To investigate whether the increased secretion of aSyn observed upon co-expression of Rab11a-WT or Rab11a-S25N occurred through changes in endocytic recycling, we measured endocytic-recycling dynamics using fluorescently labeled human transferrin. Transferrin is internalized by endocytosis after binding to its receptor on the cell surface and is recovered to the extracellular milieu by endocytic recycling (Ciechanover et al 1983). Twenty-four hours post transfection with EGFP-Rab11a-WT, EGFP-Rab11a-S25N or EGFP alone, aSyn expressing SH-SY5Y cells were loaded for 15 min with Alexa-546-labeled human transferrin and pulse chased for 10 min with non-labeled human transferrin (Figure 17A). We evaluated the percentage of Alexa-546-transferrin positive cells in each condition by fluorescence microscopy, as a measure of endosomal recycling dynamics. Compared with control transfected cells, there was no significant difference in the percentage of fluorescently labeled transferrin cells in the case of EGFP-Rab11a-WT expression (Figure 17B). In contrast, we observed a significantly higher proportion of Alexa-546-transferrin-labelled cells expressing EGFP-Rab11a-S25N when compared with EGFP expressing cells (Figure 17B). These results indicate that endocytic recycling is

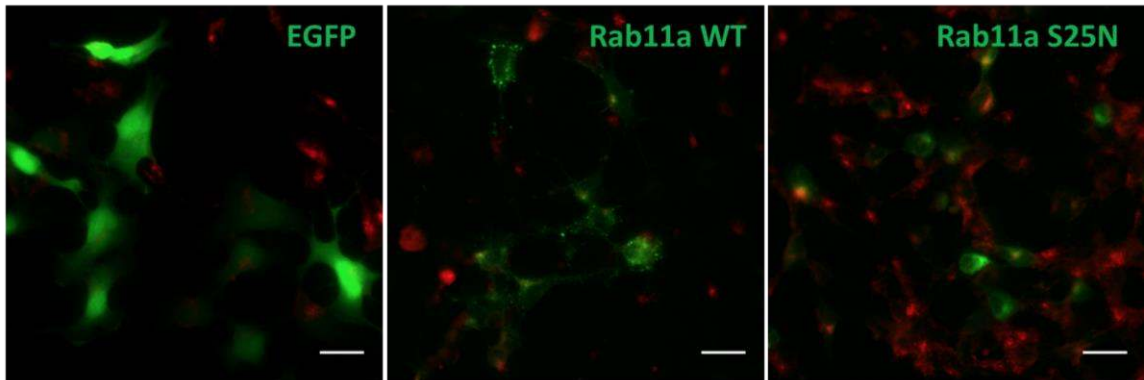
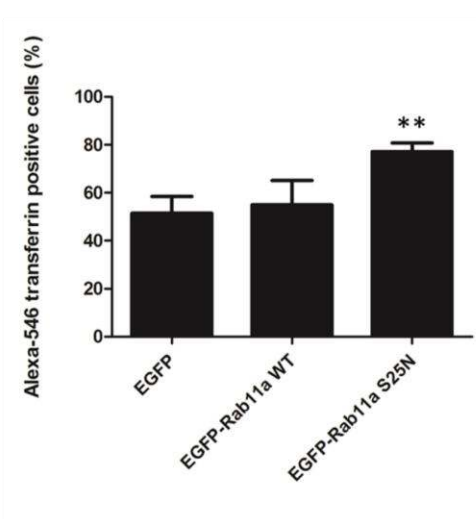
impaired in the presence of the dominant negative, GDP-bound Rab11a mutant, as less transferrin was secreted from the cells, while the expression of Rab11a-WT did not affect endocytic recycling. Therefore, we conclude that increased secretion of aSyn from SH-SY5Y cells mediated by Rab11a is not due to increased trafficking of aSyn via the endosomal recycling pathway.

### **aSyn secretion by exosomes is not increased in the presence of Rab11a-WT and Rab11a-S25N**

It has been previously shown that aSyn can be secreted from cells in association with exosomes (Alvarez-Erviti et al 2011, Danzer et al 2012, Emmanouilidou et al 2010). Exosomes are small vesicles of various sizes (40–100 nm in diameter) that are formed as intra-luminal vesicles by budding into multivesicular bodies (MVBs) and are released by fusion of MVBs with the plasma membrane (PM) (Raposo & Stoorvogel 2013).

Because of their endosomal origin, exosomes are characterized by the presence of endosome associated proteins such as Rab GTPases, SNAREs, annexins and flotillin, some of which are involved in MVB biogenesis (Alix and Tsg101) (Raposo & Stoorvogel 2013). Rab11 modulates MVB fusion and exosome release in erythroleukemic cell lines, but the exact step in which it is involved is not known (Savina et al 2002).

To test the hypothesis that Rab11a-WT or Rab11a-S25N expression leads to increased secretion of aSyn by exosomes, CM from EGFP, EGFP-Rab11a-WT or EGFP-Rab11a-S25N expressing cells was subjected to an established protocol of serial centrifugation steps for exosomal extraction (Emmanouilidou et al 2010). The pellet resulting from the last 100,000 g centrifugation step containing exosomes was subjected to immunoblot analysis using antibodies against the exosomal marker TSG101, Rab11 and aSyn (Figure 18). Quantification of aSyn in the exosomal fraction revealed lower levels of aSyn in exosomes in cells expressing EGFP-Rab11a-S25N (~30% of the control), while in cells expressing EGFP-Rab11a-WT aSyn exosomal levels were comparable with control (~90%) (Figure 18). Rab11a was also found present in the exosomal fraction (Figure 18), as expected by the endosomal origin of exosomes.

**A****B**

**Figure 17. Rab11a-S25N inhibits endosomal recycling in aSyn expressing cells.** **A.** aSyn-WT expressing SH-SY5Y cells were transfected with mock (EGFP), EGFP-Rab11a-WT or EGFP-Rab11a-S25N expressing plasmids (green). 24 h post-transfection, cells were incubated with Alexa-546 human transferrin (red) for 15 min and pulse-chased with non-labeled human transferrin to measure endocytic recycling dynamics. Cells were fixed and subjected to fluorescence microscopy analysis. Scale bar = 10  $\mu$ m. **B.** Data are represented as percentage of Alexa-546-transferrin-positive cells at 10 min pulse-chase. All the data shown are representative of at least three independent experiments (mean  $\pm$  standard deviation, \*\*  $P < 0.01$ ).

These results show that the Rab11a dominant negative mutant reduces the levels of aSyn released in association with exosomes, while Rab11a-WT does not have a major effect on exosomal release of aSyn. Therefore, we concluded that Rab11a regulates aSyn secretion by another, independent pathway.

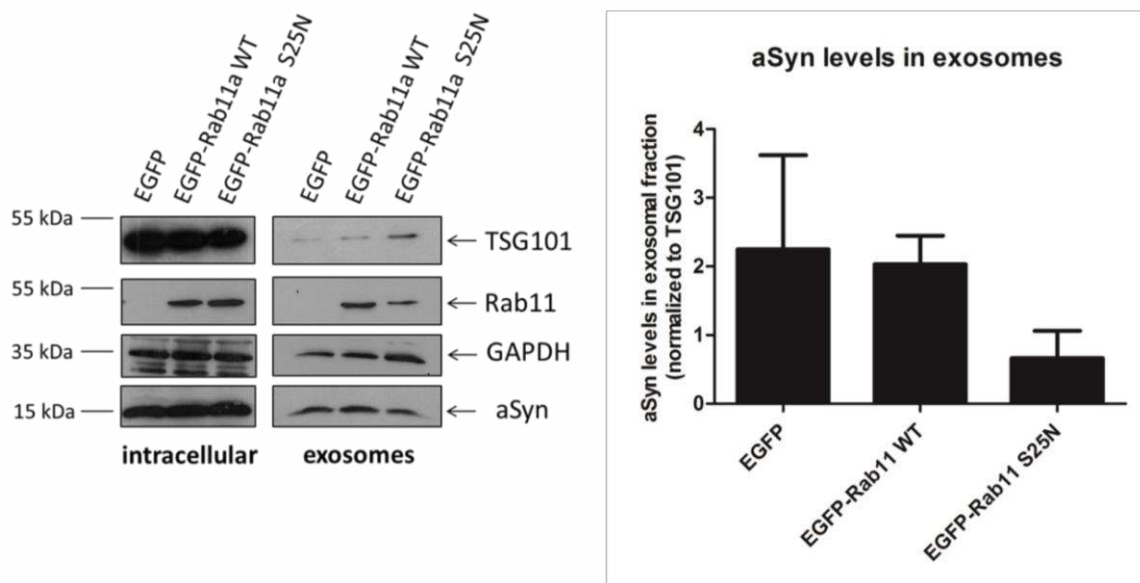


**Figure 18. Rab11a-S25N inhibits aSyn secretion by exosomes.** aSyn-WT expressing SH-SY5Y cells were transfected with mock (EGFP), EGFP-Rab11a-WT or EGFP-Rab11a-S25N expressing plasmids. 24 h post-transfection, the culture medium was replaced with 2% FBS exosome-depleted medium and conditioned for 48 h. CM was subjected to sequential centrifugation with final step at 100,000 g to extract exosomal pellet. Exosomal pellet was resuspended in RIPA buffer and analysed by immunoblotting using antibodies for the indicated proteins. A representative immunoblot of cell lysates and exosomal pellet is shown. Graph represents immunoblot quantification of aSyn levels in exosomal fraction. All the data shown are representative of at least three independent experiments.

**Brefeldin A treatment leads to increased release of aSyn and this effect is attenuated by Rab11a-WT and Rab11a-S25N expression**

Several studies showed that treatment with Brefeldin A (BFA)—a fungal metabolite blocking classical, ER/Golgi-to-PM secretory pathway—does not block aSyn secretion (Emmanouilidou et al 2010, Jang et al 2010, Lee et al 2005). Based on these findings, it was suggested that aSyn is secreted from neuronal cells via an unconventional, ER/Golgi-independent pathway. However, results from a recent study show that in enteric neurons aSyn is secreted via conventional, ER/Golgi-dependent exocytosis sensitive to BFA inhibition (Paillusson et al 2013).

Thus, to investigate whether Golgi-dependent exocytosis contributes to aSyn secretion in the presence of Rab11a-WT and Rab11a-S25N expression, aSyn expressing SH-SY5Y cells were transfected with EGFP-Rab11a-WT or EGFP-Rab11a-S25N and 24 h post-transfection were treated with 1 mg/ml BFA for 6 h. The levels of extracellular aSyn in the CM were measured by immunoblotting (Figure 19A). At the same time, the CM was used for LDH assay to assess cell death (Figure 19C). Similar to previous reports, we verified that BFA treatment did not block aSyn secretion (Figure 19A). In fact, we observed higher levels of extracellular aSyn following BFA treatment. This observation could be attributed to increased cell death after BFA treatment, as we also observed an increase in LDH activity in CM upon BFA treatment (Figure 19C). However, despite a similar increase in cell death in all conditions, the levels of aSyn in the CM did not increase significantly in case of Rab11a-WT and -S25N expression in contrast to the control (Figure 19A and 19B). These results might indicate that in the presence of Rab11a-WT and -S25N expression, there is in fact inhibition of aSyn secretion when the classical secretory pathway is blocked by BFA and this effect is masked by leakage of aSyn from dying cells. Altogether, our data suggest that Rab11a plays a role in regulating aSyn secretion.

### **Rab11a modulates aSyn aggregation and co-localizes with aSyn in intracellular inclusions**

Although the process of aSyn aggregation has been extensively studied *in vitro*, it is still unclear which cellular pathways are involved. We used an established cell model that enabled us to assess aSyn inclusion formation in an intracellular context. EGFP-Rab11a-WT, EGFP-Rab11a-S25N or EGFP alone was co-expressed in H4 human neuroglioma cells along with a C-terminal modified version of aSyn (aSynT) and Synphilin-1. This is an established paradigm of aSyn aggregation that results in the formation of LB-like inclusions (Klucken et al 2012, McLean et al 2001, Outeiro et al 2006). In this model, we counted the percentage of cells presenting aSyn inclusions versus cells that presented homogeneous aSyn staining, with no inclusions (Figure 20A). We found that both Rab11a-WT and Rab11a-S25N decreased the percentage of cells with aSyn inclusions, with a higher proportion of cells presenting homogenous aSyn staining without the presence of intracellular inclusions (Figure 20B). Interestingly, we observed the opposite effect when Rab11 was knocked down, as this resulted in an increased percentage of cells displaying

aSyn inclusions (Figure 20C). Together, these results suggest that Rab11a can modulate aSyn aggregation.

To study the sub-cellular localization of aSyn and Rab11 in the absence or presence of aSyn aggregation, EGFP-Rab11a was co-expressed together with wild-type aSyn (aSyn-WT) or with aSynT/Synphilin-1 in H4 cells, as described above. In the presence of aSyn-WT, Rab11a was normally distributed in the cell, as in the control situation (Figure 21A). Strikingly, the subcellular localization of Rab11a was changed in the presence of aSyn inclusions (Figure 21A). We found that Rab11a was co-localized inside these inclusions, together with aSyn (Figure 21B).

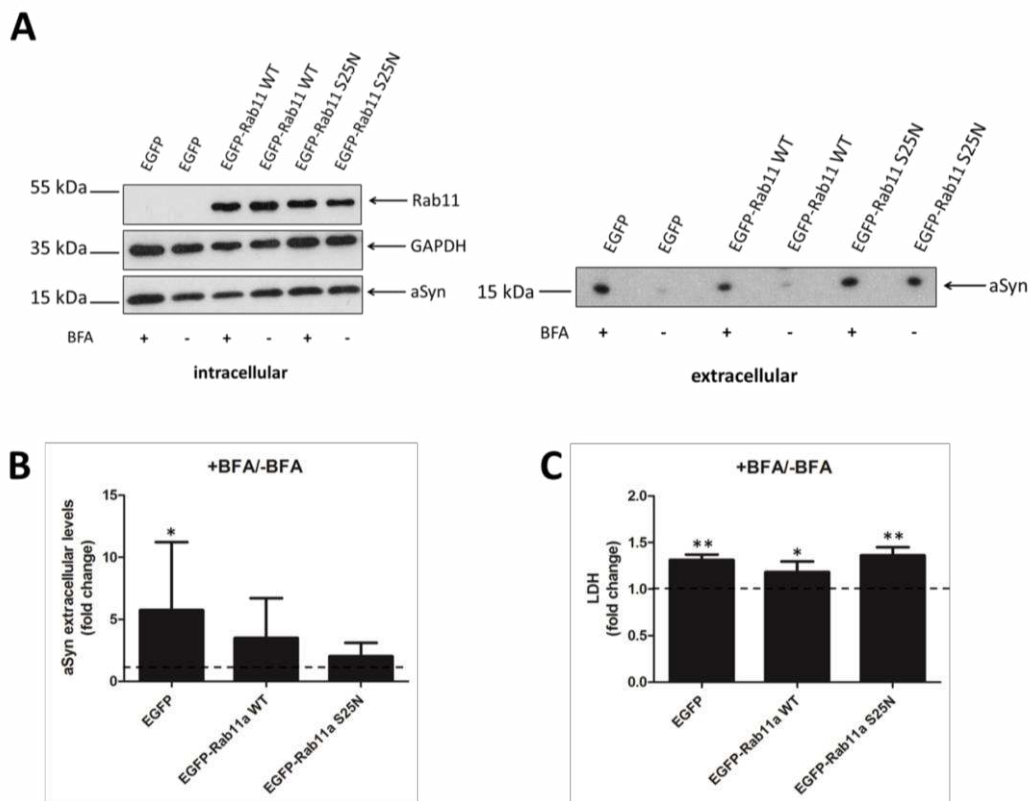


**Figure 19. BFA treatment leads to increased release of aSyn in control condition, but not in Rab11a-WT and Rab11a-S25N expressing cells.** aSyn-WT expressing SH-SY5Y cells were transfected with mock (EGFP), EGFP-Rab11a-WT or EGFP-Rab11a-S25N expressing plasmids. 24 h post-transfection, cells were pre-treated with BFA for 1 h before the culture medium was replaced and conditioned for additional 5 h in the presence of BFA. **A.** Representative immunoblot of cell lysate (intracellular) and CM (extracellular) is shown. **B.** Graphical representation of fold change of aSyn extracellular levels following BFA treatment (+BFA/-BFA). aSyn release was

significantly increased following BFA treatment in the control condition, but not in the presence of Rab11a-WT or Rab11a-S25N. **C.** LDH levels in the CM (fold change) following BFA treatment (+BFA/-BFA). Dotted line represents extracellular levels of aSyn (**B**) or LDH (**C**) in the absence of BFA treatment normalized to 100%. All the data shown are representative of at least three independent experiments (mean  $\pm$  standard deviation, \*  $P < 0.05$ , \*\*  $P < 0.01$ ).

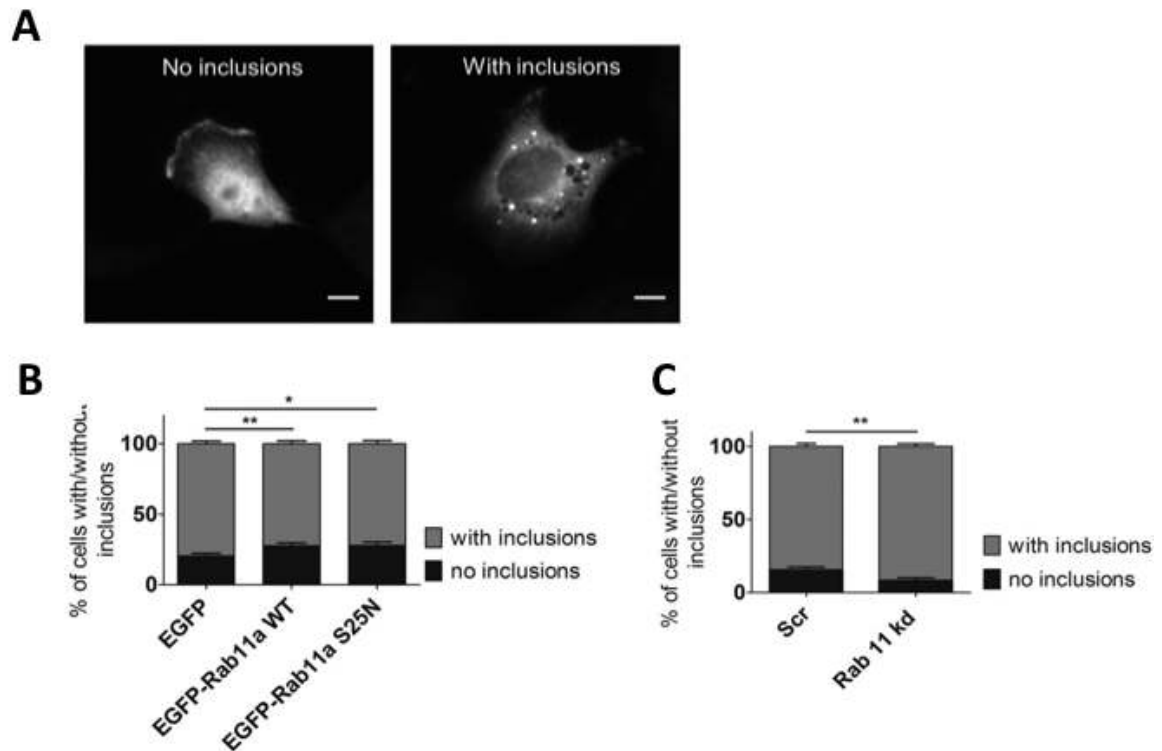


**Figure 20. Rab11 modulates aSyn aggregation.** **A.** Representative images of cells with homogenous aSyn staining (no inclusions) and with aSyn positive inclusions (with inclusions) are shown. Scale bar = 10  $\mu$ m. **B and C.** Graphs representing the percentage of cells with and without inclusions in the total population of cells positive for aSyn are shown. All the data shown are representative of at least three independent experiments (mean  $\pm$  standard deviation, \*  $P < 0.05$ , \*\*  $P < 0.01$ ).

### Rab11a reduces aSyn cytotoxicity

Considering the neuroprotective effect of Rab11 against mutant Htt in HD (Richards et al 2011, Steinert et al 2012), we investigated whether Rab11 protected against aSyn toxicity in a cell model (Outeiro et al 2006, Outeiro et al 2007). H4 cells were transfected with a plasmid expressing aSyn-WT or mock-transfected with empty vector (control), together

with EGFP, EGFP-Rab11a-WT or EGFP-Rab11a-S25N (Figure 22A). aSyn-induced toxicity was significantly reduced in the presence of Rab11a-WT or Rab11a-S25N (Figure 22A). Conversely, we observed a significant increase in aSyn toxicity upon Rab11 knockdown (Figure 22B).

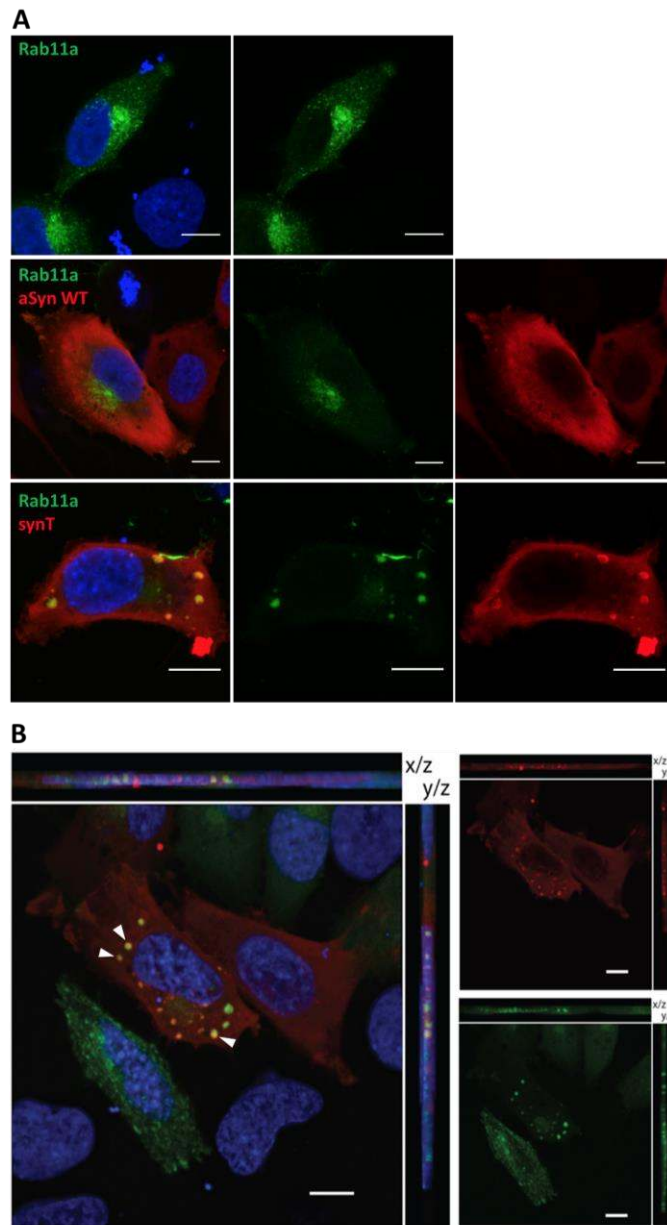


**Figure 21. Rab11a co-localizes with aSyn in intracellular inclusions, H4 cells were co-transfected either with aSyn-WT or aSynT and Synphilin-1 together with EGFP-Rab11a (green).** Cells were fixed 48 h post-transfection and subjected to immunocytochemistry for aSyn (red) followed by confocal microscopy analysis. Scale bar = 10  $\mu$ m. **A.** Rab11a changes its subcellular localization in



the presence of aSyn inclusions. **B.** Rab11a co-localizes with aSyn positive inclusions (yellow). White arrowheads point to inclusions where aSyn and Rab11 co-localize. Scale bar = 10  $\mu$ m.

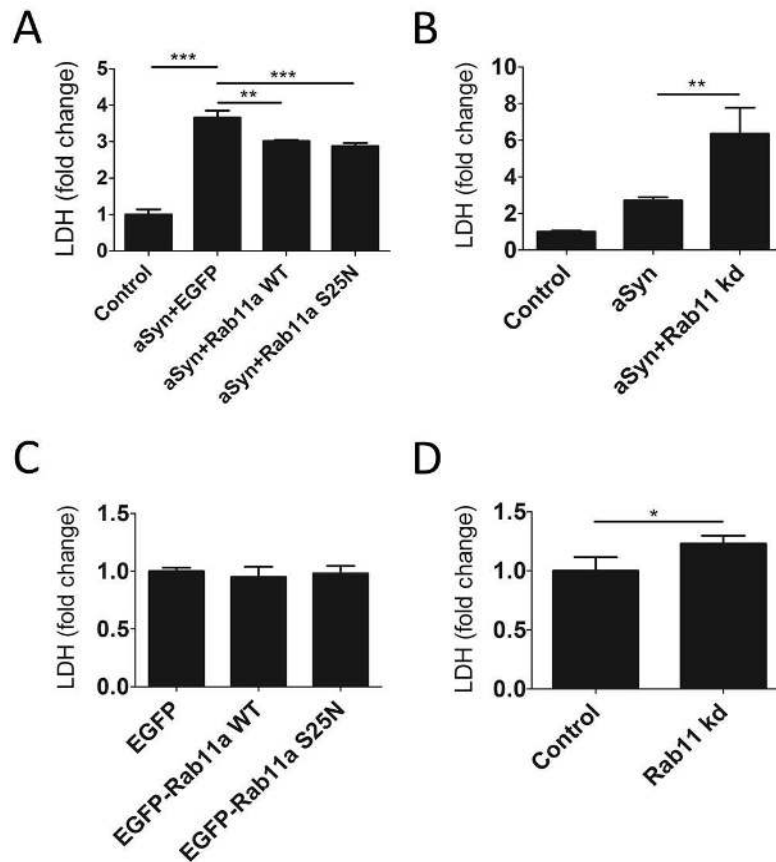


**Figure 22. Rab11 modulates aSyn toxicity.** **A and B.** H4 cells were transfected with aSyn-WT or empty vector (control) and co-transfected with EGFP-Rab11a-WT, EGFP-Rab11a-S25N or EGFP. For Rab11 knockdown, cells were transduced with an adenovirus containing miRNA construct against Rab11a or scrambled construct (control). LDH extracellular levels were measured to assess cytotoxicity. **A.** Rab11a-WT and Rab11a-S25N decrease aSyn toxicity. **B.** Rab11 knockdown increases aSyn toxicity. **C and D.** Cytotoxicity was assessed in the aSyn aggregation model (aSyn + Synphilin-1) described above. **C.** Rab11a-WT and Rab11a-S25N do not affect aSyn cytotoxicity in the aSyn aggregation model. **D.** Rab11 knockdown increases aSyn toxicity in the aSyn aggregation model. All the data shown are representative of at least three independent experiments (mean  $\pm$  standard deviation, \*  $P < 0.05$ , \*\*  $P < 0.01$ , \*\*\*  $P < 0.001$ ).

## Discussion

Several recent studies indicate that a large number of proteins without an N-terminal signal sequence for ER entry are efficiently released from cells. These include proteins such as IL-1b, acyl-CoA binding protein (AcbA), ubiquitin carboxy-terminal hydrolase, visfatin and also aSyn (Prydz et al 2013). Several mechanisms have been proposed for the transfer of molecules from the cytoplasm to the extracellular space, such as direct translocation through pores in the PM, uptake into the internal vesicles of MVBs (subsequently released as exosomes), passage via recycling endosomes or autophagosomes, incorporation into microvesicles budding outward from the PM and export via secretory lysosomes (Prydz et al 2013). aSyn has been observed inside cells in vesicles of unknown identity (Lee et al 2005) and is known to be actively secreted into the extracellular space either in free or vesicle-bound form (Emmanouilidou et al 2010, Jang et al 2010, Lee et al 2005). However, little is known about the route(s) aSyn follows to leave the cell or the mechanisms regulating aSyn secretion. It has been suggested that an endocytic pathway is involved in aSyn (Ebrahimi-Fakhari et al 2013, Emmanouilidou et al 2010, Lee et al 2005). Indeed, blocking the endosome-lysosomal pathway by methylamine or chloroquine leads to increased aSyn secretion (Emmanouilidou et al 2010). Exosomes, small secreted vesicles originating from the endocytic pathway, have also been shown to carry aSyn (Emmanouilidou et al 2010), although it seems that only a small portion of aSyn is secreted by this route (Emmanouilidou et al 2010, Hasegawa et al 2011, Jang et al 2010). In addition, impairment in MVB formation has been found to increase aSyn secretion (Hasegawa et al 2011). Notably, aSyn localization has been observed in endocytic compartments, including the recycling endosomes (Hasegawa et al 2011).

Here, we first investigated whether aSyn and Rab11 interact *in vivo*. Co-immunoprecipitation analysis of rat brain lysate demonstrates that endogenous aSyn protein does indeed interact with endogenous Rab11 (Figure 16). We next wished to explore whether Rab11 modulates aSyn secretion. It has been shown that Rab11 regulates the re-secretion of extracellularly added aSyn back into the extracellular space after its uptake by the cell (Liu et al 2009a). Furthermore, increased aSyn secretion caused by block of MVB formation using a dominant-negative mutant of vacuolar protein 4 could be restored to normal levels by simultaneous expression of Rab11a-S25N (Hasegawa et al

2011). These results point at the involvement of Rab11-regulated recycling in aSyn secretion. Therefore, we investigated the role of Rab11 in aSyn secretion by manipulating its function in the cell, either by knocking it down or expressing the Rab11a-WT or the GDP-bound inactive form of the protein. We observed that both Rab11 knockdown and expression of Rab11-S25N—which both impairs Rab11 function—lead to increased aSyn secretion. Surprisingly, the same effect, although to a lesser extent, was observed by expressing Rab11a-WT. One possible explanation is that overexpression of Rab11a-WT does not lead to an overall increased Rab11 function, as it may be competing with the endogenous Rab11 for the interacting molecules, which can be limiting factors for normal Rab11 function. This is supported by the results of the transferrin-recycling dynamics in our model. While Rab11a-S25N impairs transferrin recycling to the extracellular space, expression of Rab11a-WT did not have any effect on this process. These results together suggest that increased aSyn secretion observed after expression of Rab11a-WT or Rab11a-S25N does not occur via endosomal recycling in SH-SY5Y cells. A similar effect was observed using Rab11b-WT or Rab11b-S25N in PC12 cells expressing hGH (Khvotchev et al 2003). Both Rab11b forms increased the secretion of hGH in these cells, with Rab11a-S25N having a more pronounced effect. It has been suggested that despite leading to similar effect of increasing the constitutive exocytosis of hGH, WT and S25N Rab11b have distinct mechanisms of action. Expression of Rab11a-S25N decreased the excessive release of aSyn following a block in MVB-formation back to normal levels (Hasegawa et al 2011). This suggests that aSyn can be secreted by the way of recycling endosomes in a Rab11a-function dependent manner. Our results show that impairing Rab11a function by knockdown or expression of Rab11a-S25N leads to increased secretion of aSyn, suggesting that aSyn secretion follows other pathway(s), independent of RE when Rab11a function is impaired.

It was previously demonstrated that Rab11 has a distinct function in exocytosis depending on the cell type (Khvotchev et al 2003). While in neuronal (PC12) cells, GTP- and GDP-bound Rab11b stimulated constitutive exocytosis of hGH, in non-neuronal (HEK) cells GTP- and GDP-bound Rab11b inhibited constitutive exocytosis and caused an accumulation of cellular hGH (Khvotchev et al 2003). In this study, we have used human neuroblastoma SH-SY5Y cells, in contrast to HEK cells used by Hasegawa et al (Hasegawa et al 2011). Therefore, this might be one reason for the different effects on aSyn secretion

observed in these two studies. Another possible explanation is that aSyn can employ different pathways for its exocytosis, depending on the state of the cell. When a block in one of the pathways occurs, aSyn could be directed to another pathway(s). This would allow aSyn release to be carried out by distinct mechanisms, in response to the state of the functioning of the cell. This is supported by an observation of changes in aSyn release in response to cellular stress conditions (Jang et al 2010).

Rab11 has been implicated in regulating exosomal release in K562 erythroleukemia cells; however, the exact step remains unknown (Savina et al 2002). Since aSyn was shown to be secreted in association with exosomes, we have investigated the impact of Rab11a function on exosomal aSyn secretion. We have observed lower levels of aSyn in the exosomal fraction in cells expressing the dominant negative Rab11a-S25N mutant, while in the case of Rab11a-WT the exosomal levels of aSyn were similar to control levels (Figure 18). At the same time, Rab11a-S25N did not lead to an overall decrease in exosome release, judged by the levels of the exosomal marker TSG101 (Figure 19). These results together might indicate that impaired Rab11a function prevents aSyn entering the MVBs and exosomes, while promoting exit of aSyn from the cell through an independent pathway.

It was suggested that aSyn leaves the cell by a Golgi independent transport route. This notion is based upon results showing that aSyn secretion is not blocked by BFA, a drug that disassembles the Golgi stacks (Emmanouilidou et al 2010, Jang et al 2010, Lee et al 2005). However, insensitivity to BFA treatment by itself does not unequivocally mean that a protein normally reaches the cell surface via a nonconventional route. It is possible that certain molecules take a Golgi bypass route when the pathway they normally employ is no longer operational. Moreover, results from a recent study show that in enteric neurons aSyn is secreted via conventional, ER/Golgi-dependent exocytosis sensitive to BFA inhibition (Paillusson et al 2013). Furthermore, although BFA treatment reduced aSyn secretion in enteric neurons, it did not block it completely. Therefore, one might hypothesize that aSyn can use different pathways for exocytosis, depending on the cell type and cell condition.

We studied the involvement of Golgi-dependent pathway in aSyn secretion in the presence of Rab11a-WT or Rab11a-S25N by analyzing extracellular aSyn levels following BFA treatment. Although we observed a similar increase in cell death following the BFA

treatment in all conditions, aSyn extracellular levels were not significantly increased in the case of Rab11a-WT or Rab11a-S25N expression. Therefore, we concluded that part of aSyn can be secreted by classical ER-Golgi secretory pathway when Rab11 function is altered. Overall, our results indicate that aSyn secretion can be modulated by Rab11a and that aSyn can be secreted by different secretory pathways, depending on the condition of the cell.

Interestingly, intravesicular aSyn is more prone to aggregation than aSyn found in the cytosol (Lee et al 2005). Moreover, exposing cells to stress conditions promoting accumulation of misfolded protein leads to increased translocation of aSyn into vesicles and the consequent increase in aSyn secretion (Jang et al 2010). Furthermore, a recent study found that inhibition of the autophagy/lysosome pathway leads to increased aSyn aggregation and exocytosis (Lee et al 2013). These studies indicate that there is a connection between aSyn aggregation and aSyn secretion. Increased secretion could be a protective mechanism by the cell to dispose of misfolded and aggregated aSyn. We studied the role of Rab11a on aSyn aggregation using a cell model characterized by formation of aSyn-positive intracellular inclusions, and observed a reduction in aSyn aggregation in the presence of Rab11a-WT or Rab11a-S25N. Since knocking down Rab11 resulted in an increased proportion of cells presenting aSyn aggregates, our results suggest a GTPase independent effect of Rab11 on aSyn aggregation. Moreover, Rab11a was found to co-localize with aSyn-positive inclusions, in contrast to its normal intracellular localization in the endocytic recycling compartment, as observed in the presence of non-aggregating aSyn.

Furthermore, we addressed the effect of Rab11 on aSyn toxicity. While the presence of Rab11a-WT or Rab11a-S25N significantly decreased aSyn-induced toxicity, Rab11 knockdown resulted in a marked increase in cytotoxicity in aSyn-WT expressing cells. A similar effect was observed in the aSyn aggregation model, where Rab11 knockdown led to increase in aSyn toxicity. Interestingly, Rab11a-WT and Rab11a-S25N had no effect on aSyn toxicity in this model. Since in this model Rab11 was observed to be localized in intracellular inclusions together with aSyn, it is therefore possible that Rab11 was unable to exert a protective effect because it was being recruited from its original subcellular localization and was sequestered inside the inclusions.

Altogether, our results show, for the first time, that Rab11 interacts with aSyn inside the cell, co-localizes with aSyn in intracellular inclusions and, furthermore, modulates aSyn aggregation and toxicity, while regulating the exit of aSyn from the cell. Since we also found that Rab11 modulates aSyn-mediated behavioral deficits *in vivo* (Breda et al 2014), our studies strongly suggest Rab11 holds great potential as a therapeutic target in PD and other neurodegenerative disorders.

## Materials and Methods

### Cell culture

For aSyn secretion studies, we used SH-SY5Y cells inducibly expressing aSyn wild-type (SH-SY5Y aSyn-WT) previously described (Vekrellis et al 2009). SH-SY5Y cells overexpressing aSyn-WT were cultured in the RPMI1640 medium (Life Technologies) containing 10% fetal bovine serum (FBS), penicillin (100 U/ml), streptomycin (100 ug/ml) and 2 mM L-glutamine in the presence of 250 ug/ml G418 and 50 ug/ml hygromycin B and doxycycline (1 ug/ml; Clontech Laboratories). Expression of aSyn-WT was switched on by the removal of doxycycline from the media as described previously (Vekrellis et al 2009). For aSyn aggregation and aSyn cytotoxicity studies, we used human H4 neuroglioma cells. H4 were maintained in OPTI-MEMI (Life Technologies) supplemented with 10% FBS in the presence of penicillin (100 U/ml; Life Technologies) and streptomycin (100 ug/ml; Life Technologies).

### SH-SY5Y aSyn-WT cell line transfection and Rab11 knockdown

SH-SY5Y aSyn-WT cells were grown in the absence of doxycycline for 6 days to induce aSyn-WT expression. Cells were then seeded onto 100 mm diameter dishes ( $1.5 \times 10^6$  cells/dish) in RPMI 1640 medium containing 10% FBS 24 h prior to transfection or transduction. For Rab11 knockdown, cells were transduced with adenovirus with three distinct Rab11 miRNA constructs and incubated for 48 h before changing the medium for conditioning. For Rab11 overexpression, cells were transfected with pEGFP Rab11a-WT, pEGFP Rab11a-S25N (kind gift from Dr Chiara Zurzolo, Institut Pasteur, Paris) or empty pEGFP vector using Lipofectamine 2000 (Life Technologies). 4 h after transfection, medium was replaced with fresh growth medium.

### **Preparation of CM, LDH cytotoxicity assay and preparation of cell extracts**

24 h after transfection or 48 h after transduction, the medium was changed to RPMI 1640 medium containing 2% FBS and conditioned for 48 h. The CM from transfected or transduced cells was collected and centrifuged at 4,000 g for 10 min at 4°C to remove cell debris. For western blotting, the CM was concentrated using 3 kDa cutoff Amicon Ultra filters (Merck Millipore). CM without concentration was used to determine the membrane integrity of cells used in the experiments by measuring released LDH as described in the manufacturer's instructions (Clontech Laboratories). For extraction of cellular proteins, cells were washed 2× with cold PBS and lysed in NP-40 buffer (50 mM Tris pH 8.0, 150 mM NaCl, 1% NP-40) supplemented with protease inhibitor cocktail tablet (Roche Diagnostics).

### **Preparation of exosome-depleted medium and purification of exosomal fraction**

The depletion of the medium from bovine serum-derived exosomes was performed as described previously (Emmanouilidou et al 2010). Briefly, RPMI 1640 medium containing 20% FBS, penicillin/streptomycin and L-glutamine was centrifuged at 100,000 g for 16 h at 4°C. The supernatant was carefully removed and sterilized by filtering through a 0.2 µm filter (Whatman) and stored at 4°C until additional use in exosome preparation. Exosomal fraction from the CM was prepared as described previously (Emmanouilidou et al 2010). Briefly, SH-SY5Y aSyn-WT cells were seeded in three 100 mm dishes in 10% FBS and 24 h later transfected as described above. Twenty-four hours post-transfection, the culture medium was replaced with exosome-depleted medium diluted 10-fold with RPMI 1640 medium and conditioned for 48 h. Culture supernatants of cells were collected and spun at 300 g for 10 min to remove cells. The supernatants were then sequentially centrifuged at 2,000 g for 10 min, 10,000 g for 30 min and 100,000 g for 90 min. The pellet containing exosomes was washed once with cold PBS and centrifuged again at 100,000 g for 90 min. The resulting pellet was resuspended in 30 µl of radio immunoprecipitation assay (RIPA) buffer (50 mM Tris-HCl, pH 7.6, 150 mM NaCl, 1% NP-40, 0.5% Sodium deoxycholate and 0.1% SDS). All centrifugations were performed at 4°C.

### **Western blotting**

Protein concentration in cell extracts and concentrated CM was quantified using BCA protein assay kit (Thermo Scientific). Equal amount of total protein (250 ug for CM and 15 ug of cell lysate) was loaded on a 15% polyacrylamide separation gel and separated by SDS-PAGE using a Tetra cell (Bio-Rad). For immunoblot analysis of exosomes, whole fraction from single exosomal extraction (30 ul) was used each time. After separation by SDS-PAGE, proteins were transferred to nitrocellulose membranes using standard procedures with a Mini Trans-Blot system (Bio-Rad). Mouse anti-aSyn-1 antibody (BD Biosciences, 1:1,000), mouse anti-Rab11 (BD Biosciences, 1:1,000), mouse anti-GAPDH (Life Technologies, 1:4,000) and mouse anti-TSG101 (Abcam, 1:1000) were used. Secondary anti-mouse antibody coupled to horseradish peroxidase (GE Healthcare, 1:10,000) was used. Membranes were incubated with ECL Chemiluminescent HRP Substrate (Millipore). Densitometry analysis of the corresponding bands was performed using the ImageJ software.

### **BFA treatment**

SH-SY5Y cells expressing aSyn-WT transfected with pEGFP, pEGFP-Rab11a-WT or pEGFP-Rab11a-S25N were pre-treated with BFA (1 ug/ml; SIGMA-ALDRICH) for 1 h before the medium was changed to RPMI 1640 medium containing 2% FBS and conditioned in the presence of BFA for further 5 h. CM was collected and processed for western blot and LDH analysis as described above.

### **Transferrin pulse-chase**

SH-SY5Y cells expressing aSyn-WT were seeded on glass cover slips 24 h prior to transfection with pEGFP, pEGFP-Rab11a-WT or pEGFP-Rab11a-S25N. 24 h post-transfection, cells were washed with PBS and incubated with human Alexa-546-Transferrin (50 ug/ml; Life Technologies) at 37°C for 5 min. Cells were then washed twice with cold PBS and incubated with unlabeled human holo-transferrin (5 mg/ml; SIGMA-ALDRICH) at 37°C for 10 min. Cells were washed twice with cold PBS, fixed with 4% paraformaldehyde (PFA) for 10 min at room temperature (RT) and then mounted on glass microscopy slides in GVA mounting media (Genemed Biotechnologies). Cells were analyzed using Zeiss Axiovert 200M widefield fluorescence microscope. The percentage of



transfected cells (EGFP positive) positive for Alexa-546-Transferrin was counted using the ImageJ software. Minimum of 100 cells were counted per each condition.

#### **H4 cell line transfection, Rab11 knockdown, immunocytochemistry, microscopy analysis and cytotoxicity assays**

For intracellular aSyn aggregation experiments, H4 cells were seeded on 35 mm glass bottom imaging dishes (ibidi GmbH) 24 h prior to transfection. For Rab11 knockdown, cells were transduced with adenovirus with miRNA against Rab11 or with scrambled control (Scr). Cells were then co-transfected with aSynT (aSyn-EGFP deletion mutant WT aSyn-EGFP-D155) and Synphilin-1 in 1:1 ratio as described previously (McLean et al 2001, Outeiro et al 2006) using Fugene 6 (Promega). For Rab11 overexpression, 24 h post first transfection with aSynT and Synphilin-1, cells were further transfected with pEGFP, pEGFP-Rab11a-WT or pEGFP-Rab11a-S25N. 24 h later, cells were fixed with 4% PFA for 10 min at RT, washed twice with PBS and subjected to immunocytochemistry analysis. Briefly, cells were permeabilized with 0.5% Triton X-100 in PBS for 20 min at RT, blocked for 1 h at RT with 1% normal goat serum in 0.1% Triton X-100 in PBS, incubated with primary antibody against aSyn (mouse anti-aSyn 1:1,000; BD Biosciences) at 4°C overnight followed by secondary antibody incubation (1:1,000, goat anti-mouse IgG-Alexa568, Life Technologies) for 2 h at RT and incubated for 2 min with DAPI 1:1,000 in PBS (SIGMA-ALDRICH). Cells were then subjected to microscopy analysis using Zeiss Axiovert 200M widefield fluorescence microscope. The proportion of cells displaying aSyn-positive intracellular inclusions in the aSyn-positive cell population was determined by counting at least 100 cells in each condition using the ImageJ software.

For Rab11a and aSyn co-localization studies, H4 cells were transfected either with pSI-aSyn, a plasmid encoding for aSyn-WT (gift from Dr Bradley T. Hyman), with empty pSI plasmid or co-transfected with plasmids encoding for aSynT and Synphilin-1 as described above. 24 h post first transfection, cells were further transfected with pEGFP-Rab11a-WT and 24 h later cells were fixed and subjected to immunocytochemistry for aSyn as described above. Cells were analyzed for Rab11a and aSyn colocalization using Zeiss LSM 510 META confocal microscope followed by analysis using the ImageJ software. Sequential multi-track frames were acquired to avoid any potential crosstalk from the two fluorophores.

For aSyn cytotoxicity assay, H4 cells were transduced with adenovirus for Rab11 knockdown or transfected with pEGFP-Rab11a-WT, pEGFP-Rab11a-S25N or pEGFP as described above and co-transfected with pSI-aSyn, a plasmid encoding for aSyn-WT (gift from Dr Bradley T. Hyman), or with empty pSI plasmid. 24 h post-transfection, culture media were used to determine the levels of released LDH as described in the manufacturer's instructions (Clontech Laboratories). LDH levels in the culture media were measured in the presence of Rab11a overexpression or Rab11 knockdown in the aSyn aggregation model described above (H4 cells transfected with aSynT and Synphilin-1) in the same manner.

### **Rab11 and aSyn co-immunoprecipitation analysis**

For co-IP experiments, brain tissue from WT Sprague–Dowley adult female rats was used. Whole-brain tissue lysates were prepared with immunoprecipitation buffer (50 mM Tris–HCl pH 7.5; 0.5 mM EDTA; 150 mM NaCl; 0.05% NP40), supplemented with protease inhibitor cocktail (Roche Diagnostics) using a HT 24 bead beating homogenizer (OPS Diagnostics). Approximately 6 mg of total protein lysates were pre-cleared by incubation with 20 ul of protein G beads (Invitrogen) for 30 min at 4°C in rotation. Supernatants were recovered and incubated overnight at 4°C in rotation, with 2 ug of the immunoprecipitation antibody, anti-aSyn (C-20, Santa Cruz Biotechnologies). The next day, 40 ul of protein G beads were added for 3 h in a rotator at 4°C. Beads were washed 5× with immunoprecipitation buffer, then re-suspended in 20 ul of protein sample buffer (50 mM Tris–HCl pH6.8; 2% SDS; 10% glycerol; 1% beta-mercaptoethanol; 0.02% bromophenol blue) and boiled at 95°C for 5 min. Supernatants were resolved on a 15% SDS–PAGE gels. Proteins were transferred overnight to nitrocellulose membranes and blocked in 5% non-fat dry milk in TBS-Tween for 1 h. In order to test the co-IP with Rab11, the membranes were incubated overnight at 4°C with the primary antibody for Rab11 (BD Biosciences, 1:1000). Immunoblots were washed with TBS-Tween and incubated for 1 h at RT with the corresponding mouse-HRP secondary antibody (GE Healthcare, 1:10 000). Immunoreactivity was visualized by chemiluminescence using an ECL detection system (Millipore) and subsequent exposure to auto-radiographic film. To prove the efficiency of aSyn immunoprecipitation, the same membrane was incubated with anti-aSyn (syn-1, BD Biosciences 1:1000) for 3 h at RT and developed as described above.

### **Data analysis and statistics**

Statistical analyses were performed using Prism 6 (GraphPad Software). All values in the figures are represented as the mean  $\pm$  standard deviation. All the data shown are representative of at least three independent experiments. For transferrin pulse-chase and aSyn aggregation assay, minimum of 100 cells were analysed per condition. Statistical analysis was performed using one-way ANOVA with Bonferroni's post hoc comparison and two-tailed Student's t-test for unpaired data (\*  $P < 0.05$ , \*\*  $P < 0.01$ , \*\*\*  $P < 0.001$ ).

### **Acknowledgements**

The authors would like to thank António Temudo from Instituto de Medicina Molecular for microscopy support and to Dr Chiara Zurzolo from Institut Pasteur for kind gift of Rab11a mammalian expression vectors. Conflict of Interest statement: none declared.

### **Funding**

O.C. was supported by Fundação para a Ciência e Tecnologia, Portugal (SFRH/BD/44446/2008). T.F.O. was supported by an EMBO Installation Grant, a Marie Curie International Reintegration Grant (Neurofold), and is currently supported by the DFG Center for Nanoscale Microscopy and Molecular Physiology of the Brain. F.G. and T.F.O. have been supported by research funding from Parkinson's UK (G-1203).



### **3.3. shRNA-Based Screen Identifies Endocytic Recycling Pathway Components that Act as Genetic Modifiers of Alpha-Synuclein Aggregation, Secretion and Toxicity**

#### **Abstract**

Alpha-Synuclein (aSyn) misfolding and aggregation is common in several neurodegenerative diseases, including Parkinson's disease and dementia with Lewy bodies, which are known as Synucleinopathies. Accumulating evidence suggests that secretion and cell-to-cell trafficking of pathological forms of aSyn may explain the typical patterns of disease progression. However, the molecular mechanisms controlling aSyn aggregation and spreading of pathology are still elusive. In order to obtain unbiased information about the molecular regulators of aSyn oligomerization, we performed a microscopy-based large-scale RNAi screen in living cells. Interestingly, we identified nine Rab GTPase and kinase genes that modulated aSyn aggregation, toxicity and levels. From those, Rab8b, Rab11a, Rab13 and Slp5 were able to promote the clearance of aSyn inclusions and rescue aSyn induced toxicity. Furthermore, we found that endocytic recycling and secretion of aSyn was enhanced upon Rab11a and Rab13 expression in cells accumulating aSyn inclusions. Overall, our study resulted in the identification of new molecular players involved in the aggregation, toxicity, and secretion of aSyn, opening novel avenues for our understanding of the molecular basis of Synucleinopathies.

#### **Introduction**

Aggregation of alpha-Synuclein (aSyn) is associated with a group of disorders known as Synucleinopathies, that include Parkinson's Disease (PD), Dementia with Lewy Bodies and Multiple System Atrophy (Maroteaux et al 1988, Spillantini et al 1998a, Spillantini et al 1998b). The common pathological hallmark among these disorders is the accumulation of aSyn in aggregates within neurons, nerve fibers or glial cells (Braak et al 1999, Spillantini et al 1997). Moreover, multiplications (Singleton et al 2003) as well as point mutations (A53T, A30P, E46K, H50Q, G51D and A53E) are associated with familial forms of PD

(Appel-Cresswell et al 2013, Fares et al 2014, Kruger et al 1998, Mezey et al 1998, Pasanen et al 2014, Proukakis et al 2013, Zarranz et al 2004).

Recent findings suggest that aSyn can oligomerize into a tetramer under physiological conditions (Bartels et al 2011, Dettmer et al 2015a, Dettmer et al 2015b, Outeiro et al 2008, Wang et al 2011), although this finding remains controversial (Binolfi et al 2012, Fauvet et al 2012a, Fauvet et al 2012b). In pathological conditions, it is widely established that aSyn can enter an amyloid pathway of aggregation, first as soluble, oligomeric species that, ultimately, can accumulate in insoluble aggregates (Ding et al 2002). The role of the large protein inclusions, such as Lewy bodies (LBs), is unclear, but they may actually constitute a protective mechanism in neurons to neutralize and preclude the effects of more toxic aSyn intermediates (Diogenes et al 2012, Karpinar et al 2009, Outeiro et al 2008, Winner et al 2011).

Although the function of aSyn is still unclear, it interacts with lipid membranes (Davidson et al 1998, Outeiro & Lindquist 2003) and seems to be involved in vesicle recycling and neurotransmitter release at the synapse (Auluck et al 2010, Liu et al 2004). Moreover, it is suggested that multimeric forms of aSyn physiologically bind to phospholipids at the synapse to chaperone SNARE-complex assembly required for neurotransmitter release, while monomeric forms are increased in disease and prone to aggregate (Burre et al 2014, Burre et al 2015, Burre et al 2010, Diao et al 2013).

Work in yeast and mammalian models suggests that aSyn-mediated cytotoxicity might be associated with alterations in vesicular trafficking, such as disruption of endoplasmic reticulum to Golgi trafficking (Cooper et al 2006, Gitler et al 2008). This could be rescued by Rab (Ras analog in brain) GTPases, which play major roles in vesicular transport, tethering, docking and fusion (Stenmark 2009). Moreover, different studies have shown that dysregulation of Rab family members, such as Rab3a and Rab3b (involved in exocytosis) and Rab5 and Rab7 (involved in the endocytic pathway), are associated with aSyn-induced toxicity in dopaminergic neurons of mammalian PD models (Chung et al 2009, Dalfo et al 2004b).

Together with the Braak staging hypothesis, the finding that LB pathology might have spread in the brains of PD patients transplanted with embryonic nigral cells (Braak et al 2003, Kordower et al 2008, Li et al 2008), suggests that aSyn is able to spread in a prion-like manner in the brain. This theory has recently been supported by several studies in

mouse models (Hansen et al 2011, Luk et al 2012, Paumier et al 2015, Volpicelli-Daley et al 2014). In neurons, secretion of aSyn follows a non-classical pathway (Jang et al 2010) that is calcium-dependent and is up-regulated under stress conditions (Emmanouilidou et al 2010). In addition, aSyn can be internalized through endocytosis or the classical clathrin-dependent pathway (Ben Gedalya et al 2009, Sung et al 2001).

In LBs, aSyn is highly phosphorylated on Ser129, contrasting with only 4% of the total protein phosphorylated at this residue in normal brain (Fujiwara et al 2002, Okochi et al 2000). This suggests that phosphorylation might interfere with the aggregation process, although it is still unclear whether phosphorylation is a trigger or a consequence of aSyn aggregation. Thus, it is critical to understand whether modulating the activity of kinases and phosphatases can interfere with aSyn aggregation and/or toxicity.

Here, we conducted an unbiased RNA interference (RNAi) screen to identify modulators of aSyn oligomerization, using the bimolecular fluorescence complementation (BiFC) assay as readout. We identified genes both encoding Rab GTPases and proteins involved in signal transduction. In addition to modifying oligomerization, the identified hits also altered aSyn toxicity and later stages of the aggregation pathway. Interestingly, we found that some of the trafficking-associated identified genes also modulated the secretion of different aSyn species. Altogether, our study brings novel insight into the molecular pathways involved in aSyn aggregation, toxicity and secretion, forming the basis for the testing of novel molecules with therapeutic potential in PD and other Synucleinopathies.

## Results

### **A Live-Cell shRNA Screen Identifies Modulators of aSyn Oligomerization**

In order to understand the contribution of different cellular pathways towards aSyn aggregation, we conducted an unbiased lentiviral vector-based RNAi screen in a cellular model of aSyn oligomerization, based upon a BiFC assay that we have previously described (Outeiro et al 2008). The screen comprised 1387 genes involved in trafficking and signal transduction-related pathways (Annex 5.2.1 and Figure 23).

We identified four genes encoding Rab proteins (*RAB8B*, *RAB11A*, *RAB13* and *RAB39B*) and five genes encoding kinases or signal transduction proteins (*CAMK1*, *DYRK2*, *CC2D1A*,

*CLK4* and *SYTL5*) that modulated aSyn oligomerization (Figure 23B, 23D and Annex 5.2.2A). Interestingly, silencing of genes encoding kinases (*ALS2CR7* and *STK32B*), or phosphatases (*PSPH* and *PPP2R5E*), did not affect aSyn oligomerization but altered the subcellular distribution of the oligomers. While silencing of *ALS2CR7* or *PSPH* promoted aSyn aggregation, silencing of *STK32B* or *PPP2R5E* reduced the nuclear localization of aSyn oligomers (Annex 5.2.3).

In the remainder of the study, we focused on the genes that modified aSyn oligomerization. Evidence of gene downregulation by the shRNAs was validated by qPCR (Annex 5.2.2B) and was confirmed by at least three different shRNAs targeting the same gene. Upon silencing of the Rab GTPase genes listed above, we observed a significant increase of aSyn-BiFC fluorescence intensity, similar to the effect of silencing *CAMK1* and *DYRK2*. Conversely, the silencing of *CC2D1A*, *CLK4* and *SYTL5* led to a significant reduction of aSyn oligomerization (Figure 23B and 23D).

To further characterize the role of the hits on aSyn oligomerization, we measured the levels of aSyn in aSyn-BiFC cells where each gene was stably silenced (Figure 23C, 23D and Annex 5.2.2.C). We found that aSyn protein levels were significantly increased upon silencing of *RAB8B* or *CAMK1*. Silencing of *RAB11A*, *RAB39B* or *DYRK2* did not change the levels of aSyn, but we found a decrease upon silencing of *RAB13*, *CC2D1A*, *CLK4* and *SYTL5*. In order to correlate the levels of oligomerization with changes in the protein levels of aSyn, we compared the ratio between protein levels and fluorescence intensity (Figure 23D). The increase in aSyn oligomerization upon silencing of *RAB8B* was accompanied by an increase in levels of aSyn, suggesting the effects might be related. On the other hand, in the case of *CAMK1* silencing, the ratio of aSyn protein levels versus aSyn oligomers was  $<1$ , suggesting that the increase in oligomerization was not simply due to an increase in the levels of aSyn. Moreover, the reduced oligomerization in cells silenced for *CC2D1A*, *CLK4* or *SYTL5* might be due to reduced levels of aSyn. In contrast, the increase in aSyn oligomerization upon *RAB11A*, *RAB39B* or *DYRK2* silencing seems independent of the levels of aSyn. Interestingly, despite the observed increase in aSyn oligomerization upon *RAB13* silencing, we found a reduction in aSyn levels relative to the control. To assess whether the silencing of the candidate genes was cytotoxic, we measured the release of lactate dehydrogenase (LDH) into the media as an indicator of cell-membrane integrity. We found that silencing of *RAB8B*, *RAB13* or *CLK4* resulted in an



increase in cytotoxicity in cells with aSyn oligomers compared to cells with no aSyn ((Figure 23E and Annex 5.2.2D).

### Loss-of-Function of Rab Proteins Promotes both Oligomerization and Aggregation of aSyn

Since aSyn oligomerization precedes the formation of larger inclusions, we next asked whether the hits identified in the screen would also modulate later stages of aSyn aggregation. To test this hypothesis, we used an established model of aSyn aggregation that results in the accumulation of LB-like inclusions in H4 cells (Klucken et al 2012, McLean et al 2001, Outeiro et al 2006). We co-transfected a C-terminal modified version of aSyn (aSynT) and Synphilin-1 in cells stably transduced with lentiviruses encoding shRNAs targeting each of the identified hits, and then assessed inclusion formation using immunocytochemistry and fluorescence microscopy (Figure 24A, 24B and Annex 5.2.4A). We quantified the percentage of cells according to the pattern of aSyn distribution, *i.e.* cells with no inclusions, cells with less than ten or cells with more than ten inclusions.

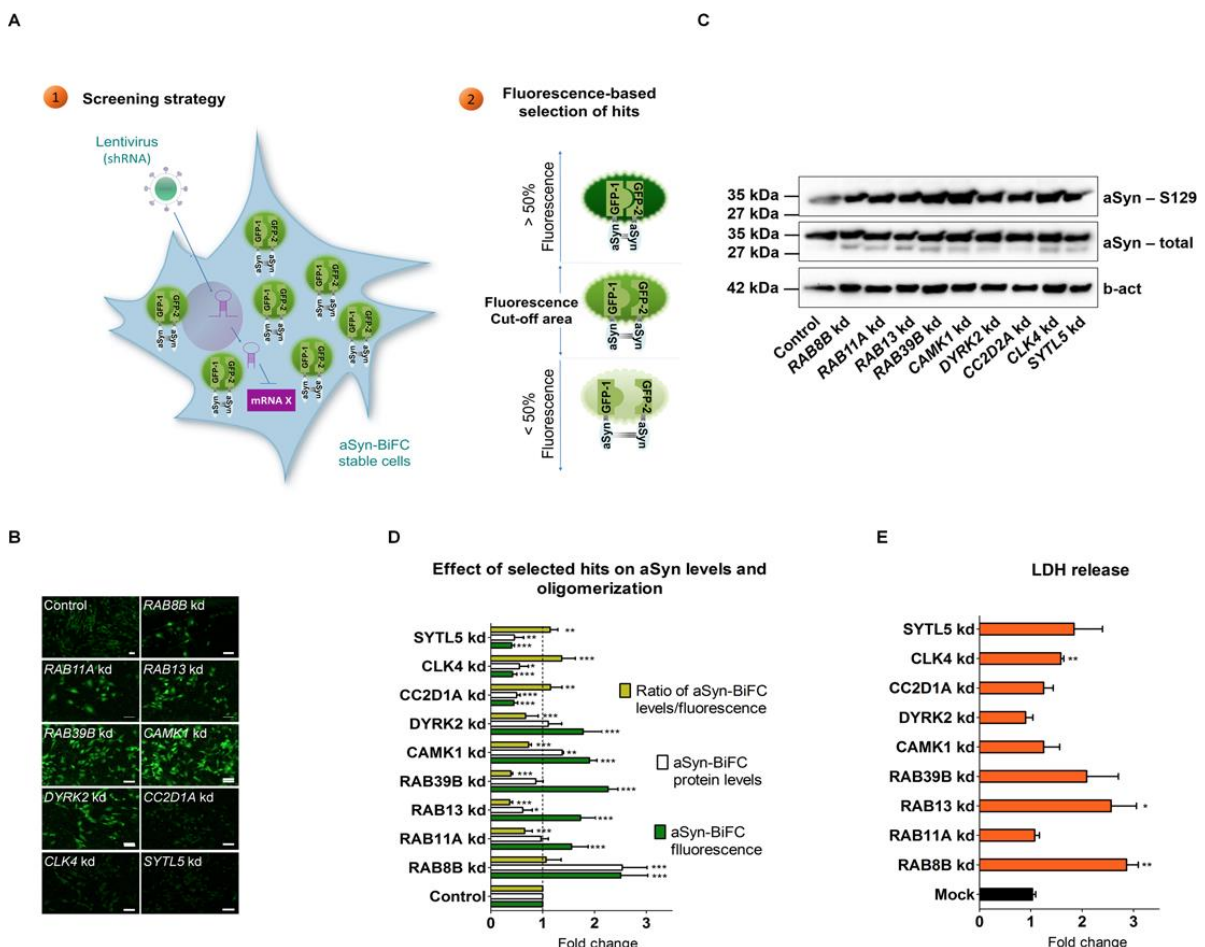


**Figure 23. RNAi-based screen for genes that modify aSyn oligomerization in living cells.** **A.** A human shRNA library targeting trafficking and phosphotransferase genes was screened using a stable cell line expressing aSyn-BiFC constructs (1). Genes modifying aSyn oligomerization by at least 50% (2) were identified using fluorescence microscopy analysis and considered for further validation. **B.** Representative live cell imaging pictures of aSyn-BiFC stable H4 cells silenced for hits that increase (*RAB8B*, *RAB11A*, *RAB13*, *RAB39B*, *CAMK1*, *DYRK2*) or decrease (*CC2D1A*, *CLK4*, *SYTL5*) aSyn oligomerization (green). A scrambled shRNA was used as control. Scale bars: 20  $\mu$ m. **C.** Representative immunoblot of aSyn-BiFC cells subjected to silencing of the selected hits **D.** Relative fluorescence quantification of aSyn oligomerization (green) and quantification of aSyn protein levels (white). The ratio of protein levels and aSyn oligomerization is presented (yellow). **E.** LDH release in the media from cells with aSyn oligomers versus no aSyn (orange). Bars represent mean  $\pm$  95% CI (\*: 0.05<p>0.01; \*\*: 0.01<p>0.001; \*\*\*: p<0.001) and are normalized to the control of at least three independent experiments. Single comparisons between the control and experimental groups were made through Wilcoxon test. Silencing of hits was performed using at least three different shRNAs against the same gene. For simplicity, only one shRNA is shown. Results with additional shRNAs are presented in Annex 5.2.2. Kd, knockdown.

In the conditions tested, more than 80% of control cells presented less than ten intracellular inclusions, 14% did not present inclusions, and less than 4% of the cells displayed ten or less inclusions. In contrast, the silencing of all the hits except *CLK4* and *DYRK2* resulted in an increase in the percentage of cells displaying aSyn inclusions (Figure 24A, 24B and Annex 5.2.4A). Moreover, with the exception of *RAB39*, the silencing of all hits caused an increase in the percentage of cells with more than 10 inclusions. This effect was stronger upon silencing of *RAB8B* (approximately 60% of cells displaying more than ten inclusions), followed by *SYTL5* (27%) and *RAB13* (15%). Together these data suggest that the hits can also modulate later steps of the aggregation process of aSyn. To assess whether the silencing of the different hits altered cytotoxicity in the aSyn aggregation model we measured cell membrane integrity, as described above. Only the silencing of *RAB8B* and *RAB39B* resulted in an increase in cytotoxicity (Figure 24C and Annex 5.2.4B). Interestingly, the silencing of *CLK4* resulted in the accumulation of inclusions with irregular shapes and silencing of *SYTL5* resulted in the accumulation of elongated cells (Annex 5.2.4C).

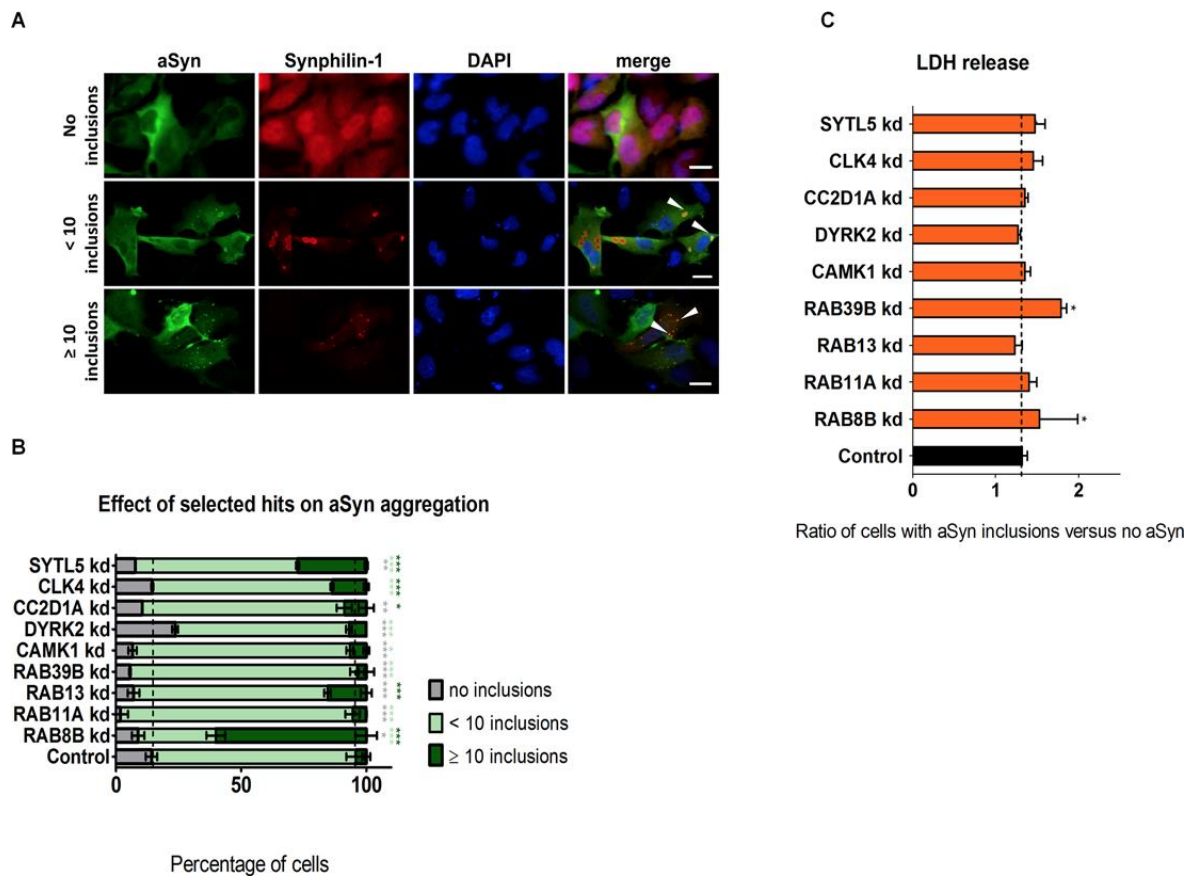


**Figure 24. Effect of silencing of selected hits on aSyn aggregation.** **A.** Stable H4 cells silenced for selected hits or with a scrambled shRNA were co-transfected with aSynT and Synphilin-1. Cells were fixed 48 h post-transfection and subjected to immunocytochemistry for aSyn (green) and for Synphilin-1 (red) followed by fluorescence microscopy. DAPI was used as a nuclear counterstain. White arrowheads point to aSyn inclusions. Scale bars: 10  $\mu$ m. **B.** Percentage of cells with no inclusions (gray), less than 10 inclusions (light green) or more than 10 inclusions (dark green). **C.** Cytotoxicity (measured by LDH release in the media) from stable cells subjected to hits silencing and normalized to control (cells transduced with scrambled shRNA). The ratio represented refers to cells with aSyn inclusions versus cells with no aSyn. Bars represent mean  $\pm$  95% CI (\*: 0.05<p>0.01; \*\*: 0.01<p>0.001; \*\*\*: p<0.001) and are normalized to the control of at least three independent experiments. Single comparisons between the control and experimental groups were made through Wilcoxon test. Kd, knockdown.

In order to further evaluate whether trafficking indeed plays a role in aSyn aggregation, we silenced another traffic component involved in exocytosis (*RAB27A*). We found that silencing of *RAB27A* increased aSyn oligomerization and did not affect aSyn levels or

cytotoxicity (Annex 5.2.5 and 5.2.6). Furthermore, in the aggregation model, it increased the percentage of cells displaying aSyn inclusions, without affecting toxicity (Annexes 5.2.5H and 5.2.5I). Thus, the effects of RAB27A silencing are consistent with those observed with the hits selected in our screen.

#### **aSyn Cell-to-Cell Trafficking is Increased upon Silencing of *RAB8B*, *RAB13* or *SYTL5***

We and others have previously shown that aSyn can be secreted and affect multiple steps of membrane trafficking (Chai et al 2013, Chutna et al 2014b, Emmanouilidou et al 2010, Lee et al 2005). Therefore, we next investigated whether the trafficking of aSyn was affected upon silencing of four selected hits (*RAB8B*, *RAB11A*, *RAB13* or *SYTL5*) and *RAB27A*, involved in different steps of intracellular trafficking.

To study cell-to-cell trafficking of aSyn, we used the aSyn-BiFC system with VENUS (Danzer et al 2012, Herrera et al 2011). Firstly, *RAB8B*, *RAB11A*, *RAB13* or *SYTL5* were silenced in H4 cells and, 24 h later, cells were transfected with either VENUS1-aSyn or aSyn-VENUS2 plasmids, separately. 24 h later, an equal number of cells transfected with VENUS1-aSyn or aSyn-VENUS2 were mixed. 72 h later, mixed cultures were analyzed by flow cytometry and microscopy for the presence of fluorescence signal, which indicates bimolecular complementation of the VENUS fluorophore and, thus, cell-to-cell trafficking of aSyn (Figure 25A). Scramble-mixed populations of VENUS1-aSyn and aSyn-VENUS2 were used to quantify cell-to-cell transfer of aSyn and used as a control to compare the effect of silencing of trafficking hits on aSyn intercellular transfer (Figure 25B). Fluorescence of cells containing a single BiFC plasmid was identical to cells without any plasmid. In the mixed population of cells that were silenced for *RAB8B*, *RAB13* and *SYTL5*, we observed a significant number of fluorescent cells, indicating that transfer of aSyn between cells occurred. By knocking down *RAB8B* or *RAB13*, we observed that the number of fluorescent cells increased to 4%, double of the control situation, while *SYTL5* knock down resulted in fluorescence in 7% of cells in population, more than three times the fluorescence of scrambled cells, while silencing of *RAB11A* or *RAB27A* had no effect (Figure 25B, 25C, 25D and Annexes 5.2.5E).

### **Endocytic Recycling of aSyn Oligomers is Mediated by Rab11a and Rab13**

Next, we assessed whether overexpression of the hits selected would have the inverse effects to those observed upon silencing. For this, we expressed Rab8b, Rab11a, Rab13 and Slp5 in aSyn oligomerization model. In the case of Rab8b, Rab11a or Rab13, we compared the effects of overexpressing wild type forms, constitutively active mutants (Rab8b-Q67L, Rab11a-Q70L and Rab13-Q67L), or dominant-negative mutants (Rab8b-T22N, Rab11a-S25N and Rab13-T22N). We found that overexpression of wild type forms or the constitutively active mutants of the Rab proteins significantly reduced aSyn oligomerization, while overexpression of Slp5 had no effect (Figure 26A, 26B and Annexes 5.2.7, 5.2.8, 5.2.9 and 5.2.10). Overexpression of wild type or mutant forms of Rab13 reduced almost four times aSyn oligomerization. The dominant negative form of Rab8b, Rab8b-T22N, had a more attenuated effect on aSyn oligomerization compared to Rab8b-WT or Rab8b-Q67L. The dominant negative mutant of Rab11a did not change aSyn oligomerization.

To investigate whether the endocytic recycling pathway was altered in the presence of aSyn oligomers, we monitored the distribution of fluorescently-labeled Transferrin (Tf), which follows the endocytic recycling pathway and marks the endocytic recycling compartment (ERC). As expected, Tf accumulated in ERC in control cells without aSyn. In contrast, in cells expressing aSyn-BiFC, Tf lost the preferential accumulation in the ERC, appearing at the periphery of the cell (Figure 26A and Annex 5.2.10B). We measured the fluorescence intensity of Alexa-647-Tf and observed that the expression of wild type forms of Rab11a or Rab13 decreased the amount of the Tf within cells. In contrast, the dominant-negative forms of Rab11a and Rab13 showed a stronger Tf intracellular signal than control (Figure 26C and Annexes 5.2.8 and 5.2.9). These results indicate that overexpression of the selected Rab hits restores endocytic recycling in cells accumulating aSyn oligomers. We also found that expression of Slp5 did not alter the intracellular Tf signal, while Rab8b increased it (Figure 26C and Annexes 5.2.7A and 5.2.10A).

To further determine if aSyn oligomers were secreted from cells, we measured the levels of aSyn both in the media and in cell lysates. We observed no differences in the intracellular levels of aSyn. Moreover, although secretion was slightly increased upon overexpression of all hits, only Slp5 overexpression significantly increased aSyn secretion (Figure 26E). Given that cells overexpressing each of the selected hits showed reduced

cytotoxicity (Figure 26D), we concluded that the release of aSyn was not due to cell death. Overall, our results suggest that the overexpression of Rab11a and Rab13, but not Rab8b or Slp5, promotes endocytic recycling of aSyn oligomers. Also, the Slp5-mediated release of aSyn oligomers does not appear to be due to increased trafficking of aSyn via the endocytic recycling pathway.

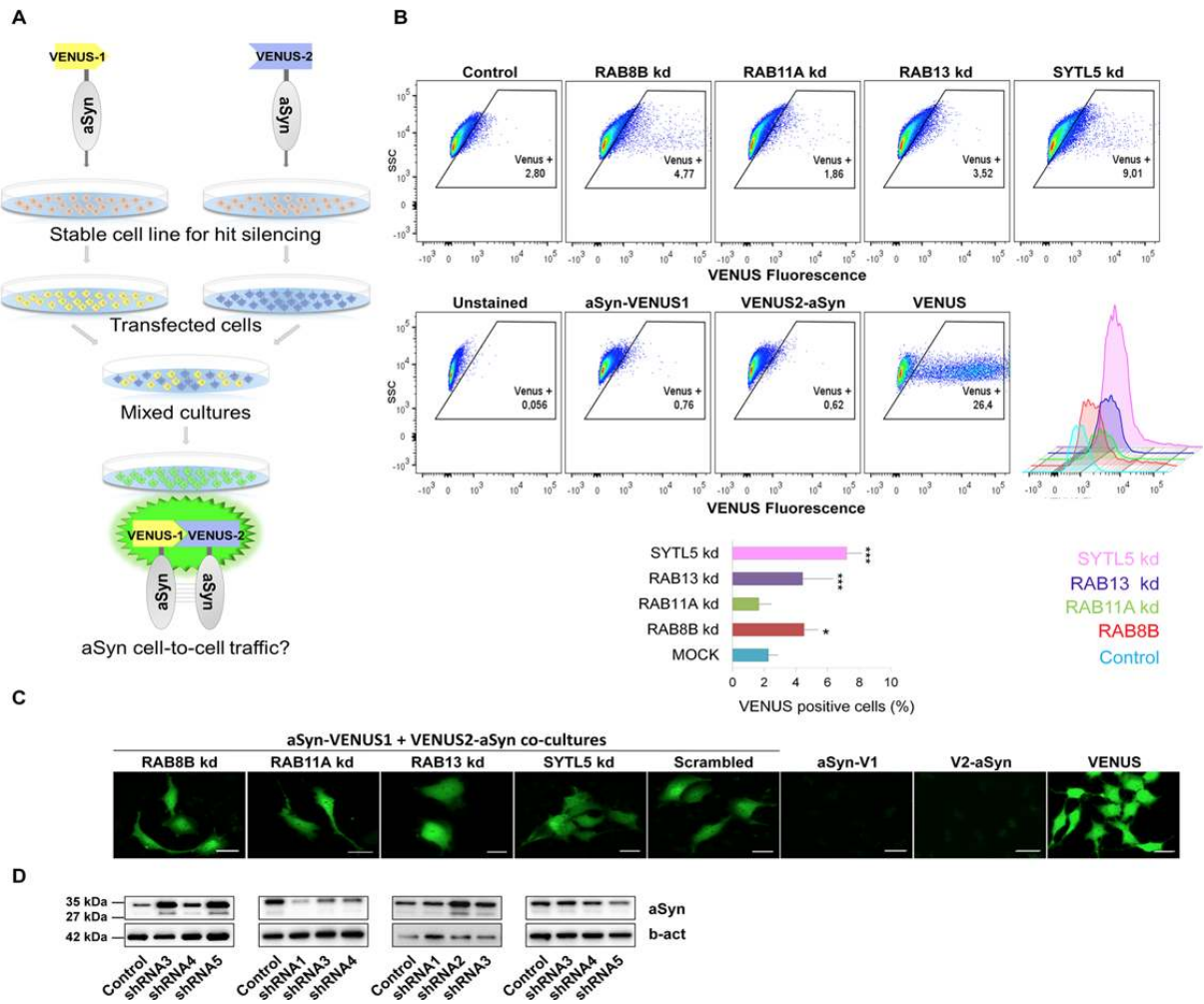


**Figure 25. Silencing of *RAB8B*, *RAB13* or *SYTL5* increases aSyn cell-to-cell trafficking.** **A.** Experimental design of aSyn cell-to-cell trafficking assay. Stable cells silenced for *RAB8B*, *RAB11A*, *RAB13*, *SYTL5* with a scrambled shRNA were transfected separately with plasmids encoding either VENUS1-aSyn or aSyn-VENUS2. 24 h later, cells were mixed and co-cultured for 72 h. Upon release and uptake of the aSyn-VENUS fusions, reconstitution of the fluorescence signal can be detected inside cells, and the signal quantified through flow cytometry or microscopy. **B.** VENUS positive cells were monitored by flow cytometry. A representative result is shown as side scatter

(SSC) versus VENUS fluorescence, with the corresponding histogram. The percentage of VENUS positive cells is indicated by the mean  $\pm$  95% CI of at least three independent experiments. **C.** *In vivo* imaging of aSyn-VENUS1 and VENUS2-aSyn mixed cells subjected to silencing of the selected hits. Scale bar: 20  $\mu$ m. **D.** Immunoblotting analysis of, total aSyn and beta-actin. Bars represent mean  $\pm$  95% CI (\*: 0.05<p>0.01; \*\*: 0.01<p>0.001; \*\*\*: p<0.001) and are normalized to the control of at least three independent experiments. Single comparisons between the control and experimental groups were made through Wilcoxon test. Kd, knockdown.

### **Overexpression of Rab11a and Rab13 Increases aSyn Secretion and Clearance of aSyn Inclusions**

To further explore the role of the hits identified on aSyn inclusion formation, we used the aSyn aggregation model and overexpressed Rab8b, Rab11a, Rab13 or Slp5. We found that wild type and constitutively active forms of Rab8b, Rab11a and Rab13 significantly decreased the percentage of cells with aSyn inclusions, when compared with the dominant negative forms or control. A similar effect was verified with the overexpression of Slp5 (Figure 27A and 27B). These results are consistent with those obtained upon silencing of the same genes (Fig 24B). Interestingly, in cells lacking aSyn inclusions, Rab8b, Rab11a, Rab13 and Slp5 were normally distributed in the cell, as in the control situation (Figure 26A, and Annexes 5.2.7, 5.2.8, 5.2.9 and 5.2.10). However, we found that in cells with aSyn inclusions, these four proteins changed their subcellular localization and co-localized with the inclusions (Figure 27A and Annexes 5.2.7, 5.2.8, 5.2.9 and 5.2.10). Together, these results suggest that Rab8b, Rab11a, Rab13 or Slp5 can modulate aSyn aggregation and can be recruited into inclusions.

To investigate whether endocytic recycling was altered in the presence of aSyn inclusions, we monitored this process using Alexa-647-labeled Tf. Normally, Tf accumulates in the ERC. In our experiments, we found that Slp5 and wild type or constitutively active mutant forms of Rab8b, Rab11 and Rab13 decreased the intracellular fluorescence signal of Tf. In contrast, cells expressing the dominant-negative forms of these Rabs displayed similar fluorescence intensity to the controls (Fig 27C). These results indicated that recycling through the endocytic recycling pathway was compromised in cells with aSyn inclusions, as more Tf accumulated inside the cells, and that overexpression of wild type and



constitutively-active forms of Rab8b, Rab11a, and Rab13, and Slp5, could rescue this defect.

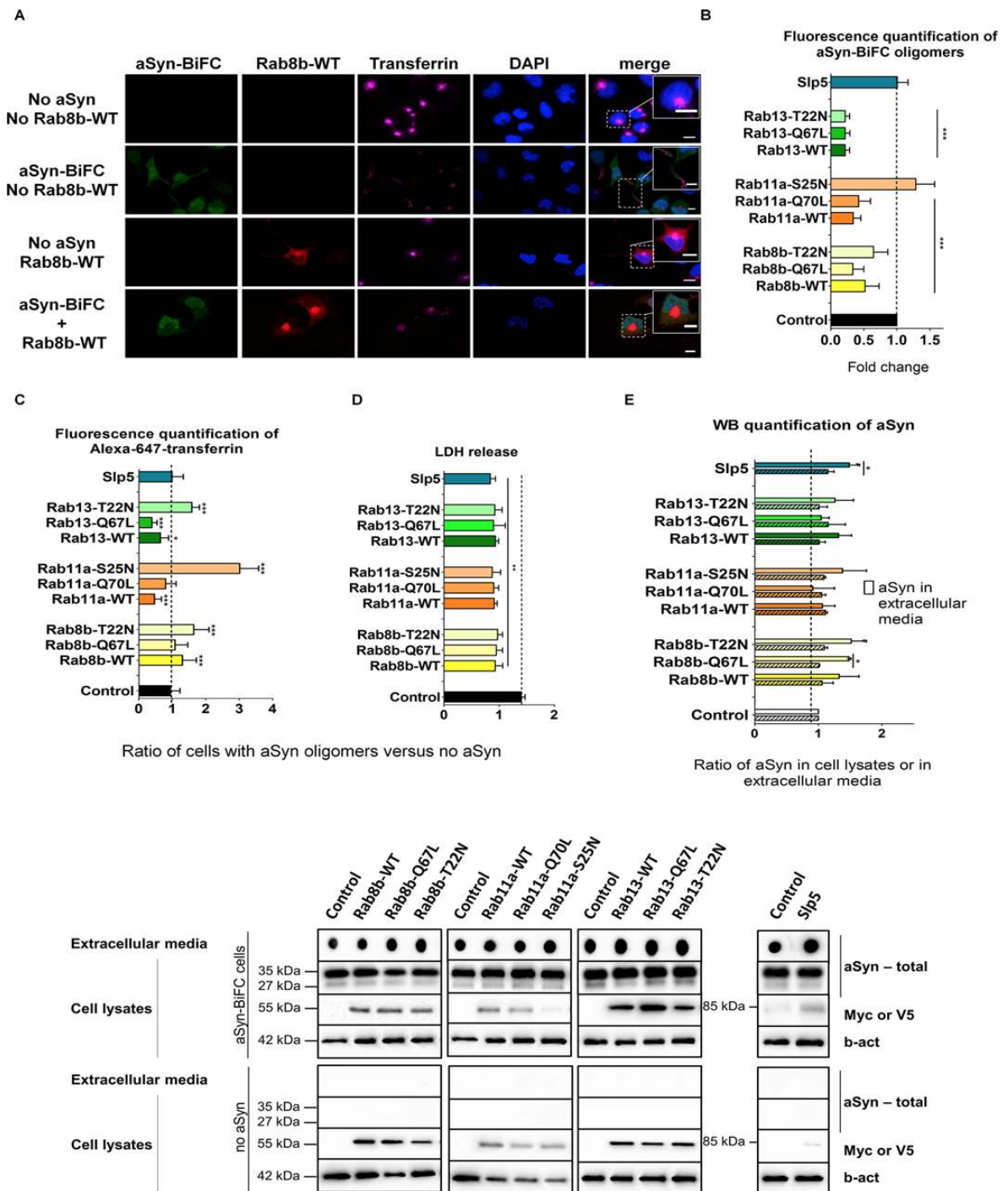


**Figure 26. Overexpression of selected hits reduces aSyn oligomerization and modulates endocytic recycling and secretion.** **A.** H4 stable cells for aSyn-BiFC (green) or H4 cells with no aSyn were transfected with constructs expressing Rab8b, Rab11a, Rab13, Slp5 (red) or empty vector. 48 h post-transfection, media with no serum was replaced in cells for 1 h. Cells were



incubated with Alexa-647 human transferrin (magenta) for 30 min, prior to fixation. DAPI was used as a nuclear counterstain. Cells were subjected to confocal microscopy. For simplicity, because all expressed hits have similar subcellular locations, only wild type form of Rab8b is shown. Imaging of the remaining constructs is presented in Annexes 5.2.7, 5.2.8, 5.2.9 and 5.2.10. Squares are regions zoomed-in showing transferrin localization within endocytic recycling compartment in cells with no aSyn oligomers or hit, at cells extremities in cells with aSyn oligomers and no hit, and colocalizing the hit in cells with or without aSyn. Scale bars: 10  $\mu$ m. **B.** Relative aSyn-BiFC fluorescence upon hits overexpression compared to the control (empty vector transfection). **C.** Quantification of Alexa-647 transferrin intensity normalized to the control condition. The represented ratio refers to cells with aSyn oligomers versus cells with no aSyn. **D.** LDH extracellular levels were measured to assess cytotoxicity. The ratio represented refers to cells with aSyn oligomers versus cells with no aSyn. **E.** Relative quantification of aSyn intracellular total protein (stripe pattern) and extracellular conditioned media (clear pattern) for each condition. A representative immunoblot is shown. In graphs, Rab8b is represented in yellow, Rab11a in orange, Rab13 in green and Slp5 in blue. Bars represent mean  $\pm$  95% CI (\*: 0.05<p>0.01; \*\*: 0.01<p>0.001; \*\*\*: p<0.001) and are normalized to the control of at least three independent experiments. Single comparisons between the control and experimental groups were made through Wilcoxon test.

To determine whether Rab8b, Rab11a, Rab13 or Slp5 played a role in aSyn secretion when this protein is aggregated, we measured the levels of aSyn in conditioned media. We found that aSyn secretion was not changed by Slp5 (Figure 27E). However, wild type forms of the Rabs increased aSyn secretion. To further confirm that the increased levels of extracellular aSyn were not due to increased cell death, we measured the release of LDH, and found that all the hits tested were protective (Figure 27D).

Altogether these results show that overexpression of Rab8b, Rab11a, Rab13 or Slp5 reduces aSyn aggregation, and that the subcellular localization of these proteins is altered in the presence of aSyn inclusions, since they all co-localize. Overexpression of these Rabs also promotes aSyn secretion, which can occur through the endocytic recycling pathway. Thus, the increased aSyn secretion upon Rab8b, Rab11a and Rab13 overexpression can explain the decrease of aSyn inclusions within the cells, as this effect is not related with an increase in cell death.

## Discussion

Increasing evidence suggests that pre-fibrillar, oligomeric forms of aSyn are the toxic species that lead to pathology (Karpinar et al 2009, Lashuel et al 2002, Winner et al 2011). The main objective of this study was to identify regulators of aSyn oligomerization, an early step of the aggregation process that precedes the formation of larger protein assemblies typically referred to as protein aggregates. To do this, we performed an RNAi screen targeting 76 membrane trafficking and 1311 phosphotransferase genes using a cell model of aSyn oligomerization. Interestingly, given the uniqueness of our approach, based on live-cell imaging of aSyn oligomers, the screen also enabled us to identify genes that did not alter aSyn oligomerization but modified the subcellular distribution of the oligomeric species.

With respect to the primary goal of the screen, we identified four genes encoding Rab proteins (*RAB8B*, *RAB11A*, *RAB13* and *RAB39B*) and five genes encoding phosphotransferase proteins (*CAMK1*, *DYRK2*, *CC2D1A*, *CLK4* and *SYTL5*) that modulated both oligomerization and aggregation (except *DYRK2*) of aSyn.

Regarding the effect of the hits on aSyn oligomerization and protein levels, we identified hits that increased both parameters, as in the case of *RAB8B* and *CAMK1*. Interestingly, silencing of *RAB8B*, but not *CAMK1*, is toxic in the presence of aSyn oligomers. The fact that *RAB8B* silencing is also toxic in the presence of aSyn inclusions suggests this is a relevant modulator at two different stages of aSyn aggregation process. Camk1 is a Calmodulin-dependent kinase that plays a role in axonal growth (Ageta-Ishihara et al 2009). Until now Camk1 activity had not been associated with aSyn. However, Camk2 seems to play an essential role in the redistribution of aSyn during neurotransmitter release at the synapse (Liu et al 2007). Moreover, Camk2 forms a complex with aSyn and seems to regulate its oligomerization status (Martinez et al 2003). If Camk1 and Camk2 share some functionality, this might explain the stronger downstream effect of *CAMK1* silencing, with a more pronounced effect on oligomerization rather than on the levels of aSyn. We also identified hits that decreased both aSyn oligomerization and protein levels; for example, the silencing of *CC2D1A*, *CLK4* and *SYTL5* decreased oligomerization probably because they reduce the levels of aSyn. Silencing of *CLK4*, but not of *CC2D1A* and *SYTL5*, is toxic to the cells. Thus, we can speculate that, at least for *CC2D1A* and *SYTL5*, the effects

observed are not due to cytotoxicity, as membrane integrity is preserved, and these hits can be further tested as candidate therapeutic modulators in Synucleinopathies.

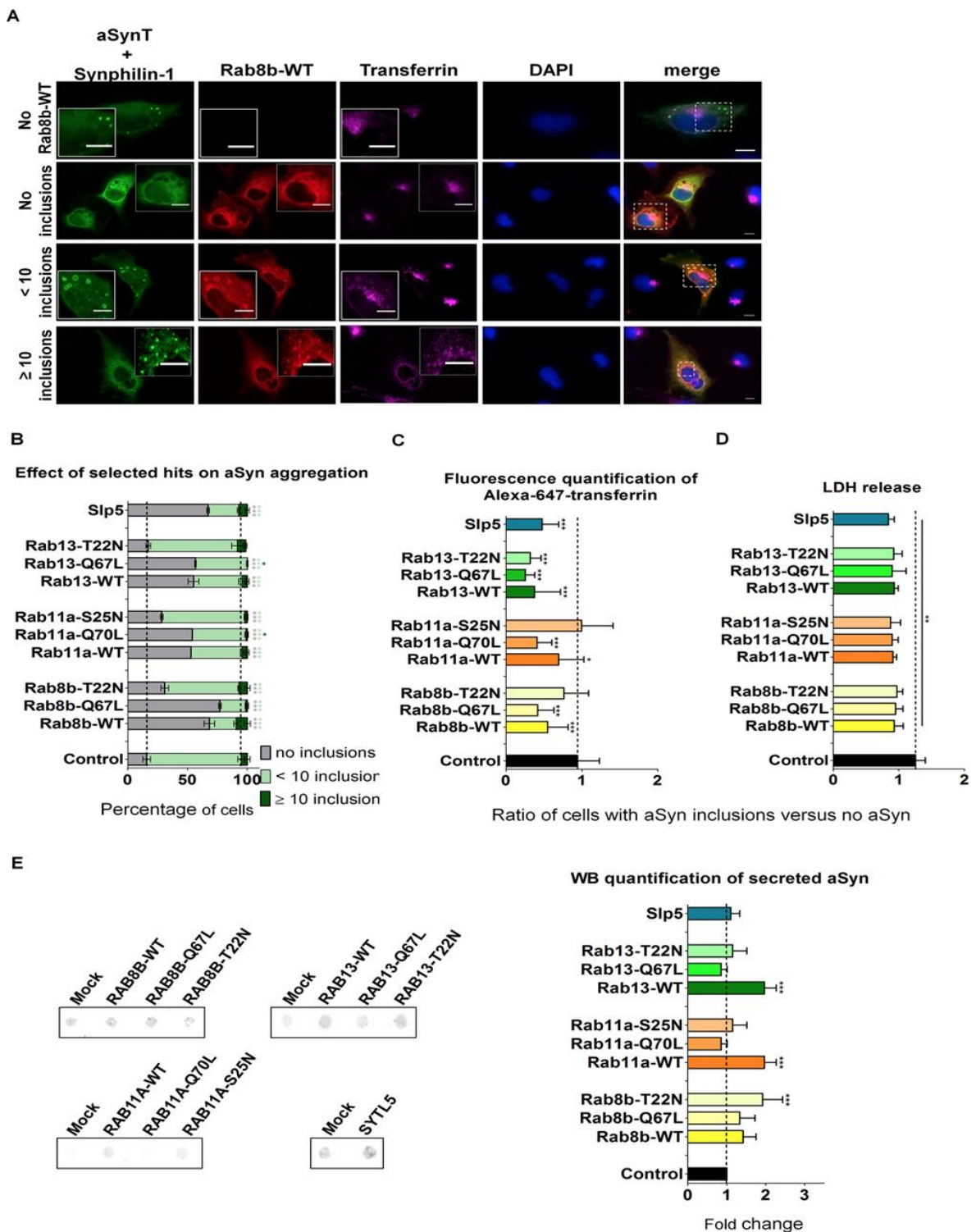


Figure 27. Overexpression of Rab8b, Rab11a, Rab13 and Slp5 reduces aSyn aggregation and modulates endosomal recycling and secretion. A. H4 cells were triple-transfected with aSynT,

Synphilin-1 and constructs expressing Rab8b, Rab11a, Rab13, Slp5 (red) or empty vector. 48 h post-transfection, media with no serum was replaced in cells for 1 h. Cells were incubated with Alexa-647 human transferrin (magenta) for 30 min, prior to fixation and subjected to immunocytochemistry for aSyn (green), and followed by confocal microscopy. DAPI was used as a nuclear counterstain. Control with empty vector is shown. Amplifications within cells were made to show co-localization between aSyn, the hit and transferring within inclusions. For simplicity, only Rab8b-WT is shown. Imaging of the remaining constructs is shown in Annexes 5.2.7, 5.2.8, 5.2.9 and 5.2.10. Scale bars: 10  $\mu$ m. **B.** Quantification of the number of aSyn inclusions per cell. The cells displaying aSyn inclusions were divided in: cells with no inclusions (represented in black), cells with less than 10 inclusions (in light gray) and cells with more than 10 inclusions (in dark gray). Only triple transfected cells were considered for the quantifications. **C.** Quantification of alexa-647 transferrin intensity normalized to the control condition. **D.** Cytotoxicity was measured by the LDH-release assay. The represented ratios in C and D refers to cells with aSyn inclusions versus cells with no aSyn **E.** Representative immunoblot of extracellular conditioned media from cells overexpressing the selected genes in the aSyn aggregation model, and respective quantification. In graphs, Rab8b is represented in yellow, Rab11a in orange, Rab13 in green and Slp5 in blue. Bars represent mean  $\pm$  95% CI (\*: 0.05<p>0.01; \*\*: 0.01<p>0.001; \*\*\*: p<0.001) and are normalized to the control of at least three independent experiments. Single comparisons between the control and experimental groups were made through Wilcoxon test.

Moreover, we also found hits that had a direct effect on oligomerization without changing the levels of aSyn; silencing of *RAB11A*, *RAB39B* and *DYRK2* increased oligomerization without affecting the levels of aSyn. Silencing of *RAB39B* was toxic in the aSyn aggregation model but not in the oligomerization model. Thus, from a therapeutic perspective, hits that modify oligomerization or aggregation without altering the levels of aSyn are of great interest. Finally, we found one hit (*RAB13*) that increased oligomerization while reducing the levels of aSyn. When overexpressed, this gene was protective against toxicity, reduced oligomerization and did not alter the levels of aSyn. In total, our findings reveal an intricate connection between aSyn aggregation, toxicity and levels that will need to be further investigated in future studies.

Four out of the nine modifiers of aSyn oligomerization and aggregation were Rab small GTPases. Rab GTPases are a family of more than 60 members in humans that are master regulators of intracellular formation of vesicles, motility and release, thereby playing a

key role in neuronal trafficking (reviewed in (Eisbach & Outeiro 2013, Villarroel-Campos et al 2014)). Rab GTPases switch between GDP-bound (inactive) and GTP-bound (active) states to regulate downstream cellular functions. It is the activation by a guanine-nucleotide exchange factor (GEF) that converts an inactive Rab into the active GTP-bound form (Seabra & Wasmeier 2004). Active Rab GTPases can bind Rab effectors, which control the spatiotemporal regulation of Rab steps within cells. Given the importance of Rab GTPases and their effectors in the regulation of membrane trafficking, several human disorders have been associated with their dysfunction, in particular diseases affecting neuronal cells (reviewed in (Seixas et al 2013)).

Although the hits identified fall into several different functional classes, all but *SYTL5* affect neuronal trafficking (Ageta-Ishihara et al 2009, Di Giovanni et al 2005, Giannandrea et al 2010, Greenfield et al 2002, Hattula et al 2002, Jain et al 2014, Martinelli et al 2012, Slepak et al 2012). We focused on hits involved in secretion, as this process might underlie the spreading and transmission of aSyn pathology in the brain (Braak et al 2003). Thus, we further characterized the effect of Rab8b, Rab11a, Rab13 and Slp5 on aSyn aggregation. Rab8 is associated with actin and microtubule cell reorganization and polarized trafficking to dynamic cell surface structures (Hattula et al 2002). Interestingly, Rab8 is able to reconstitute Golgi morphology in cellular models of PD (Rendon et al 2013) and, in addition, we recently reported that aSyn interacts with Rab8a. Moreover, we also found that Rab8 rescues the aSyn-dependent loss of dopaminergic neurons in *Drosophila* (Yin et al 2014). Here, we showed that silencing of Rab8b increased the accumulation of oligomeric or aggregated species of aSyn and was toxic to cells, while overexpression of Rab8b reverted those effects. Rab11a is ubiquitously expressed with preferential localization to ERC. Defective trafficking of Rab11 from the ERC has been implicated in AD, HD and PD (Greenfield et al 2002, Li et al 2009, Liu et al 2009a). Rab11a is involved in the process of exocytosis of aSyn via RE (Liu et al 2009a). Silencing of Rab11a increased accumulation of oligomeric or aggregated aSyn, while overexpression of Rab11a was protective and reverted the oligomerization and aggregation of aSyn, as we previously reported in independent studies (Breda et al 2014, Chutna et al 2014b). Rab13 mediates trafficking between the trans-Golgi network and recycling endosomes (Nokes et al 2008) and it is associated with neuronal plasticity, neurite outgrowth, cell migration and regulation of tight junctions. Interestingly, we found that Rab13 silencing

was toxic to cells with aSyn oligomers but not to cells with aSyn inclusions. On the other hand, overexpression of Rab13 reduced aSyn toxicity in both cell models. We also found that Rab11a and Rab13 decrease the amount of intracellular Tf both in the models of aSyn oligomerization and aggregation. Moreover, secretion of aSyn is also differentially affected depending on the cell model, suggesting that the endocytic recycling pathway might be used to clear aSyn aggregates, possibly through secretion. Slp5 is a calcium-dependent protein that belongs to the Synaptotagmin-like protein family. Proteins from this family contain tandem C2 domains that bind phospholipids and proteins associated with the plasma membrane. Slp5 interacts with GTP-bound Rab27a, Rab3a and Rab6a, but not with Rab8 or Rab11a (Kuroda et al 2002b). As an effector of Rab27a, Slp5 mediates the tethering/docking of Rab27a-positive vesicles to the plasma membrane (Fukuda 2013). Moreover, it can modulate the Rab27a-mediated transport of Cystic Fibrosis Transmembrane conductance Regulator (CFTR) to the membrane (Saxena & Kaur 2006). Slp5 can be found in the brain and in other tissues, and was shown to promote exocytosis of dense core in PC12 cells (Fukuda 2003). On other hand, *SYTL5* was also identified in another RNAi screen as player in chemotaxis (Colvin et al 2010), being potentially important in the generation of inflammatory responses. To the best of our knowledge, Slp5 had not been previously associated with brain disorders. Here, we showed that Slp5 silencing decreases aSyn oligomerization and increases the number of aSyn inclusions per cell. Moreover, the recycling endocytic pathway is active upon Slp5 overexpression in cells presenting aSyn inclusions, but the levels of aSyn secretion are not altered (Figure 28 and Annex 5.2.6).

Interestingly, *RAB27A* was not identified in our primary RNAi screen (Annex 5.2.1). We hypothesize that this might be due to redundancy between Rab27 isoforms and also because this GTPase has at least eleven different effectors (Fukuda 2013) that may mask the effects of RNAi-mediated silencing. Although silencing of *RAB27A* does not affect aSyn oligomerization or secretion, it promotes aggregation (Annex 5.2.5). This further supports the hypothesis that trafficking components are key players in aSyn homeostasis.

Remarkably, we found that overexpression of Rab8, Rab11a, Rab13 and Slp5 significantly increases the percentage of cells without inclusions to 50-75%. Although future studies will be important to further clarify the precise molecular mechanisms involved, it is possible that these proteins reduce aSyn aggregation by affecting its release. A second

important observation showed that, in the remaining cells displaying aSyn inclusions, Rab8, Rab11a, Rab13 and Slp5 localized in the inclusions together with aSyn. Therefore, and as previously suggested, the sequestration of the Rabs in the inclusions may affect their function (Chutna et al 2014a).

Additional studies will be necessary to clarify the relationship between the genes we identified and their cellular functions, especially those related to the endocytic recycling pathway. For example, in addition to Rab11a, Rab8 also assists the transport of Tf within cells and colocalizes with Slp1 and Slp4 (Hattula et al 2006, Kuroda et al 2002a). In fact, in cells with no inclusions, transferrin (Tf) labels the endocytic recycling compartment (ERC). In cells with inclusions, the ERC location of Tf was maintained but the signal was weaker. However, if one of the selected traffic hits is overexpressed in cells with few aSyn inclusions, Tf can be seen at i) the ERC (as the traffic hit) and ii) in aSyn inclusions, co-localizing with the hit. If the number of inclusions is higher, Tf signal loses the ERC location (as the overexpressed hit) and is redistributed in inclusions. This sequential difference in Tf location reflects the possible redistribution of trafficking players and, thus, represents an alteration in the endocytic recycling machinery promoted by aSyn aggregation. This effect can synergistically be explained by a first cellular attempt to flow the excess of aSyn within the cell specifically when it is aggregated. The increase in aSyn secretion in the aSyn aggregation model (upon expression of all selected hits) suggests that endocytic recycling is being activated as less Tf signal is detected. However, when there are more inclusions in the cells there is a higher chance that the hits will be sequestered in the inclusions. aSyn is known to be secreted under physiological conditions, possibly via unconventional exocytosis, as it lacks an ER-targeting signal peptide. Although the precise mechanisms involved are still unclear, multiple secretory pathways have been described (Lee et al 2005). However, it was demonstrated that pathological and aggregated species of aSyn can also be secreted (Pacheco et al 2012). This suggests that misfolded and aggregated aSyn is a key agent for the propagation of PD pathology by a prion-like mechanism (Bernis et al 2015, Tyson et al 2015). In this context, aggregation can be viewed as a protective mechanism, as it could arrest the toxic species that would otherwise be secreted. This is consistent with several observations by different groups, including our own, that protein aggregates (or at least some types of aggregates) appear to be less toxic than smaller, oligomeric species. It is possible that,

after a certain threshold, the cumulative failure of cellular quality control systems, together with the secretion of aSyn, disrupts the initial cellular attempt to contain pathological aSyn species. As a result, toxic species of aSyn can spread in a prion-like manner.

Since we found that silencing of *RAB8B*, *RAB13* or *SYTL5* augmented aSyn cell-to-cell transfer (Figure 25B and 25C), these genes emerge as potential modifiers of the spreading of aSyn pathology. Transfecting independent cells with VENUS1-aSyn or aSyn-VENUS2 plasmids for 24h, and then mixing equal numbers of each cell population, enables the study of aSyn cell-to-cell transmission using the split-VENUS BiFC system. We observed a two to threefold increase in aSyn cell-to-cell transfer upon silencing of *RAB8B*, *RAB13* or *SYTL5*, while silencing of *RAB11A* or *RAB27A* had no effect when compared to scramble-infected cells. This is further supported by a stronger signal in the immunoblot of at least two of three shRNAs used to silence *RAB8B*, *RAB13* or *SYTL5*. Linking these results with the oligomerization state of aSyn, silencing of both *RAB8B* and *RAB13* promoted aSyn oligomerization, probably because the balance between the entrance and exit of aSyn is increased in those cells. On the other hand, silencing of *SYTL5* decreased oligomerization and increased cell-to-cell transfer of aSyn. Recently, aSyn was shown to be secreted by exosomes (Alvarez-Erviti et al 2011, Danzer et al 2012, Emmanouilidou et al 2010). Given that Slp5 is an effector protein of Rab27a involved in exosome-mediated secretion (Ostrowski et al 2010) and that, upon silencing, intercellular trafficking of aSyn is increased, this confirms that aSyn transmission also occurs by pathways independent of exosomes, as previously reported (Chutna et al 2014b, Danzer et al 2012, Ejlerskov et al 2013). Silencing of *RAB11A* did not affect the cell-to-cell trafficking of aSyn (Figure 25). Hence, the increase in aSyn dimerization induced by silencing of *RAB11A* might reflect the impairment of the endocytic recycling pathway, one of the routes through which aSyn oligomers can be released (Danzer et al 2012).

In this study we showed that traffic-related modulators of aSyn oligomerization can reverse toxicity and reduce aggregation by increasing secretion of aSyn. Altogether, the genetic screen we performed serves not only as a proof of concept for the identification of genetic modifiers of aSyn aggregation, but provides novel insight into the molecular underpinnings of PD and other Synucleinopathies. Ultimately, future validation in animal



models will establish which of the identified genes holds greater potential as targets for therapeutic intervention.

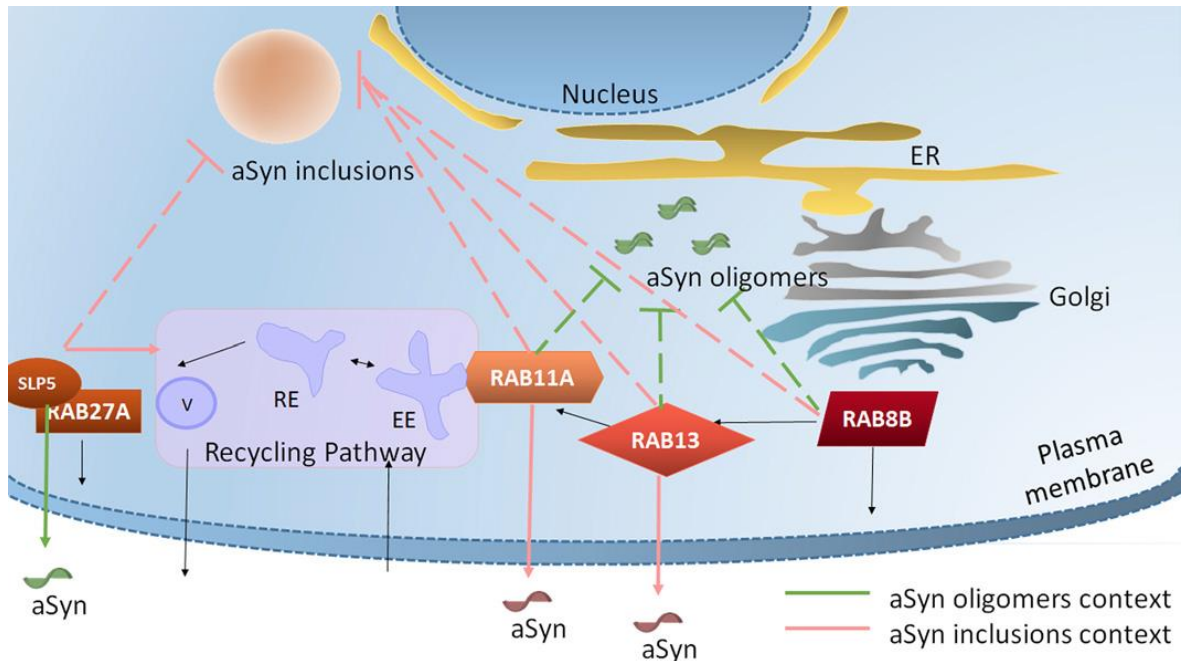


**Figure 28. Rab8b, Rab11a, Rab13 and Slp5 are involved in different steps of cellular trafficking and modulate different aggregated species of aSyn.** Rab8b is localized in cell membranes and vesicles and may be involved in polarized vesicular trafficking (endoplasmic reticulum (ER) to plasma membrane) and, specifically, in neurotransmitter release. Rab11a regulates endocytic recycling pathway and participates specifically in transferrin recycling. Rab13 plays a role in regulating membrane trafficking between trans-Golgi network, recycling endosomes (RE) and cell/tight junctions. Slp5 is localized throughout the nucleus and cytosol, and binds to phospholipidic structures. Slp5 is a Rab27a effector protein and plays a role in exocytosis. Rab8b, Rab11a and Rab13 overexpression rescues aSyn-induced toxicity and inhibits its oligomerization and aggregation. Moreover, Rab11a and Rab13 increases aSyn secretion through recycling endocytic route only when aSyn inclusions are present within cells. Although Slp5 also rescues aSyn-induced toxicity when oligomerization or aggregation are the readout, it increases aSyn secretion only in a context of aSyn oligomerization. EE, early endosome; V, vesicle.

## Materials and Methods

### Cell Culture, Transfections, Infections and Immunocytochemistry

Human H4 neuroglial cells (HTB-148 - ATCC, Manassas, VA, USA) were maintained in Opti-MEM medium supplemented with 10% of fetal bovine serum (FBS) (Life Technologies), and incubated at 37°C, 5% CO<sub>2</sub>. Cells were plated 24 h prior to transfection until 80% of confluence. Transfections were performed using Fugene 6 (Promega) according to the manufacturer's instructions.

aSyn-BiFC stable cell lines were obtained by transfecting H4 cells with GN-link-aSyn and aSyn-GC constructs (Outeiro et al 2008) and maintained with G418 and Hygromycin B antibiotics (both at 100 µg/ml, InvivoGen) in Opti-MEM media with 10% FBS. GFP reconstitution assay was made as previously described (Outeiro et al 2008) and the brightest cells were viably separated using a fluorescence activated cell sorter. After growth of these selected cells, sorting and regrowth was repeated until we obtained a homogeneously fluorescent aSyn-BiFC cell line.

To generate stable cell lines with hits silencing, H4 cells or aSyn-BiFC stable cells were seeded on 10 cm plates 24 h prior to infection. Cells were infected as described (Moffat et al 2006) with lentiviruses. Infected cells were selected with 5 µg/ml puromycin antibiotic (Invivogen) 48 h later and maintained with antibiotic in media.

### RNAi, High-content Fluorescence Imaging and Analysis

#### *Generation and Titer of Lentiviruses*

Lentiviral plasmids encoding shRNAs for traffic and phosphotransferase genes were obtained from the library of the RNAi Consortium (TRC). Plasmids were purified with the QiaPrep miniprep kit (QIAGEN IZASA Portugal) and transfected into HEK293T cells with a three-plasmid system to produce lentiviruses with a very high titer of 10<sup>7</sup> CFU/ml (Moffat et al 2006) following the standard procedures.

#### *aSyn-BiFC Cells Infection*

1.0x10<sup>4</sup> stable aSyn-BiFC cells were plated in 96 well, clear bottomed, black polystyrene plates (Corning). 24 h later, the medium was carefully removed without disturbing the cells at the bottom. Cells were then infected with virus containing shRNAs for the silencing of kinases-, phosphatases- and traffic-related genes. 3-5 different shRNAs per

gene were used in an arrayed format. 20 ul of virus with polybrene (1:1000 final concentration) was added. The 96-well plates were then centrifuged at 2200 rpm for 90 min at 37°C. After centrifugation, medium was removed and 200 ul/well of fresh Opti-MEM medium was added. 48 h post-infection, cells were washed with PBS and media (Opti-MEM with no phenol red, Life technologies) was replaced. Fluorescent images were obtained from living cells using Axiovert200M microscope (Carl Zeiss MicroImaging). Over than 100 cells were acquired for each field imaging and fluorescent intensities were calculated through ImageJ software. Fluorescent screening was repeated at least three independent times and hits were selected based on the ratio of fluorescent averages. Genes which upon silencing reduced or increased the levels of GFP fluorescence by at least 50% were selected for subsequent confirmation and analysis in secondary assays. Cells were observed with 20x objective for quantification analysis and with a 63x objective for subcellular localization studies. ImageJ was used to convert the average GFP fluorescence of each cell to average pixel intensity. Values were then averaged for each condition, and statistical differences between a baseline condition and an experimental condition were calculated.

For the selected hits, production of lentiviruses was repeated as described above.  $5.0 \times 10^5$  stable aSyn-BiFC cells or H4 cells were plated in 6-well plates, and infected with 500ul of viruses with polybrene (1:1000 final concentration). The 6-well plates were then centrifuged at 2200 rpm for 90 min at 37°C. After centrifugation, medium was removed and 200 ul/well of fresh Opti-MEM medium was added. The plates were incubated for 48 h. Cells were selected with 5ug/ml of puromycin (final concentration).

### **Real Time PCR**

$1.5 \times 10^6$  aSyn-BiFC cells were plated in 10 cm plates and infected with selected hits as described (Moffat et al 2006). 48 h post-infection, total RNA was extracted from cell lysates with Trizol reagent (Invitrogen) in accordance with the manufacturer's instruction. 1µg of RNA was reverse transcribed into cDNA using Superscript First Strand Synthesis Kit (Invitrogen). PCR amplification was performed by using 2µl of cDNA with SYBR Green master mix (Sigma-Aldrich). Primers used for real time PCR were chosen using Primer 3, Net Primer and BLAST software to ensure specificity. RT-PCR primers here used were: for *RAB8B*, forward 5'-ATGAGGCTGGAATCCACTTG, reverse 5'-ATGAGGCTGGAATCCACTTG;

for *RAB11A*, forward 5'-CATGTTCCACCAACCACTGA, reverse 5'-GTCATTCGGGACAAGTGGAT; for *RAB13*, forward 5'-CAAGACAATAACTACTGCCTACTACCG, reverse 5'-AAGCCTCATCCACATTCATACTG; for *RAB39B*, forward 5'-AGTTCCGGCTCATTGTCATC, reverse 5'-ATCTGGAGCTTGATGCGTTT; for *CAMK1*, forward 5'-AAGAGCAAGTGGAAAGCAAGC, reverse 5'-AGTGAGGAGTGGTAGGGAAGC; for *DYRK2*, forward 5'-CCAGAAGTAGCAGCAGGACC, reverse 5'-CCCACTGTTGTAAGCCCATT; for *CC2D1A*, forward 5'-ATCTGGATGTCTTTGTTCGGTT, reverse 5'-TTGATGCCCTTGGTCTGG; for *CLK4*, forward 5'-GGTTGGTCTCAGCCTTGTG, reverse 5'-TGTGTTGTGGTATGGGTCCTAA; for *SYTL5*, forward 5'-AGCAAAGCCACCAAGCAC, reverse 5'-CTGAGAGTCCATCCAATCCAC; for *ACTB* (beta-actin, endogenous control), forward 5'-GGACTTCGAGCAAGAGATGG, reverse 5'-AGCACTGTGTTGGCGTACAG.

### **Fluorescent-Activated Cell Sorting for Cell-to-Cell Trafficking Assay**

1.5x10<sup>6</sup> H4 stable cells with hit silencing (*RAB8B*, *RAB11A*, *RAB13* or *SYTL5*) per dish were plated and transfected in 10 cm dishes. 24 h later, cells were transfected cells with VENUS1-aSyn or aSyn-VENUS2 vectors independently (Danzer et al 2012). 24 h later, 0.5x10<sup>6</sup> of transfected cells with VENUS1-aSyn and aSyn-VENUS2 constructs were mixed. 72 h after, trypsin was added to each plate and neutralized with media (Opti-MEM+10% FBS). Cell suspension was centrifuged at 1100 rpm for 10 min, the supernatant aspirated and the pellet reconstituted in phosphate buffered saline (PBS). The resulting supernatant was filtered with cell strainer caps into polypropylene tubes (both from BD Biosciences). VENUS Fluorescence was measured on a BD LSRFortessa (BD Biosciences) and detected also at Axiovert200M microscope (Carl Zeiss MicroImaging).

### **Overexpression Constructs**

In order to generate pcDNA ENTR BP myc-mCherry-C2 mouse Rab8b, pcDNA ENTR BP V5-mCherry-C2 mouse Rab11a and pcDNA ENTR BP V5-mCherry-C2 mouse Rab13, pcDNA ENTR BP myc-mCherry-C2 or pcDNA ENTR BP V5-mCherry-C2, mammalian expression vectors were used. These mammalian expression vectors were previously generated by inserting a polylinker containing several restriction sites into pcDNA6.2GW/Em-GFP, a mammalian expression Gateway (Invitrogen) previously digested with DraI/XhoI followed by insertion of myc-mCherry-C2 or V5-mCherry-C2, previously synthesized into

NheI/BamHI. Rab8b, Rab11a and Rab13 mouse coding sequence and part of 3' UTR were produced by RT-PCR amplification using total RNA isolated from at-T20 cell line as a template, digested with EcoRI/Sall and cloned with the same restriction enzymes into the mammalian expression vectors. The primers here used were: for Rab8b, forward 5'-AGTGAATTCATGGCGAAGACGTACGATTATCTGTTC, reverse 5'-GACCGTCTGACTCACAGGAGACTGCACCGGAAGAA; for Rab11a, forward 5'-TGAGGAATTCATGGGCACCCGCGACGACGAGTA, reverse 5'-AATAGTCTGACCATGCTGGTTGCTGAATATGGTG; for Rab13, forward 5'-CCCGGCGCCCCAGTGGAATTCATGGCCAAAG, reverse 5'-GTGCGTCTGACAGCCTCTCAGGACCCTAACC. Rab8b (Q67L and T22N), Rab11a (Q70L and S25N) and Rab13 (Q67L and T22N) mutants were generated by PCR mutagenesis and using the following primers: for Rab8b-Q67L, forward 5'-GGCCTGGAAAGATTCCGAACAATTACG, reverse 5'-CGCCGTGTCCCATATCTGAAGTTTAAT; for Rab8b-T22N, forward 5'-GACTCCGGCGTTGGCAAGAACTGC, reverse 5'-GCCGATGAGCAGCAGCTTGAACAGATA; for Rab11a-Q70L, forward 5'-GGGCTGGAGCGGTACAGGGCTATAAC, reverse 5'-TGCTGTGTCCCATATCTGTGCCTTTAT; for Rab11a-S25N, forward 5'-GGTGTGGAAAGAATAACCTCCTGTCT, reverse 5'-AGAATCTCCAATAAGGACAACCTTTA; for Rab13-Q67L, forward 5'-GGCCTAGAACGATTCAAGACAATAACT, reverse 5'-AGCCGTGTCCACACTTGCAGTTTGAT; for Rab13-T22N, forward 5'-TCGGGGGTGGGCAAGAATTGT, reverse 5'-GTCCCCGATGAGCAGCAACTTGAAGAG. In order to generate pENTR V5-C2 mouse Syt15 and pENTR GFP-C2 mouse Syt15, Gateway mammalian expression vectors previously described were used (Seixas et al 2012). Syt15 mouse coding sequence was produced by RT-PCR amplification of total RNA isolated from mouse brain as template (using the primers forward 5'-TCGAAGCTTCGGATCCATGTCTAAGAACTCAGAGTTCATC and reverse 5'-CTAGTCTGACTCAGAGCCTACATTTCCGCGCATGCT), digested with HindIII/Sall and cloned into pENTR GFP-C2 with the same restriction enzymes.

### **aSyn-BiFC Cells Transfection with Overexpressed Hit Vectors, Transferrin Labeling and Imaging**

For overexpression assays, H4 cells or aSyn-BiFC stable cells were seeded 24 h prior to transfection (on 35 mm glass bottom lbi-treated imaging dishes, lbindi GmbH) for

immunocytochemistry and cell imaging or on 6 well plates for immunoblotting or cytotoxicity assays). Cells were transfected with wild type, constitutively active and dominant negative mutants of pcDNA ENTR BP myc-mCherry-C2-RAB8B (RAB8B-WT, RAB8B-Q67L, RAB8B-T22N), pcDNA ENTR BP myc-mCherry-C2-RAB11A (RAB11A-WT, RAB11A-Q70L, RAB11A-S25N), pcDNA ENTR BP V5-mCherry-C2-RAB13 (RAB13-WT, RAB13-Q67L, RAB13-T22N), pENTR V5-C2-SYLT5 constructs or empty vector (plasmids were a kind gift of Dr. José S. Ramalho, Universidade Nova de Lisboa, Portugal). 48 h post-transfection, cells were washed with PBS and incubated with media with no serum for 1 h. 50 µg/ml of Alexa-633-Tf (Life Technologies) were added for 30 min. Cells were then washed with PBS and fixed with 4% paraformaldehyde for 10 min and washed again. Immunocytochemistry was performed only for SYTL5 construct, using primary antibody (mouse anti-V5, Cell Signaling) and secondary antibody (goat anti-mouse IgG-Alexa568, Life Technologies). Nuclear staining was made using 1 µg/ml of Hoechst 33342 dye (Sigma Aldrich) for 2 min. Cells were washed and imaged in PBS. Cells were imaged using a Zeiss LSM 710 microscope with a 63× 1.4 NA oil immersion objective. Fluorescence emission was detected for Hoechst, GFP, mCherry and Far-red: excitation at 405 nm (band pass 420-480), 488 nm (band pass 505-550), 561 nm (band pass 575-615), 633 nm (647 – 754). Pinhole was at 160 µm for all channels and 2-10% of transmission was used.

### **Transferrin Labeling, Immunocytochemistry and Imaging in aSyn Aggregation Cell Model**

For loss-of-function assays, stable H4 cells for hit silencing were seeded in 35 mm glass bottom imaging dishes (ibidi GmbH) 24 h prior to transfection and were co-transfected with aSynT and Synphilin-1-V5 as previously described (Chutna et al 2014b) and subjected to immunocytochemistry 48 h later. For overexpression assays, triple transfections were performed with aSynT, Synphilin-1-V5 and mCherry-Rabs or GFP-Slp5 plasmids and Tf incubation was made as described for aSyn-BiFC cells. Then, cells were permeabilized with 0.5% Triton X-100 in PBS for 20 min at RT, blocked for 1 h at RT with 1% normal goat serum in 0.1% Triton X-100 in PBS, incubated with primary antibody against aSyn (mouse anti-aSyn 1:1000; BD Biosciences) and Synphilin-1-V5 (only for loss of function assays; mouse anti-V5, 1:1000, Cell Signaling) at 4°C overnight followed by secondary antibody incubation (1:1000, goat anti-mouse IgG-Alexa488 for aSynT (or igG-Alexa 568 for aSynT

when co-transfected with GFP-SYTL5) and goat anti-mouse IgG-Alexa568 (Life Technologies) for Synphilin-1-V5 (only for loss-of-function assays), for 2 h at RT. Nuclear staining was made using 1 µg/ml of Hoechst 33342 dye (Sigma Aldrich) for 2 min. Cells were washed and imaged in PBS. Cells were then subjected to microscopy analysis using Zeiss Axiovert 200M for loss of function assays or Zeiss 710 confocal microscope for overexpression assays using the same settings used for dimerization model. The proportion of cells displaying aSyn-positive intracellular inclusions in the aSyn-positive cell population was determined by counting at least 100 cells in each condition. Moreover, for overexpression assays, Alexa-546-Tf fluorescence intensity was also determined using ImageJ.

### **Immunoblotting of Intracellular Proteins**

Total protein extracts were obtained 48 h post-transfection using standard procedures. Briefly, cells were washed twice in PBS and lysed in NP40 buffer (glycerol 10%, Hepes 20mM pH7.9, KCl 10mM, EDTA 1 mM, NP40 0.2 %, DTT 1mM) containing protease and phosphatase inhibitors cocktail (1 tablet/10ml, Roche Diagnostics). Cell debris was spun down at 2,500 rpm for 10 min and supernatant were sonicated at 10mA for 15 s (Soniprep 150). Protein concentration was determined using the BCA protein assay (Thermo Scientific) and 20 µg of protein lysates were resolved in 12% SDS-PAGE. Resolved proteins were transferred to nitrocellulose membranes. After quick washing in TBS-T (Tris buffered saline and 0.1% Tween 20), membranes were blocked either in 5% non-fat dry milk in TBS-T or in 5% BSA in TBS-T for 1 h and then incubated with primary antibodies in 5% BSA in TBS overnight at 4°C. The primary antibodies used were mouse anti-aSyn, 1:1,000, BD Transduction; mouse anti-pS129-aSyn 1:1,000 Wako Chemicals USA; mouse anti beta-actin, 1:4,000, Sigma; mouse anti-V5, 1:1,000, Cell Signaling; mouse anti-myc, 1:1,000, Santa Cruz. The membrane was then washed three times for 10 min each in TBS-T at room temperature and probed with IgG horseradish peroxidase-conjugated (HRP) anti-mouse secondary antibody (1:10,000) for 1 h at room temperature. The membrane was washed again four times for 15 min each with TBS-T and the signal was detected with an ECL chemiluminescence kit (Millipore Immobilon Western Chemiluminescent HRP Substrate).

### **Immunoblotting of Extracellular aSyn**

1.5x10<sup>5</sup> cells were plated in 6 well plates one day prior to transfection (for overexpression assays). 48 h post-transfection or seeding (for loss-of-function assays we used stable cell lines with hits silencing), media was extracted. Using a dot-blot apparatus with a nitrocellulose membrane, 380 ul of media were loaded into wells of the dot blot templates and proteins were trapped on the membrane by vacuum. Blocking, washing and detection was made as described above, by immunoblotting the membrane.

### **Cytotoxicity Assays**

For aSyn cytotoxicity assay, stable H4 cells for aSyn-BiFC system or H4 cells were transduced with lentiviruses (for assays with hits loss-of-function) or transfected with overexpression vectors as described above (for overexpression assays). 48 h post-transfection or transduction, culture media was used to determine the levels of released LDH as described in the manufacturer's instructions (Clontech Laboratories). LDH levels in the culture media were measured and ratio of toxicity between cells with aSyn dimers versus cells with no aSyn was determined.

### **Statistical Analysis**

Statistical significance was determined using the paired t-test with Wilcoxon matched pairs test and 95% confidence interval. Differences were considered statistically significant when  $p \leq 0.05$ . Analyses were performed using the Graphpad Prism 5.0 software (GraphPad Software, CA, USA).

### **Acknowledgements**

The authors would like to thank Bioimaging Unit from Instituto de Medicina Molecular for support with imaging.



## **3.4 Antibodies Against Alpha-Synuclein Reduce Oligomerization in Living Cells**

### **Abstract**

Recent research implicates soluble aggregated forms of aSyn as neurotoxic species with a central role in the pathogenesis of Parkinson's disease and related disorders. The pathway by which aSyn aggregates is believed to occur in a step-wise manner, in which dimers and smaller oligomers are initially formed. Here, we studied the effects of monoclonal aSyn antibodies on the early stages of aggregation using the bimolecular fluorescence complementation (BiFC) assay. As shown by widefield and confocal microscopy, cells treated for 48 h with monoclonal antibodies displayed various degrees of antibody internalization. As indicated by decreased GFP fluorescence signal, C-terminal and oligomer-selective aSyn antibodies reduced the extent of aSyn dimerization/oligomerization. Furthermore, ELISA measurements on lysates and conditioned media from antibody treated cells displayed lower aSyn levels compared to untreated cells, suggesting increased protein turnover. Taken together, our results propose that extracellular administration of monoclonal antibodies can modify or inhibit early steps in the aggregation process of aSyn, thus providing further support for passive immunization against diseases with aSyn pathology.

### **Introduction**

Parkinson's disease, dementia with Lewy bodies and multiple system atrophy are neurodegenerative disorders characterized by the loss of neurons in the brain along with the presence of large intracellular protein inclusions known as Lewy bodies (Singleton et al 2003, Wakabayashi et al 1998). The major protein component of Lewy bodies is alpha-Synuclein (aSyn), a 140 amino acid long protein with a partially unfolded structure (Spillantini et al 1997). Although aSyn has a largely unknown function, recent findings

suggest it to be involved in neurotransmitter regulation. For example, aSyn may regulate the reuptake of dopamine into striatum of transgenic mice (Chadchankar et al 2011) or be more generally involved in synaptic release by promoting SNARE complex assembly (Burre et al 2010).

The aggregation cascade of aSyn is believed to begin with the formation of dimers and smaller oligomers before the appearance of larger oligomers or protofibrils (Uversky et al 2001). Such soluble pre-aggregated species have been demonstrated to have toxic properties and may thus play a central role in pathogenesis (Danzer et al 2007, Lee et al 2004a, Nasstrom et al 2011a, Outeiro et al 2008, Tsika et al 2010). In addition, the disease associated mutations in the gene encoding for aSyn have been found to increase the formation of oligomers/protofibrils, further supporting the pathogenic significance of such species (Conway et al 1998, Giasson et al 1999, Greenbaum et al 2005).

aSyn aggregation has been widely studied in cell culture models. By overexpressing aSyn, intracellular inclusions can be induced in a wide range of cell types via various aggregation-promoting conditions (Desplats et al 2009, Waxman & Giasson 2010). Early stages of protein aggregation can be assessed with protein-fragment complementation techniques (Outeiro & Kazantsev 2008, Remy & Michnick 1999). One such method, the bimolecular fluorescence complementation (BiFC) assay, has previously been adopted for the study of aSyn aggregation (Outeiro et al 2008).

In the last decade, immunotherapy has emerged as a promising tool to target and clear protein pathology in neurodegenerative diseases. With active immunization of transgenic a $\beta$  precursor protein (APP) mice, using fibrils of the a $\beta$ , a distinct reduction of a $\beta$  pathology could be seen (Schenk et al 1999). In addition, a $\beta$  immunization has been found to alleviate memory impairment in transgenic animal models (Morgan et al 2000). Instead of vaccination in Alzheimer's disease, focus has now been set on passive treatment with antibodies against A $\beta$ . Such an approach has proven to be equally efficient in both cell and animal models and is likely to be a safer therapeutic option, as T-cell mediated side effects can be avoided (Lord et al 2009, Tampellini et al 2007).

Immunotherapy has now also begun to be evaluated as an approach to treat aSyn pathology. In one study, active immunization with aSyn on transgenic mice showed that the pathology was less pronounced in vaccinated mice as compared to placebo (Masliah

et al 2005). As for passive immunotherapy against aSyn pathology, no studies have been published to date.

Here, we have explored the use of monoclonal aSyn antibodies to target dimerization/ and oligomerization on a cell culture model, using BiFC.

## Results

### Characterization of mAb49/G

Immunization of mice with 4-hydroxynonenal (HNE)-stabilized aSyn oligomers resulted in several monoclonal antibodies, among which mAb49/G was chosen for this study. By inhibition ELISA, the binding of mAb49/G to an HNE-stabilized aSyn oligomer coated plate was inhibited by addition of serially diluted aSyn species. When adding aSyn oligomers, the IC<sub>50</sub> levels were in the low nanomolar range (0,7 nM) whereas the addition of at least 80 nM aSyn monomers were needed to quench the same signal, indicating a strong selectivity of mAb49/G for oligomeric aSyn (Figure 29).

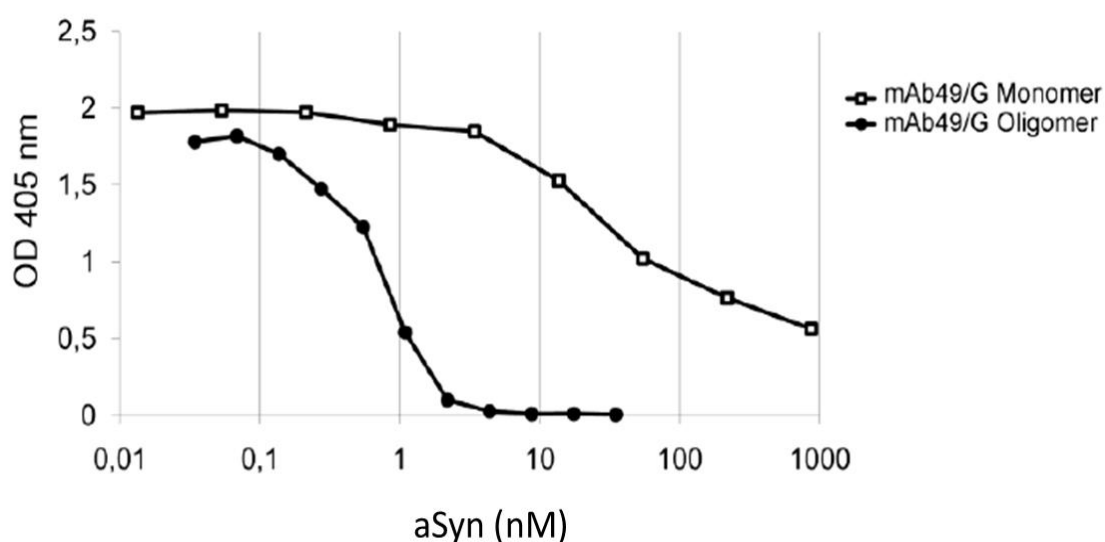


**Figure 29.** Characterization of mAb49/G by inhibition ELISA. Binding of mAb49/G to aSyn monomers (□) or aSyn oligomers (●) was analyzed on HNE stabilized aSyn oligomer coated plates. On the x-axis, the molar concentration of aSyn is displayed. The IC<sub>50</sub> values are calculated as the concentration of either aSyn monomers or aSyn oligomers needed to quench half of the signal in the ELISA. Note that, due to uncertainties concerning the size of the aSyn oligomers used in this

assay, the concentration in pM for both species is based on the molecular weight of one aSyn monomer. These data are representative of at least three independent experiments.

### **Cellular internalization of the aSyn antibodies**

Antibody uptake was studied with immunocytochemistry followed by widefield and confocal microscopy. After 48 h of transfection with the two aSyn-BiFC constructs, GFP fluorescence was detected with widefield microscopy indicating dimerization/oligomerization of aSyn (Figure 30D). In parallel experiments, cells transfected with the same constructs and immediately treated with the mAb49/G, mAb211 and mAb5C2 antibodies for 48 h, displayed occasional small punctae of aSyn in the cell soma after immunostaining with secondary antibodies (Figure 30A, 30B and 30C, arrows). Interestingly, these punctae partly co-occurred with GFP-positive signals, indicating internalization of the extracellularly added aSyn antibodies mAb49/G and mAb211 (Figure 30A, 30B, arrows). However, by examining inclusion staining for the 5C2 antibody, cells exhibited red signals with no co-occurring GFP-fluorescence indicating binding to monomeric forms of the aSyn-BiFC for this particular antibody (Figure 30C, arrows).

To ensure that the antibodies were truly taken up, cells were also analyzed by confocal microscopy. All antibodies were then found to get internalized by obtaining z-slice images, but the intracellular presence of mAb49/G and mAb211 was especially pronounced. Moreover, the antibodies labeled several small inclusions throughout the cell soma but were not found to stain the nucleus (Figure 31A-C). For comparison, cells were subjected to ordinary immunocytochemistry using the mAb49/G, mAb211 and 5C2 as primary antibodies (Figure 31D-F). Indeed, a similar pattern of immunofluorescence staining was detected in those cells confirming antibody localization to small inclusions of aSyn in the cell soma (Figure 31A-C).

To control for passive uptake of the antibodies as a result of DNA transfection, we performed experiments in which the antibodies were incubated with or without the presence of Fugene 6. However, we could not see any difference in antibody uptake between these two experimental conditions, thus indicating that the antibody uptake was not dependent on the presence of cell permeabilization reagents (data not shown).

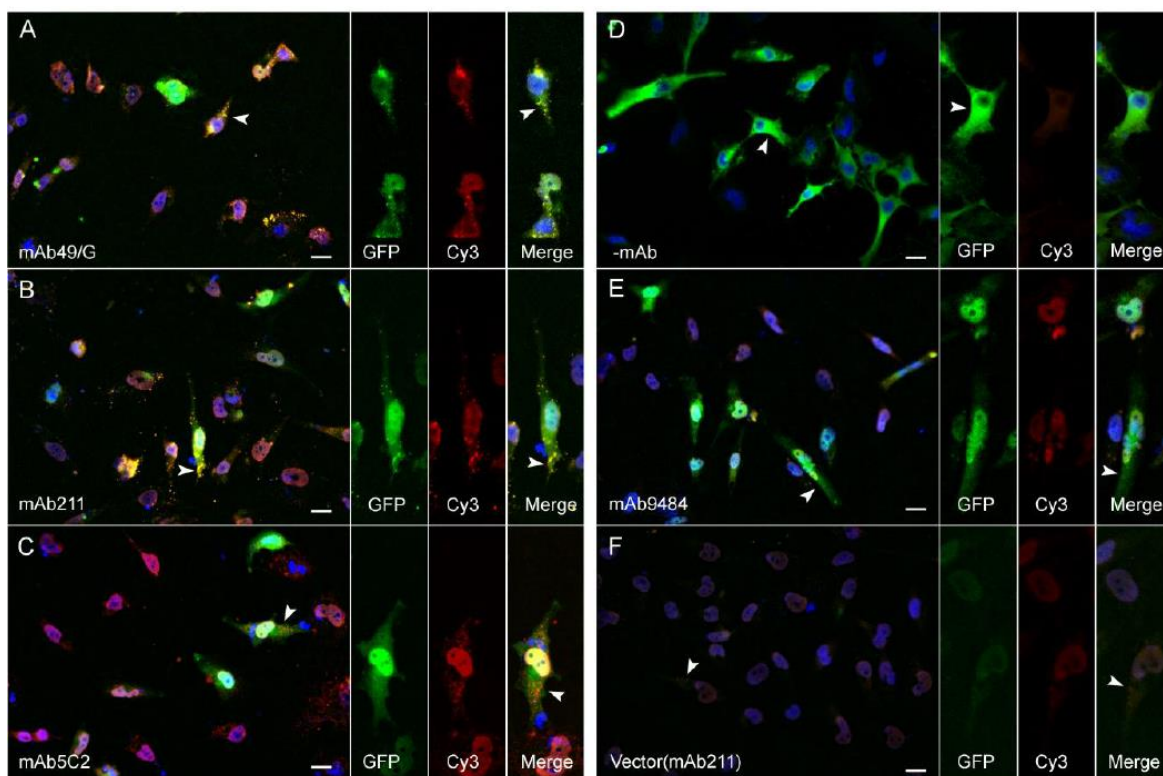


**Figure 30.** Immunocytochemistry with anti-mouse secondary antibodies (red) displays internalization of the aSyn monoclonal antibodies. Forty-eight hours after transfection with the two aSyn-BiFC constructs, cells displayed GFP fluorescence in the whole cell soma (green) (D). Cells transfected with the constructs and treated with the aSyn antibodies mAb49/G and mAb211 displayed less diffuse GFP fluorescence but more localized GFP-puncta (A, B, arrows). These signals occasionally co-occurred with signals from an anti-mouse secondary antibody, indicating internalization of the treatment antibodies (A-B). Cells treated with the mAb5C2 antibody only displayed diffuse GFP-fluorescence in the whole cell soma (C). After staining with an anti-mouse secondary antibody red puncta could be detected in these cells indicating no co-occurrence with GFP (C). 40x magnification. Scale bar 20  $\mu$ m.

#### **Reduced oligomerization after treatment with C-terminal specific and oligomer selective aSyn antibodies**

H4 neuroglioma cells were transfected with the two aSyn-BiFC constructs. Forty-eight hours after transfection, GFP fluorescence could be detected in the cell soma in

approximately 50% of the cells, indicating aSyn dimerization/oligomerization (Figure 32D). The fluorescence in aSyn-BiFC transfected cells corresponded to a robust increase in fluorescence (2.7-fold over expression to vector controls).

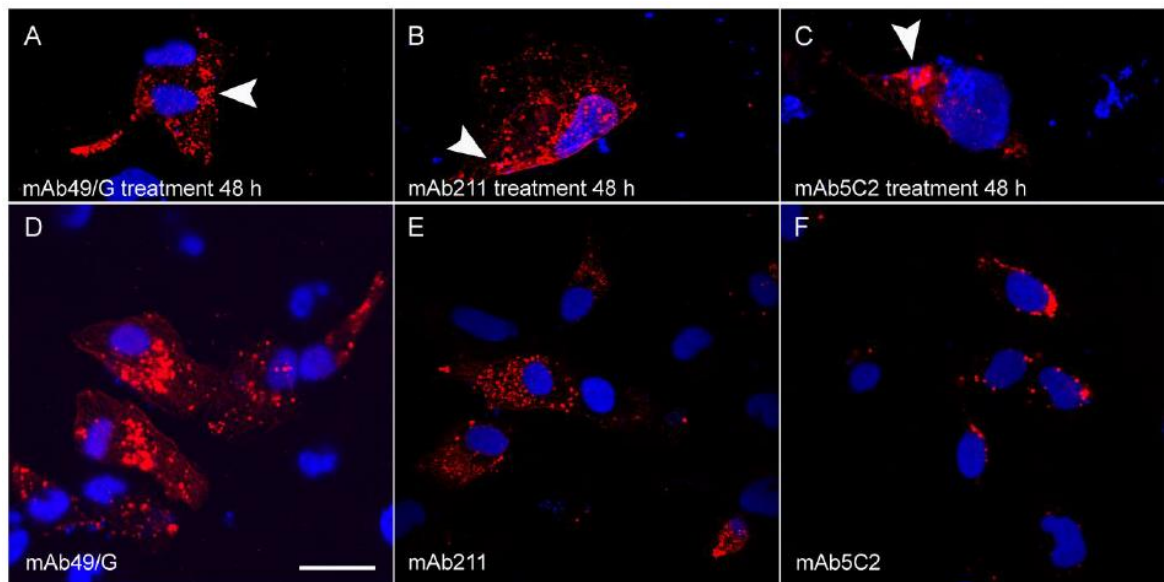


**Figure 31. Confocal microscopy showing internalization of the aSyn antibodies.** Forty-eight hours after addition of the mAb49/G, mAb211 and 5C2 aSyn antibodies, red punctate staining was detected within the cells (A, B and C). For comparison purposes, ordinary immunocytochemistry was carried out using mAb49/G, mAb211 and mAb5C2 as primary antibodies (D, E and F). 63x magnification. Scale bar 20  $\mu\text{m}$ .

In parallel experiments, aSyn antibodies were added to the cell media immediately after transfection. Addition of the aSyn C-terminal antibodies mAb49/G and mAb211 reduced the GFP fluorescence significantly (1.4- and 1.5-fold over expression to vector controls, respectively,  $p < 0.05$ ,  $p < 0.01$ ). With the aSyn mid-region antibody mAb5C2, raised against the non-A $\beta$  component (NAC) region, there was no reduction (2.5-fold over expression to vector controls) of GFP fluorescence (Figure 32C).

Thus, treatment with C-terminal aSyn antibodies resulted in decreased formation of aSyn dimers/oligomers (Figure 32A and 32B), whereas treatment with the mid-region antibody mAb5C2 did not seem to affect the extent of aSyn oligomerization. To ensure that the effects were specific to the aSyn antibodies, the monoclonal GAPDH antibody mAb9484

was added in parallel. No apparent decrease (2.6-fold over expression to vector controls) of GFP fluorescence was seen with this antibody, thus indicating that aSyn oligomerization was not affected by an irrelevant monoclonal antibody (Figure 32E).

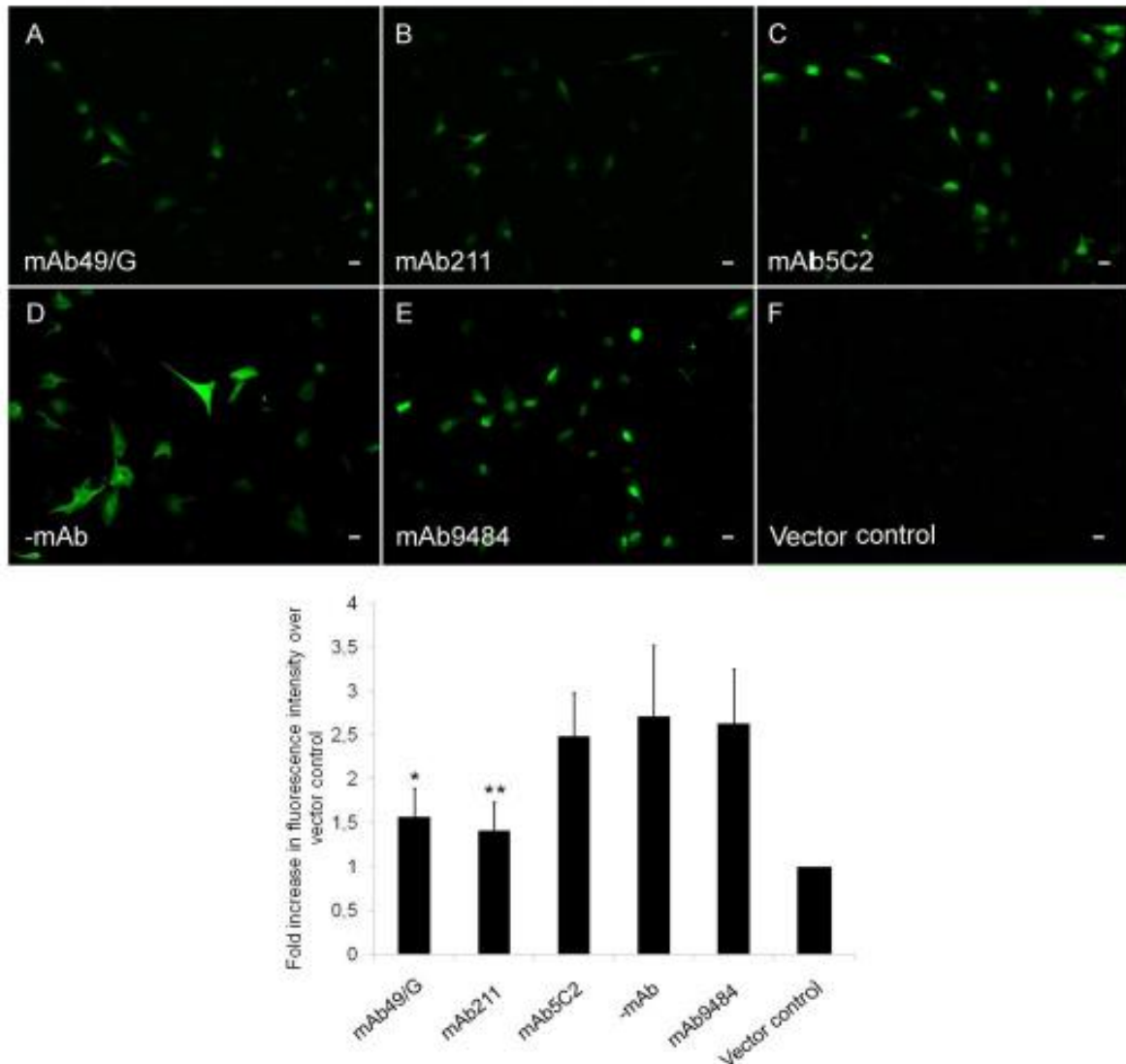


**Figure 32. aSyn dimerization/oligomerization, as shown by GFP fluorescence reconstitution.** 48 h after transfection with the aSyn-BiFC constructs, the H4 cells exhibited robust GFP fluorescence (2.7-fold over expression to vector controls) throughout the cell soma and nucleus (D and G). When cells were treated with the aSyn C-terminal specific antibodies mAb49/G and mAb211 the GFP fluorescence was significantly ( $*p<0.05$ ,  $**p<0.01$ ) reduced (1.4- and 1.5-fold over expression to vector controls respectively) indicating less dimerization/oligomerization (A, B and G). The mAb5C2 antibody targeting the non-A $\beta$  component (NAC) region of aSyn did not show any reduction (2.5-fold over expression to vector controls) of GFP fluorescence, indicating no effect on the formation of dimers/oligomers (C and G). With the monoclonal antibody mAb9484 against

GAPDH, no apparent effect (2.6-fold over expression to vector controls) on dimerization/oligomerization could be seen (E and G). 20X magnification. Scale bar 20 $\mu$ m.

### **Decreased intra and extracellular levels of aSyn from antibody treated cells**

A sandwich ELISA was used to measure aSyn levels in lysate and conditioned media from the same cells that were analyzed for BiFC. In lysates from BiFC expressing cells (with no mAb added), aSyn levels were calculated to 5.6 ng/ml (Figure 33A). In comparison, levels of aSyn in lysates treated with aSyn antibodies for 48 h were 2.8 ng/ml with mAb49/G treatment (\*p<0.04), 3.9 ng/ml with mAb211 (\*p<0.05) and 3.3 ng/ml with mAb5C2 (\*p<0.05), indicating reduced aSyn levels in cell lysate with antibody treatment (Figure 33A).

In conditioned media from untreated cells, aSyn levels were calculated to be 6.9 ng/ml (Figure 33B). In media from cells treated with aSyn antibodies for 48 h, aSyn levels were 3.2 ng/ml after treatment with mAb49/G (\*p<0.05), 2.2 ng/ml with mAb211 (\*p<0.05) and 2.3 ng/ml (\*p<0.05) with mAb5C2 (Figure 33B).

## **Discussion**

The use of immunotherapy to prevent or clear abnormal protein aggregates has emerged as a promising tool to treat neurodegenerative diseases. Also, disorders with aggregated aSyn may be targeted with immunotherapy and active immunization in transgenic mice has indeed been shown to reduce the accumulation of aSyn in the brain (Masliah et al 2005). Although in that study it was proposed that immunization resulted in degradation of aSyn via the lysosomal pathway, it is still largely unknown by which mechanisms intraneuronal aSyn aggregates can be cleared (Masliah et al 2005).

There is an ongoing debate whether extracellularly administered antibodies can enter the cell and affect intracellular pathology. Indeed, antibodies utilized in cancer research have been shown to effectively bind to its target after cell internalization (Hagan et al 1986). In addition, more recent work showed that antibodies directed against APP can maintain its biological activity and remain associated with its target after internalization (Tampellini et al 2007). In the present study we could detect aSyn antibodies within the cells after 48 h



(Figure 31A, B and C) of incubation and find that they co-occurred with the aSyn dimers/oligomers (Figure 30A and B).

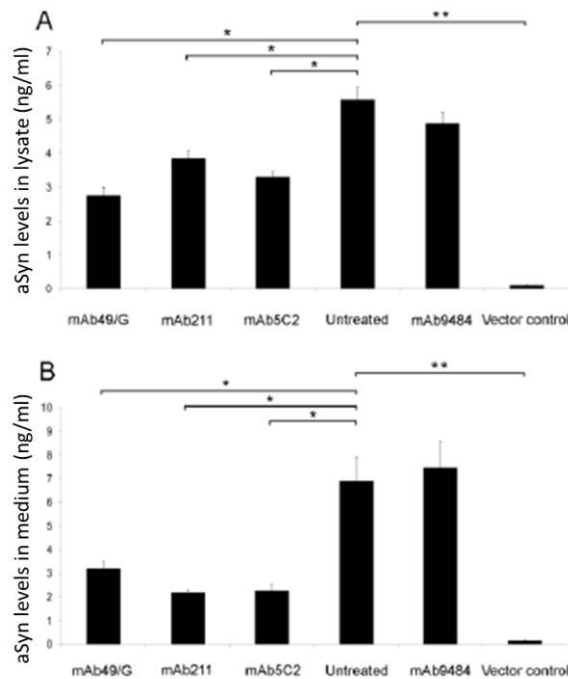


**Figure 33.** ELISA measurement of aSyn levels in lysates and media from BiFC expressing cells. In BiFC expressing cells (-mAb), the levels were 5.6 ng/ml (A), with mAb49/G treatment 2.8 ng/ml (\* $p < 0.04$ ), mAb211 treatment 3.9 ng/ml (\* $p < 0.05$ ) and with mAb5C2 treatment 3.3 ng/ml (\* $p < 0.05$ ) showing a reduction in protein content (A). In conditioned media from untreated cells (-mAb) the aSyn levels were 6.9 ng/ml (B). In media from antibody treated cells, the levels were 3.2 ng/ml for mAb49/G (\* $p < 0.05$ ), 2.2 ng/ml for mAb211 (\* $p < 0.05$ ) and 2.3 ng/ml (\* $p < 0.05$ ) with mAb5C2 (B).

Although our study indicates that aSyn can be targeted intracellularly, aggregated soluble species may also be possible to target in the extracellular space. Indeed, several recent studies on cells and transgenic mice have indicated cell-to-cell propagation of aSyn pathology. In addition, neuropathological analyses of Parkinson’s disease brains that had been transplanted with fetal mesencephalic dopaminergic neurons displayed Lewy bodies in the grafted cells, suggesting a similar propagation mechanism in the human brain (Li et al 2008).

Our findings demonstrate that extracellularly added aSyn antibodies reduced aSyn dimerization/oligomerization in living cells. Previously, *in vitro* studies have shown that aSyn aggregation can be decreased by expressing single chain fragments, i.e. intrabodies, targeting the C-terminus of aSyn (Zhou et al 2004a).

We found that both the oligomer-selective antibody mAb49/G and the mAb211 antibody, raised against the C-terminal part of aSyn (epitope 121-125), were efficient in reducing aSyn dimerization/oligomerization (Figure 32A and B). On the contrary, the mid-region antibody mAb5C2 did not significantly reduce the degree of dimer/oligomer formation.

The inhibiting effect on oligomerization by mAb49/G was somewhat expected as we believe that this antibody recognizes an epitope exclusively present in the oligomeric structure of aSyn. Moreover, the efficient prevention with the C-terminal aSyn antibody was also not entirely surprising. We and others have described that oligomers and fibrils of aSyn expose C-terminal epitopes (Gai et al 2003, Nasstrom et al 2011a) and aSyn antibodies directed against such epitopes seem to be more efficient in clearing aSyn pathology in transgenic mice (Eliezer Masliah, personal communication). Along the same lines, the lack of effect on lowering dimer/oligomer levels for the 5C2 antibody in the current study could be explained by the fact that its hydrophobic NAC-region epitope (61-95) is hidden in the oligomeric core (Giasson et al 2001).

To further investigate antibody effects on aSyn oligomerization, we utilized ELISA to measure levels of aSyn in cell lysates and conditioned media from wells under the various experimental conditions. Similar studies with extracellular addition of antibodies against APP have pointed to an antibody-directed clearance of A $\beta$  via the endosomal/lysosomal pathway (Tampellini et al 2007). In agreement with these findings, we showed that the levels of aSyn were decreased both in cell lysate and conditioned media after antibody treatment, indicating an increased protein turnover in treated cells (Figure 33A and 33B).

The finding that the NAC-specific 5C2 antibody influenced aSyn levels in both cell lysate and conditioned media without affecting oligomer formation is intriguing (Figure 32C, 33A and 33B). Presumably, the 5C2 antibody fails to affect dimerization/oligomerization of aSyn but can bind to the monomeric aSyn-BiFC in which the NAC region is exposed. Thereby, also this antibody can facilitate protein turnover, thus explaining the decreased total aSyn levels seen in the ELISA. However, the oligomer-selective mAb49/G and C-

terminal mAb211 antibodies would be more suitable antibody candidates, as they are targeting pathological aSyn aggregates rather than the physiological protein.

In summary, we have studied the effects of monoclonal aSyn antibodies on the early stages of oligomerization in H4 cells. We could show that extracellularly administered C-terminal and oligomer-selective aSyn antibodies are efficiently internalized, have an inhibiting effect on aSyn oligomer formation and facilitates protein turnover. Thus, these results provide further support for passive immunotherapy against Synucleinopathies.

## **Materials and Methods**

### **aSyn constructs**

The G-N-155-aSyn and aSyn-G-156-C constructs used for the BiFC assay were generated as described earlier (Outeiro et al 2008). For all transfection experiments, an empty pcDNA3.1 expression vector (Invitrogen, Carlsbad, CA) was used as control.

### **Cell culture**

H4 neuroglioma cells were cultured at 37°C and 5% CO<sub>2</sub> in OPTI-MEM (Invitrogen) and supplemented with 10% fetal bovine serum (FBS) (Invitrogen) and 4 mM Glutamine (Invitrogen).

### **Antibodies**

The following aSyn monoclonal antibodies (mAb) were used for cell culture treatment: mAb211 (Santa Cruz Biotechnology, Santa Cruz, CA), mAb5C2 (Santa Cruz Biotechnology) and the oligomer-selective antibody mAb49/G (BioArctic Neuroscience, Stockholm, Sweden). The monoclonal GAPDH antibody 9484 (Abcam, Cambridge, UK) was used as a negative treatment control. All antibodies used for cellular treatment were diluted in TBS to reach a final concentration of 1 µg/ml in the extracellular media. For the sandwich ELISA, the Syn-1 (BD Biosciences, Franklin Lakes, NJ) and FL-140 (Santa Cruz Biotechnology) aSyn antibodies were used for capture and detection, respectively. For immunocytochemistry experiments, anti-mouse Cy3 or Alexa594 conjugated secondary antibodies (Invitrogen) were used.

### **Generation of the oligomer-selective aSyn antibody mAb49/G**

Balb/c mice (The Jackson Laboratory, Bar Harbor, Maine) were immunized with 4-hydroxy-2-nonenal (HNE) stabilized aSyn oligomers [11] diluted 1:1 with Freund's adjuvant. After repeated boosts, immunized mice with high serum titers were sacrificed for isolation of spleen cells. Next, the spleen cells were fused with SP2/0 myeloma cells. Hybridomas were screened for anti-aSyn reactivity with ELISA and positive clones underwent at least two rounds of limiting dilution assay to ensure monoclonality. The IsoStrip kit (Roche Diagnostics, Basel, Switzerland) was used to determine isotype and subclass of the antibody. The mAb49/G IgG1 antibody was then purified from the conditioned media with affinity chromatography using Protein G-Sepharose (GE Healthcare, Uppsala, Sweden). All experiments involving animals were approved by the local ethical committee (decision numbers N417/08; 2009-01-15).

### **Inhibition ELISA**

An inhibition ELISA assay was performed as described previously, using aSyn monomers and HNE stabilized aSyn oligomers as antigen competitors (Englund et al 2007).

### **Transfection and addition of monoclonal antibodies**

Prior to the day of transfection, cells were seeded onto 35 mm poly-D-lysine coated culture plates (MatTek Cultureware, Ashland, MA) at a density of  $1.5 \times 10^5$  cells/plate. Transfection of H4 cells were carried out with a 1:5 ratio ( $\mu\text{g DNA} : \mu\text{l Fugene 6}$ ), using the Fugene 6 Transfection reagent (Roche Diagnostics). In brief, the culture medium was replaced with medium containing 1% FBS, transfected and left to incubate at 37°C for 24 h. For bioimaging, to ensure optimal reconstitution of the two GFP fragments, cells were incubated over night at 30°C (Hu et al 2002, Outeiro et al 2008). Moreover, cells were treated or untreated at time zero of transfection with either of the mAb211, mAb5C2 or mAb49/G aSyn antibodies or with the mAb9484 GAPDH antibody for 48 h at a final antibody concentration of 1  $\mu\text{g/ml}$ .

### **Immunocytochemistry**

Cells were washed with PBS and subsequently fixed for 10 min in 4% paraformaldehyde (PFA). After permeabilization for 20 min in 0.1% Triton X-100 at room temperature, the cells were blocked with 1.5% normal goat serum (NGS) (Invitrogen) for 2 h. After washing with PBS, cells were incubated with a Cy3 conjugated secondary antibody (Invitrogen) (1:5000 in 1.5% NGS) for 1 h. Finally, cells were stained with DAPI (Invitrogen) (1:20000 in 1.5% NGS) for 10 min.

Control cells were stained using the mouse monoclonal aSyn antibodies mAb49/G (BioArctic Neuroscience), mAb211 (Santa Cruz Biotechnology) and mAb5C2 (Santa Cruz Biotechnology) (1:500 in 1.5% NGS) for 2 h. Next, cells were probed with the Alexa-Fluor 594 conjugated secondary antibody (Invitrogen) (1:5000 in 1.5% NGS) for 1 h. Finally, cells were stained with DAPI (Invitrogen) (1:20000 in 1.5% NGS) for 10 min. All incubations were performed at room temperature.

To control for unspecific binding of the secondary antibodies, cells were treated only with a mouse secondary antibody and compared to buffer treated controls. To control for passive uptake of the aSyn antibodies as an effect of DNA-transfection, additional experiments in which the antibodies were added with and without simultaneous administration of Fugene 6 were carried out.

Cells were analyzed with confocal microscopy using a LSM 510 META instrument (Carl Zeiss Microimaging) where single plane and z-slice images of antibody internalization were obtained.

### **Fixing cells and fluorescence microscopy**

At the end of the treatment, cells were washed with PBS and subsequently fixed for 10 min in 4% paraformaldehyde (PFA). To study GFP fluorescence the cells were analyzed using an Axiovert 200M widefield fluorescence microscope (Carl Zeiss Microimaging GmbH, Jena, Germany). The cells were observed using an Epi-fluorescence illuminator equipped with a FITC filter. Eight random sites in the well for each condition were observed using a 20X objective.

### **Quantification of fluorescence intensity**

For quantification of pixel intensities, the ImageJ (NIH, Bethesda, MD) software was used. The GFP fluorescence was converted to average pixel intensities for each condition. The intensities for each captured frame are presented as fold increase in fluorescence over vector transfected controls. To test for statistically significant differences, groups were subjected to one-way ANOVA. Probability values <0.05 were considered significant using a two-tailed confidence interval.

### **Preparation of conditioned media and cell lysates**

Forty-eight hours after transfection and antibody treatment, the conditioned media was recovered and centrifuged at 2,150 x g at 4°C for 10 min. To concentrate the samples, the conditioned media was freeze-dried and re-dissolved in CellyticM (Sigma-Aldrich, St. Louis, MO) lysis buffer supplemented with protease inhibitor cocktail (Roche Diagnostics). The cells were washed with PBS, lysed with CellyticM (Sigma-Aldrich) and supplemented with a protease inhibitor cocktail (Roche Diagnostics). The lysate was collected and centrifuged at 4°C for 10 min and 20,800 x g. Protein concentrations in conditioned media and lysates were determined with the BCA Protein Assay Reagent (Thermo Fisher Scientific, Rockford, IL).

### **Sandwich ELISA**

A 96-well high binding plate polystyrene microtiter plate (Corning) was coated with 200 ng/well of Syn-1 (BD Biosciences) in PBS and incubated at 4°C overnight. The solution was removed from each well and the cells were blocked with 1% BSA / 0.15% Kathon for 1 h at room temperature. The samples, including a standard series of recombinant aSyn diluted in 1% BSA, 0.05% Tween and 0.15 % Kathon, were added to the wells and incubated with shaking at room temperature for 2 h. After washing, the FL-140 polyclonal aSyn antibody (Santa Cruz Biotechnology) was diluted to 1 µg/ml and added to the wells, followed by shaking at room temperature for 1 h. Next, the wells were washed and an anti-rabbit horse radish peroxidase (HRP) coupled detection antibody (Pierce, Rockford, IL, USA) was added at a final concentration of 0.4 µg/ml. After a further incubation for 1 h, the wells were washed and the K-blue aqueous substrate (TMB) was used as substrate for HRP. Before measurement, the reaction was stopped using 1 M H<sub>2</sub>SO<sub>4</sub>. The plate was

measured using a SpectraMAX 190 (Molecular Devices, Palo Alto, CA) spectrophotometer at 450 nm. The data for each sample was calculated as the means of three separate wells.

### **Acknowledgements**

This work was supported by grants from Swedish Research Council (2006-2822(LL); 2006-6326 and 2006-3464(MI)), Uppsala Berzelii Technology Center for Neurodiagnostics, Swedish Brain Foundation, Lundbeck foundation, Swedish Alzheimer Foundation, Swedish Parkinson Foundation, Swedish Society of Medicine, Hans and Helen Danielsson, Lennart and Christina Kahlén, Stohne's Foundation, Söderström-Königska Foundation, Swedish Dementia Foundation, Björklund's Foundation for ALS research, Magn Bergwall Foundation, Thore Nilsson Foundation, Old Servants' Foundation, Åhlén Foundation, Loo and Hans Osterman's Foundation, Jeansson's Foundation, Larsson-Röst's Foundation, Golje's Foundation. SG is supported by a PhD fellowship from AXA Research Fund. TFO is supported by Fundacao para a Ciencia e Tecnologia (FCT), an EMBO Installation Grant, and a Marie Curie International Reintegration Grant (Neurofold).





## **IV. C**onclusions and **F**uture **D**irections

---

**This chapter contains parts of the following publication:**

Goncalves, S. A. and T. F. Outeiro (2016). **Traffic jams and the complex role of alpha-Synuclein aggregation in Parkinson's disease.** *Small GTPases*: 1-7.



A common pathological event among diverse NDs is the misfolding and accumulation of different proteins in the brain. These processes are thought to potentiate aberrant PPIs that culminate in the disruption of several biological processes and, ultimately, in neuronal loss. Although protein aggregates are a common hallmark in several disorders, the cellular context leading to their generation remains unclear. A major limitation in the diagnosis of NDs is that it is done in a very advanced phase of the pathology, a time that coincides with a substantial and irreversible loss of neuronal cells.

PD is an incurable ND and represents significant costs to individuals, care-givers and society. It is defined at post-mortem by the loss of dopamine neurons in the *substantia nigra* together with the presence of LBs and LNs. Dysfunction of the affected neurons heralds impaired trafficking, to which DA neurons are particularly dependent and thus more vulnerable to its disturbance (Hunn et al 2015). The novel clarifications regarding PD have been clarifying the mechanistic explanation beyond its pathology.

The elucidation of the molecular mechanisms involved in aSyn misfolding and the associated proteotoxicity is essential for the design of novel therapeutic strategies and to devise alternative approaches to diagnose PD at earlier stages. Here, we used cellular models to investigate the molecular mechanisms underlying both oligomeric and aggregated aSyn, by characterizing intra- and intercellular dynamics of this protein and by identifying molecular partners that allowed novel insights in the function of aSyn.

Traditionally, aSyn was assumed to be predominantly localized in presynaptic terminals and also in the cytoplasm. Its presence in the nucleus and mitochondria was later described (Goers et al 2003, Kontopoulos et al 2006, Siddiqui et al 2012). aSyn has been proven to be highly mobile as studies *in vitro* and *in vivo* with photobleaching of GFP-tagged aSyn at the synapse, showed a quick recovery after photobleaching (Fortin et al 2004, Unni et al 2010). We have found that the availability of the N-terminal region is determinant for the entry of aSyn into the nucleus. We have also determined that missense mutations, S129 phosphorylation, or HSP70 can modulate that characteristic of aSyn dynamics. While A30P increases the tendency to enter in nucleus, E46K and A53T reverse the nuclear flux of aSyn. Moreover, PLK2, the best well characterized kinase that phosphorylates aSyn at S129 residue, potentiates the cytoplasmic location of aSyn. This is consistent with the fact that aSyn is mainly phosphorylated in the disease context but not in normal conditions. HSP70 chaperone boosted the dynamics between nucleus and

cytoplasm compartments probably maintaining the cell homeostasis and biological viability in the presence of a monomeric form of aSyn.

Other studies suggest that the C-terminal region of aSyn might be important for the targeting of aSyn to the nucleus (Specht et al 2005, Xu et al 2006). Although this can be partially puzzling facing our results, we believe this is not contradicting our findings as those results refer to aSyn localization while we studied its dynamics. Specht and colleagues expressed deletion mutants of aSyn and found out that the C-terminal domain of aSyn has a predominant nuclear localization while N-terminal fragment is excluded from nucleus (Specht et al 2005). While we cannot compare results because we used the full-length aSyn in our studies, we observed that aSyn is basally localized in both compartments, although the velocity rate at which this protein is transferred from one compartment to another differs and depends on the availability of the N-terminal. Xu et al all observed aSyn at both compartments but it was upon stress conditions that the C-terminal fragment of aSyn was translocated to the nucleus, while full-length protein remained in cytoplasm (Xu et al 2006). As in the present work we observed that the presence of HSP70, which binds to aSyn through its NAC domain (Roodveldt et al 2009), shifts aSyn into the nucleus, what we add to the literature is that the C-terminal is required for chaperone binding, as already described, but it is the availability of the N-terminal of aSyn that facilitates the entrance into the nucleus. Finally, Ma et al found out that aSyn nuclear import is mediated by importin-alpha and that 1-60 and 103-140 residues are essential for intranuclear localization (Ma et al 2014).

Recent findings claim aSyn naturally exists as a tetramer, and that monomeric forms of aSyn are deleterious to the cell (Bartels et al 2011, Dettmer et al 2015b). If so, we can consider we characterized the shuttling between nucleus and cytoplasm of the monomeric forms of aSyn and PAGFP fusion constructs having in the light the availability of N- or C-terminal of aSyn. aSyn is under the molecular weight cut-off of the nuclear pore (40kDa) which means it can enter the nucleus (Keminer & Peters 1999). However, tetrameric or larger forms of aSyn cannot cross the nuclear pore complex. We speculate that the monomeric/oligomeric forms, other than the stable tetramers, are the ones that can enter those compartments in pathological sceneries. As increasing evidences suggests they are the pathologic species, this corroborates their association with cell toxicity, when levels of aSyn are increased in nuclei or mitochondria in PD context (Cole et al 2008). As

proof of concept, it was demonstrated that aSyn downregulates c-Jun N-terminal kinase, protecting cells against oxidative stress, upregulates Caveolin-1 expression and downregulates ERK expression which may play a role in the pathogenesis of PD (Hashimoto et al 2002, Surgucheva et al 2005). Moreover, it reduces anti-apoptotic Bcl-xL expression and increases the pro-apoptotic Bcl2-associated X protein (Bax) (Seo et al 2002). Finally, aSyn can bind to a promoter of Peroxisome proliferator-activated receptor gamma co-activator 1-alpha (PGC-1a) transcriptional co-activator, which reduces its expression upon oxidative stress (Siddiqui et al 2012). Thus, two scenarios of interaction between aSyn and mitochondria may occur: aSyn direct interaction with mitochondria, with subsequent transportation into the organelle which can cause dysfunction, or it could impair transcription of nuclear-encoded genes enrolled in mitochondrial function (Surguchov 2015).

In the nucleus, aSyn interact with histones, inhibits acetylation, enhances chromatin binding and inhibits transcription of genes involved in the mitochondrial biogenesis in the cells (Kontopoulos et al 2006). The interaction between aSyn and histones may reduce the pool of free histones available for DNA binding, leading to destabilization of nucleosomes and to subsequent transcription deregulation. By this way, aSyn action in the nucleus is associated with neurotoxicity. Concordantly, aSyn N-terminal was previously related with an increase in the level of intracellular reactive oxygen species (ROS), changes in mitochondrial morphology and membrane permeability (Shen et al 2014).

Remains to be clarified the mechanism that leads to aSyn entrance in the nucleus. While it seems a fine-tuned regulation, localization of aSyn in the nucleus and mitochondria may be an important key to unravel the etiology of Synucleinopathies.

Recent studies with tissue from PD patients and animal models suggest that oligomeric species of aSyn are toxic to the neurons, suggesting that the large cytoplasmic inclusions are the result of a protective mechanism to avoid the accumulation of the more toxic species (Goncalves et al 2016, Outeiro et al 2008, Winner et al 2011). In this context, modifying the oligomerization process of aSyn, either by inhibiting the initial interactions that drive the formation of oligomeric species, or by promoting the formation of cytoplasmic protein inclusions that consume oligomeric species, appears as promising strategies. However, promoting inclusion formation requires caution, as aggregates may

also disrupt cellular functions, perhaps by physically clogging specific compartments in the cell. Overall, these concepts demand additional investigation.

We used cell-based models of Synucleinopathy to screen a collection of shRNAs, targeting 76 genes associated with intracellular transport and 1311 genes involved in signal transduction players. The objective was to identify modifiers of aSyn oligomerization, using the BiFC assay as readout. With this approach (Goncalves et al 2010, Outeiro et al 2008), we identified 9 genetic modifiers of aSyn oligomerization (Goncalves et al 2016). Interestingly, the hits we identified were functionally related, and associated with neuronal trafficking processes. We then focused our subsequent studies on hits involved in secretion, as this process might be related to the process of spreading and transmission of pathological forms of aSyn between cells in the brain, in a prion-like manner (Braak et al 2003). This hypothesis is consistent with the detection of aSyn pathology in neuronal grafts in PD patients after transplantation of midbrain cells (Li et al 2008). aSyn was shown to be secreted via non-classical exocytosis and, not exclusively, in association with exosomes (Danzer et al 2011, Emmanouilidou et al 2010, Lee et al 2005, Sung et al 2005). This is also in agreement with the presence of aSyn in cerebrospinal fluid (El-Agnaf et al 2003, Lee et al 2006).

Thus, although we believe that the remaining five genes identified in our RNAi-based screen deserve further examination, as they are thought to play relevant roles in neuronal cells (Annex 5.2.11.), we selected four hits identified in our screen based on their involvement in different steps of cellular trafficking: *RAB8B*, *RAB11A*, *RAB13* and *SYTL5*. Rab8 is associated with actin and microtubule reorganization and with polarized trafficking to dynamic cell surface structures (Hattula et al 2002). In addition, it is able to reconstitute Golgi morphology in cellular models of PD (Rendon et al 2013) and, as we independently showed (Breda et al 2014), to rescue aSyn induced loss of dopaminergic neurons in *Drosophila* (Yin et al 2014). Rab11a is a ubiquitously expressed protein with predominant localization at the endosomal recycling compartment/recycling endosome (ERC/RE). Strikingly, defects in trafficking from the ERC has been previously implicated in AD, HD and PD (Greenfield et al 2002, Li et al 2009, Liu et al 2009a). Rab11a is involved in the process of exocytosis of aSyn via RE (Liu et al 2009a). Rab13 mediates trafficking between the trans-Golgi network and REs (Nokes et al 2008). Moreover, it has been associated with neuronal plasticity, neurite outgrowth, cell migration and regulation of

tight junctions, all of which are important pathways in normal neuronal biology (Di Giovanni et al 2005, Marzesco et al 2002, Wu et al 2011b). *SYTL5* is an effector protein of Rab27a and mediates the transport of vesicle-Rab27a complex along the cytoskeleton until the plasma membrane is reached, forming a docking/tethering complex that then releases the vesicles (Fukuda 2013).

In our validation assays, we investigated the effect of the selected hits on aSyn accumulation, toxicity and secretion, assays that we have previously described (Lazaro et al 2014). We found that silencing Rab8b, Rab11a and Rab13 rescued aSyn-induced toxicity and reduced the accumulation of both oligomeric and aggregated forms of aSyn. Moreover, Rab11a and Rab13 increased aSyn secretion through the recycling endocytic route when aSyn inclusions were present. When soluble, oligomeric aSyn were present, those two genes still promoted recycling endocytic pathway but not alter the levels of aSyn secretion.

We also showed that Rab11 interacts with aSyn *in vivo* and modulates its secretion through a pathway that does not occur through exosomes or endocytic recycling (Chutna et al 2014b). This emphasizes the contribution of Rab11a, an endocytic recycling marker, specifically to aSyn oligomerization and aggregation dynamics, that we now found to involve the RE pathway.

Although Slp5 rescues the toxicity associated both with aSyn oligomerization and aggregation levels, we found it to affect the later stages of aggregation. Moreover, we found that Slp5 increased the secretion of aSyn in the oligomerization model, in a manner that was independent of the endocytic recycling pathway. Given that Slp5 is an effector protein of Rab27a, involved in secretion through exosomes, our finding supports the idea that the release of aSyn can, at least in part, occur via exosomes, as other studies have suggested ((Alvarez-Erviti et al 2011, Chutna et al 2014b, Danzer et al 2012, Ejlerskov et al 2013, Emmanouilidou et al 2010)).

The common effect among the four trafficking hits was that Rab8b, Rab11a, Rab13 and Slp5 promoted similar effects in the aSyn aggregation cell model. Upon silencing, they increased the number of inclusions per cell. Conversely, upon overexpression, they reduced the percentage of cells with inclusions in 50%-90% and also reduced aSyn toxicity. Importantly, in cells with inclusions, the trafficking proteins co-localized with aSyn in inclusions. This could either be due to the recruitment of the various proteins into

the inclusions, due to the sticky nature of the inclusions, or due to a cellular response in order to try to contain aSyn accumulation (Goncalves et al 2016). This is in agreement with the interaction between aSyn and Rab8 in brain tissue from patients who showed Lewy body pathology but not in control tissue (Dalfo et al 2004a). In addition, Rab8 (as well as Rab3a and Rab5) co-immunoprecipitates with aSyn in the extracts from A30P transgenic mice (Dalfo et al 2004b). Importantly, Rab8 is also potentially linked to HD as in the presence of mutant Huntingtin (Htt), post-Golgi Rab8 dependent trafficking to lysosomes is compromised (del Toro et al 2009).

Thus, it seems logical to hypothesize that future therapeutic strategies might be designed to target and correct neuronal trafficking defects, as this can be related to (i) autophagy-mediated protein degradation, known to be essential in maintaining the overall cellular proteostasis, and (ii) to the spreading of aSyn pathology in the brain. Additional studies using other cell and animal models will continue to shed light into the role of intracellular trafficking plays in PD and other Synucleinopathies.

Therapeutics may rely on immunotherapy, drug- and/or gene-mediated strategies. The challenge of targeting the molecules, genes or virus to the brain and across the BBB is the major limitation. However, elegant systems to circumvent this barrier are under development. These include liposomes, viral delivery systems and also the transvascular delivery of siRNA (Gonçalves et al 2012). By associating specific brain-recognizable decoys, a successful delivery might be achieved. Importantly, the effectiveness and timeliness of the present strategies might depend on the stage of the disease and also the exact causative mechanisms, suggesting that tailored-therapeutics must be developed.

Advances in drug development suggest that antibodies can cross the blood-brain barrier in limited quantities. Here we proposed that extracellular administration of monoclonal antibodies can modify or inhibit early steps in the aggregation process of aSyn, thus providing further support for passive immunization against diseases with aSyn pathology (Nasstrom et al 2011b). Supporting this line of thought, immunotherapy for Alzheimer's disease has shown that targeting a $\beta$  with antibodies can reduce pathology in both mouse models and human brain. Notably, the antibodies penetration into the BBB is still under the desired concentrations for an effective therapeutic results (Yu & Watts 2013) and further technology advances may be needed to transpose to the clinics the new therapeutic hypothesis that are arising from basic molecular biology.



aSyn seems to behave as a prionic protein, as its aggregated form is found in grafts from foetal tissue 11-16 years after transplantation (Kordower et al 2008, Li et al 2008). Still, grafts transplantation can be a way to delay prionic spread of the protein in mid-term, as for instance, within 18 months, no overt pathology were found after transplantation and motor improvements are noticeable (Kordower et al 1995). In the long term, as disturbances in cellular trafficking seems to be a major pathological consequence of all PD forms, therapy may rely in strategies to restore cellular trafficking and the secondary roads linked to it, as autophagy.

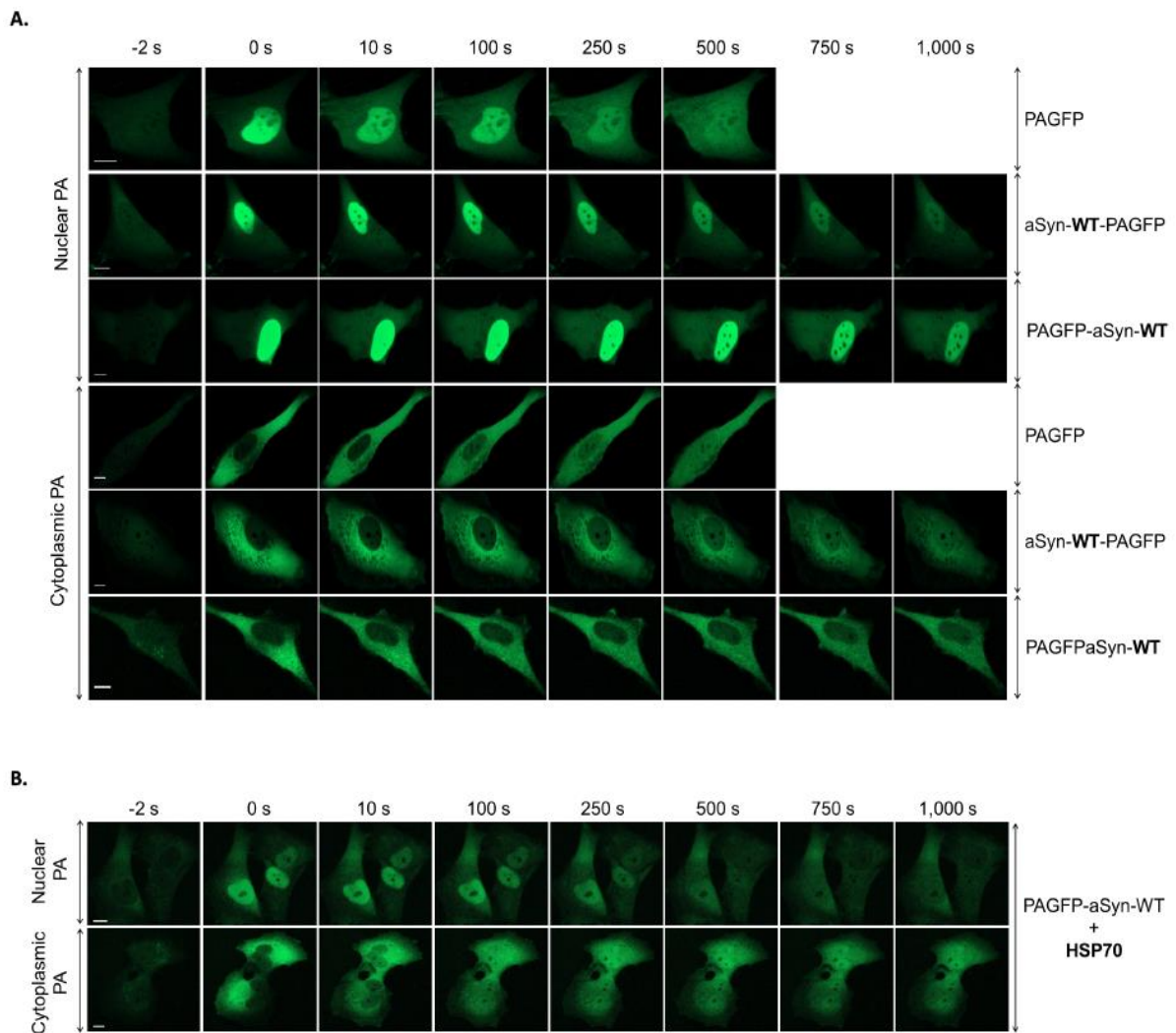


## V. Annexes

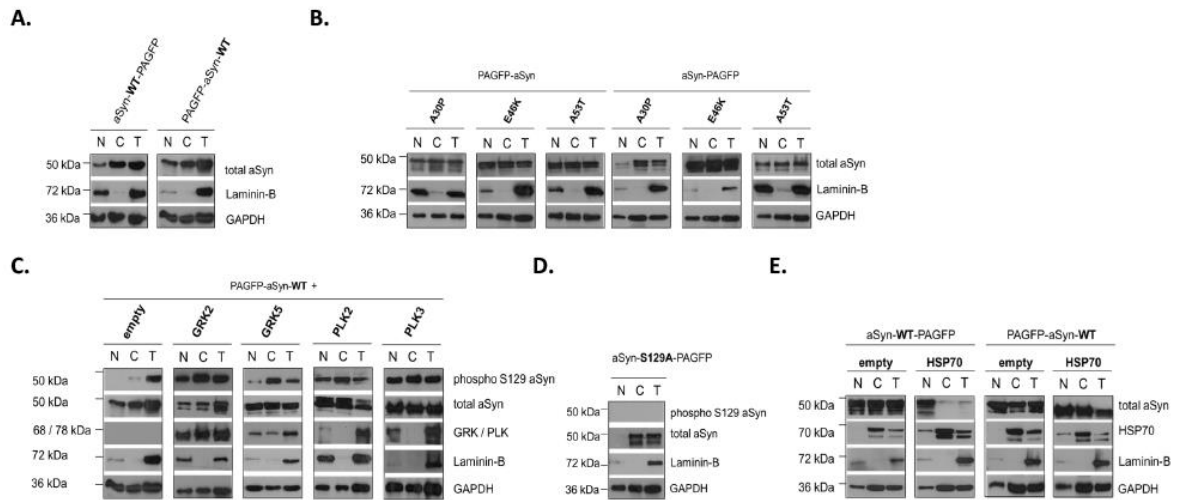
---



## 5.1. Assessing the Subcellular Dynamics of Alpha-Synuclein using Photoactivation Microscopy



**Annex 5.1.1. Subcellular dynamics of aSyn-WT.** **A.** Distribution of PAGFP, aSyn-WT-PAGFP or PAGFP-aSyn-WT in H4 cells before (-2 s), during (0 s) and after (10, 100, 250, 500, 750 and 1,000 s) nuclear and cytoplasmic photoactivation. **B.** Distribution of PAGFP-aSyn-WT co-expressed with HSP70 in H4 cells before (-2 s), during (0 s) and after (10, 100, 250, 500, 750 and 1,000 s) nuclear or cytoplasmic photoactivation. Scale bars: 10  $\mu$ m.



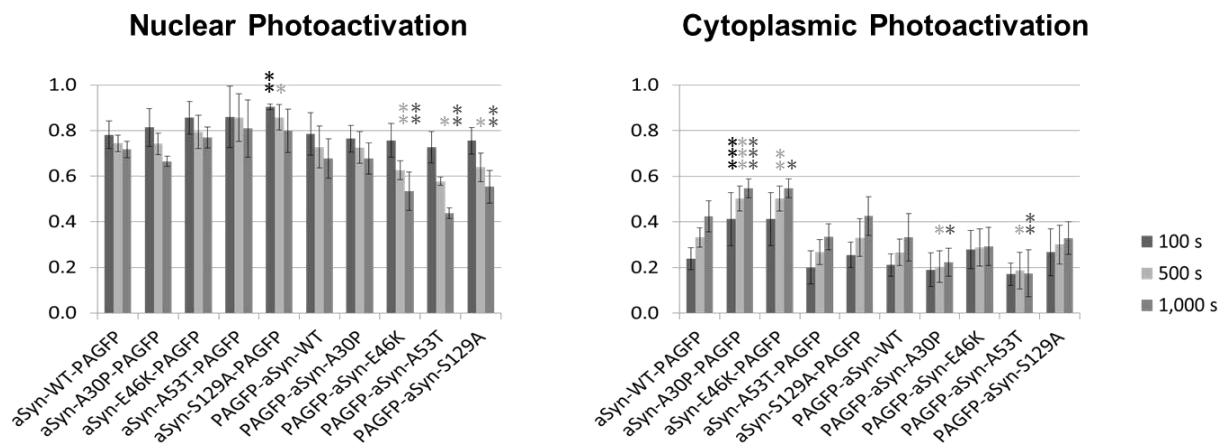
**Annex 5.1.2 Immunoblotting analysis of nuclear and cytosolic protein extracts from cells expressing fusion constructs of aSyn and PAGFP.** **A.** aSyn-WT reporter proteins. **B.** A30P, E46K and A53T aSyn reporter proteins. **C.** PAGFP-aSyn-WT with GRK2, GRK5, PLK2 and PLK3. **D.** PAGFP-aSyn-S129A. **E.** aSyn-WT in the presence or absence of HSP70. N: nuclear fraction; C: cytoplasmic fraction; T: total fraction.

### Annex 5.1.3 Relative nuclear fluorescence of aSyn upon photoactivation.

A. Relative nuclear fluorescence of aSyn variants 100 s, 500 s and 1,000 s after photoactivation.												
Constructs	Nuclear Photoactivation						Cytoplasmic Photoactivation					
	100 s		500 s		1,000 s		100 s		500 s		1,000 s	
	N <sup>1</sup>	p-value <sup>2</sup>	N	p-value	N	p-value	N	p-value	N	p-value	N	p-value
aSyn-WT-PAGFP	0.7815 ± 0.0600		0.7448 ± 0.0358		0.7174 ± 0.0355		0.2391 ± 0.0481		0.3316 ± 0.0427		0.4243 ± 0.0681	
aSyn-A30P-PAGFP	0.8141 ± 0.0831	0.2837	0.7420 ± 0.0473	0.1530	0.6649 ± 0.0226	0.1010	0.4124 ± 0.1165	0.0007***	0.5028 ± 0.0542	< 0.0001***	0.5473 ± 0.0419	0.0003***
aSyn-E46K-PAGFP	0.8564 ± 0.0711	0.9357	0.7934 ± 0.0729	0.2001	0.7700 ± 0.0460	0.6237	0.4124 ± 0.1165	0.0723	0.5028 ± 0.0542	0.0044**	0.5473 ± 0.0419	0.0445*
aSyn-A53T-PAGFP	0.8601 ± 0.1340	0.9813	0.8579 ± 0.1043	0.6783	0.8090 ± 0.1252	0.7762	0.2013 ± 0.0730	0.9610	0.2673 ± 0.0541	0.8710	0.3346 ± 0.0571	0.8149
aSyn-S129A-PAGFP	0.9045 ± 0.013	0.0044**	0.8577 ± 0.0561	0.0124*	0.7988 ± 0.0959	0.2517	0.2553 ± 0.0568	0.6577	0.3304 ± 0.0826	0.9823	0.4256 ± 0.0845	0.9803
PAGFP-aSyn-WT	0.7849 ± 0.0931		0.7277 ± 0.0917		0.6776 ± 0.0866		0.211 ± 0.049		0.2661 ± 0.0579		0.3321 ± 0.1032	
PAGFP-aSyn-A30P	0.7643 ± 0.0580	0.5901	0.7254 ± 0.0696	0.9525	0.6778 ± 0.0678	0.9943	0.1898 ± 0.0734	0.4367	0.2036 ± 0.0690	0.0411	0.2223 ± 0.0615	0.0185
PAGFP-aSyn-E46K	0.7570 ± 0.0747	0.4815	0.6262 ± 0.0410	0.0096**	0.5338 ± 0.0842	0.001**	0.2787 ± 0.0840	0.0541	0.2881 ± 0.0816	0.5480	0.2921 ± 0.083	0.5419
PAGFP-aSyn-A53T	0.7262 ± 0.0682	0.3995	0.5774 ± 0.0184	0.0346*	0.4378 ± 0.0239	0.0013**	0.1709 ± 0.0490	0.1350	0.1861 ± 0.0808	0.0282*	0.1749 ± 0.1039	0.0096**
PAGFP-aSyn-S129A	0.7554 ± 0.0582	0.5668	0.6387 ± 0.0628	0.0282*	0.5540 ± 0.0715	0.0099**	0.2668 ± 0.1025	0.3967	0.3007 ± 0.0852	0.2817	0.3285 ± 0.0714	0.4130

<sup>1</sup> N: Nuclear fluorescence. For simplicity, the cytoplasmic fluorescence values were suppressed, as they can be represented by 1-N, being the p-value the same of N.

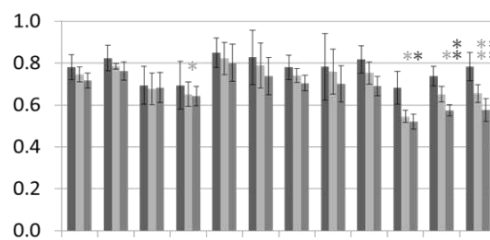
<sup>2</sup> P-values obtained from two-tailed unpaired Student's t-test with 95% of confidence interval ( $\alpha=0.05$ ). Fisher tests comparing the variances between the experimental and control groups revealed the variances are not significantly different.



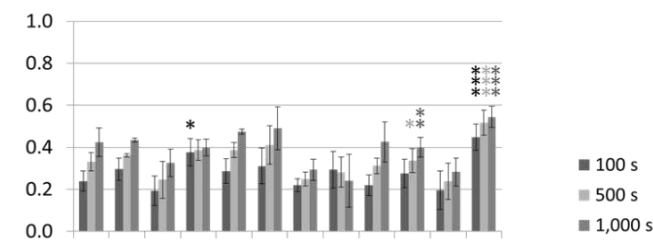
B. Relative nuclear fluorescence of aSyn-WT in the presence of selected genes at 100 s, 500 s and 1,000 s after photoactivation.

Constructs	Nuclear Photoactivation						Cytoplasmic Photoactivation					
	100 s		500 s		1,000 s		100 s		500 s		1,000 s	
	N <sup>1</sup>	p <sup>2</sup>	N	p	N	p		p	N	p	N	p
aSyn-WT-PAGFP + empty	0.7815 ± 0.0600		0.7448 ± 0.0358		0.7174 ± 0.0355		0.2391 ± 0.0481		0.3316 ± 0.0427		0.4243 ± 0.0681	
aSyn-WT-PAGFP + GRK2	0.8235 ± 0.0612	0.3651	0.7849 ± 0.0138	0.0818	0.7625 ± 0.0436	0.2804	0.2960 ± 0.0538	0.2442	0.3622 ± 0.0068	0.2875	0.4352 ± 0.0096	0.7980
aSyn-WT-PAGFP + GRK5	0.6937 ± 0.0902	0.1562	0.6766 ± 0.0763	0.1564	0.6826 ± 0.0714	0.5656	0.1939 ± 0.0711	0.4128	0.2455 ± 0.0880	0.2023	0.3259 ± 0.0656	0.1458
aSyn-WT-PAGFP + PLK2	0.6940 ± 0.1147	0.1793	0.6512 ± 0.0581	0.0118*	0.6424 ± 0.0461	0.0574	0.3766 ± 0.0661	0.0124*	0.3868 ± 0.0487	0.1285	0.3995 ± 0.0404	0.5332
aSyn-WT-PAGFP + PLK3	0.8507 ± 0.0702	0.1335	0.8220 ± 0.0761	0.0928	0.8018 ± 0.0880	0.2525	0.2876 ± 0.0591	0.3003	0.3880 ± 0.0362	0.1165	0.4756 ± 0.0118	0.1874
aSyn-WT-PAGFP + HSP70	0.8273 ± 0.1305	0.5472	0.7890 ± 0.1067	0.4624	0.7387 ± 0.0887	0.7705	0.3116 ± 0.0848	0.2203	0.4115 ± 0.0926	0.2083	0.4917 ± 0.1019	0.3420
PAGFP-aSyn-WT + empty	0.7803 ± 0.0582		0.7413 ± 0.0338		0.7037 ± 0.0372		0.2191 ± 0.0306		0.2489 ± 0.0338		0.2935 ± 0.0503	
PAGFP-aSyn-WT + GRK2	0.7820 ± 0.1604	0.9844	0.7591 ± 0.1073	0.7608	0.7016 ± 0.0857	0.9653	0.2939 ± 0.0881	0.1334	0.2823 ± 0.0711	0.3973	0.2413 ± 0.1253	0.6214
PAGFP-aSyn-WT + GRK5	0.8170 ± 0.0648	0.5186	0.7533 ± 0.0534	0.7438	0.6900 ± 0.0463	0.7104	0.2196 ± 0.0484	0.9867	0.3121 ± 0.0369	0.1027	0.4264 ± 0.0962	0.0773
PAGFP-aSyn-WT + PLK2	0.6826 ± 0.0793	0.1841	0.5455 ± 0.0299	0.0141*	0.5204 ± 0.0348	0.0364*	0.2765 ± 0.0676	0.1486	0.3373 ± 0.0569	0.0207*	0.4001 ± 0.0457	0.0058**
PAGFP-aSyn-WT + PLK3	0.7376 ± 0.0456	0.3446	0.6516 ± 0.0361	0.0198*	0.5745 ± 0.0262	0.0038**	0.1956 ± 0.0911	0.1702	0.2394 ± 0.0860	0.1573	0.2832 ± 0.0665	0.1646

Nuclear Photoactivation



Cytoplasmic Photoactivation



<sup>1</sup> N: Nuclear fluorescence. For simplicity, the cytoplasmic fluorescence values were suppressed, as they can be represented by 1-N, being the p-value the same of N.

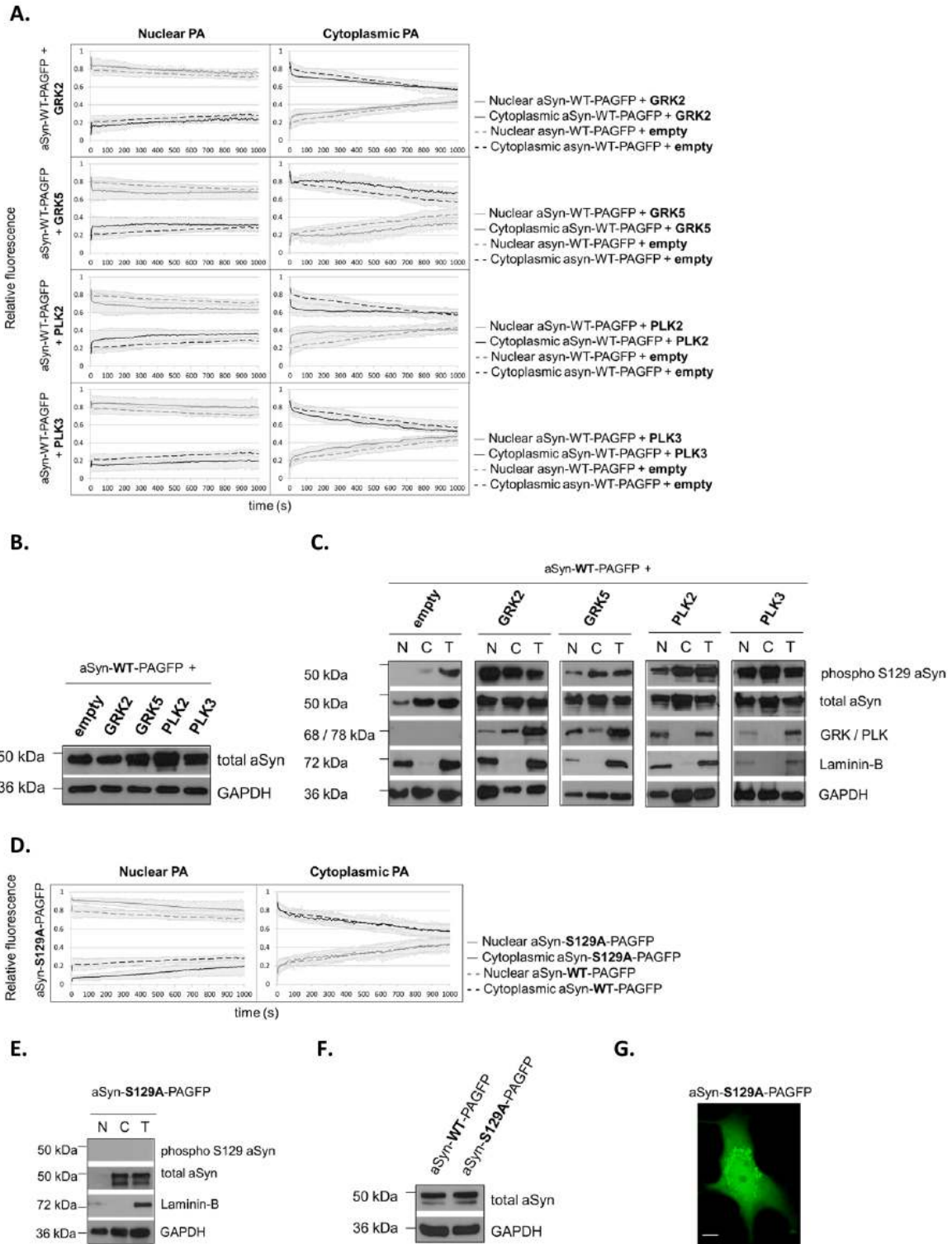
<sup>2</sup> P-values obtained from two-tailed unpaired Student's t-test with 95% of confidence interval ( $\alpha=0.05$ ). Fisher tests comparing the variances between the experimental and control groups revealed the variances are not significantly different.

aSyn-WT-PAGFP + empty  
aSyn-WT-PAGFP + GRK2  
aSyn-WT-PAGFP + GRK5  
aSyn-WT-PAGFP + PLK2  
aSyn-WT-PAGFP + PLK3  
PAGFP-aSyn-WT + HSP70  
PAGFP-aSyn-WT + empty  
PAGFP-aSyn-WT + GRK2  
PAGFP-aSyn-WT + GRK5  
PAGFP-aSyn-WT + PLK2  
PAGFP-aSyn-WT + PLK3  
PAGFP-aSyn-WT + HSP70

aSyn-WT-PAGFP + empty  
aSyn-WT-PAGFP + GRK2  
aSyn-WT-PAGFP + GRK5  
aSyn-WT-PAGFP + PLK2  
aSyn-WT-PAGFP + PLK3  
PAGFP-aSyn-WT + HSP70  
PAGFP-aSyn-WT + empty  
PAGFP-aSyn-WT + GRK2  
PAGFP-aSyn-WT + GRK5  
PAGFP-aSyn-WT + PLK2  
PAGFP-aSyn-WT + PLK3  
PAGFP-aSyn-WT + HSP70

■ 100 s  
■ 500 s  
■ 1,000 s





**Annex 5.1.4. Effect of S129 phosphorylation status on the subcellular dynamics of aSyn-WT-PAGFP.** **A.** Fluorescence intensities after photoactivation in the nucleus (light grey lines) and in the cytoplasm (dark grey lines) of aSyn-WT-PAGFP fusion proteins co-expressed with GRK2, GRK5,

PLK2 and PLK3 (solid lines) over time. Fluorescence intensities of photoactivated control aSyn-WT-PAGFP constructs after co-transfection with an empty vector are shown in dashed lines. Values are mean  $\pm$  standard deviation of 15 cells analyzed per condition; **B.** Immunoblotting analysis of total aSyn levels in cells expressing aSyn-WT-PAGFP or aSyn-S129A-PAGFP; **C.** Immunoblotting analysis of aSyn-WT-PAGFP construct co-expressed with GRK2, GRK5, PLK2 and PLK3. N: nuclear fraction; C: cytoplasmic fraction; T: total fraction; **D.** Fluorescence intensities after photoactivation in the nucleus (light grey) and in the cytoplasm (dark grey) of aSyn-S129A-PAGFP fusion proteins (solid lines) over time. Fluorescence intensities of photoactivated control aSyn-WT-PAGFP fusion proteins are shown in dashed lines. Values are mean  $\pm$  standard deviation of up to 15 cells analyzed for each condition; **E.** Immunoblotting analysis of cells expressing aSyn-S129A-PAGFP. N: nuclear fraction; C: cytoplasmic fraction; T: total fraction; **F.** Immunoblotting analysis of total aSyn levels in cells expressing aSyn-WT-PAGFP or aSyn-S129A-PAGFP; **G.** Cytosolic inclusions in cells expressing aSyn-S129A-PAGFP. Images were taken 500 s after photoactivation in the nucleus in order to increase the contrast of the cytosolic inclusions. Scale bar: 10  $\mu$ m.

### Annex 5.1.5. aSyn intracellular dynamics upon photoactivation.

Construct	aSyn Dynamics <sup>1</sup>	
	Nuclear PA <sup>2</sup>	Cytoplasmic PA
	WT-aSyn dynamics	
aSyn-WT-PAGFP	N <sup>3</sup>	C+N <sup>4</sup>
PAGFP-aSyn-WT	N	C <sup>5</sup>
	PD-associated aSyn mutants dynamics	
aSyn-A30P-PAGFP	N	<i>C+N quickly</i>
PAGFP- aSyn-A30P	N	C
aSyn-E46K-PAGFP	N	<i>C+N quickly</i>
PAGFP-aSyn-E46K	<i>N+C<sup>6</sup></i>	C
aSyn-A53T-PAGFP	N	C+N
PAGFP-aSyn-A53T	<i>N+C</i>	C
	Phosphorylated aSyn dynamics	
aSyn-WT-PAGFP + empty	N	C+N
PAGFP-aSyn-WT + empty	N	C
WT-aSyn-PAGFP + GRK2	N	C+N
PAGFP-aSyn-WT + GRK2	N	C
aSyn- WT-PAGFP + GRK5	N	C+N
PAGFP-aSyn-WT + GRK5	N	<i>C+N</i>
aSyn-WT-PAGFP + PLK2	N	C+N
PAGFP-aSyn-WT + PLK2	<i>N+C</i>	C
aSyn-WT-PAGFP + PLK3	N	C+N
PAGFP-aSyn-WT + PLK3	<i>N+C</i>	C
aSyn-S129A-PAGFP	N	C+N
PAGFP-aSyn-S129A	<i>N+C</i>	C
	aSyn dynamics in the presence of HSP70 chaperone	
WT-aSyn-PAGFP + HSP70	N	C+N
PAGFP-aSyn-WT + HSP70	<i>N+C</i>	<i>C+N quickly</i>

<sup>1</sup> aSyn subcellular localization: cytoplasm and nucleus

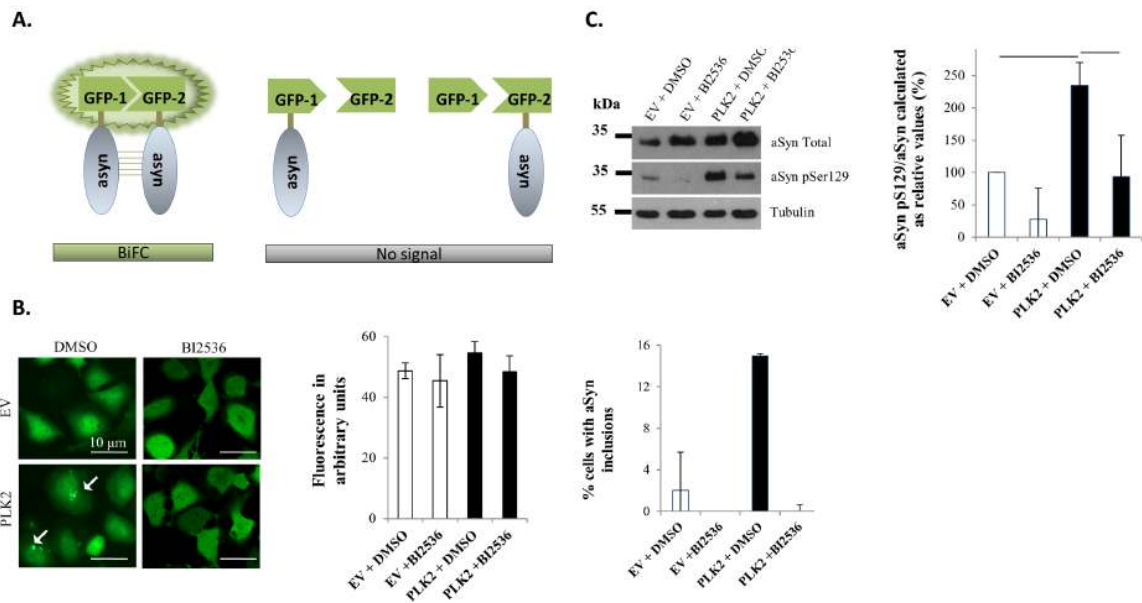
<sup>2</sup> PA: photoactivation

<sup>3</sup> N: maintained in the nucleus

<sup>4</sup> C+N: spread from the cytoplasm to the nucleus

<sup>5</sup> C: maintained in the cytoplasm

<sup>6</sup> N+C: spread from the nucleus to the cytoplasm



**Annex 5.1.6. PLK2 promotes aSyn inclusion formation in human cells.** **A.** Schematic representation of the BiFC assay. Two aSyn molecules are fused to two non-fluorescent halves of a fluorescent reporter, in this case, GFP. If the proteins interact, they bring together the halves of the reporter protein and reconstitute the functional fluorophore. Protein complementation occurs only when aSyn is fused to fragments of GFP, and not observed when a GFP fragments alone are expressed. **B.** Microscopy analysis of H4 cells stably transfected with GN-link-aSyn+aSyn-GC and transiently co-transfected either with PLK2 or an empty vector (EV), in the presence (BI2536) or absence (DMSO) of a kinase inhibitor. aSyn fluorescence intensity is quantified in arbitrary units. The percentage of cells with aSyn inclusions is shown. **C.** H4 cells stably transfected with GN-link-aSyn+aSyn-GC were immunoblotted 48 h post transient co-transfection either with PLK2 or empty control (EV), in the presence (BI2536) or absence (DMSO) of a kinase inhibitor, using antibodies against aSyn phosphorylated on Ser-129 and total aSyn. Ser-129 phosphorylation levels were normalized for the total amount of aSyn (mean  $\pm$  standard deviation) and relative to the EV + DMSO condition. All data presented are representative of three independent experiments. Statistical analysis was performed using two-tailed Student's t test for unpaired data (\*= $p < 0.05$ ), (\*\*= $p < 0.005$ ).

## 5.2. shRNA-Based Screen Identifies Endocytic Recycling Pathway Components that Act as Genetic Modifiers of Alpha-Synuclein Aggregation, Secretion and Toxicity

Annex 5.2.1. List of screened genes in the RNAi assay using aSyn-BiFC stable cells as readout. **A.** Human trafficking collection **B.** Human kinases / phosphatases collection.

A. Human trafficking collection					
Gene name	NM_Id	Gene name	NM_Id	Gene name	NM_Id
<b>BET1L</b>	NM_016526	<b>RAB10</b>	NM_016131	<b>RAB37</b>	NM_175738
<b>BNIP1</b>	NM_001205	<b>RAB11A</b>	NM_004663	<b>RAB38</b>	NM_022337
<b>EPIM</b>	NM_001980	<b>RAB11B</b>	NM_004218	<b>RAB39</b>	NM_017516
<b>GOSR1</b>	NM_004871	<b>RAB13</b>	NM_002870	<b>RAB39B</b>	NM_171998
<b>GOSR2</b>	NM_004287	<b>RAB14</b>	NM_016322	<b>RAB40B</b>	NM_006822
<b>RAB1B</b>	NM_030981	<b>RAB15</b>	NM_198686	<b>RAB40C</b>	NM_021168
<b>RAB2B</b>	NM_032846	<b>RAB17</b>	NM_022449	<b>SEC22L2</b>	NM_012430
<b>RAB2</b>	NM_002865	<b>RAB18</b>	NM_021252	<b>SEC22L3</b>	NM_004206
<b>RAB3A</b>	NM_002866	<b>RAB20</b>	NM_017817	<b>SNAP29</b>	NM_004782
<b>RAB3B</b>	NM_002867	<b>RAB21</b>	NM_014999	<b>STX11</b>	NM_003764
<b>RAB3C</b>	NM_138453	<b>RAB22A</b>	NM_020673	<b>STX12</b>	NM_177424
<b>RAB3D</b>	NM_004283	<b>RAB23</b>	NM_016277	<b>STX17</b>	NM_017919
<b>RAB4A</b>	NM_004578	<b>RAB24</b>	NM_130781	<b>STX1A</b>	NM_004603
<b>RAB4B</b>	NM_016154	<b>RAB25</b>	NM_020387	<b>STX3A</b>	NM_004177
<b>RAB5A</b>	NM_004162	<b>RAB26</b>	NM_014353	<b>STX4A</b>	NM_004604
<b>RAB5B</b>	NM_002868	<b>RAB27A</b>	NM_004580	<b>STX5A</b>	NM_003164
<b>Mk,RAB5C</b>	NM_004583	<b>RAB27B</b>	NM_004163	<b>STX6</b>	NM_005819
<b>RAB6A</b>	NM_002869	<b>RAB28</b>	NM_004249	<b>STX7</b>	NM_003569
<b>RAB6B</b>	NM_016577	<b>RAB30</b>	NM_014488	<b>STX8</b>	NM_004853
<b>RAB6C</b>	NM_032144	<b>RAB31</b>	NM_006868	<b>SYBL1</b>	NM_005638
<b>RAB7</b>	NM_004637	<b>RAB32</b>	NM_006834	<b>VAMP3</b>	NM_004781
<b>RAB7L1</b>	NM_003929	<b>RAB33A</b>	NM_004794	<b>VTI1A</b>	NM_145206
<b>RAB8A</b>	NM_005370	<b>RAB33B</b>	NM_031296	<b>VTI1B</b>	NM_006370
<b>RAB8B</b>	NM_016530	<b>RAB34</b>	NM_031934	<b>YKT6</b>	NM_006555
<b>RAB9A</b>	NM_004251	<b>RAB35</b>	NM_006861		

<b>RAB9B</b>	NM_016370	<b>RAB36</b>	NM_004914		
<b>B. Human kinases / phosphatases collection</b>					
<b>Gene name</b>	<b>NM_Id</b>	<b>Gene name</b>	<b>NM_Id</b>	<b>Gene name</b>	<b>NM_Id</b>
<b>AAK1</b>	NM_014911	<b>ALS2CR2</b>	NM_018571	<b>C3orf29</b>	NM_022485
<b>AATK</b>	XM_375495	<b>ALS2CR7</b>	NM_139158	<b>C3orf48</b>	NM_144714
<b>ABL1</b>	NM_005157	<b>AMHR2</b>	NM_020547	<b>C7orf16</b>	NM_006658
<b>ABL1</b>	NM_007313	<b>ANKK1</b>	NM_178510	<b>C9orf96</b>	XM_376921
<b>ABL2</b>	NM_005158	<b>ANP32A</b>	NM_006305	<b>CABC1</b>	NM_020247
<b>ACACB</b>	NM_001093	<b>APC</b>	NM_000038	<b>CALM1</b>	NM_006888
<b>ACP1</b>	NM_007099	<b>APPL</b>	NM_012096	<b>CALM2</b>	NM_001743
<b>ACP6</b>	NM_016361	<b>ARAF</b>	NM_001654	<b>CALM3</b>	NM_005184
<b>ACPL2</b>	NM_152282	<b>ARF1</b>	NM_001658	<b>CAMK1</b>	NM_003656
<b>ACPP</b>	NM_001099	<b>ARHGAP29</b>	NM_004815	<b>CAMK1D</b>	NM_020397
<b>ACPT</b>	NM_080789	<b>ARHGEF2</b>	NM_004723	<b>CAMK1G</b>	NM_020439
<b>ACVR1</b>	NM_001105	<b>ARMET</b>	NM_006010	<b>CAMK2A</b>	NM_171825
<b>ACVR1B</b>	NM_004302	<b>ARPP-21</b>	NM_198399	<b>CAMK2B</b>	NM_001220
<b>ACVR1B</b>	NM_020328	<b>ATM</b>	NM_000051	<b>CAMK2D</b>	NM_001221
<b>ACVR1C</b>	NM_145259	<b>ATP6V0E2L</b>	XM_088142	<b>CAMK2G</b>	NM_001222
<b>ACVR2A</b>	NM_001616	<b>ATPBD3</b>	NM_145232	<b>CAMK2N1</b>	NM_018584
<b>ACVR2B</b>	NM_001106	<b>ATR</b>	NM_001184	<b>CAMK4</b>	NM_001744
<b>ADAM2</b>	NM_001464	<b>AURKA</b>	NM_003600	<b>CAMKK1</b>	NM_172207
<b>ADCK1</b>	NM_020421	<b>AURKAIP1</b>	NM_017900	<b>CAMKK2</b>	NM_153499
<b>ADCK2</b>	NM_052853	<b>AURKB</b>	NM_004217	<b>CAMKV</b>	NM_024046
<b>ADCK5</b>	NM_174922	<b>AURKC</b>	NM_003160	<b>CARKL</b>	NM_013276
<b>ADK</b>	NM_001123	<b>AXL</b>	NM_001699	<b>CASK</b>	NM_003688
<b>ADPGK</b>	NM_031284	<b>AXL</b>	NM_021913	<b>CBL</b>	NM_005188
<b>ADRBK1</b>	NM_001619	<b>BCKDK</b>	NM_005881	<b>CC2D1A</b>	NM_017721
<b>ADRBK2</b>	NM_005160	<b>BCL2</b>	NM_000633	<b>CCL2</b>	NM_002982
<b>AGTR2</b>	NM_000686	<b>BCL2L11</b>	NM_138621	<b>CCNB3</b>	NM_033670
<b>AK1</b>	NM_000476	<b>BCR</b>	NM_004327	<b>CCND1</b>	NM_053056
<b>AK2</b>	NM_001625	<b>BLK</b>	NM_001715	<b>CCR2</b>	NM_000648
<b>AK3</b>	NM_016282	<b>BMP2K</b>	NM_017593	<b>Ccr2</b>	NM_009915
<b>AK3L1</b>	NM_013410	<b>BMP2KL</b>	XM_293293	<b>CCRK</b>	NM_178432
<b>AK5</b>	NM_012093	<b>BMPR1A</b>	NM_004329	<b>CCRN4L</b>	NM_012118
<b>AK7</b>	NM_152327	<b>BMPR1B</b>	NM_001203	<b>CD40</b>	NM_001250
<b>AKAP3</b>	NM_006422	<b>BMPR2</b>	NM_001204	<b>CDC14A</b>	NM_003672

<b>AKAP4</b>	NM_003886	<b>BMX</b>	NM_001721	<b>CDC14C</b>	NM_152627
<b>AKAP5</b>	NM_004857	<b>BPNT1</b>	NM_006085	<b>CDC2</b>	NM_001786
<b>AKAP6</b>	NM_004274	<b>BRAF</b>	NM_004333	<b>CDC25A</b>	NM_001789
<b>AKAP7</b>	NM_004842	<b>BRCA1</b>	NM_007294	<b>CDC25B</b>	NM_004358
<b>AKAP8</b>	NM_005858	<b>BRCA2</b>	NM_000059	<b>CDC25C</b>	NM_001790
<b>AKAP8L</b>	NM_014371	<b>BRD2</b>	NM_005104	<b>CDC2L1</b>	NM_001787
<b>AKAP9</b>	NM_005751	<b>BRD3</b>	NM_007371	<b>CDC2L2</b>	NM_024011
<b>AKAP10</b>	NM_007202	<b>BRD4</b>	NM_058243	<b>CDC2L5</b>	NM_003718
<b>AKAP11</b>	NM_016248	<b>BRDT</b>	NM_001726	<b>CDC2L6</b>	NM_015076
<b>AKAP12</b>	NM_005100	<b>BRSK1</b>	NM_032430	<b>CDC42BPA</b>	NM_014826
<b>AKAP13</b>	NM_006738	<b>BRSK2</b>	NM_003957	<b>CDC42BPA</b>	NM_003607
<b>AKAP14</b>	NM_178813	<b>BTK</b>	NM_000061	<b>CDC42BPB</b>	NM_006035
<b>AKT1</b>	NM_005163	<b>BUB1</b>	NM_004336	<b>CDC42BPG</b>	XM_290516
<b>AKT2</b>	NM_001626	<b>BUB1B</b>	NM_001211	<b>CDC42SE2</b>	NM_020240
<b>AKT3</b>	NM_005465	<b>C11orf17</b>	NM_020642	<b>CDC7</b>	NM_003503
<b>ALK</b>	NM_004304	<b>C14orf41</b>	XM_495996	<b>CDH1</b>	NM_004360
<b>ALPK1</b>	NM_025144	<b>C15orf42</b>	NM_152259	<b>CDK10</b>	NM_003674
<b>ALPK2</b>	NM_052947	<b>C17orf51</b>	XM_378661	<b>CDK10</b>	NM_052987
<b>ALPK3</b>	NM_020778	<b>C17orf75</b>	NM_022344	<b>CDK2</b>	NM_001798
<b>CDK2</b>	NM_052827	<b>CSK</b>	NM_004383	<b>DOK1</b>	NM_001381
<b>CDK4</b>	NM_000075	<b>CSMD1</b>	NM_033225	<b>DTYMK</b>	NM_012145
<b>CDK5</b>	NM_004935	<b>CSNK1A1</b>	NM_001892	<b>DULLARD</b>	NM_015343
<b>CDK5R1</b>	NM_003885	<b>CSNK1A1L</b>	NM_145203	<b>DUSP1</b>	NM_004417
<b>CDK6</b>	NM_001259	<b>CSNK1D</b>	NM_001893	<b>DUSP3</b>	NM_004090
<b>CDK7</b>	NM_001799	<b>CSNK1D</b>	NM_139062	<b>DUSP4</b>	NM_001394
<b>CDK8</b>	NM_001260	<b>CSNK1E</b>	NM_001894	<b>DUSP5</b>	NM_004419
<b>CDK9</b>	NM_001261	<b>CSNK1E</b>	NM_152221	<b>DUSP6</b>	NM_001946
<b>CDKL1</b>	NM_004196	<b>CSNK1G2</b>	NM_001319	<b>DUSP8</b>	NM_004420
<b>CDKL2</b>	NM_003948	<b>CSNK1G3</b>	NM_004384	<b>DUSP9</b>	NM_001395
<b>CDKL3</b>	NM_016508	<b>CSNK2A1</b>	NM_001895	<b>DUSP10</b>	NM_007207
<b>CDKL4</b>	XM_293029	<b>CSNK2A1</b>	NM_177559	<b>DUSP11</b>	NM_003584
<b>CDKL5</b>	NM_003159	<b>CSNK2A2</b>	NM_001896	<b>DUSP12</b>	NM_007240
<b>CDKN1A</b>	NM_000389	<b>CTDP1</b>	NM_004715	<b>DUSP13</b>	NM_016364
<b>CDKN1B</b>	NM_004064	<b>CTDSP2</b>	NM_005730	<b>DUSP14</b>	NM_007026
<b>CDKN1C</b>	NM_000076	<b>CYLD</b>	NM_015247	<b>DUSP15</b>	NM_080611
<b>CDKN2A</b>	NM_058197	<b>DAB2IP</b>	NM_032552	<b>DUSP18</b>	NM_152511
<b>CDKN2C</b>	NM_001262	<b>DAPK1</b>	NM_004938	<b>DUSP19</b>	NM_080876

<b>CERK</b>	NM_182661	<b>DAPK2</b>	NM_014326	<b>DUSP21</b>	NM_022076
<b>CERKL</b>	NM_201548	<b>DAPK3</b>	NM_001348	<b>DUSP22</b>	NM_020185
<b>CHEK1</b>	NM_001274	<b>DAPP1</b>	NM_014395	<b>DUSP26</b>	NM_024025
<b>CHEK2</b>	NM_007194	<b>DBF4</b>	NM_006716	<b>DUSP27</b>	XM_043739
<b>CHKA</b>	NM_001277	<b>DCAMKL1</b>	NM_004734	<b>DVL1</b>	NM_004421
<b>CHKB</b>	NM_005198	<b>DCAMKL2</b>	NM_152619	<b>DVL2</b>	NM_004422
<b>CHUK</b>	NM_001278	<b>DCAMKL3</b>	XM_047355	<b>DYRK1A</b>	NM_001396
<b>CIB2</b>	NM_006383	<b>DCC</b>	NM_005215	<b>DYRK1B</b>	NM_004714
<b>CIB3</b>	NM_054113	<b>DCK</b>	NM_000788	<b>DYRK2</b>	NM_003583
<b>CIB4</b>	XM_059399	<b>DDR1</b>	NM_001954	<b>DYRK3</b>	NM_003582
<b>CILP</b>	NM_003613	<b>DDR2</b>	NM_006182	<b>DYRK4</b>	NM_003845
<b>CINP</b>	NM_032630	<b>DGKA</b>	NM_001345	<b>DYSF</b>	NM_003494
<b>CIT</b>	NM_007174	<b>DGKB</b>	NM_004080	<b>E2F1</b>	NM_005225
<b>CKB</b>	NM_001823	<b>DGKD</b>	NM_003648	<b>EEF2K</b>	NM_013302
<b>CKM</b>	NM_001824	<b>DGKE</b>	NM_003647	<b>EGFR</b>	NM_005228
<b>CKMT1B</b>	NM_020990	<b>DGKG</b>	NM_001346	<b>EGLN1</b>	NM_022051
<b>CKMT2</b>	NM_001825	<b>DGKH</b>	NM_152910	<b>EGLN3</b>	NM_022073
<b>CKS1B</b>	NM_001826	<b>DGKI</b>	NM_004717	<b>EIF2AK1</b>	NM_014413
<b>CKS2</b>	NM_001827	<b>DGKK</b>	XM_066534	<b>EIF2AK2</b>	NM_002759
<b>CLK1</b>	NM_004071	<b>DGKQ</b>	NM_001347	<b>EIF2AK3</b>	NM_004836
<b>CLK2</b>	NM_003993	<b>DGKZ</b>	NM_003646	<b>ELAC2</b>	NM_018127
<b>CLK3</b>	NM_003992	<b>DGUOK</b>	NM_001929	<b>ELAVL4</b>	NM_021952
<b>CLK4</b>	NM_020666	<b>DHH</b>	NM_021044	<b>ENDOG</b>	NM_004435
<b>CMPK</b>	NM_016308	<b>DKC1</b>	NM_001363	<b>ENPP1</b>	NM_006208
<b>CNKS1R</b>	NM_006314	<b>DKFZp686K16132</b>	XM_371497	<b>ENPP6</b>	NM_153343
<b>CNKS1R3</b>	NM_173515	<b>DKFZp761P0423</b>	XM_291277	<b>ENPP7</b>	NM_178543
<b>CNP</b>	NM_033133	<b>DLEC1</b>	NM_005106	<b>EP300</b>	NM_001429
<b>COL3A1</b>	NM_000090	<b>DLG1</b>	NM_004087	<b>EPB41L4A</b>	NM_022140
<b>COL4A3BP</b>	NM_005713	<b>DLG2</b>	NM_001364	<b>EPHA1</b>	NM_005232
<b>CPNE1</b>	NM_152928	<b>DLG4</b>	NM_001365	<b>EPHA2</b>	NM_004431
<b>CPNE2</b>	NM_152727	<b>DMBT1</b>	NM_004406	<b>EPHA3</b>	NM_005233
<b>CPNE3</b>	NM_003909	<b>DMPK</b>	NM_004409	<b>EPHA4</b>	NM_004438
<b>CPT2</b>	NM_000098	<b>DNA2L</b>	XM_166103	<b>EPHA5</b>	NM_004439
<b>CRKL</b>	NM_005207	<b>DNAJC6</b>	NM_014787	<b>EPHA6</b>	NM_173655
<b>CRKRS</b>	NM_016507	<b>DOCK2</b>	NM_004946	<b>EPHA6</b>	XM_114973
<b>CSF1R</b>	NM_005211	<b>DOCK4</b>	NM_014705	<b>EPHA7</b>	NM_004440
<b>EPHA8</b>	NM_020526	<b>FRAP1</b>	NM_004958	<b>HECW1</b>	NM_015052



<b>EPHA10</b>	NM_173641	<b>FRK</b>	NM_002031	<b>HGF</b>	NM_000601
<b>EPHB1</b>	NM_004441	<b>FRMD1</b>	NM_024919	<b>HGS</b>	NM_004712
<b>EPHB2</b>	NM_004442	<b>FRMPD2</b>	NM_152428	<b>HINT3</b>	NM_138571
<b>EPHB3</b>	NM_004443	<b>FUK</b>	NM_145059	<b>HIPK2</b>	NM_022740
<b>EPHB4</b>	NM_004444	<b>FUS</b>	NM_004960	<b>HIPK3</b>	NM_005734
<b>EPHB6</b>	NM_004445	<b>FXN</b>	NM_000144	<b>HIPK4</b>	NM_144685
<b>EPM2A</b>	NM_005670	<b>FYN</b>	NM_002037	<b>HK1</b>	NM_033498
<b>ERBB2</b>	NM_004448	<b>Gabra1</b>	NM_010250	<b>HK2</b>	NM_000189
<b>ERBB3</b>	NM_001982	<b>Gabra2</b>	NM_008066	<b>HK3</b>	NM_002115
<b>ERBB4</b>	NM_005235	<b>Gabra3</b>	NM_008067	<b>HNRPA2B1</b>	NM_002137
<b>EREG</b>	NM_001432	<b>Gabra5</b>	NM_176942	<b>HRAS</b>	NM_176795
<b>ERN1</b>	NM_001433	<b>GAK</b>	NM_005255	<b>HRAS</b>	NM_005343
<b>ESR1</b>	NM_000125	<b>GALK1</b>	NM_000154	<b>HRASLS</b>	NM_020386
<b>ETNK1</b>	NM_018638	<b>GALK2</b>	NM_002044	<b>HSP90AA1</b>	NM_005348
<b>ETNK2</b>	NM_018208	<b>GAPVD1</b>	XM_044196	<b>HSPA5</b>	NM_005347
<b>EVI1</b>	NM_005241	<b>GBL</b>	NM_022372	<b>HSPB8</b>	NM_014365
<b>EXO1</b>	NM_130398	<b>GCK</b>	NM_033507	<b>HUNK</b>	NM_014586
<b>EXOSC10</b>	NM_002685	<b>GCKR</b>	NM_001486	<b>IBTK</b>	XM_371835
<b>EXT1</b>	NM_000127	<b>GEFT</b>	NM_133483	<b>ICK</b>	NM_014920
<b>EXT2</b>	NM_000401	<b>GGTL3</b>	NM_178025	<b>IGBP1</b>	NM_001551
<b>EZH1</b>	NM_001991	<b>GK</b>	NM_000167	<b>IGF1</b>	NM_000618
<b>EZH2</b>	NM_004456	<b>GK2</b>	NM_033214	<b>IGF1R</b>	NM_000875
<b>FAM62A</b>	NM_015292	<b>GKAP1</b>	NM_025211	<b>IHH</b>	XM_050846
<b>FAS</b>	NM_000043	<b>GLI2</b>	NM_030379	<b>IHPK2</b>	NM_016291
<b>FASN</b>	NM_004104	<b>GMFB</b>	NM_004124	<b>IHPK3</b>	NM_054111
<b>FASTK</b>	NM_006712	<b>GMFG</b>	NM_004877	<b>IKBKAP</b>	NM_003640
<b>FCRL2</b>	NM_030764	<b>GMIP</b>	NM_016573	<b>IKBKE</b>	NM_014002
<b>FER</b>	NM_005246	<b>GNB2L1</b>	NM_006098	<b>ILK</b>	NM_004517
<b>FER1L3</b>	NM_013451	<b>GNE</b>	NM_005476	<b>ILKAP</b>	NM_030768
<b>FES</b>	NM_002005	<b>GPR109A</b>	NM_177551	<b>ILVBL</b>	NM_176826
<b>FGFR1</b>	NM_000604	<b>Gpr109a</b>	NM_030701	<b>INPP4A</b>	NM_001566
<b>FGFR2</b>	NM_000141	<b>Gpr12</b>	NM_008151	<b>INPP4B</b>	NM_003866
<b>FGFR3</b>	NM_000142	<b>GPSM2</b>	NM_013296	<b>INPP5D</b>	NM_005541
<b>FGFR4</b>	NM_002011	<b>GRK1</b>	NM_002929	<b>INPP5E</b>	NM_019892
<b>FGR</b>	NM_005248	<b>GRK4</b>	NM_005307	<b>INPP5F</b>	NM_014937
<b>FIGN</b>	NM_018086	<b>GRK5</b>	NM_005308	<b>INPPL1</b>	NM_001567
<b>FLJ21438</b>	XM_029084	<b>GRK6</b>	NM_002082	<b>INSR</b>	NM_000208

<b>FLJ23356</b>	NM_032237	<b>GRK7</b>	NM_139209	<b>INSRR</b>	NM_014215
<b>FLJ25006</b>	NM_144610	<b>GSC</b>	NM_173849	<b>IPMK</b>	NM_152230
<b>FLJ30092</b>	XM_497354	<b>GSG2</b>	NM_031965	<b>IRAK1</b>	NM_001569
<b>FLJ30698</b>	XM_375602	<b>GSK3A</b>	NM_019884	<b>IRAK2</b>	NM_001570
<b>FLJ32658</b>	NM_144688	<b>GSK3B</b>	NM_002093	<b>IRAK3</b>	NM_007199
<b>FLJ40125</b>	NM_178494	<b>GTF2H1</b>	NM_005316	<b>IRAK4</b>	NM_016123
<b>FLJ40852</b>	NM_173677	<b>GUCY2C</b>	NM_004963	<b>IRS1</b>	NM_005544
<b>FLT1</b>	NM_002019	<b>GUCY2F</b>	NM_001522	<b>ITCH</b>	NM_031483
<b>FLT3</b>	NM_004119	<b>GUK1</b>	NM_000858	<b>ITGAV</b>	NM_002210
<b>FLT3LG</b>	NM_001459	<b>GZMA</b>	NM_006144	<b>ITGB3</b>	NM_000212
<b>FLT4</b>	NM_002020	<b>GZMB</b>	NM_004131	<b>ITK</b>	NM_005546
<b>FN3K</b>	NM_022158	<b>GZMH</b>	NM_033423	<b>ITPK1</b>	NM_014216
<b>FN3KRP</b>	NM_024619	<b>GZMK</b>	NM_002104	<b>ITPKA</b>	NM_002220
<b>FNDC3B</b>	NM_022763	<b>GZMM</b>	NM_005317	<b>ITPKB</b>	NM_002221
<b>FOXO1A</b>	NM_002015	<b>HABP2</b>	NM_004132	<b>ITPKC</b>	NM_025194
<b>FOXO3A</b>	NM_001455	<b>HCK</b>	NM_002110	<b>ITSN1</b>	NM_003024
<b>ITSN2</b>	NM_019595	<b>LOC440091</b>	XM_495916	<b>MAP4K5</b>	NM_006575
<b>JAK1</b>	NM_002227	<b>LOC440345</b>	XM_496125	<b>MAPK1</b>	NM_138957
<b>JAK2</b>	NM_004972	<b>LOC440354</b>	XM_496137	<b>MAPK3</b>	NM_002746
<b>JAK3</b>	NM_000215	<b>LOC440388</b>	XM_496170	<b>MAPK4</b>	NM_002747
<b>JUN</b>	NM_002228	<b>LOC440820</b>	XM_496519	<b>MAPK6</b>	NM_002748
<b>KALRN</b>	NM_007064	<b>LOC441655</b>	XM_497366	<b>MAPK7</b>	NM_139034
<b>KDR</b>	NM_002253	<b>LOC441759</b>	XM_497498	<b>MAPK7</b>	NM_139032
<b>KHK</b>	NM_000221	<b>LOC441812</b>	XM_497579	<b>MAPK8</b>	NM_139049
<b>KIAA0226</b>	XM_032901	<b>LOC441868</b>	XM_497647	<b>MAPK8IP1</b>	NM_005456
<b>KIAA0999</b>	NM_025164	<b>LOC442075</b>	XM_497910	<b>MAPK8IP2</b>	NM_012324
<b>KIAA1303</b>	NM_020761	<b>LOC442558</b>	XM_499301	<b>MAPK8IP3</b>	NM_015133
<b>KIAA1446</b>	NM_020836	<b>LOC644379</b>	XM_372273	<b>MAPK9</b>	NM_139069
<b>KIAA1639</b>	XM_290923	<b>LOC644644</b>	XM_372274	<b>MAPK9</b>	NM_002752
<b>KIAA1706</b>	NM_030636	<b>LOC647208</b>	XM_496155	<b>MAPK10</b>	NM_002753
<b>KIAA1804</b>	NM_032435	<b>LOC91461</b>	XM_038576	<b>MAPK10</b>	NM_138982
<b>KIAA2002</b>	XM_370878	<b>LRPPRC</b>	NM_133259	<b>MAPK11</b>	NM_002751
<b>KIDINS220</b>	XM_291015	<b>LRRK1</b>	NM_024652	<b>MAPK12</b>	NM_002969
<b>KIT</b>	NM_000222	<b>LRRK2</b>	XM_058513	<b>MAPK13</b>	NM_002754
<b>KLHL23</b>	NM_144711	<b>LTK</b>	NM_002344	<b>MAPK14</b>	NM_001315
<b>KRAS</b>	NM_033360	<b>LYK5</b>	NM_153335	<b>MAPK14</b>	NM_139012
<b>KRAS</b>	NM_004985	<b>LYN</b>	NM_002350	<b>MAPK15</b>	NM_139021

<b>KSR1</b>	XM_290793	<b>MADD</b>	NM_003682	<b>MAPKAP1</b>	NM_024117
<b>KSR2</b>	NM_173598	<b>MAGI3</b>	NM_020965	<b>MAPKAP2</b>	NM_032960
<b>LATS1</b>	NM_004690	<b>MAK</b>	NM_005906	<b>MAPKAP3</b>	NM_004635
<b>LATS2</b>	NM_014572	<b>MAMDC1</b>	NM_182830	<b>MAPKAP5</b>	NM_003668
<b>LCK</b>	NM_005356	<b>MAMDC2</b>	NM_153267	<b>MAPKBP1</b>	XM_031706
<b>LIG4</b>	NM_002312	<b>MAP2K1</b>	NM_002755	<b>MARK1</b>	NM_018650
<b>LIMK1</b>	NM_002314	<b>MAP2K1IP1</b>	NM_021970	<b>MARK2</b>	NM_004954
<b>LIMK2</b>	NM_016733	<b>MAP2K2</b>	NM_030662	<b>MARK3</b>	NM_002376
<b>LMTK3</b>	XM_055866	<b>MAP2K3</b>	NM_002756	<b>MASA</b>	NM_021204
<b>LOC283155</b>	XM_208545	<b>MAP2K4</b>	NM_003010	<b>MAST1</b>	NM_014975
<b>LOC283871</b>	XM_208887	<b>MAP2K5</b>	NM_145162	<b>MAST2</b>	NM_015112
<b>LOC375133</b>	NM_199345	<b>MAP2K6</b>	NM_002758	<b>MAST3</b>	XM_038150
<b>LOC375449</b>	NM_198828	<b>MAP2K7</b>	NM_005043	<b>MAST4</b>	XM_291141
<b>LOC387870</b>	XM_291991	<b>MAP3K1</b>	XM_042066	<b>MASTL</b>	NM_032844
<b>LOC387927</b>	XM_370726	<b>MAP3K2</b>	NM_006609	<b>MATK</b>	NM_002378
<b>LOC388259</b>	XM_370975	<b>MAP3K3</b>	NM_002401	<b>MAX</b>	NM_002382
<b>LOC389069</b>	XM_371588	<b>MAP3K4</b>	NM_005922	<b>MBIP</b>	NM_016586
<b>LOC389772</b>	XM_372128	<b>MAP3K5</b>	NM_005923	<b>MCTP1</b>	NM_024717
<b>LOC389873</b>	XM_372233	<b>MAP3K6</b>	NM_004672	<b>MCTP2</b>	NM_018349
<b>LOC390641</b>	XM_497469	<b>MAP3K7</b>	NM_145332	<b>MELK</b>	NM_014791
<b>LOC390705</b>	XM_372626	<b>MAP3K7IP1</b>	NM_006116	<b>MEN1</b>	NM_000244
<b>LOC390877</b>	XM_372705	<b>MAP3K8</b>	NM_005204	<b>MERTK</b>	NM_006343
<b>LOC390975</b>	XM_372749	<b>MAP3K9</b>	XM_027237	<b>MET</b>	NM_000245
<b>LOC391025</b>	XM_372775	<b>MAP3K10</b>	NM_002446	<b>MFN2</b>	NM_014874
<b>LOC391428</b>	XM_372953	<b>MAP3K11</b>	NM_002419	<b>MGC16169</b>	NM_033115
<b>LOC391533</b>	XM_497921	<b>MAP3K12</b>	NM_006301	<b>MGC42105</b>	NM_153361
<b>LOC392226</b>	XM_498286	<b>MAP3K13</b>	NM_004721	<b>MINK1</b>	NM_015716
<b>LOC392265</b>	XM_498294	<b>MAP3K14</b>	NM_003954	<b>MINPP1</b>	NM_004897
<b>LOC400301</b>	XM_375150	<b>MAP3K15</b>	XM_372199	<b>MKNK1</b>	NM_003684
<b>LOC400708</b>	XM_375632	<b>MAP4K1</b>	NM_007181	<b>MKNK2</b>	NM_017572
<b>LOC400927</b>	XM_376010	<b>MAP4K2</b>	NM_004579	<b>MLCK</b>	NM_182493
<b>LOC402679</b>	XM_377958	<b>MAP4K3</b>	NM_003618	<b>MLH1</b>	NM_000249
<b>LOC402679</b>	XM_380022	<b>MAP4K4</b>	NM_145687	<b>MLH3</b>	NM_014381
<b>MLKL</b>	NM_152649	<b>NLK</b>	NM_016231	<b>PDK1</b>	NM_002610
<b>MLLT7</b>	NM_005938	<b>NME1</b>	NM_000269	<b>PDK2</b>	NM_002611
<b>MOBK1B</b>	NM_018221	<b>NME2</b>	NM_002512	<b>PDK4</b>	NM_002612
<b>MOBKL1A</b>	NM_173468	<b>NME3</b>	NM_002513	<b>PDPK1</b>	NM_002613

<b>MOBKL2A</b>	NM_130807	<b>NME4</b>	NM_005009	<b>PDXK</b>	NM_003681
<b>MOBKL2B</b>	NM_024761	<b>NME5</b>	NM_003551	<b>PFKFB1</b>	NM_002625
<b>MORC1</b>	NM_014429	<b>NME7</b>	NM_013330	<b>PFKFB2</b>	NM_006212
<b>MORC3</b>	NM_015358	<b>NPR2</b>	NM_000907	<b>PFKFB4</b>	NM_004567
<b>MOS</b>	NM_005372	<b>NR1H4</b>	NM_005123	<b>PFKL</b>	NM_002626
<b>MPP1</b>	NM_002436	<b>NR1I2</b>	NM_003889	<b>PFKM</b>	NM_000289
<b>MPP2</b>	NM_005374	<b>NR1I3</b>	NM_005122	<b>PFKP</b>	NM_002627
<b>MPP3</b>	NM_001932	<b>NRAS</b>	NM_002524	<b>PFTK1</b>	NM_012395
<b>MRE11A</b>	NM_005591	<b>NRBP1</b>	NM_013392	<b>PGK1</b>	NM_000291
<b>MSH2</b>	NM_000251	<b>NRBP2</b>	NM_178564	<b>PGK2</b>	NM_138733
<b>MSH5</b>	NM_025259	<b>NRGN</b>	NM_006176	<b>PHACTR1</b>	XM_166420
<b>MST1R</b>	NM_002447	<b>NRK</b>	NM_198465	<b>PHACTR2</b>	XM_376540
<b>MTM1</b>	NM_000252	<b>NTRK1</b>	NM_002529	<b>PHACTR3</b>	NM_080672
<b>MTMR1</b>	NM_003828	<b>NTRK2</b>	NM_006180	<b>PHACTR4</b>	NM_023923
<b>MTMR2</b>	NM_016156	<b>NTRK3</b>	NM_002530	<b>PHKA1</b>	NM_002637
<b>MTMR3</b>	NM_021090	<b>NUAK1</b>	NM_014840	<b>PHKA2</b>	NM_000292
<b>MTMR4</b>	NM_004687	<b>NUAK2</b>	NM_030952	<b>PHKB</b>	NM_000293
<b>MTMR6</b>	NM_004685	<b>NUCKS1</b>	NM_022731	<b>PHKG1</b>	NM_006213
<b>MTMR8</b>	NM_017677	<b>NUDT8</b>	NM_181843	<b>PHKG2</b>	NM_000294
<b>MTMR9</b>	NM_015458	<b>OBSCN</b>	NM_052843	<b>PHLPP</b>	NM_194449
<b>MTMR10</b>	NM_017762	<b>OTOF</b>	NM_194323	<b>PHLPL</b>	XM_041191
<b>MTMR12</b>	NM_019061	<b>OXSR1</b>	NM_005109	<b>PHOSPHO1</b>	NM_178500
<b>MUSK</b>	NM_005592	<b>P15RS</b>	NM_018170	<b>PI4K2B</b>	NM_018323
<b>MVK</b>	NM_000431	<b>PACSIN1</b>	NM_020804	<b>PI4KII</b>	NM_018425
<b>MYB</b>	NM_005375	<b>PACSIN2</b>	NM_007229	<b>PICK1</b>	NM_012407
<b>MYC</b>	NM_002467	<b>PACSIN3</b>	NM_016223	<b>PIK3AP1</b>	NM_152309
<b>MYLK</b>	NM_053028	<b>PAK1</b>	NM_002576	<b>PIK3C2A</b>	NM_002645
<b>MYLK2</b>	NM_033118	<b>PAK2</b>	NM_002577	<b>PIK3C2B</b>	NM_002646
<b>MYO3A</b>	NM_017433	<b>PAK3</b>	NM_002578	<b>PIK3C2G</b>	NM_004570
<b>MYO3B</b>	NM_138995	<b>PAK4</b>	NM_005884	<b>PIK3C3</b>	NM_002647
<b>MYO9B</b>	NM_004145	<b>PAK6</b>	NM_020168	<b>PIK3CA</b>	NM_006218
<b>MYST2</b>	NM_007067	<b>PAK7</b>	NM_020341	<b>PIK3CB</b>	NM_006219
<b>NADK</b>	NM_023018	<b>PANK1</b>	NM_138316	<b>PIK3CD</b>	NM_005026
<b>NAGK</b>	NM_017567	<b>PANK2</b>	NM_024960	<b>PIK3CG</b>	NM_002649
<b>NBN</b>	NM_002485	<b>PANK3</b>	NM_024594	<b>PIK3R1</b>	NM_181504
<b>NEDD4L</b>	NM_015277	<b>PANK4</b>	NM_018216	<b>PIK3R1</b>	XM_043865
<b>NEK1</b>	NM_012224	<b>PAP2D</b>	XM_375754	<b>PIK3R2</b>	NM_005027

<b>NEK2</b>	NM_002497	<b>PAPSS1</b>	NM_005443	<b>PIK3R3</b>	NM_003629
<b>NEK3</b>	NM_152720	<b>PASK</b>	NM_015148	<b>PIK3R4</b>	NM_014602
<b>NEK4</b>	NM_003157	<b>PBK</b>	NM_018492	<b>PIK3R5</b>	NM_014308
<b>NEK5</b>	XM_292160	<b>PCK1</b>	NM_002591	<b>PIM1</b>	NM_002648
<b>NEK6</b>	NM_014397	<b>PCK2</b>	NM_004563	<b>PIM2</b>	NM_006875
<b>NEK7</b>	NM_133494	<b>PCTK1</b>	NM_033018	<b>PIM3</b>	NM_001001852
<b>NEK8</b>	NM_178170	<b>PCTK2</b>	NM_002595	<b>PIN1</b>	NM_006221
<b>NEK9</b>	NM_033116	<b>PCTK3</b>	NM_002596	<b>PINK1</b>	NM_032409
<b>NEK10</b>	NM_152534	<b>PDGFB</b>	NM_002608	<b>PIP5K1A</b>	NM_003557
<b>NEK11</b>	NM_024800	<b>PDGFRA</b>	NM_006206	<b>PIP5K1B</b>	NM_003558
<b>NF1</b>	NM_000267	<b>PDGFRB</b>	NM_002609	<b>PIP5K1C</b>	NM_012398
<b>NF2</b>	NM_000268	<b>PDGFR1</b>	NM_006207	<b>PIP5K2A</b>	NM_005028
<b>NKX3-1</b>	NM_006167	<b>PDIK1L</b>	NM_152835	<b>PIP5K2B</b>	NM_003559
<b>PIP5K2C</b>	NM_024779	<b>PPM2C</b>	NM_018444	<b>PPP3R2</b>	NM_147180
<b>PKIA</b>	NM_006823	<b>PPME1</b>	NM_016147	<b>PPP4C</b>	NM_002720
<b>PKIB</b>	NM_032471	<b>PPP1CA</b>	NM_002708	<b>PPP4R1</b>	NM_005134
<b>PKIG</b>	NM_181805	<b>PPP1CB</b>	NM_002709	<b>PPP4R1L</b>	XM_086650
<b>PKM2</b>	NM_182471	<b>PPP1CC</b>	NM_002710	<b>PPP4R2</b>	NM_174907
<b>PKMYT1</b>	NM_004203	<b>PPP1R10</b>	NM_002714	<b>PPP5C</b>	NM_006247
<b>PKN1</b>	NM_002741	<b>PPP1R11</b>	NM_021959	<b>PPP6C</b>	NM_002721
<b>PKN2</b>	NM_006256	<b>PPP1R12A</b>	NM_002480	<b>PPTC7</b>	NM_139283
<b>PLA2G4B</b>	NM_005090	<b>PPP1R12B</b>	NM_002481	<b>PRKAA1</b>	NM_006251
<b>PLAUR</b>	NM_002659	<b>PPP1R12C</b>	NM_017607	<b>PRKAA2</b>	NM_006252
<b>PLCB1</b>	NM_182734	<b>PPP1R13B</b>	NM_015316	<b>PRKAB2</b>	NM_005399
<b>PLCB2</b>	NM_004573	<b>PPP1R14A</b>	NM_033256	<b>PRKACA</b>	NM_002730
<b>PLCB3</b>	NM_000932	<b>PPP1R14B</b>	XM_370630	<b>PRKACB</b>	NM_002731
<b>PLCB4</b>	NM_000933	<b>PPP1R14C</b>	NM_030949	<b>PRKAG1</b>	NM_002733
<b>PLCD1</b>	NM_006225	<b>PPP1R14D</b>	NM_017726	<b>PRKAG2</b>	NM_016203
<b>PLCD4</b>	NM_032726	<b>PPP1R15A</b>	NM_014330	<b>PRKAG3</b>	NM_017431
<b>PLCG1</b>	NM_002660	<b>PPP1R15B</b>	NM_032833	<b>PRKAR1A</b>	NM_002734
<b>PLCG2</b>	NM_002661	<b>PPP1R16A</b>	NM_032902	<b>PRKAR1B</b>	NM_002735
<b>PLCL1</b>	NM_006226	<b>PPP1R16B</b>	NM_015568	<b>PRKAR2A</b>	NM_004157
<b>PLCL2</b>	NM_015184	<b>PPP1R1A</b>	NM_006741	<b>PRKAR2B</b>	NM_002736
<b>PLCZ1</b>	NM_033123	<b>PPP1R1B</b>	NM_032192	<b>PRKCA</b>	NM_002737
<b>PLD1</b>	NM_002662	<b>PPP1R1C</b>	XM_087137	<b>PRKCB1</b>	NM_002738
<b>PLK1</b>	NM_005030	<b>PPP1R2</b>	NM_006241	<b>PRKCBP1</b>	NM_183048
<b>PLK2</b>	NM_006622	<b>PPP1R2P9</b>	NM_025210	<b>PRKCD</b>	NM_006254

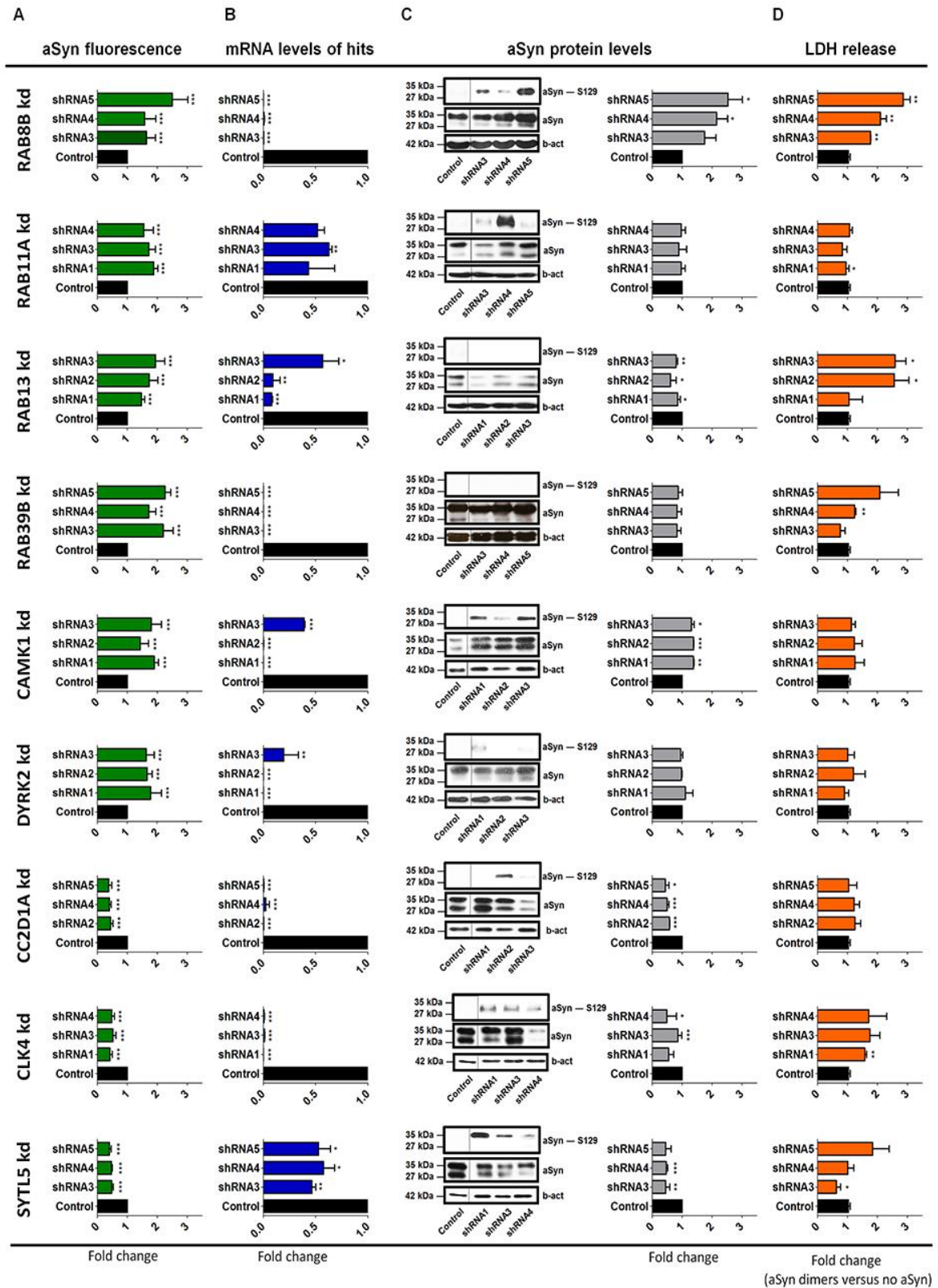
<b>PLK3</b>	NM_004073	<b>PPP1R3A</b>	NM_002711	<b>PRKCDBP</b>	NM_145040
<b>PLK4</b>	NM_014264	<b>PPP1R3B</b>	NM_024607	<b>PRKCE</b>	NM_005400
<b>PMS1</b>	NM_000534	<b>PPP1R3C</b>	NM_005398	<b>PRKCG</b>	NM_002739
<b>PMVK</b>	NM_006556	<b>PPP1R3D</b>	NM_006242	<b>PRKCH</b>	NM_006255
<b>PNCK</b>	NM_198452	<b>PPP1R3E</b>	XM_033391	<b>PRKCI</b>	NM_002740
<b>POT1</b>	NM_015450	<b>PPP1R3F</b>	XM_372210	<b>PRKCQ</b>	NM_006257
<b>PPAP2A</b>	NM_003711	<b>PPP1R3G</b>	XM_371796	<b>PRKCSH</b>	NM_001001329
<b>PPAP2C</b>	NM_003712	<b>PPP1R7</b>	NM_002712	<b>PRKCZ</b>	NM_002744
<b>PPAPDC1A</b>	XM_113641	<b>PPP1R8</b>	NM_002713	<b>PRKD1</b>	NM_002742
<b>PPAPDC2</b>	NM_203453	<b>PPP1R9A</b>	XM_371933	<b>PRKD2</b>	NM_016457
<b>PPARA</b>	NM_005036	<b>PPP1R9B</b>	NM_032595	<b>PRKD3</b>	NM_005813
<b>PPARD</b>	NM_006238	<b>PPP2CA</b>	NM_002715	<b>PRKDC</b>	NM_006904
<b>Pparg</b>	NM_011146	<b>PPP2CB</b>	NM_004156	<b>PRKG1</b>	NM_006258
<b>PPARG</b>	NM_138712	<b>PPP2R1A</b>	NM_014225	<b>PRKG2</b>	NM_006259
<b>PPEF1</b>	NM_006240	<b>PPP2R1B</b>	NM_002716	<b>PRKRA</b>	NM_003690
<b>PPEF2</b>	NM_006239	<b>PPP2R2A</b>	NM_002717	<b>PRKX</b>	NM_005044
<b>PPFIA1</b>	NM_003626	<b>PPP2R2B</b>	NM_004576	<b>PRKY</b>	NM_002760
<b>PPFIA2</b>	NM_003625	<b>PPP2R2C</b>	NM_020416	<b>PRPF4B</b>	NM_003913
<b>PPFIA3</b>	NM_003660	<b>PPP2R2C</b>	NM_181876	<b>PRPS1</b>	NM_002764
<b>PPFIA4</b>	XM_046751	<b>PPP2R3A</b>	NM_002718	<b>PRPS2</b>	NM_002765
<b>PPFIBP1</b>	NM_003622	<b>PPP2R3B</b>	NM_013239	<b>PRSS7</b>	NM_002772
<b>PPM1A</b>	NM_021003	<b>PPP2R5A</b>	NM_006243	<b>PSKH1</b>	NM_006742
<b>PPM1B</b>	NM_002706	<b>PPP2R5B</b>	NM_006244	<b>PSKH2</b>	NM_033126
<b>PPM1D</b>	NM_003620	<b>PPP2R5C</b>	NM_002719	<b>PSMD14</b>	NM_005805
<b>PPM1E</b>	NM_014906	<b>PPP2R5D</b>	NM_006245	<b>PSPH</b>	NM_004577
<b>PPM1F</b>	NM_014634	<b>PPP2R5E</b>	NM_006246	<b>PSTPIP1</b>	NM_003978
<b>PPM1H</b>	XM_350880	<b>PPP3CA</b>	NM_000944	<b>PSTPIP2</b>	NM_024430
<b>PPM1K</b>	NM_152542	<b>PPP3CB</b>	NM_021132	<b>PTBP1</b>	NM_002819
<b>PPM1L</b>	NM_139245	<b>PPP3CC</b>	NM_005605	<b>PTCH</b>	NM_000264
<b>PPM1M</b>	NM_144641	<b>PPP3R1</b>	NM_000945	<b>PTCH2</b>	NM_003738
<b>PTEN</b>	NM_000314	<b>R3HDM2</b>	NM_014925	<b>RPS6KC1</b>	NM_012424
<b>PTHR1</b>	NM_000316	<b>RAD50</b>	NM_005732	<b>RPS6KL1</b>	NM_031464
<b>PTK2</b>	NM_005607	<b>RAF1</b>	NM_002880	<b>RSC1A1</b>	NM_006511
<b>PTK2B</b>	NM_004103	<b>RAGE</b>	NM_014226	<b>RXRA</b>	NM_002957
<b>PTK6</b>	NM_005975	<b>RASA1</b>	NM_022650	<b>RXRB</b>	NM_021976
<b>PTK7</b>	NM_002821	<b>RASA2</b>	NM_006506	<b>RXRG</b>	NM_006917
<b>PTK9</b>	NM_002822	<b>RASA3</b>	NM_007368	<b>RYK</b>	NM_002958

<b>PTK9L</b>	NM_007284	<b>RASAL2</b>	NM_004841	<b>SAG</b>	NM_000541
<b>PTN</b>	NM_002825	<b>RASSF5</b>	NM_031437	<b>SBF1</b>	NM_002972
<b>PTP4A1</b>	NM_003463	<b>RB1</b>	NM_000321	<b>SBF2</b>	NM_030962
<b>PTP4A2</b>	NM_003479	<b>RBKS</b>	NM_022128	<b>SBK1</b>	XM_370948
<b>PTP4A3</b>	NM_007079	<b>RBL1</b>	NM_002895	<b>SCAP1</b>	NM_003726
<b>PTPDC1</b>	NM_152422	<b>RBL2</b>	NM_005611	<b>SCYL1</b>	NM_020680
<b>PTPLA</b>	NM_014241	<b>RCSD1</b>	NM_052862	<b>SCYL2</b>	NM_017988
<b>PTPLAD2</b>	XM_376819	<b>REL</b>	NM_002908	<b>SCYL3</b>	NM_020423
<b>PTPMT1</b>	XM_374879	<b>RET</b>	NM_000323	<b>SDHD</b>	NM_003002
<b>PTPN1</b>	NM_002827	<b>RET</b>	NM_020629	<b>SETD2</b>	NM_012271
<b>PTPN2</b>	NM_002828	<b>RFK</b>	NM_018339	<b>SF1</b>	NM_004630
<b>PTPN3</b>	NM_002829	<b>RFP</b>	NM_006510	<b>SFN</b>	NM_006142
<b>PTPN4</b>	NM_002830	<b>RGS3</b>	NM_144489	<b>SGK</b>	NM_005627
<b>PTPN5</b>	NM_032781	<b>RHEB</b>	NM_005614	<b>SGK2</b>	NM_170693
<b>PTPN6</b>	NM_002831	<b>RIC8B</b>	NM_018157	<b>SGK3</b>	NM_013257
<b>PTPN7</b>	NM_002832	<b>RIMS1</b>	NM_014989	<b>SGK3</b>	NM_170709
<b>PTPN9</b>	NM_002833	<b>RIMS4</b>	NM_182970	<b>SH2D1A</b>	NM_002351
<b>PTPN12</b>	NM_002835	<b>RIOK1</b>	NM_031480	<b>SH2D1B</b>	NM_053282
<b>PTPN13</b>	NM_006264	<b>RIOK2</b>	NM_018343	<b>SH3KBP1</b>	NM_031892
<b>PTPN14</b>	NM_005401	<b>RIPK1</b>	NM_003804	<b>SHC1</b>	NM_003029
<b>PTPN18</b>	NM_014369	<b>RIPK2</b>	NM_003821	<b>SHH</b>	NM_000193
<b>PTPN21</b>	NM_007039	<b>RIPK3</b>	NM_006871	<b>SIRPA</b>	NM_080792
<b>PTPN22</b>	NM_012411	<b>RIPK4</b>	NM_020639	<b>SIRPB2</b>	XM_209363
<b>PTPN23</b>	NM_015466	<b>RIPK5</b>	NM_015375	<b>SIRPD</b>	NM_178460
<b>PTPRA</b>	NM_002836	<b>RNASEL</b>	NM_021133	<b>SIRT2</b>	NM_012237
<b>PTPRB</b>	NM_002837	<b>RNF180</b>	NM_178532	<b>SKI</b>	NM_003036
<b>PTPRC</b>	NM_002838	<b>RNGTT</b>	NM_003800	<b>SKIP</b>	XM_051221
<b>PTPRCAP</b>	NM_005608	<b>ROCK1</b>	NM_005406	<b>SKIP</b>	NM_016532
<b>PTPRD</b>	NM_002839	<b>ROCK2</b>	NM_004850	<b>Slc1a3</b>	NM_148938
<b>PTPRE</b>	NM_006504	<b>ROR1</b>	NM_005012	<b>SLC22A18</b>	NM_002555
<b>PTPRF</b>	NM_002840	<b>ROR2</b>	NM_004560	<b>Slc26a9</b>	NM_177243
<b>PTPRG</b>	NM_002841	<b>ROS1</b>	NM_002944	<b>SLK</b>	NM_014720
<b>PTPRH</b>	NM_002842	<b>RP11-145H9.1</b>	XM_373109	<b>SMAD2</b>	NM_005901
<b>PTPRJ</b>	NM_002843	<b>RP6-213H19.1</b>	NM_016542	<b>SMAD4</b>	NM_005359
<b>PTPRK</b>	NM_002844	<b>RPA1</b>	NM_002945	<b>SMARCB1</b>	NM_003073
<b>PTPRM</b>	NM_002845	<b>RPA2</b>	NM_002946	<b>SMG1</b>	NM_014006
<b>PTPRN</b>	NM_002846	<b>RPGRIP1</b>	NM_020366	<b>SMG6</b>	NM_017575

<b>PTPRN2</b>	NM_002847	<b>RPH3A</b>	NM_014954	<b>SNAI3</b>	XM_370995
<b>PTPRO</b>	NM_002848	<b>RPS6</b>	NM_001010	<b>SNF1LK</b>	NM_173354
<b>PTPRR</b>	NM_002849	<b>RPS6KA1</b>	NM_002953	<b>SNF1LK2</b>	NM_015191
<b>PTPRS</b>	NM_002850	<b>RPS6KA2</b>	NM_021135	<b>SNRK</b>	NM_017719
<b>PTPRT</b>	NM_007050	<b>RPS6KA3</b>	NM_004586	<b>SOCS5</b>	NM_014011
<b>PTPRU</b>	NM_005704	<b>RPS6KA4</b>	NM_003942	<b>SOD1</b>	NM_000454
<b>PTPRV</b>	XM_086287	<b>RPS6KA5</b>	NM_004755	<b>SOX2</b>	NM_003106
<b>PTPRZ1</b>	NM_002851	<b>RPS6KA6</b>	NM_014496	<b>SPEG</b>	NM_005876
<b>PXK</b>	NM_017771	<b>RPS6KB1</b>	NM_003161	<b>SRMS</b>	NM_080823
<b>R3HDM1</b>	NM_015361	<b>RPS6KB2</b>	NM_003952	<b>SRPK2</b>	NM_003138
<b>SSH1</b>	NM_018984	<b>TESK1</b>	NM_006285	<b>TYROBP</b>	NM_003332
<b>SSH2</b>	NM_033389	<b>TESK2</b>	NM_007170	<b>UCK1</b>	NM_031432
<b>SSH3</b>	NM_017857	<b>TEX14</b>	NM_031272	<b>UCK2</b>	NM_012474
<b>STAC3</b>	NM_145064	<b>TGFA</b>	NM_003236	<b>UCKL1</b>	NM_017859
<b>STK3</b>	NM_006281	<b>TGFBR1</b>	NM_004612	<b>UGP2</b>	NM_006759
<b>STK4</b>	NM_006282	<b>TGFBR2</b>	NM_003242	<b>UHMK1</b>	NM_144624
<b>STK10</b>	NM_005990	<b>THBS1</b>	NM_003246	<b>ULK1</b>	NM_003565
<b>STK11</b>	NM_000455	<b>THOC4</b>	NM_005782	<b>ULK2</b>	NM_014683
<b>STK11IP</b>	NM_052902	<b>TIAM1</b>	NM_003253	<b>ULK3</b>	NM_015518
<b>STK16</b>	NM_003691	<b>TIE1</b>	NM_005424	<b>ULK4</b>	NM_017886
<b>STK17A</b>	NM_004760	<b>TINF2</b>	NM_012461	<b>UNC13B</b>	NM_006377
<b>STK17B</b>	NM_004226	<b>TJP2</b>	NM_004817	<b>UNK</b>	XM_062966
<b>STK19</b>	NM_004197	<b>TK1</b>	NM_003258	<b>UNK</b>	XM_171165
<b>STK23</b>	NM_014370	<b>TK2</b>	NM_004614	<b>UNK</b>	XM_291584
<b>STK24</b>	NM_003576	<b>TLK1</b>	NM_012290	<b>UNK</b>	XM_291786
<b>STK25</b>	NM_006374	<b>TLK2</b>	NM_006852	<b>UNK</b>	XM_370946
<b>STK31</b>	NM_032944	<b>TNFRSF11B</b>	NM_002546	<b>UNK</b>	XM_371492
<b>STK32A</b>	NM_145001	<b>TNIK</b>	XM_039796	<b>UNK</b>	XM_372542
<b>STK32B</b>	NM_018401	<b>TNK1</b>	NM_003985	<b>UNK</b>	XM_372625
<b>STK32C</b>	NM_173575	<b>TNK2</b>	NM_005781	<b>UNK</b>	XM_372987
<b>STK33</b>	NM_030906	<b>TNKS</b>	NM_003747	<b>UNK</b>	XM_373224
<b>STK35</b>	NM_080836	<b>TNNI3K</b>	NM_015978	<b>UNK</b>	XM_373298
<b>STK36</b>	NM_015690	<b>TNS1</b>	NM_022648	<b>UNK</b>	XM_373815
<b>STK38</b>	NM_007271	<b>TNS3</b>	NM_022748	<b>UNK</b>	XM_376585
<b>STK38L</b>	NM_015000	<b>TP53RK</b>	NM_033550	<b>UNK</b>	XM_376950
<b>STK39</b>	NM_013233	<b>TPD52L3</b>	NM_033516	<b>UNK</b>	XM_377635
<b>STK40</b>	NM_032017	<b>TPK1</b>	NM_022445	<b>UNK</b>	XM_378103

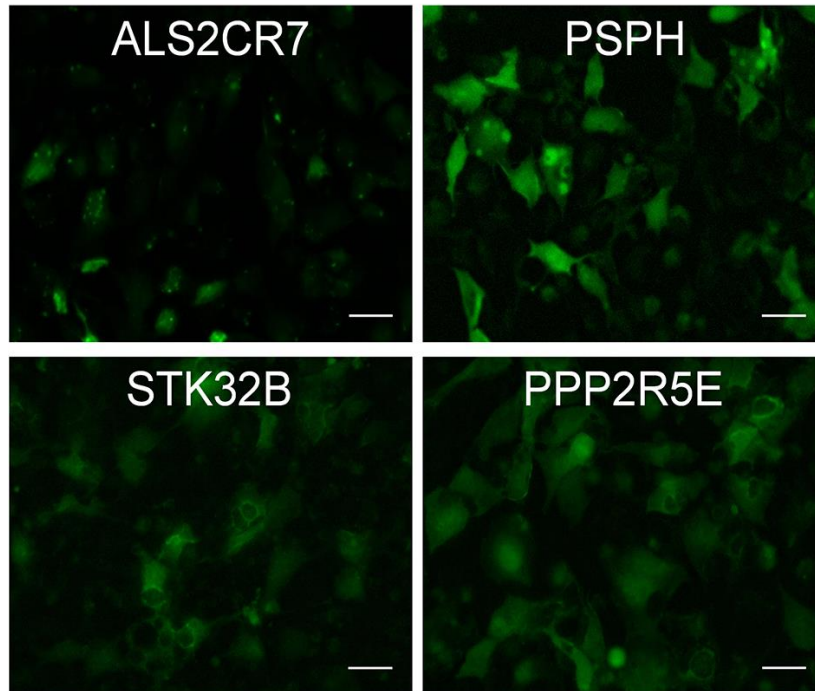


<b>STYK1</b>	NM_018423	<b>TPTE2</b>	NM_130785	<b>UNK</b>	XM_378155
<b>STYX</b>	NM_145251	<b>TPTEps1</b>	XM_495953	<b>UNK</b>	XM_378664
<b>STYXL1</b>	NM_016086	<b>TRAF3IP3</b>	NM_025228	<b>UNK</b>	XM_495804
<b>SUV39H2</b>	NM_024670	<b>TRIB1</b>	NM_025195	<b>UNK</b>	XM_496486
<b>SUZ12</b>	NM_015355	<b>TRIB2</b>	NM_021643	<b>UNK</b>	XM_496630
<b>SYK</b>	NM_003177	<b>TRIB3</b>	NM_021158	<b>UNK</b>	XM_496720
<b>SYT2</b>	NM_177402	<b>TRIO</b>	NM_007118	<b>UNK</b>	XM_496793
<b>SYT4</b>	NM_020783	<b>TRPM6</b>	NM_017662	<b>UNK</b>	XM_496862
<b>SYT5</b>	NM_003180	<b>TRPM7</b>	NM_017672	<b>UNK</b>	XM_497237
<b>SYT11</b>	NM_152280	<b>TRPV5</b>	NM_019841	<b>UNK</b>	XM_497414
<b>SYT14</b>	NM_153262	<b>TRPV6</b>	NM_018646	<b>UNK</b>	XM_497433
<b>SYT16</b>	NM_031914	<b>TSC1</b>	NM_000368	<b>UNK</b>	XM_497521
<b>SYT17</b>	NM_016524	<b>TSC2</b>	NM_000548	<b>UNK</b>	XM_497706
<b>SYTL5</b>	NM_138780	<b>TSKS</b>	NM_021733	<b>UNK</b>	XM_497790
<b>TAF1</b>	NM_004606	<b>TSSK1</b>	NM_032028	<b>UNK</b>	XM_497791
<b>TAF1L</b>	NM_153809	<b>TSSK2</b>	NM_053006	<b>UNK</b>	XM_497812
<b>TAOK1</b>	NM_020791	<b>TSSK3</b>	NM_052841	<b>UNK</b>	XM_497846
<b>TAOK2</b>	NM_016151	<b>TSSK4</b>	NM_174944	<b>UNK</b>	XM_497909
<b>TAOK2</b>	NM_004783	<b>TSSK6</b>	NM_032037	<b>UNK</b>	XM_498204
<b>TAOK3</b>	NM_016281	<b>TTBK1</b>	XM_166453	<b>UNK</b>	XM_498243
<b>TBK1</b>	NM_013254	<b>TTBK2</b>	NM_173500	<b>UNK</b>	XM_498259
<b>TEC</b>	NM_003215	<b>TTK</b>	NM_003318	<b>UNK</b>	XM_498262
<b>TEK</b>	NM_000459	<b>TTN</b>	NM_003319	<b>UNK</b>	XM_499394
<b>TENC1</b>	NM_170754	<b>TTRAP</b>	NM_016614	<b>UNK</b>	XM_499479
<b>TEP1</b>	NM_007110	<b>TXK</b>	NM_003328	<b>VAV1</b>	NM_005428
<b>TERF1</b>	NM_017489	<b>TYK2</b>	NM_003331	<b>VHL</b>	NM_000551
<b>TERF2IP</b>	NM_018975	<b>TYRO3</b>	NM_006293	<b>VRK1</b>	NM_003384
<b>VRK2</b>	NM_006296	<b>WNK4</b>	NM_032387	<b>XRCC6</b>	NM_001469
<b>VRK3</b>	NM_016440	<b>WNT1</b>	NM_005430	<b>XYLB</b>	NM_005108
<b>WEE1</b>	NM_003390	<b>WT1</b>	NM_024426	<b>YES1</b>	NM_005433
<b>WIF1</b>	NM_007191	<b>WTAP</b>	NM_004906	<b>YSK4</b>	NM_025052
<b>WNK1</b>	NM_018979	<b>WWP2</b>	NM_007014	<b>ZAK</b>	NM_016653
<b>WNK2</b>	NM_006648	<b>XRCC4</b>	NM_022406	<b>ZAP70</b>	NM_001079
<b>WNK3</b>	NM_020922	<b>XRCC5</b>	NM_021141	<b>ZC3HC1</b>	NM_016478



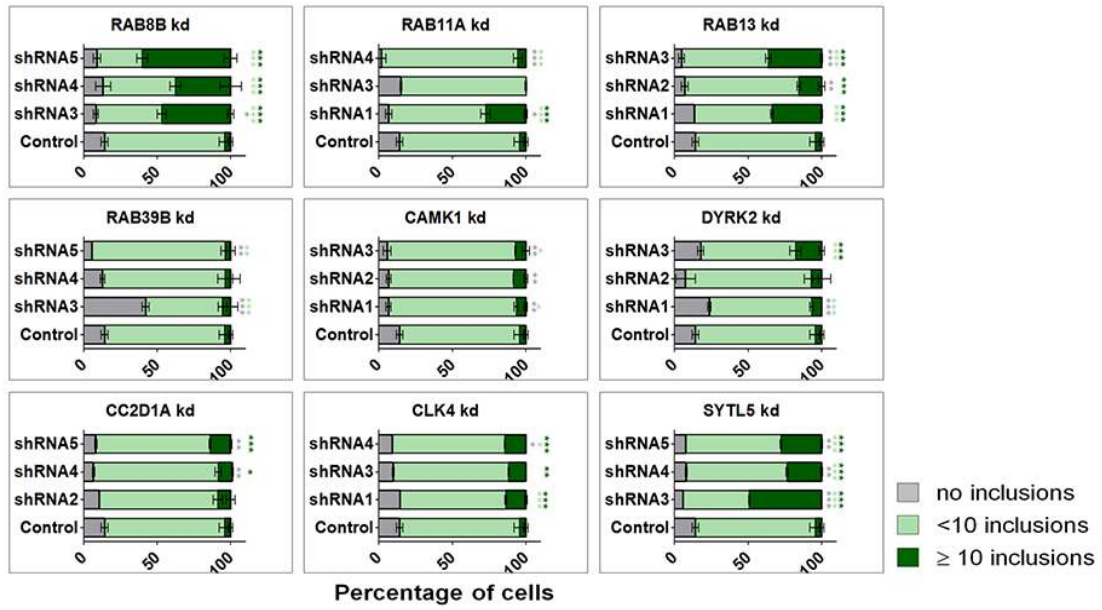
**Annex 5.2.2. Silencing of specific trafficking and kinase genes modifies aSyn oligomerization. A.** Quantification of relative fluorescence intensity of aSyn-BiFC stable H4 cells submitted to silencing

of *RAB8B*, *RAB11A*, *RAB13*, *RAB39B*, *CAMK1*, *DYRK2*, *CC2D1A*, *CLK4* and *SYTL5*. Three different shRNAs were used per gene. **B.** mRNA levels of cells submitted to silencing of the hits normalized to control cells. **C.** Immunoblotting analysis of S129 phosphorylated aSyn, total aSyn and beta-actin. Quantification of aSyn protein levels from aSyn-BiFC cells submitted to silencing of the selected hits **D.** Cytotoxicity (measured by LDH release in media from cells with aSyn oligomers versus no aSyn) normalized to control cells. All the quantifications presented are normalized to the control cells infected with a scrambled shRNA. Bars represent mean  $\pm$  95% CI (\*:  $0.05 < p < 0.01$ ; \*\*:  $0.01 < p < 0.001$ ; \*\*\*:  $p < 0.001$ ) and are normalized to the control of at least three independent experiments. Single comparisons between the control and experimental groups were made through Wilcoxon test. kd, knockdown.

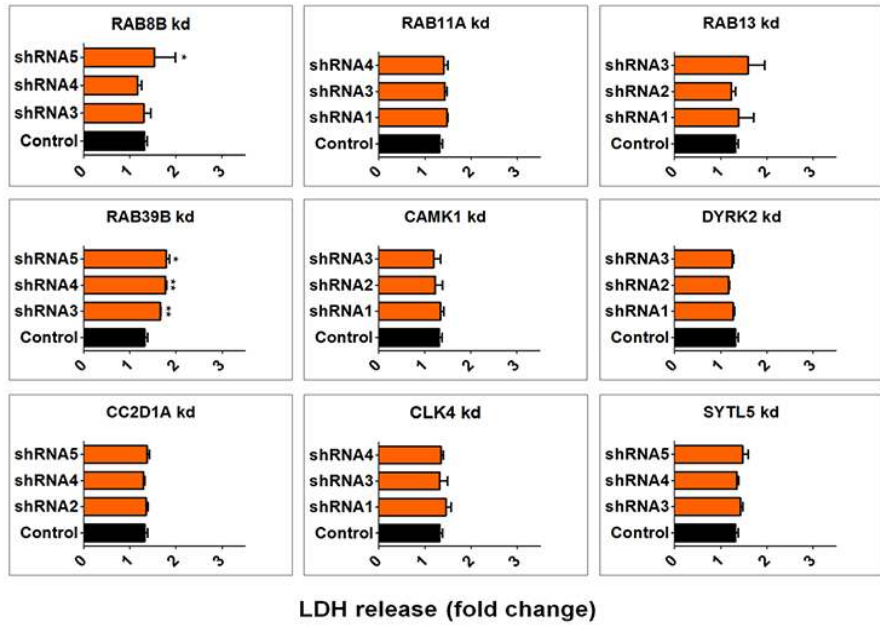


**Annex 5.2.3. Silencing of specific phosphotransferase genes does not affect aSyn oligomerization but alters the distribution of oligomers.** Upon silencing of *ALS2CR7* or *PSPH*, aSyn aggregates are seen within cells. Silencing of *STK32B* and *PPP2R5E* leads to a reduced fluorescence in the nucleus. In addition, a ring of fluorescent signal surrounding the nucleus is observed. Scale bars: 20  $\mu\text{m}$ .

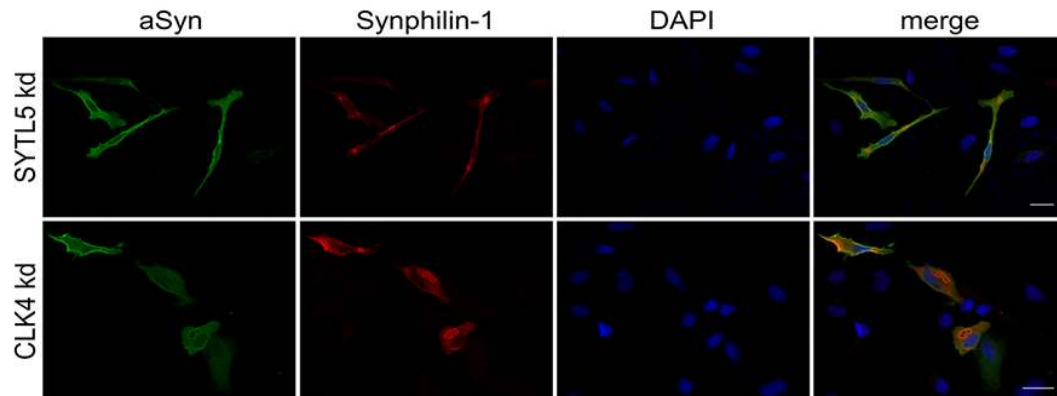
A



B

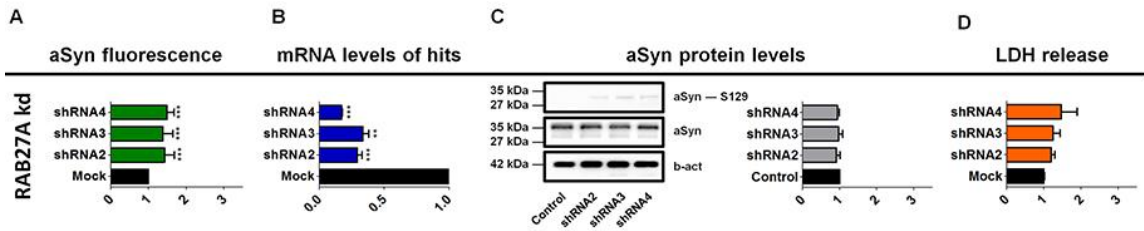


C

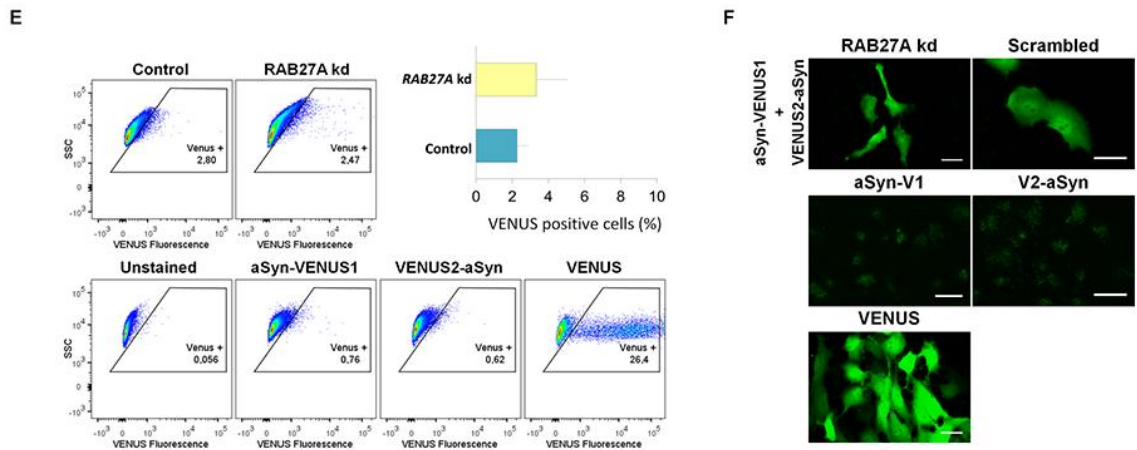


**Annex 5.2.4. Silencing of selected hits alters aSyn aggregation and cellular homeostasis. A.** Quantification of the number of aSyn inclusions per cell. 3 different shRNAs per gene were used. The number of inclusions was divided in the following categories: no inclusions (gray), less than 10 inclusions (light green) and more than 10 inclusions (dark green). **B.** Cytotoxicity (measured by LDH release in media) from cells with aSyn inclusions versus no aSyn and normalized to control cells. All quantifications are normalized to the control (scrambled infected cells). Bars represent mean  $\pm$  95% CI (\*:  $0.05 < p < 0.01$ ; \*\*:  $0.01 < p < 0.001$ ; \*\*\*:  $p < 0.001$ ) and are normalized to the control of at least three independent experiments. Single comparisons between the control and experimental groups were made through Wilcoxon test. **C.** Immunohistochemistry of cells expressing aSyn and silenced for *CLK4* and *SYTL5*. Silencing of *SYTL5* in aSyn-expressing cells promote cell elongation. Upon *CLK4* depletion, aSyn inclusions adopt an amorphous shape. Scale bars: 20  $\mu$ m. Kd, knockdown.

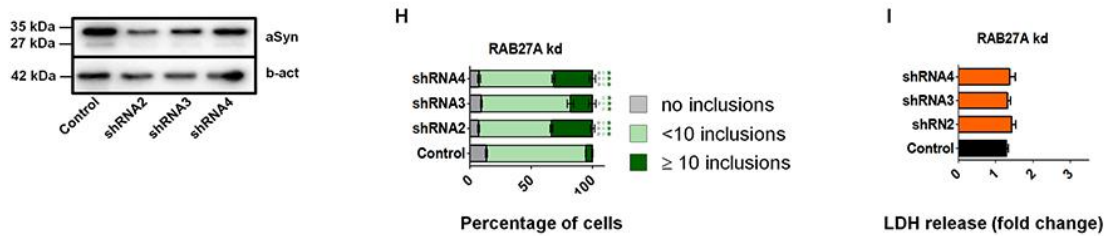
### Effect of Rab27A kd on aSyn oligomerization model



### Effect of Rab27A kd on aSyn cell-to-cell traffic



### Effect of Rab27A kd on aSyn aggregation



**Annex 5.2.5. Silencing of *RAB27A* alters aggregation of aSyn.** **A.** Quantification of relative fluorescence intensity of aSyn-BiFC stable H4 cells submitted to silencing of *RA27A*. Three different shRNAs were tested. **B.** mRNA levels of cells submitted to silencing of the *RAB27A* normalized to control cells (cells transduced with scrambled shRNA). **C.** Immunoblotting analysis of S129 phosphorylated aSyn, total aSyn and beta-actin. Quantification of aSyn protein levels from aSyn-BiFC cells submitted to silencing of *RAB27A*. **D.** Cytotoxicity (measured by LDH release in media from cells with aSyn oligomers versus no aSyn) normalized to control cells. **E.** VENUS positive cells were monitored by flow cytometry. A representative result is shown as side scatter (SSC) versus VENUS fluorescence, with the corresponding histogram. **F.** *In vivo* imaging of aSyn-VENUS1 and VENUS2-aSyn mixed cells subjected to silencing of *RAB27A*. Scale bar: 20  $\mu$ m. **G.**

Immunoblotting analysis of total aSyn and beta-actin. **H.** Percentage of cells with no inclusions (gray), less than 10 inclusions (light green) or more than 10 inclusions (dark green). **I.** Cytotoxicity (measured by LDH release in the media) from stable cells subjected to *RAB27A* silencing and normalized to control. Bars represent mean  $\pm$  95% CI (\*:  $0.05 < p < 0.01$ ; \*\*:  $0.01 < p < 0.001$ ; \*\*\*:  $p < 0.001$ ) and are normalized to the control of at least three independent experiments. Single comparisons between the control and experimental groups were made Wilcoxon test. Kd, knockdown.



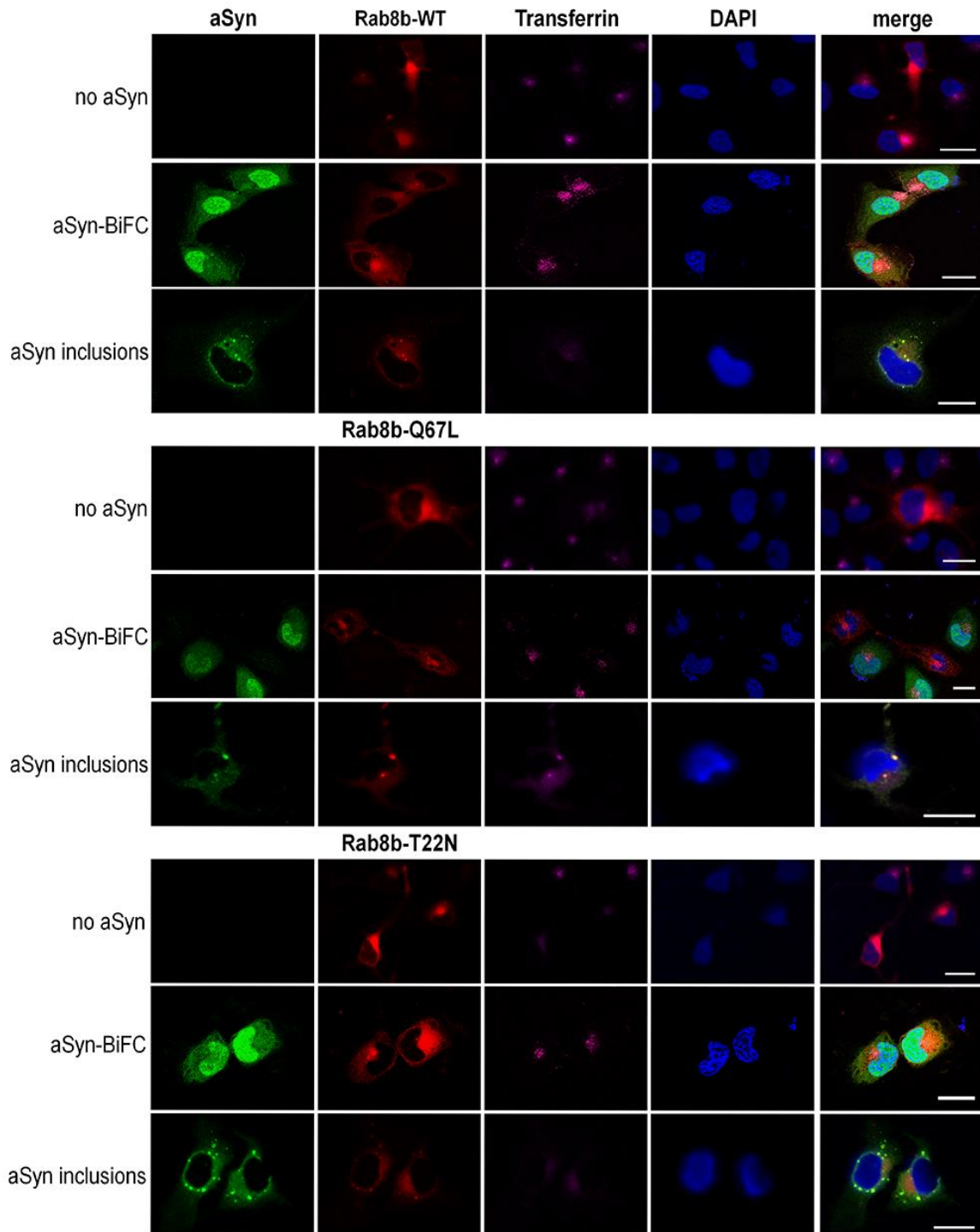
Annex 5.2.6. Summary of the effect of traffic players on oligomerization and aggregation of aSyn.

	aSyn-BiFC system									
	Fluorescence intensity		aSyn protein levels		Cell-to-cell traffic	Secretion	Cytotoxicity		Transferrin intensity	
	KD <sup>1</sup>	OE <sup>2</sup>	KD	OE	KD	OE	KD	OE	KD	OE
<i>RAB8B</i>	↑	↓	↑	↔	↑	↔	↑	↓	-	↑
<i>RAB11A</i>	↑	↓	↔	↔	↔	↔	↔	↓	-	↓
<i>RAB13</i>	↑	↓	↓	↔	↑	↔	↑	↓	-	↓
<i>RAB39B</i>	↑	-	↔	-	-	-	↔	-	-	-
<i>CAMK1</i>	↑	-	↑	-	-	-	↔	-	-	-
<i>DYRK2</i>	↑	-	↔	-	-	-	↔	-	-	-
<i>CC2D1A</i>	↓	-	↓	-	-	-	↔	-	-	-
<i>CLK4</i>	↓	-	↓	-	-	-	↑	-	-	-
<i>SYTL5</i>	↓	↔	↓	↔	↑	↑	↔	↓	-	↔

	aSyn aggregation											
	number of inclusions per cell						Secretion		Cytotoxicity		Transferrin intensity	
	no inclusions		<10		>10							
	KD	OE	KD	OE	KD	OE	KD	OE	KD	OE	KD	OE
<i>RAB8B</i>	↓	↑	↓	↓	↑	↔	-	↔	↑	↓	-	↓
<i>RAB11A</i>	↓	↑	↑	↓	↔	↔	-	↑	↔	↓	-	↓
<i>RAB13</i>	↓	↑	↔	↓	↑	↔	-	↑	↔	↓	-	↓
<i>RAB39B</i>	↓	-	↑	-	↔	-	-	-	↑	-	-	-
<i>CAMK1</i>	↓	-	↑	-	↔	-	-	-	↔	-	-	-
<i>DYRK2</i>	↑	-	↓	-	↔	-	-	-	↔	-	-	-
<i>CC2D1A</i>	↓	-	↔	-	↑	-	-	-	↔	-	-	-
<i>CLK4</i>	↔	-	↓	-	↑	-	-	-	↔	-	-	-
<i>SYTL5</i>	↓	↑	↓	↓	↑	↔	-	↔	↔	↓	-	↓

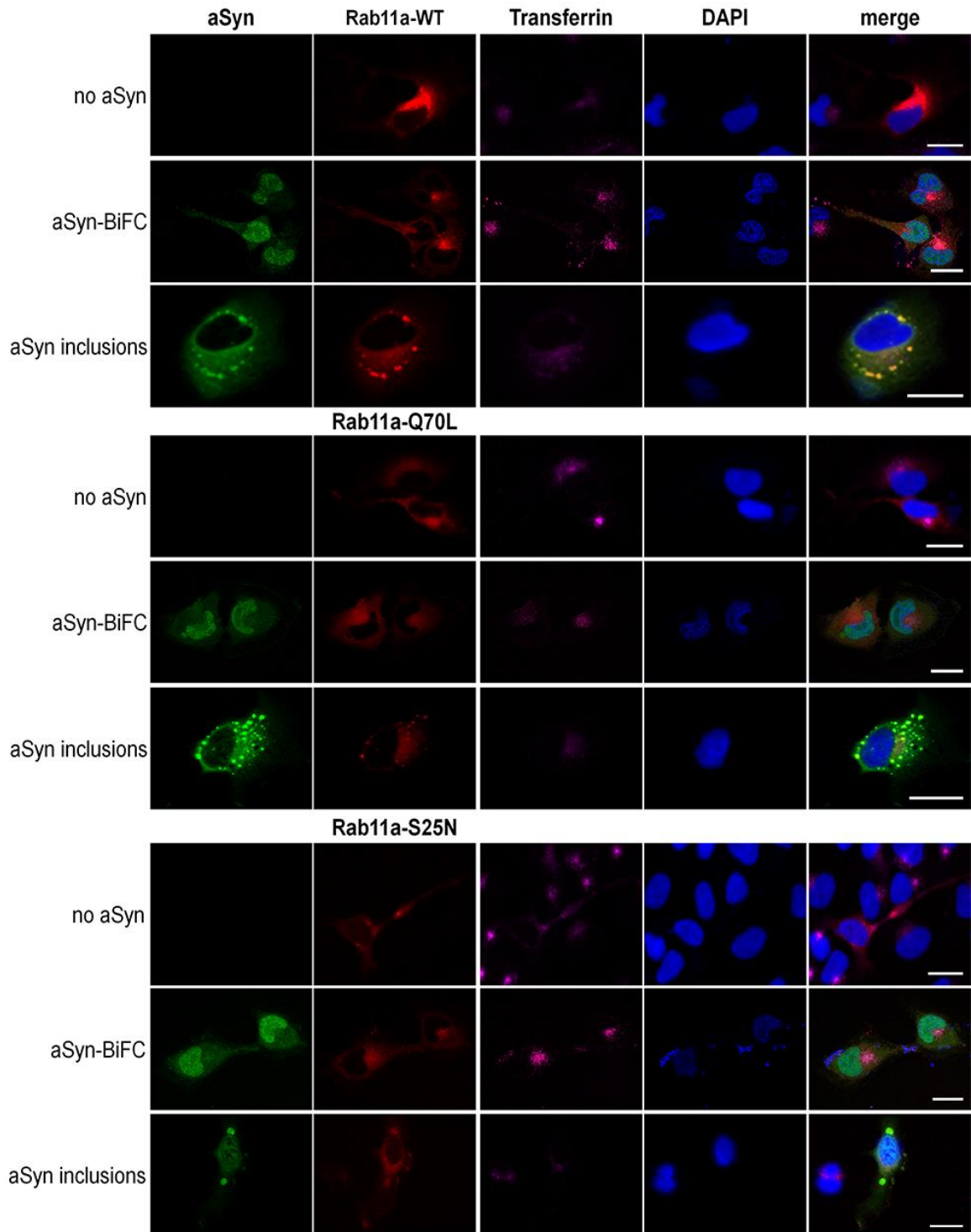
<sup>1</sup> KD, knockdown

<sup>2</sup> OE, overexpression



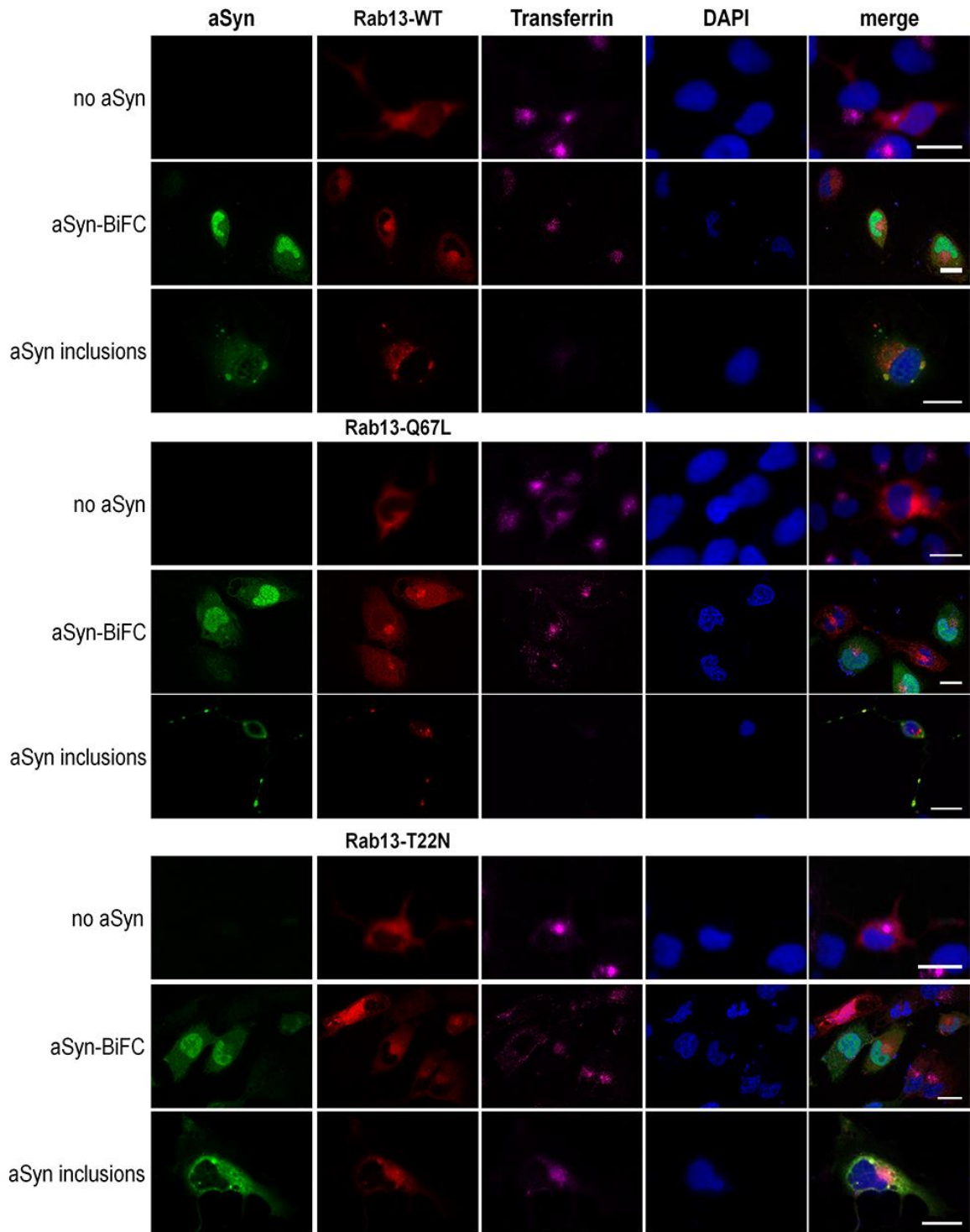
**Annex 5.2.7. Overexpression of Rab8b at different steps of aSyn aggregation.** H4 cells with no aSyn or stable for aSyn-BiFC (green) were transfected with Rab8b-WT, -Q67L and -T22N constructs. To promote the formation of aSyn inclusions, cells were triple-transfected with aSynT, Synphilin-1 and the same constructs referred above. 48 h post-transfection, media with no serum was replaced in cells for 1 h. Cells were incubated with Alexa-647 human transferrin (magenta) for

30 min, prior to fixation. DAPI was used as a nuclear counterstain. Only for aSyn aggregation model, cells were subjected to immunocytochemistry for aSyn (green) followed by confocal microscopy. Scale bars: 20  $\mu$ m. Control cells are represented in Annex 5.2.10B.



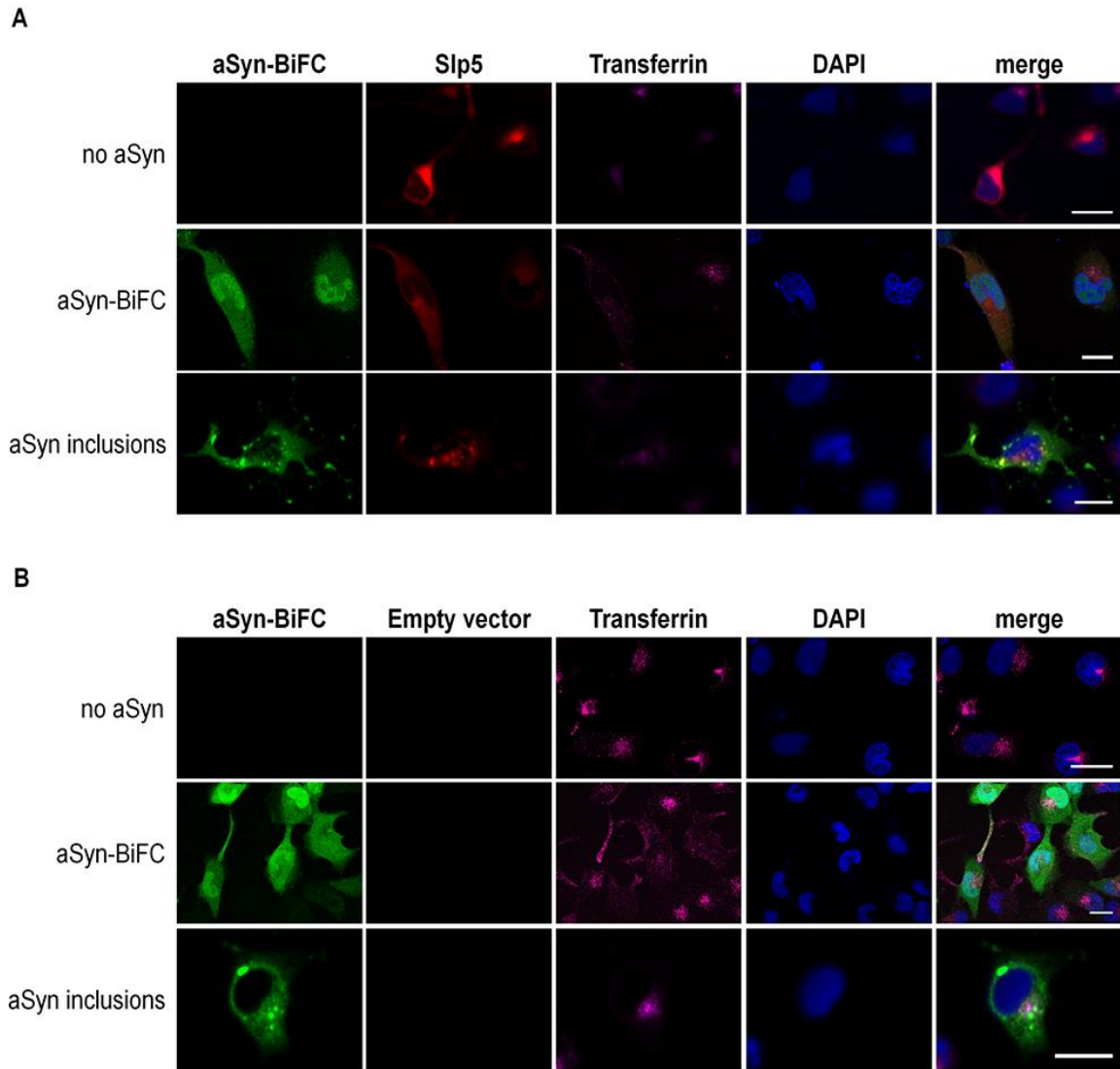
**Annex 5.2.8. Overexpression of Rab11a at different steps of aSyn aggregation.** H4 cells with no aSyn or stable for aSyn-BiFC (green) were transfected with constructs expressing Rab11a-WT, Q70L and -S25N. To promote the formation of aSyn inclusions, cells were triple-transfected with aSynT, Synphilin-1 and the same constructs referred above. 48 h post-transfection, media with no serum was replaced in cells for 1 h. Cells were incubated with Alexa-647 human transferrin

(magenta) for 30 min, prior to fixation. DAPI was used as a nuclear counterstain. Only for aSyn aggregation model, cells were subjected to immunocytochemistry for aSyn (green) followed by confocal microscopy. Scale bars: 20  $\mu\text{m}$ . Control cells are represented in Annex 5.2.10B.



**Annex 5.2.9. Overexpression of Rab13 at different steps of aSyn aggregation.** H4 cells with no aSyn or stable for aSyn-BiFC (green) were transfected with constructs expressing Rab13-WT, -67L and -T22N. To promote the formation of aSyn inclusions, cells were triple-transfected with aSynT, Synphilin-1 and the same constructs referred above. 48 h post-transfection, media with no serum was replaced in cells for 1 h. Cells were incubated with Alexa-647 human transferrin (magenta) for

30 min, prior to fixation. DAPI was used as a nuclear counterstain. Only for aSyn aggregation model, cells were subjected to immunocytochemistry for aSyn (green) followed by confocal microscopy. Scale bars: 20  $\mu$ m. Control cells are represented in Annex 5.2.10B.



**Annex 5.2.10. Overexpression of SLP5 at different steps of aSyn aggregation.** H4 cells with no aSyn or stable for aSyn-BiFC (green) were transfected with **(A)** SLP5 or **(B)** empty vector. To promote the formation of aSyn inclusions, cells were triple-transfected with aSynT, Synphilin-1 and the same constructs referred above. 48 h post-transfection, media with no serum was replaced in cells for 1 h. Cells were incubated with Alexa-647 human transferrin (magenta) for 30 min, prior to fixation. DAPI was used as a nuclear counterstain. Only for aSyn aggregation model, cells were subjected to immunocytochemistry for aSyn (green) followed by confocal microscopy. Scale bars: 20  $\mu$ m.



**Annex 5.2.11. Neuronal roles and effects of knockdown of the genes identified on aSyn oligomerization and aggregation models**

Hit	Role in neuronal processes	Effect of knockdown on aSyn				
		oligomerization			Aggregation	
		Fluorescence intensity	protein levels	Cytotoxicity	inclusions per cell	Cytotoxicity
<b>RAB39B</b>	<ul style="list-style-type: none"> <li>Trafficking from the endoplasmic reticulum to the Golgi</li> <li>Mutations associated with intellectual disabilities, epilepsy and cognitive impairment (Mata et al 2015)</li> <li>Deletion identified in three cases with early-onset Parkinsonism and intellectual disability; deregulates aSyn homeostasis with aSyn reactive-LB and neurites</li> <li>T168K missense mutation was found in a fourth patient with similar symptoms (Wilson et al 2014)</li> <li>Co-localization with Huntingtin, translocating it to ER (Yao et al 2015)</li> </ul>	↑	↔	↔	↑	↑
<b>CAMK1</b>	<ul style="list-style-type: none"> <li>Calmodulin-dependent kinase that plays a role in axonal growth (Ageta-Ishihara et al 2009)</li> <li>Camk2 forms a complex with aSyn and regulates oligomerization (Martinez et al 2003)</li> </ul>	↑	↑	↔	↑	↔
<b>DYRK2</b>	<ul style="list-style-type: none"> <li>Dual-specificity tyrosine and serine/threonine phosphorylation-regulated kinase, involved in cytoskeletal organization and decreases both axon/dendrite growth and branching (Slepek et al 2012)</li> </ul>	↑	↔	↔	↓	↔
<b>CC2D1A</b>	<ul style="list-style-type: none"> <li>Coiled-coil and C2 domain containing 1A (<i>Cc2d1a</i>) is a transcriptional repressor inhibited by calcium, involved in neuronal differentiation and regulation of endosomal sorting complexes required for transport (Martinelli et al 2012)</li> <li>Cc2d1a regulates NF-κB activity (Manzini et al 2014)</li> <li>C-terminal deletion in <i>CC2D1A</i> is linked to mental retardation (Basel-Vanagaite et al 2006)</li> </ul>	↓	↓	↔	↑	↔
<b>CLK4</b>	<ul style="list-style-type: none"> <li>Cdc2-like kinase 4 is a protein involved in phosphorylation of serine/arginine rich proteins within spliceosome</li> <li>CLKs were also recently involved in the pathophysiology of Alzheimer's disease (Jain et al 2014)</li> </ul>	↓	↓	↑	↑	↔



## VI. References

---



- Aarsland D, Kurz MW. 2010. The epidemiology of dementia associated with Parkinson disease. *J Neurol Sci* 289: 18-22
- Abbas N, Lucking CB, Ricard S, Durr A, Bonifati V, et al. 1999. A wide variety of mutations in the parkin gene are responsible for autosomal recessive parkinsonism in Europe. French Parkinson's Disease Genetics Study Group and the European Consortium on Genetic Susceptibility in Parkinson's Disease. *Hum Mol Genet* 8: 567-74
- Abeliovich A, Schmitz Y, Farinas I, Choi-Lundberg D, Ho WH, et al. 2000. Mice lacking alpha-synuclein display functional deficits in the nigrostriatal dopamine system. *Neuron* 25: 239-52
- Ageta-Ishihara N, Takemoto-Kimura S, Nonaka M, Adachi-Morishima A, Suzuki K, et al. 2009. Control of cortical axon elongation by a GABA-driven Ca<sup>2+</sup>/calmodulin-dependent protein kinase cascade. *J Neurosci* 29: 13720-9
- Alvarez-Erviti L, Seow Y, Schapira AH, Gardiner C, Sargent IL, et al. 2011. Lysosomal dysfunction increases exosome-mediated alpha-synuclein release and transmission. *Neurobiol Dis* 42: 360-7
- Anderie I, Schulz I, Schmid A. 2007. Direct interaction between ER membrane-bound PTP1B and its plasma membrane-anchored targets. *Cell Signal* 19: 582-92
- Anderson JP, Walker DE, Goldstein JM, de Laat R, Banducci K, et al. 2006. Phosphorylation of Ser-129 is the dominant pathological modification of alpha-synuclein in familial and sporadic Lewy body disease. *J Biol Chem* 281: 29739-52
- Anwar S, Peters O, Millership S, Ninkina N, Doig N, et al. 2011. Functional alterations to the nigrostriatal system in mice lacking all three members of the synuclein family. *J Neurosci* 31: 7264-74
- Aosaki T, Miura M, Suzuki T, Nishimura K, Masuda M. 2010. Acetylcholine-dopamine balance hypothesis in the striatum: an update. *Geriatrics & gerontology international* 10 Suppl 1: S148-57
- Appel-Cresswell S, Vilarino-Guell C, Encarnacion M, Sherman H, Yu I, et al. 2013. Alpha-synuclein p.H50Q, a novel pathogenic mutation for Parkinson's disease. *Movement disorders : official journal of the Movement Disorder Society* 28: 811-3
- Arawaka S, Wada M, Goto S, Karube H, Sakamoto M, et al. 2006. The role of G-protein-coupled receptor kinase 5 in pathogenesis of sporadic Parkinson's disease. *J Neurosci* 26: 9227-38
- Armstrong RA, Cairns NJ, Lantos PL. 2006. Multiple system atrophy (MSA): topographic distribution of the alpha-synuclein-associated pathological changes. *Parkinsonism Relat Disord* 12: 356-62
- Auluck PK, Caraveo G, Lindquist S. 2010. alpha-Synuclein: membrane interactions and toxicity in Parkinson's disease. *Annu Rev Cell Dev Biol* 26: 211-33
- Auluck PK, Chan HY, Trojanowski JQ, Lee VM, Bonini NM. 2002. Chaperone suppression of alpha-synuclein toxicity in a Drosophila model for Parkinson's disease. *Science* 295: 865-8

- Azeredo da Silveira S, Schneider BL, Cifuentes-Diaz C, Sage D, Abbas-Terki T, et al. 2009. Phosphorylation does not prompt, nor prevent, the formation of alpha-synuclein toxic species in a rat model of Parkinson's disease. *Hum Mol Genet* 18: 872-87
- Baba M, Nakajo S, Tu PH, Tomita T, Nakaya K, et al. 1998. Aggregation of alpha-synuclein in Lewy bodies of sporadic Parkinson's disease and dementia with Lewy bodies. *Am J Pathol* 152: 879-84
- Bandopadhyay R, de Belleruche J. 2009. Pathogenesis of Parkinson's disease: emerging role of molecular chaperones. *Trends Mol Med*
- Bartels T, Choi JG, Selkoe DJ. 2011. alpha-Synuclein occurs physiologically as a helically folded tetramer that resists aggregation. *Nature* 477: 107-10
- Basel-Vanagaite L, Attia R, Yahav M, Ferland RJ, Anteki L, et al. 2006. The CC2D1A, a member of a new gene family with C2 domains, is involved in autosomal recessive non-syndromic mental retardation. *J Med Genet* 43: 203-10
- Basso E, Antas P, Marijanovic Z, Goncalves S, Tenreiro S, Outeiro TF. 2013. PLK2 modulates alpha-synuclein aggregation in yeast and mammalian cells. *Mol Neurobiol* 48: 854-62
- Bauer PO, Nukina N. 2009. The pathogenic mechanisms of polyglutamine diseases and current therapeutic strategies. *Journal of neurochemistry* 110: 1737-65
- Bayer TA, Jakala P, Hartmann T, Egensperger R, Buslei R, et al. 1999. Neural expression profile of alpha-synuclein in developing human cortex. *Neuroreport* 10: 2799-803
- Beach TG, Adler CH, Sue LI, Vedders L, Lue L, et al. 2010. Multi-organ distribution of phosphorylated alpha-synuclein histopathology in subjects with Lewy body disorders. *Acta Neuropathol* 119: 689-702
- Ben Gedalya T, Loeb V, Israeli E, Altschuler Y, Selkoe DJ, Sharon R. 2009. Alpha-synuclein and polyunsaturated fatty acids promote clathrin-mediated endocytosis and synaptic vesicle recycling. *Traffic* 10: 218-34
- Berge G, Sando SB, Rongve A, Aarsland D, White LR. 2014. Apolipoprotein E epsilon2 genotype delays onset of dementia with Lewy bodies in a Norwegian cohort. *J Neurol Neurosurg Psychiatry* 85: 1227-31
- Bernis ME, Babila JT, Breid S, Wusten KA, Wullner U, Tamguney G. 2015. Prion-like propagation of human brain-derived alpha-synuclein in transgenic mice expressing human wild-type alpha-synuclein. *Acta Neuropathol Commun* 3: 75
- Biernat J, Gustke N, Drewes G, Mandelkow EM, Mandelkow E. 1993. Phosphorylation of Ser262 strongly reduces binding of tau to microtubules: distinction between PHF-like immunoreactivity and microtubule binding. *Neuron* 11: 153-63
- Binolfi A, Theillet FX, Selenko P. 2012. Bacterial in-cell NMR of human alpha-synuclein: a disordered monomer by nature? *Biochem Soc Trans* 40: 950-4
- Bodner CR, Maltsev AS, Dobson CM, Bax A. 2010. Differential phospholipid binding of alpha-synuclein variants implicated in Parkinson's disease revealed by solution NMR spectroscopy. *Biochemistry* 49: 862-71

- Bohren KM, Nadkarni V, Song JH, Gabbay KH, Owerbach D. 2004. A M55V polymorphism in a novel SUMO gene (SUMO-4) differentially activates heat shock transcription factors and is associated with susceptibility to type I diabetes mellitus. *J Biol Chem* 279: 27233-8
- Bonifati V, Rizzu P, van Baren MJ, Schaap O, Breedveld GJ, et al. 2003. Mutations in the DJ-1 gene associated with autosomal recessive early-onset parkinsonism. *Science* 299: 256-9
- Bonini NM, Giasson BI. 2005. Snaring the function of alpha-synuclein. *Cell* 123: 359-61
- Borghi R, Marchese R, Negro A, Marinelli L, Forloni G, et al. 2000. Full length alpha-synuclein is present in cerebrospinal fluid from Parkinson's disease and normal subjects. *Neurosci Lett* 287: 65-7
- Braak H, Braak E, Yilmazer D, de Vos RA, Jansen EN, et al. 1994. Amygdala pathology in Parkinson's disease. *Acta neuropathologica* 88: 493-500
- Braak H, de Vos RA, Bohl J, Del Tredici K. 2006. Gastric alpha-synuclein immunoreactive inclusions in Meissner's and Auerbach's plexuses in cases staged for Parkinson's disease-related brain pathology. *Neurosci Lett* 396: 67-72
- Braak H, Del Tredici K. 2004. Poor and protracted myelination as a contributory factor to neurodegenerative disorders. *Neurobiol Aging* 25: 19-23
- Braak H, Del Tredici K, Rub U, de Vos RA, Jansen Steur EN, Braak E. 2003. Staging of brain pathology related to sporadic Parkinson's disease. *Neurobiol Aging* 24: 197-211
- Braak H, Sandmann-Keil D, Gai W, Braak E. 1999. Extensive axonal Lewy neurites in Parkinson's disease: a novel pathological feature revealed by alpha-synuclein immunocytochemistry. *Neurosci Lett* 265: 67-9
- Bracha-Drori K, Shichrur K, Katz A, Oliva M, Angelovici R, et al. 2004. Detection of protein-protein interactions in plants using bimolecular fluorescence complementation. *Plant J* 40: 419-27
- Bras J, Guerreiro R, Darwent L, Parkkinen L, Ansorge O, et al. 2014. Genetic analysis implicates APOE, SNCA and suggests lysosomal dysfunction in the etiology of dementia with Lewy bodies. *Hum Mol Genet* 23: 6139-46
- Breda C, Nugent ML, Estranero JG, Kyriacou CP, Outeiro TF, et al. 2014. Rab11 modulates alpha-synuclein mediated defects in synaptic transmission and behaviour. *Hum Mol Genet*
- Brundin P, Li JY, Holton JL, Lindvall O, Revesz T. 2008. Research in motion: the enigma of Parkinson's disease pathology spread. *Nat Rev Neurosci* 9: 741-5
- Brundin P, Melki R, Kopito R. 2010. Prion-like transmission of protein aggregates in neurodegenerative diseases. *Nat Rev Mol Cell Biol* 11: 301-7
- Burre J. 2015. The Synaptic Function of alpha-Synuclein. *Journal of Parkinson's disease* 5: 699-713
- Burre J, Sharma M, Sudhof TC. 2014. alpha-Synuclein assembles into higher-order multimers upon membrane binding to promote SNARE complex formation. *Proceedings of the National Academy of Sciences of the United States of America* 111: E4274-83

- Burre J, Sharma M, Sudhof TC. 2015. Definition of a molecular pathway mediating alpha-synuclein neurotoxicity. *J Neurosci* 35: 5221-32
- Burre J, Sharma M, Tsetsenis T, Buchman V, Etherton MR, Sudhof TC. 2010. Alpha-synuclein promotes SNARE-complex assembly in vivo and in vitro. *Science* 329: 1663-7
- Chadchankar H, Ihalainen J, Tanila H, Yavich L. 2011. Decreased reuptake of dopamine in the dorsal striatum in the absence of alpha-synuclein. *Brain Res* 1382: 37-44
- Chai YJ, Kim D, Park J, Zhao H, Lee SJ, Chang S. 2013. The secreted oligomeric form of alpha-synuclein affects multiple steps of membrane trafficking. *FEBS Lett* 587: 452-9
- Chandra S, Chen X, Rizo J, Jahn R, Sudhof TC. 2003. A broken alpha-helix in folded alpha-synuclein. *J Biol Chem* 278: 15313-8
- Chandra S, Gallardo G, Fernandez-Chacon R, Schluter OM, Sudhof TC. 2005. Alpha-synuclein cooperates with CSPalpha in preventing neurodegeneration. *Cell* 123: 383-96
- Chartier-Harlin MC, Kachergus J, Roumier C, Mouroux V, Douay X, et al. 2004. Alpha-synuclein locus duplication as a cause of familial Parkinson's disease. *Lancet* 364: 1167-9
- Chaturvedi RK, Beal MF. 2008. PPAR: a therapeutic target in Parkinson's disease. *J Neurochem* 106: 506-18
- Chen B, Liu Q, Ge Q, Xie J, Wang ZW. 2007. UNC-1 regulates gap junctions important to locomotion in *C. elegans*. *Curr Biol* 17: 1334-9
- Chen CD, Oh SY, Hinman JD, Abraham CR. 2006. Visualization of APP dimerization and APP-Notch2 heterodimerization in living cells using bimolecular fluorescence complementation. *J Neurochem* 97: 30-43
- Chen L, Feany MB. 2005. Alpha-synuclein phosphorylation controls neurotoxicity and inclusion formation in a *Drosophila* model of Parkinson disease. *Nat Neurosci* 8: 657-63
- Chen L, Periquet M, Wang X, Negro A, McLean PJ, et al. 2009. Tyrosine and serine phosphorylation of alpha-synuclein have opposing effects on neurotoxicity and soluble oligomer formation. *J Clin Invest* 119: 3257-65
- Chiba-Falek O, Touchman JW, Nussbaum RL. 2003. Functional analysis of intra-allelic variation at NACP-Rep1 in the alpha-synuclein gene. *Hum Genet* 113: 426-31
- Chu J, Zhang Z, Zheng Y, Yang J, Qin L, et al. 2009. A novel far-red bimolecular fluorescence complementation system that allows for efficient visualization of protein interactions under physiological conditions. *Biosens Bioelectron* 25: 234-9
- Chu Y, Morfini GA, Langhamer LB, He Y, Brady ST, Kordower JH. 2012. Alterations in axonal transport motor proteins in sporadic and experimental Parkinson's disease. *Brain* 135: 2058-73
- Chung CY, Koprach JB, Hallett PJ, Isacson O. 2009. Functional enhancement and protection of dopaminergic terminals by RAB3B overexpression. *Proc Natl Acad Sci U S A* 106: 22474-9



- Chutna O, Goncalves S, Villar-Pique A, Guerreiro P, Marijanovic Z, et al. 2014a. The small GTPase Rab11 co-localizes with alpha-synuclein in intracellular inclusions and modulates its aggregation, secretion and toxicity. *Hum Mol Genet* 23: 6732-45
- Chutna O, Goncalves S, Villar-Pique A, Guerreiro P, Marijanovic Z, et al. 2014b. The small GTPase Rab11 co-localizes with alpha-synuclein in intracellular inclusions and modulates its aggregation, secretion and toxicity. *Hum Mol Genet*
- Ciechanover A, Schwartz AL, Lodish HF. 1983. Sorting and recycling of cell surface receptors and endocytosed ligands: the asialoglycoprotein and transferrin receptors. *J Cell Biochem* 23: 107-30
- Cole NB, Dieuliis D, Leo P, Mitchell DC, Nussbaum RL. 2008. Mitochondrial translocation of alpha-synuclein is promoted by intracellular acidification. *Exp Cell Res* 314: 2076-89
- Colvin RA, Means TK, Diefenbach TJ, Moita LF, Friday RP, et al. 2010. Synaptotagmin-mediated vesicle fusion regulates cell migration. *Nature immunology* 11: 495-502
- Conway KA, Harper JD, Lansbury PT. 1998. Accelerated in vitro fibril formation by a mutant alpha-synuclein linked to early-onset Parkinson disease. *Nat Med* 4: 1318-20
- Cookson MR. 2012. Cellular effects of LRRK2 mutations. *Biochem Soc Trans* 40: 1070-3
- Cooper AA, Gitler AD, Cashikar A, Haynes CM, Hill KJ, et al. 2006. Alpha-synuclein blocks ER-Golgi traffic and Rab1 rescues neuron loss in Parkinson's models. *Science* 313: 324-8
- Crews L, Mizuno H, Desplats P, Rockenstein E, Adame A, et al. 2008. Alpha-synuclein alters Notch-1 expression and neurogenesis in mouse embryonic stem cells and in the hippocampus of transgenic mice. *J Neurosci* 28: 4250-60
- Critchley M. 1957. Medical aspects of boxing, particularly from a neurological standpoint. *British medical journal* 1: 357-62
- Croisier E, Moran LB, Dexter DT, Pearce RK, Graeber MB. 2005. Microglial inflammation in the parkinsonian substantia nigra: relationship to alpha-synuclein deposition. *J Neuroinflammation* 2: 14
- Crowther RA, Jakes R, Spillantini MG, Goedert M. 1998. Synthetic filaments assembled from C-terminally truncated alpha-synuclein. *FEBS Lett* 436: 309-12
- Dalfo E, Barrachina M, Rosa JL, Ambrosio S, Ferrer I. 2004a. Abnormal alpha-synuclein interactions with rab3a and rabphilin in diffuse Lewy body disease. *Neurobiol Dis* 16: 92-7
- Dalfo E, Gomez-Isla T, Rosa JL, Nieto Bodelon M, Cuadrado Tejedor M, et al. 2004b. Abnormal alpha-synuclein interactions with Rab proteins in alpha-synuclein A30P transgenic mice. *J Neuropathol Exp Neurol* 63: 302-13
- Dalfo E, Portero-Otin M, Ayala V, Martinez A, Pamplona R, Ferrer I. 2005. Evidence of oxidative stress in the neocortex in incidental Lewy body disease. *J Neuropathol Exp Neurol* 64: 816-30
- Damier P, Hirsch EC, Agid Y, Graybiel AM. 1999. The substantia nigra of the human brain. II. Patterns of loss of dopamine-containing neurons in Parkinson's disease. *Brain* 122 ( Pt 8): 1437-48

- Danzer KM, Haasen D, Karow AR, Moussaud S, Habeck M, et al. 2007. Different species of alpha-synuclein oligomers induce calcium influx and seeding. *J Neurosci* 27: 9220-32
- Danzer KM, Kranich LR, Ruf WP, Cagsal-Getkin O, Winslow AR, et al. 2012. Exosomal cell-to-cell transmission of alpha synuclein oligomers. *Molecular neurodegeneration* 7: 42
- Danzer KM, Krebs SK, Wolff M, Birk G, Hengerer B. 2009. Seeding induced by alpha-synuclein oligomers provides evidence for spreading of alpha-synuclein pathology. *J Neurochem* 111: 192-203
- Danzer KM, Ruf WP, Putcha P, Joyner D, Hashimoto T, et al. 2011. Heat-shock protein 70 modulates toxic extracellular alpha-synuclein oligomers and rescues trans-synaptic toxicity. *FASEB J* 25: 326-36
- Davidson WS, Jonas A, Clayton DF, George JM. 1998. Stabilization of alpha-synuclein secondary structure upon binding to synthetic membranes. *J Biol Chem* 273: 9443-9
- de Lau LM, Breteler MM. 2006. Epidemiology of Parkinson's disease. *Lancet Neurol* 5: 525-35
- Dedmon MM, Christodoulou J, Wilson MR, Dobson CM. 2005. Heat shock protein 70 inhibits alpha-synuclein fibril formation via preferential binding to prefibrillar species. *J Biol Chem* 280: 14733-40
- del Toro D, Alberch J, Lazaro-Dieguez F, Martin-Ibanez R, Xifro X, et al. 2009. Mutant huntingtin impairs post-Golgi trafficking to lysosomes by delocalizing optineurin/Rab8 complex from the Golgi apparatus. *Mol Biol Cell* 20: 1478-92
- Desplats P, Lee HJ, Bae EJ, Patrick C, Rockenstein E, et al. 2009. Inclusion formation and neuronal cell death through neuron-to-neuron transmission of alpha-synuclein. *Proc Natl Acad Sci U S A* 106: 13010-5
- Dettmer U, Newman AJ, Luth ES, Bartels T, Selkoe D. 2013. In vivo cross-linking reveals principally oligomeric forms of alpha-synuclein and beta-synuclein in neurons and non-neural cells. *J Biol Chem* 288: 6371-85
- Dettmer U, Newman AJ, Soldner F, Luth ES, Kim NC, et al. 2015a. Parkinson-causing alpha-synuclein missense mutations shift native tetramers to monomers as a mechanism for disease initiation. *Nature communications* 6: 7314
- Dettmer U, Newman AJ, von Saucken VE, Bartels T, Selkoe D. 2015b. KTEGV repeat motifs are key mediators of normal alpha-synuclein tetramerization: Their mutation causes excess monomers and neurotoxicity. *Proceedings of the National Academy of Sciences of the United States of America* 112: 9596-601
- Devi L, Raghavendran V, Prabhu BM, Avadhani NG, Anandatheerthavarada HK. 2008. Mitochondrial import and accumulation of alpha-synuclein impair complex I in human dopaminergic neuronal cultures and Parkinson disease brain. *J Biol Chem* 283: 9089-100
- Di Giovanni S, De Biase A, Yakovlev A, Finn T, Beers J, et al. 2005. In vivo and in vitro characterization of novel neuronal plasticity factors identified following spinal cord injury. *J Biol Chem* 280: 2084-91
- Diao J, Burre J, Vivona S, Cipriano DJ, Sharma M, et al. 2013. Native alpha-synuclein induces clustering of synaptic-vesicle mimics via binding to phospholipids and synaptobrevin-2/VAMP2. *Elife* 2: e00592

- Dickson DW, Braak H, Duda JE, Duyckaerts C, Gasser T, et al. 2009. Neuropathological assessment of Parkinson's disease: refining the diagnostic criteria. *Lancet Neurol* 8: 1150-7
- Ding TT, Lee SJ, Rochet JC, Lansbury PT, Jr. 2002. Annular alpha-synuclein protofibrils are produced when spherical protofibrils are incubated in solution or bound to brain-derived membranes. *Biochemistry* 41: 10209-17
- Diogenes MJ, Dias RB, Rombo DM, Vicente Miranda H, Maiolino F, et al. 2012. Extracellular alpha-synuclein oligomers modulate synaptic transmission and impair LTP via NMDA-receptor activation. *J Neurosci* 32: 11750-62
- Dixit R, Ross JL, Goldman YE, Holzbaur EL. 2008. Differential regulation of dynein and kinesin motor proteins by tau. *Science* 319: 1086-9
- Dodson MW, Zhang T, Jiang C, Chen S, Guo M. 2012. Roles of the Drosophila LRRK2 homolog in Rab7-dependent lysosomal positioning. *Hum Mol Genet* 21: 1350-63
- Duda JE, Giasson BI, Chen Q, Gur TL, Hurtig HI, et al. 2000. Widespread nitration of pathological inclusions in neurodegenerative synucleinopathies. *The American journal of pathology* 157: 1439-45
- Ebrahimi-Fakhari D, Saidi LJ, Wahlster L. 2013. Molecular chaperones and protein folding as therapeutic targets in Parkinson's disease and other synucleinopathies. *Acta Neuropathol Commun* 1: 79
- Ebrahimi-Fakhari D, Wahlster L, McLean PJ. 2012. Protein degradation pathways in Parkinson's disease: curse or blessing. *Acta Neuropathol* 124: 153-72
- Edvardson S, Cinnamon Y, Ta-Shma A, Shaag A, Yim YI, et al. 2012. A deleterious mutation in DNAJC6 encoding the neuronal-specific clathrin-uncoating co-chaperone auxilin, is associated with juvenile parkinsonism. *PLoS One* 7: e36458
- Eisbach SE, Outeiro TF. 2013. Alpha-synuclein and intracellular trafficking: impact on the spreading of Parkinson's disease pathology. *J Mol Med (Berl)* 91: 693-703
- Ejlertskov P, Rasmussen I, Nielsen TT, Bergstrom AL, Tohyama Y, et al. 2013. Tubulin polymerization-promoting protein (TPPP/p25alpha) promotes unconventional secretion of alpha-synuclein through exophagy by impairing autophagosome-lysosome fusion. *J Biol Chem* 288: 17313-35
- El-Agnaf OM, Salem SA, Paleologou KE, Cooper LJ, Fullwood NJ, et al. 2003. Alpha-synuclein implicated in Parkinson's disease is present in extracellular biological fluids, including human plasma. *FASEB J* 17: 1945-7
- Emanuele M, Chiergatti E. 2015. Mechanisms of alpha-synuclein action on neurotransmission: cell-autonomous and non-cell autonomous role. *Biomolecules* 5: 865-92
- Emmanouilidou E, Melachroinou K, Roumeliotis T, Garbis SD, Ntzouni M, et al. 2010. Cell-produced alpha-synuclein is secreted in a calcium-dependent manner by exosomes and impacts neuronal survival. *J Neurosci* 30: 6838-51
- Engelender S, Kaminsky Z, Guo X, Sharp AH, Amaravi RK, et al. 1999. Synphilin-1 associates with alpha-synuclein and promotes the formation of cytosolic inclusions. *Nat Genet* 22: 110-4

- Englund H, Sehlin D, Johansson AS, Nilsson LN, Gellerfors P, et al. 2007. Sensitive ELISA detection of amyloid-beta protofibrils in biological samples. *J Neurochem* 103: 334-45
- Esseltine JL, Ferguson SS. 2013. Regulation of G protein-coupled receptor trafficking and signaling by Rab GTPases. *Small GTPases* 4: 132-5
- Fahn S. 2000. The spectrum of levodopa-induced dyskinesias. *Ann Neurol* 47: S2-9; discussion S9-11
- Fan Y, Limprasert P, Murray IV, Smith AC, Lee VM, et al. 2006. Beta-synuclein modulates alpha-synuclein neurotoxicity by reducing alpha-synuclein protein expression. *Hum Mol Genet* 15: 3002-11
- Fares MB, Ait-Bouziad N, Dikiy I, Mbefo MK, Jovicic A, et al. 2014. The novel Parkinson's disease linked mutation G51D attenuates in vitro aggregation and membrane binding of alpha-synuclein, and enhances its secretion and nuclear localization in cells. *Hum Mol Genet* 23: 4491-509
- Farrer M, Chan P, Chen R, Tan L, Lincoln S, et al. 2001. Lewy bodies and parkinsonism in families with parkin mutations. *Ann Neurol* 50: 293-300
- Fauvet B, Fares MB, Samuel F, Dikiy I, Tandon A, et al. 2012a. Characterization of semisynthetic and naturally Nalpha-acetylated alpha-synuclein in vitro and in intact cells: implications for aggregation and cellular properties of alpha-synuclein. *J Biol Chem* 287: 28243-62
- Fauvet B, Mbefo MK, Fares MB, Desobry C, Michael S, et al. 2012b. alpha-Synuclein in central nervous system and from erythrocytes, mammalian cells, and Escherichia coli exists predominantly as disordered monomer. *J Biol Chem* 287: 15345-64
- Feany MB, Bender WW. 2000. A Drosophila model of Parkinson's disease. *Nature* 404: 394-8
- Fields S, Song O. 1989. A novel genetic system to detect protein-protein interactions. *Nature* 340: 245-6
- Fiske M, Valtierra S, Solvang K, Zorniak M, White M, et al. 2011. Contribution of Alanine-76 and Serine Phosphorylation in alpha-Synuclein Membrane Association and Aggregation in Yeasts. *Parkinsons Dis* 2011: 392180
- Flower TR, Chesnokova LS, Froelich CA, Dixon C, Witt SN. 2005. Heat shock prevents alpha-synuclein-induced apoptosis in a yeast model of Parkinson's disease. *J Mol Biol* 351: 1081-100
- Fombonne J, Rabizadeh S, Banwait S, Mehlen P, Bredesen DE. 2009. Selective vulnerability in Alzheimer's disease: amyloid precursor protein and p75(NTR) interaction. *Annals of neurology* 65: 294-303
- Fortin DL, Troyer MD, Nakamura K, Kubo S, Anthony MD, Edwards RH. 2004. Lipid rafts mediate the synaptic localization of alpha-synuclein. *J Neurosci* 24: 6715-23
- Freichel C, Neumann M, Ballard T, Muller V, Woolley M, et al. 2007. Age-dependent cognitive decline and amygdala pathology in alpha-synuclein transgenic mice. *Neurobiol Aging* 28: 1421-35
- Fujita M, Sugama S, Sekiyama K, Sekigawa A, Tsukui T, et al. 2010. A beta-synuclein mutation linked to dementia produces neurodegeneration when expressed in mouse brain. *Nat Commun* 1: 110

- Fujiwara H, Hasegawa M, Dohmae N, Kawashima A, Masliah E, et al. 2002. alpha-Synuclein is phosphorylated in synucleinopathy lesions. *Nature cell biology* 4: 160-4
- Fukuda M. 2003. Slp4-a/granuphilin-a inhibits dense-core vesicle exocytosis through interaction with the GDP-bound form of Rab27A in PC12 cells. *The Journal of biological chemistry* 278: 15390-6
- Fukuda M. 2013. Rab27 effectors, pleiotropic regulators in secretory pathways. *Traffic* 14: 949-63
- Funke SA, Birkmann E, Henke F, Gortz P, Lange-Asschenfeldt C, et al. 2007. Single particle detection of Abeta aggregates associated with Alzheimer's disease. *Biochemical and biophysical research communications* 364: 902-7
- Gai WP, Pountney DL, Power JH, Li QX, Culvenor JG, et al. 2003. alpha-Synuclein fibrils constitute the central core of oligodendroglial inclusion filaments in multiple system atrophy. *Exp Neurol* 181: 68-78
- Gaig C, Marti MJ, Ezquerra M, Rey MJ, Cardozo A, Tolosa E. 2007. G2019S LRRK2 mutation causing Parkinson's disease without Lewy bodies. *J Neurol Neurosurg Psychiatry* 78: 626-8
- Galvin JE, Giasson B, Hurtig HI, Lee VM, Trojanowski JQ. 2000. Neurodegeneration with brain iron accumulation, type 1 is characterized by alpha-, beta-, and gamma-synuclein neuropathology. *Am J Pathol* 157: 361-8
- Galvin JE, Schuck TM, Lee VM, Trojanowski JQ. 2001. Differential expression and distribution of alpha-, beta-, and gamma-synuclein in the developing human substantia nigra. *Exp Neurol* 168: 347-55
- Gandia J, Galino J, Amaral OB, Soriano A, Lluís C, et al. 2008. Detection of higher-order G protein-coupled receptor oligomers by a combined BRET-BiFC technique. *FEBS Lett* 582: 2979-84
- Garcia-Reitböck P, Anichtchik O, Bellucci A, Iovino M, Ballini C, et al. 2010. SNARE protein redistribution and synaptic failure in a transgenic mouse model of Parkinson's disease. *Brain* 133: 2032-44
- Gehl C, Waadt R, Kudla J, Mendel RR, Hansch R. 2009. New GATEWAY vectors for high throughput analyses of protein-protein interactions by bimolecular fluorescence complementation. *Mol Plant* 2: 1051-8
- Gelb DJ, Oliver E, Gilman S. 1999. Diagnostic criteria for Parkinson disease. *Arch Neurol* 56: 33-9
- George JM, Jin H, Woods WS, Clayton DF. 1995. Characterization of a novel protein regulated during the critical period for song learning in the zebra finch. *Neuron* 15: 361-72
- Giannandrea M, Bianchi V, Mignogna ML, Sirri A, Carrabino S, et al. 2010. Mutations in the small GTPase gene RAB39B are responsible for X-linked mental retardation associated with autism, epilepsy, and macrocephaly. *Am J Hum Genet* 86: 185-95
- Giasson BI, Duda JE, Murray IV, Chen Q, Souza JM, et al. 2000. Oxidative damage linked to neurodegeneration by selective alpha-synuclein nitration in synucleinopathy lesions. *Science* 290: 985-9
- Giasson BI, Murray IV, Trojanowski JQ, Lee VM. 2001. A hydrophobic stretch of 12 amino acid residues in the middle of alpha-synuclein is essential for filament assembly. *J Biol Chem* 276: 2380-6

- Giasson BI, Uryu K, Trojanowski JQ, Lee VM. 1999. Mutant and wild type human alpha-synucleins assemble into elongated filaments with distinct morphologies in vitro. *J Biol Chem* 274: 7619-22
- Gitler AD, Bevis BJ, Shorter J, Strathearn KE, Hamamichi S, et al. 2008. The Parkinson's disease protein alpha-synuclein disrupts cellular Rab homeostasis. *Proc Natl Acad Sci U S A* 105: 145-50
- Goedert M, Spillantini MG, Del Tredici K, Braak H. 2013. 100 years of Lewy pathology. *Nature reviews. Neurology* 9: 13-24
- Goers J, Manning-Bog AB, McCormack AL, Millett IS, Doniach S, et al. 2003. Nuclear localization of alpha-synuclein and its interaction with histones. *Biochemistry* 42: 8465-71
- Goetz CG, Poewe W, Rascol O, Sampaio C. 2005. Evidence-based medical review update: pharmacological and surgical treatments of Parkinson's disease: 2001 to 2004. *Mov Disord* 20: 523-39
- Gonçalves S, Vicente Miranda H, Outeiro TF. 2012. Novel Molecular Therapeutics in Parkinson's Disease In *Human Molecular Therapeutics*, ed. RR David Whitehouse, pp. 245-65. UK: John Wiley & Sons
- Goncalves SA, Macedo D, Raquel H, Simoes PD, Giorgini F, et al. 2016. shRNA-Based Screen Identifies Endocytic Recycling Pathway Components That Act as Genetic Modifiers of Alpha-Synuclein Aggregation, Secretion and Toxicity. *PLoS genetics* 12: e1005995
- Goncalves SA, Matos JE, Outeiro TF. 2010. Zooming into protein oligomerization in neurodegeneration using BiFC. *Trends Biochem Sci* 35: 643-51
- Gorbatyuk OS, Li S, Sullivan LF, Chen W, Kondrikova G, et al. 2008. The phosphorylation state of Ser-129 in human alpha-synuclein determines neurodegeneration in a rat model of Parkinson disease. *Proc Natl Acad Sci U S A* 105: 763-8
- Greenbaum EA, Graves CL, Mishizen-Eberz AJ, Lupoli MA, Lynch DR, et al. 2005. The E46K mutation in alpha-synuclein increases amyloid fibril formation. *J Biol Chem* 280: 7800-7
- Greenfield JP, Leung LW, Cai D, Kaasik K, Gross RS, et al. 2002. Estrogen lowers Alzheimer beta-amyloid generation by stimulating trans-Golgi network vesicle biogenesis. *J Biol Chem* 277: 12128-36
- Greggio E, Zambrano I, Kaganovich A, Beilina A, Taymans JM, et al. 2008. The Parkinson disease-associated leucine-rich repeat kinase 2 (LRRK2) is a dimer that undergoes intramolecular autophosphorylation. *The Journal of biological chemistry* 283: 16906-14
- Griesbeck O, Baird GS, Campbell RE, Zacharias DA, Tsien RY. 2001. Reducing the environmental sensitivity of yellow fluorescent protein. Mechanism and applications. *The Journal of biological chemistry* 276: 29188-94
- Grundke-Iqbal I, Iqbal K, Quinlan M, Tung YC, Zaidi MS, Wisniewski HM. 1986. Microtubule-associated protein tau. A component of Alzheimer paired helical filaments. *J Biol Chem* 261: 6084-9
- Gunther EC, Strittmatter SM. 2010. beta-amyloid oligomers and cellular prion protein in Alzheimer's disease. *J Mol Med* 88: 331-38

- Haberman A, Williamson WR, Epstein D, Wang D, Rina S, et al. 2012. The synaptic vesicle SNARE neuronal Synaptobrevin promotes endolysosomal degradation and prevents neurodegeneration. *J Cell Biol* 196: 261-76
- Hagan PL, Halpern SE, Dillman RO, Shawler DL, Johnson DE, et al. 1986. Tumor size: effect on monoclonal antibody uptake in tumor models. *J Nucl Med* 27: 422-7
- Hansen C, Angot E, Bergstrom AL, Steiner JA, Pieri L, et al. 2011. alpha-Synuclein propagates from mouse brain to grafted dopaminergic neurons and seeds aggregation in cultured human cells. *J Clin Invest* 121: 715-25
- Hara K, Momose Y, Tokiguchi S, Shimohata M, Terajima K, et al. 2007. Multiplex families with multiple system atrophy. *Arch Neurol* 64: 545-51
- Hara T, Nakamura K, Matsui M, Yamamoto A, Nakahara Y, et al. 2006. Suppression of basal autophagy in neural cells causes neurodegenerative disease in mice. *Nature* 441: 885-9
- Hardy J, Selkoe DJ. 2002. The amyloid hypothesis of Alzheimer's disease: progress and problems on the road to therapeutics. *Science* 297: 353-6
- Hartl FU, Bracher A, Hayer-Hartl M. 2011. Molecular chaperones in protein folding and proteostasis. *Nature* 475: 324-32
- Hartl FU, Hayer-Hartl M. 2009. Converging concepts of protein folding in vitro and in vivo. *Nat Struct Mol Biol* 16: 574-81
- Hasegawa T, Konno M, Baba T, Sugeno N, Kikuchi A, et al. 2011. The AAA-ATPase VPS4 regulates extracellular secretion and lysosomal targeting of alpha-synuclein. *PLoS One* 6: e29460
- Hashimoto M, Hsu LJ, Rockenstein E, Takenouchi T, Mallory M, Masliah E. 2002. alpha-Synuclein protects against oxidative stress via inactivation of the c-Jun N-terminal kinase stress-signaling pathway in neuronal cells. *J Biol Chem* 277: 11465-72
- Hashimoto M, Rockenstein E, Mante M, Mallory M, Masliah E. 2001. beta-Synuclein inhibits alpha-synuclein aggregation: a possible role as an anti-parkinsonian factor. *Neuron* 32: 213-23
- Hattula K, Furuhejm J, Arffman A, Peranen J. 2002. A Rab8-specific GDP/GTP exchange factor is involved in actin remodeling and polarized membrane transport. *Mol Biol Cell* 13: 3268-80
- Hattula K, Furuhejm J, Tikkanen J, Tanhuanpaa K, Laakkonen P, Peranen J. 2006. Characterization of the Rab8-specific membrane traffic route linked to protrusion formation. *J Cell Sci* 119: 4866-77
- Hejjaoui M, Butterfield S, Fauvet B, Vercruyse F, Cui J, et al. 2012. Elucidating the role of C-terminal post-translational modifications using protein semisynthesis strategies: alpha-synuclein phosphorylation at tyrosine 125. *J Am Chem Soc* 134: 5196-210
- Henley SM, Frost C, MacManus DG, Warner TT, Fox NC, Tabrizi SJ. 2006. Increased rate of whole-brain atrophy over 6 months in early Huntington disease. *Neurology* 67: 694-6

- Herl L, Thomas AV, Lill CM, Banks M, Deng A, et al. 2009. Mutations in amyloid precursor protein affect its interactions with presenilin/gamma-secretase. *Mol Cell Neurosci* 41: 166-74
- Herrera F, Tenreiro S, Miller-Fleming L, Outeiro TF. 2011. Visualization of cell-to-cell transmission of mutant huntingtin oligomers. *PLoS Curr* 3: RRN1210
- Hirsch EC, Hunot S, Hartmann A. 2005. Neuroinflammatory processes in Parkinson's disease. *Parkinsonism Relat Disord* 11 Suppl 1: S9-S15
- Hodara R, Norris EH, Giasson BI, Mishizen-Eberz AJ, Lynch DR, et al. 2004. Functional consequences of alpha-synuclein tyrosine nitration: diminished binding to lipid vesicles and increased fibril formation. *J Biol Chem* 279: 47746-53
- Hoffman-Zacharska D, Koziorowski D, Ross OA, Milewski M, Poznanski J, et al. 2013. Novel A18T and pA29S substitutions in alpha-synuclein may be associated with sporadic Parkinson's disease. *Parkinsonism Relat Disord* 19: 1057-60
- Horstink M, Tolosa E, Bonuccelli U, Deuschl G, Friedman A, et al. 2006. Review of the therapeutic management of Parkinson's disease. Report of a joint task force of the European Federation of Neurological Societies (EFNS) and the Movement Disorder Society-European Section (MDS-ES). Part II: late (complicated) Parkinson's disease. *Eur J Neurol* 13: 1186-202
- Hoyer W, Cherny D, Subramaniam V, Jovin TM. 2004. Impact of the acidic C-terminal region comprising amino acids 109-140 on alpha-synuclein aggregation in vitro. *Biochemistry* 43: 16233-42
- Hsu LJ, Mallory M, Xia Y, Veinbergs I, Hashimoto M, et al. 1998. Expression pattern of synucleins (non-Abeta component of Alzheimer's disease amyloid precursor protein/alpha-synuclein) during murine brain development. *J Neurochem* 71: 338-44
- Hsu LJ, Sagara Y, Arroyo A, Rockenstein E, Sisk A, et al. 2000. alpha-synuclein promotes mitochondrial deficit and oxidative stress. *Am J Pathol* 157: 401-10
- Hu CD, Chinenov Y, Kerppola TK. 2002. Visualization of interactions among bZIP and Rel family proteins in living cells using bimolecular fluorescence complementation. *Mol Cell* 9: 789-98
- Hu CD, Kerppola TK. 2003. Simultaneous visualization of multiple protein interactions in living cells using multicolor fluorescence complementation analysis. *Nat Biotechnol* 21: 539-45
- Hunn BH, Cragg SJ, Bolam JP, Spillantini MG, Wade-Martins R. 2015. Impaired intracellular trafficking defines early Parkinson's disease. *Trends in neurosciences* 38: 178-88
- Hyun CH, Yoon CY, Lee HJ, Lee SJ. 2013. LRRK2 as a Potential Genetic Modifier of Synucleinopathies: Interlacing the Two Major Genetic Factors of Parkinson's Disease. *Exp Neurobiol* 22: 249-57
- Inglis KJ, Chereau D, Brigham EF, Chiou SS, Schobel S, et al. 2009. Polo-like kinase 2 (PLK2) phosphorylates alpha-synuclein at serine 129 in central nervous system. *J Biol Chem* 284: 2598-602
- Irwin DJ, Lee VM, Trojanowski JQ. 2013. Parkinson's disease dementia: convergence of alpha-synuclein, tau and amyloid-beta pathologies. *Nature reviews. Neuroscience* 14: 626-36



- Jain P, Karthikeyan C, Moorthy NS, Waiker DK, Jain AK, Trivedi P. 2014. Human CDC2-like kinase 1 (CLK1): a novel target for Alzheimer's disease. *Curr Drug Targets* 15: 539-50
- Jakes R, Spillantini MG, Goedert M. 1994. Identification of two distinct synucleins from human brain. *FEBS Lett* 345: 27-32
- Jang A, Lee HJ, Suk JE, Jung JW, Kim KP, Lee SJ. 2010. Non-classical exocytosis of alpha-synuclein is sensitive to folding states and promoted under stress conditions. *J Neurochem* 113: 1263-74
- Jenco JM, Rawlingson A, Daniels B, Morris AJ. 1998. Regulation of phospholipase D2: selective inhibition of mammalian phospholipase D isoenzymes by alpha- and beta-synucleins. *Biochemistry* 37: 4901-9
- Jensen PH, Hager H, Nielsen MS, Hojrup P, Gliemann J, Jakes R. 1999. alpha-synuclein binds to Tau and stimulates the protein kinase A-catalyzed tau phosphorylation of serine residues 262 and 356. *J Biol Chem* 274: 25481-9
- Jo E, Fuller N, Rand RP, St George-Hyslop P, Fraser PE. 2002. Defective membrane interactions of familial Parkinson's disease mutant A30P alpha-synuclein. *J Mol Biol* 315: 799-807
- Johnsson N, Varshavsky A. 1994. Split ubiquitin as a sensor of protein interactions in vivo. *Proc Natl Acad Sci U S A* 91: 10340-4
- Juenemann K, Reits EA. 2012. Alternative macroautophagic pathways. *International journal of cell biology* 2012: 189794
- Jung JJ, Tiwari A, Inamdar SM, Thomas CP, Goel A, Choudhury A. 2012. Secretion of soluble vascular endothelial growth factor receptor 1 (sVEGFR1/sFlt1) requires Arf1, Arf6, and Rab11 GTPases. *PLoS One* 7: e44572
- Junn E, Mouradian MM. 2001. Apoptotic signaling in dopamine-induced cell death: the role of oxidative stress, p38 mitogen-activated protein kinase, cytochrome c and caspases. *J Neurochem* 78: 374-83
- Karpinar DP, Baliya MB, Kugler S, Opazo F, Rezaei-Ghaleh N, et al. 2009. Pre-fibrillar alpha-synuclein variants with impaired beta-structure increase neurotoxicity in Parkinson's disease models. *EMBO J* 28: 3256-68
- Kayed R, Head E, Sarsoza F, Saing T, Cotman CW, et al. 2007. Fibril specific, conformation dependent antibodies recognize a generic epitope common to amyloid fibrils and fibrillar oligomers that is absent in prefibrillar oligomers. *Mol Neurodegener* 2: 18
- Keminer O, Peters R. 1999. Permeability of single nuclear pores. *Biophys J* 77: 217-28
- Kerppola TK. 2006. Visualization of molecular interactions by fluorescence complementation. *Nat Rev Mol Cell Biol* 7: 449-56
- Kerppola TK. 2008. Bimolecular fluorescence complementation: visualization of molecular interactions in living cells. *Methods Cell Biol* 85: 431-70
- Khvotchev MV, Ren M, Takamori S, Jahn R, Sudhof TC. 2003. Divergent functions of neuronal Rab11b in Ca<sup>2+</sup>-regulated versus constitutive exocytosis. *J Neurosci* 23: 10531-9

- Kitada T, Asakawa S, Hattori N, Matsumine H, Yamamura Y, et al. 1998. Mutations in the parkin gene cause autosomal recessive juvenile parkinsonism. *Nature* 392: 605-8
- Klein C, Westenberger A. 2012. Genetics of Parkinson's disease. *Cold Spring Harb Perspect Med* 2: a008888
- Klucken J, Outeiro TF, Nguyen P, McLean PJ, Hyman BT. 2006. Detection of novel intracellular alpha-synuclein oligomeric species by fluorescence lifetime imaging. *Faseb J* 20: 2050-7
- Klucken J, Poehler AM, Ebrahimi-Fakhari D, Schneider J, Nuber S, et al. 2012. Alpha-synuclein aggregation involves a bafilomycin A 1-sensitive autophagy pathway. *Autophagy* 8: 754-66
- Klucken J, Shin Y, Masliah E, Hyman BT, McLean PJ. 2004. Hsp70 Reduces alpha-Synuclein Aggregation and Toxicity. *J Biol Chem* 279: 25497-502
- Komatsu M, Waguri S, Chiba T, Murata S, Iwata J, et al. 2006. Loss of autophagy in the central nervous system causes neurodegeneration in mice. *Nature* 441: 880-4
- Kontopoulos E, Parvin JD, Feany MB. 2006. Alpha-synuclein acts in the nucleus to inhibit histone acetylation and promote neurotoxicity. *Hum Mol Genet* 15: 3012-23
- Kordower JH, Chu Y, Hauser RA, Freeman TB, Olanow CW. 2008. Lewy body-like pathology in long-term embryonic nigral transplants in Parkinson's disease. *Nat Med* 14: 504-6
- Kordower JH, Freeman TB, Snow BJ, Vingerhoets FJ, Mufson EJ, et al. 1995. Neuropathological evidence of graft survival and striatal reinnervation after the transplantation of fetal mesencephalic tissue in a patient with Parkinson's disease. *N Engl J Med* 332: 1118-24
- Korvatska O, Strand NS, Berndt JD, Strovast T, Chen DH, et al. 2013. Altered splicing of ATP6AP2 causes X-linked parkinsonism with spasticity (XPDS). *Hum Mol Genet* 22: 3259-68
- Krantz DE, Peter D, Liu Y, Edwards RH. 1997. Phosphorylation of a vesicular monoamine transporter by casein kinase II. *J Biol Chem* 272: 6752-9
- Kruger R, Kuhn W, Muller T, Woitalla D, Graeber M, et al. 1998. Ala30Pro mutation in the gene encoding alpha-synuclein in Parkinson's disease. *Nat Genet* 18: 106-8
- Kuhla B, Boeck K, Luth HJ, Schmidt A, Weigle B, et al. 2006. Age-dependent changes of glyoxalase I expression in human brain. *Neurobiol Aging* 27: 815-22
- Kulisevsky J, Pagonabarraga J, Pascual-Sedano B, Garcia-Sanchez C, Gironell A, Trapecio Group S. 2008. Prevalence and correlates of neuropsychiatric symptoms in Parkinson's disease without dementia. *Movement disorders : official journal of the Movement Disorder Society* 23: 1889-96
- Kuroda TS, Fukuda M, Ariga H, Mikoshiba K. 2002a. The Slp homology domain of synaptotagmin-like proteins 1-4 and Slac2 functions as a novel Rab27A binding domain. *J Biol Chem* 277: 9212-8
- Kuroda TS, Fukuda M, Ariga H, Mikoshiba K. 2002b. Synaptotagmin-like protein 5: a novel Rab27A effector with C-terminal tandem C2 domains. *Biochem Biophys Res Commun* 293: 899-906

- Kuwahara T, Koyama A, Koyama S, Yoshina S, Ren CH, et al. 2008. A systematic RNAi screen reveals involvement of endocytic pathway in neuronal dysfunction in alpha-synuclein transgenic *C. elegans*. *Hum Mol Genet* 17: 2997-3009
- Kuwahara T, Tonegawa R, Ito G, Mitani S, Iwatsubo T. 2012. Phosphorylation of alpha-synuclein protein at Ser-129 reduces neuronal dysfunction by lowering its membrane binding property in *Caenorhabditis elegans*. *J Biol Chem* 287: 7098-109
- Langowski J. 2008. Protein-protein interactions determined by fluorescence correlation spectroscopy. *Methods Cell Biol* 85: 471-84
- Lanktree MB, Guo Y, Murtaza M, Glessner JT, Bailey SD, et al. 2011. Meta-analysis of Dense Genecentric Association Studies Reveals Common and Uncommon Variants Associated with Height. *Am J Hum Genet* 88: 6-18
- Lashuel HA, Petre BM, Wall J, Simon M, Nowak RJ, et al. 2002. Alpha-synuclein, especially the Parkinson's disease-associated mutants, forms pore-like annular and tubular protofibrils. *J Mol Biol* 322: 1089-102
- Lavedan C, Leroy E, Dehejia A, Buchholtz S, Dutra A, et al. 1998. Identification, localization and characterization of the human gamma-synuclein gene. *Hum Genet* 103: 106-12
- Lazaro DF, Rodrigues EF, Langohr R, Shahpasandzadeh H, Ribeiro T, et al. 2014. Systematic comparison of the effects of alpha-synuclein mutations on its oligomerization and aggregation. *PLoS genetics* 10: e1004741
- Lee HJ, Cho ED, Lee KW, Kim JH, Cho SG, Lee SJ. 2013. Autophagic failure promotes the exocytosis and intercellular transfer of alpha-synuclein. *Exp Mol Med* 45: e22
- Lee HJ, Khoshaghideh F, Patel S, Lee SJ. 2004a. Clearance of alpha-synuclein oligomeric intermediates via the lysosomal degradation pathway. *J Neurosci* 24: 1888-96
- Lee HJ, Kim C, Lee SJ. 2010. Alpha-synuclein stimulation of astrocytes: Potential role for neuroinflammation and neuroprotection. *Oxid Med Cell Longev* 3: 283-7
- Lee HJ, Patel S, Lee SJ. 2005. Intravesicular localization and exocytosis of alpha-synuclein and its aggregates. *J Neurosci* 25: 6016-24
- Lee HJ, Suk JE, Bae EJ, Lee JH, Paik SR, Lee SJ. 2008. Assembly-dependent endocytosis and clearance of extracellular alpha-synuclein. *Int J Biochem Cell Biol* 40: 1835-49
- Lee JC, Langen R, Hummel PA, Gray HB, Winkler JR. 2004b. Alpha-synuclein structures from fluorescence energy-transfer kinetics: implications for the role of the protein in Parkinson's disease. *Proc Natl Acad Sci U S A* 101: 16466-71
- Lee PH, Lee G, Park HJ, Bang OY, Joo IS, Huh K. 2006. The plasma alpha-synuclein levels in patients with Parkinson's disease and multiple system atrophy. *J Neural Transm (Vienna)* 113: 1435-9
- Lesage S, Anheim M, Letournel F, Bousset L, Honore A, et al. 2013. G51D alpha-synuclein mutation causes a novel parkinsonian-pyramidal syndrome. *Ann Neurol* 73: 459-71

- Lewy F. 1912. Paralysis agitans, Pathologische Anatomie In *Handbuch der Neurologie*, ed. MA Lewandowsky, G. Berlin: Springer-Verlag
- Li JY, Englund E, Holton JL, Soulet D, Hagell P, et al. 2008. Lewy bodies in grafted neurons in subjects with Parkinson's disease suggest host-to-graft disease propagation. *Nat Med* 14: 501-3
- Li X, Sapp E, Chase K, Comer-Tierney LA, Masso N, et al. 2009. Disruption of Rab11 activity in a knock-in mouse model of Huntington's disease. *Neurobiol Dis* 36: 374-83
- Li X, Valencia A, Sapp E, Masso N, Alexander J, et al. 2010. Aberrant Rab11-dependent trafficking of the neuronal glutamate transporter EAAC1 causes oxidative stress and cell death in Huntington's disease. *J Neurosci* 30: 4552-61
- Liepelt-Scarfone I, Pilotto A, Muller K, Bormann C, Gauss K, et al. 2015. Autonomic dysfunction in subjects at high risk for Parkinson's disease. *Journal of neurology* 262: 2643-52
- Lippincott-Schwartz J, Altan-Bonnet N, Patterson GH. 2003. Photobleaching and photoactivation: following protein dynamics in living cells. *Nat Cell Biol* Suppl: S7-14
- Liu J, Zhang JP, Shi M, Quinn T, Bradner J, et al. 2009a. Rab11a and HSP90 regulate recycling of extracellular alpha-synuclein. *J Neurosci* 29: 1480-5
- Liu N, Bonini NM. 2006. Hosting neurotoxicity in polyglutamine disease. *Cell* 127: 1299-300
- Liu S, Fa M, Ninan I, Trinchese F, Dauer W, Arancio O. 2007. Alpha-synuclein involvement in hippocampal synaptic plasticity: role of NO, cGMP, cGK and CaMKII. *Eur J Neurosci* 25: 3583-96
- Liu S, Ninan I, Antonova I, Battaglia F, Trinchese F, et al. 2004. alpha-Synuclein produces a long-lasting increase in neurotransmitter release. *EMBO J* 23: 4506-16
- Liu W, Vives-Bauza C, Acin-Perez R, Yamamoto A, Tan Y, et al. 2009b. PINK1 defect causes mitochondrial dysfunction, proteasomal deficit and alpha-synuclein aggregation in cell culture models of Parkinson's disease. *PLoS One* 4: e4597
- Lord A, Gumucio A, Englund H, Sehlin D, Sundquist VS, et al. 2009. An amyloid-beta protofibril-selective antibody prevents amyloid formation in a mouse model of Alzheimer's disease. *Neurobiol Dis* 36: 425-34
- Lou H, Montoya SE, Alerte TN, Wang J, Wu J, et al. 2010. Serine 129 phosphorylation reduces the ability of alpha-synuclein to regulate tyrosine hydroxylase and protein phosphatase 2A in vitro and in vivo. *J Biol Chem* 285: 17648-61
- Lowe J, Blanchard A, Morrell K, Lennox G, Reynolds L, et al. 1988. Ubiquitin is a common factor in intermediate filament inclusion bodies of diverse type in man, including those of Parkinson's disease, Pick's disease, and Alzheimer's disease, as well as Rosenthal fibres in cerebellar astrocytomas, cytoplasmic bodies in muscle, and mallory bodies in alcoholic liver disease. *The Journal of pathology* 155: 9-15
- Lozano AM, Snyder BJ, Hamani C, Hutchison WD, Dostrovsky JO. 2010. Basal ganglia physiology and deep brain stimulation. *Mov Disord* 25 Suppl 1: S71-5

- Luk KC, Kehm V, Carroll J, Zhang B, O'Brien P, et al. 2012. Pathological alpha-synuclein transmission initiates Parkinson-like neurodegeneration in nontransgenic mice. *Science* 338: 949-53
- Luth ES, Bartels T, Dettmer U, Kim NC, Selkoe DJ. 2015. Purification of alpha-synuclein from human brain reveals an instability of endogenous multimers as the protein approaches purity. *Biochemistry* 54: 279-92
- Ma KL, Song LK, Yuan YH, Zhang Y, Han N, et al. 2014. The nuclear accumulation of alpha-synuclein is mediated by importin alpha and promotes neurotoxicity by accelerating the cell cycle. *Neuropharmacology* 82: 132-42
- MacLeod DA, Rhinn H, Kuwahara T, Zolin A, Di Paolo G, et al. 2013. RAB7L1 interacts with LRRK2 to modify intraneuronal protein sorting and Parkinson's disease risk. *Neuron* 77: 425-39
- Maday S, Wallace KE, Holzbaur EL. 2012. Autophagosomes initiate distally and mature during transport toward the cell soma in primary neurons. *J Cell Biol* 196: 407-17
- Maeta K, Mori K, Takatsume Y, Izawa S, Inoue Y. 2005. Diagnosis of cell death induced by methylglyoxal, a metabolite derived from glycolysis, in *Saccharomyces cerevisiae*. *FEMS Microbiol Lett* 243: 87-92
- Mahul-Mellier AL, Fauvet B, Gysbers A, Dikiy I, Oueslati A, et al. 2014. c-Abl phosphorylates alpha-synuclein and regulates its degradation: implication for alpha-synuclein clearance and contribution to the pathogenesis of Parkinson's disease. *Hum Mol Genet* 23: 2858-79
- Manzini MC, Xiong L, Shaheen R, Tambunan DE, Di Costanzo S, et al. 2014. CC2D1A regulates human intellectual and social function as well as NF-kappaB signaling homeostasis. *Cell Rep* 8: 647-55
- Maroteaux L, Campanelli JT, Scheller RH. 1988. Synuclein: a neuron-specific protein localized to the nucleus and presynaptic nerve terminal. *J Neurosci* 8: 2804-15
- Marques O, Outeiro TF. 2012. Alpha-synuclein: from secretion to dysfunction and death. *Cell Death Dis* 3: e350
- Marsden CD. 1982. The mysterious motor function of the basal ganglia: the Robert Wartenberg Lecture. *Neurology* 32: 514-39
- Martinelli N, Hartlieb B, Usami Y, Sabin C, Dordor A, et al. 2012. CC2D1A is a regulator of ESCRT-III CHMP4B. *J Mol Biol* 419: 75-88
- Martinez J, Moeller I, Erdjument-Bromage H, Tempst P, Luring B. 2003. Parkinson's disease-associated alpha-synuclein is a calmodulin substrate. *J Biol Chem* 278: 17379-87
- Marzesco AM, Dunia I, Pandjaitan R, Recouvreur M, Dauzonne D, et al. 2002. The small GTPase Rab13 regulates assembly of functional tight junctions in epithelial cells. *Mol Biol Cell* 13: 1819-31
- Masliah E, Hashimoto M. 2002. Development of new treatments for Parkinson's disease in transgenic animal models: a role for beta-synuclein. *Neurotoxicology* 23: 461-8
- Masliah E, Rockenstein E, Adame A, Alford M, Crews L, et al. 2005. Effects of alpha-synuclein immunization in a mouse model of Parkinson's disease. *Neuron* 46: 857-68

- Mata IF, Jang Y, Kim CH, Hanna DS, Dorschner MO, et al. 2015. The RAB39B p.G192R mutation causes X-linked dominant Parkinson's disease. *Molecular neurodegeneration* 10: 50
- Matsuda W, Furuta T, Nakamura KC, Hioki H, Fujiyama F, et al. 2009. Single nigrostriatal dopaminergic neurons form widely spread and highly dense axonal arborizations in the neostriatum. *J Neurosci* 29: 444-53
- Mbefo MK, Paleologou KE, Boucharaba A, Oueslati A, Schell H, et al. 2010. Phosphorylation of synucleins by members of the Polo-like kinase family. *J Biol Chem* 285: 2807-22
- McCann H, Stevens CH, Cartwright H, Halliday GM. 2014. alpha-Synucleinopathy phenotypes. *Parkinsonism Relat Disord* 20 Suppl 1: S62-7
- McGeer PL, Itagaki S, Boyes BE, McGeer EG. 1988. Reactive microglia are positive for HLA-DR in the substantia nigra of Parkinson's and Alzheimer's disease brains. *Neurology* 38: 1285-91
- McLean PJ, Kawamata H, Hyman BT. 2001. Alpha-synuclein-enhanced green fluorescent protein fusion proteins form proteasome sensitive inclusions in primary neurons. *Neuroscience* 104: 901-12
- McLean PJ, Ribich S, Hyman BT. 2000. Subcellular localization of alpha-synuclein in primary neuronal cultures: effect of missense mutations. *J Neural Transm Suppl*: 53-63
- Mezey E, Dehejia AM, Harta G, Tresser N, Suchy SF, et al. 1998. Alpha synuclein is present in Lewy bodies in sporadic Parkinson's disease. *Mol Psychiatry* 3: 493-9
- Moffat J, Grueneberg DA, Yang X, Kim SY, Kloepfer AM, et al. 2006. A lentiviral RNAi library for human and mouse genes applied to an arrayed viral high-content screen. *Cell* 124: 1283-98
- Morell M, Espargaro A, Aviles FX, Ventura S. 2008. Study and selection of in vivo protein interactions by coupling bimolecular fluorescence complementation and flow cytometry. *Nat Protoc* 3: 22-33
- Morgan D, Diamond DM, Gottschall PE, Ugen KE, Dickey C, et al. 2000. A beta peptide vaccination prevents memory loss in an animal model of Alzheimer's disease. *Nature* 408: 982-5
- Mougenot AL, Nicot S, Bencsik A, Morignat E, Verchere J, et al. 2012. Prion-like acceleration of a synucleinopathy in a transgenic mouse model. *Neurobiol Aging* 33: 2225-8
- Multiple-System Atrophy Research C. 2013. Mutations in COQ2 in familial and sporadic multiple-system atrophy. *N Engl J Med* 369: 233-44
- Murray IV, Giasson BI, Quinn SM, Koppaka V, Axelsen PH, et al. 2003. Role of alpha-synuclein carboxy-terminus on fibril formation in vitro. *Biochemistry* 42: 8530-40
- Nagai T, Ibata K, Park ES, Kubota M, Mikoshiba K, Miyawaki A. 2002. A variant of yellow fluorescent protein with fast and efficient maturation for cell-biological applications. *Nature biotechnology* 20: 87-90
- Nasstrom T, Fagerqvist T, Barbu M, Karlsson M, Nikolajeff F, et al. 2011a. The lipid peroxidation products 4-oxo-2-nonenal and 4-hydroxy-2-nonenal promote the formation of alpha-synuclein oligomers with distinct biochemical, morphological, and functional properties. *Free Radic Biol Med* 50: 428-37

- Nasstrom T, Goncalves S, Sahlin C, Nordstrom E, Screpanti Sundquist V, et al. 2011b. Antibodies against alpha-synuclein reduce oligomerization in living cells. *PLoS One* 6: e27230
- Negro A, Brunati AM, Donella-Deana A, Massimino ML, Pinna LA. 2002. Multiple phosphorylation of alpha-synuclein by protein tyrosine kinase Syk prevents eosin-induced aggregation. *FASEB J* 16: 210-2
- Nemani VM, Lu W, Berge V, Nakamura K, Onoa B, et al. 2010. Increased expression of alpha-synuclein reduces neurotransmitter release by inhibiting synaptic vesicle recluster after endocytosis. *Neuron* 65: 66-79
- Nervi A, Reitz C, Tang MX, Santana V, Piriz A, et al. 2011. Familial aggregation of dementia with Lewy bodies. *Arch Neurol* 68: 90-3
- Ninkina N, Peters O, Millership S, Salem H, van der Putten H, Buchman VL. 2009. Gamma-synucleinopathy: neurodegeneration associated with overexpression of the mouse protein. *Hum Mol Genet* 18: 1779-94
- Nishioka K, Wider C, Vilarino-Guell C, Soto-Ortolaza AI, Lincoln SJ, et al. 2010. Association of alpha-, beta-, and gamma-synuclein with diffuse lewy body disease. *Arch Neurol* 67: 970-5
- Nokes RL, Fields IC, Collins RN, Folsch H. 2008. Rab13 regulates membrane trafficking between TGN and recycling endosomes in polarized epithelial cells. *J Cell Biol* 182: 845-53
- Oh SY, Chen CD, Abraham CR. 2010. Cell-type dependent modulation of Notch signaling by the amyloid precursor protein. *J Neurochem* 113: 262-74
- Oh SY, Ellenstein A, Chen CD, Hinman JD, Berg EA, et al. 2005. Amyloid precursor protein interacts with notch receptors. *J Neurosci Res* 82: 32-42
- Ohtake H, Limprasert P, Fan Y, Onodera O, Kakita A, et al. 2004. Beta-synuclein gene alterations in dementia with Lewy bodies. *Neurology* 63: 805-11
- Okochi M, Walter J, Koyama A, Nakajo S, Baba M, et al. 2000. Constitutive phosphorylation of the Parkinson's disease associated alpha-synuclein. *J Biol Chem* 275: 390-7
- Olanow CW, Agid Y, Mizuno Y, Albanese A, Bonuccelli U, et al. 2004. Levodopa in the treatment of Parkinson's disease: current controversies. *Mov Disord* 19: 997-1005
- Orenstein SJ, Kuo SH, Tasset I, Arias E, Koga H, et al. 2013. Interplay of LRRK2 with chaperone-mediated autophagy. *Nat Neurosci* 16: 394-406
- Ostrerova N, Petrucelli L, Farrer M, Mehta N, Choi P, et al. 1999. alpha-Synuclein shares physical and functional homology with 14-3-3 proteins. *J Neurosci* 19: 5782-91
- Ostrowski M, Carmo NB, Krumeich S, Fanget I, Raposo G, et al. 2010. Rab27a and Rab27b control different steps of the exosome secretion pathway. *Nature cell biology* 12: 19-30; sup pp 1-13
- Oueslati A, Paleologou KE, Schneider BL, Aebischer P, Lashuel HA. 2012. Mimicking phosphorylation at serine 87 inhibits the aggregation of human alpha-synuclein and protects against its toxicity in a rat model of Parkinson's disease. *J Neurosci* 32: 1536-44

- Outeiro TF, Kazantsev A. 2008. Drug Targeting of alpha-Synuclein Oligomerization in Synucleinopathies. *Perspect Medicin Chem* 2: 41-9
- Outeiro TF, Klucken J, Bercury K, Tetzlaff J, Putcha P, et al. 2009. Dopamine-induced conformational changes in alpha-synuclein. *PLoS One* 4: e6906
- Outeiro TF, Klucken J, Strathearn KE, Liu F, Nguyen P, et al. 2006. Small heat shock proteins protect against alpha-synuclein-induced toxicity and aggregation. *Biochem Biophys Res Commun* 351: 631-8
- Outeiro TF, Kontopoulos E, Altmann SM, Kufareva I, Strathearn KE, et al. 2007. Sirtuin 2 inhibitors rescue alpha-synuclein-mediated toxicity in models of Parkinson's disease. *Science* 317: 516-9
- Outeiro TF, Lindquist S. 2003. Yeast cells provide insight into alpha-synuclein biology and pathobiology. *Science* 302: 1772-5
- Outeiro TF, Putcha P, Tetzlaff JE, Spoelgen R, Koker M, et al. 2008. Formation of toxic oligomeric alpha-synuclein species in living cells. *PLoS One* 3: e1867
- Outeiro TF, Tetzlaff J. 2007. Mechanisms of disease II: cellular protein quality control. *Semin Pediatr Neurol* 14: 15-25
- Pacheco C, Aguayo LG, Opazo C. 2012. An extracellular mechanism that can explain the neurotoxic effects of alpha-synuclein aggregates in the brain. *Front Physiol* 3: 297
- Paillusson S, Clairembault T, Biraud M, Neunlist M, Derkinderen P. 2013. Activity-dependent secretion of alpha-synuclein by enteric neurons. *J Neurochem* 125: 512-7
- Paleologou KE, Oueslati A, Shakked G, Rospigliosi CC, Kim HY, et al. 2010. Phosphorylation at S87 is enhanced in synucleinopathies, inhibits alpha-synuclein oligomerization, and influences synuclein-membrane interactions. *J Neurosci* 30: 3184-98
- Pals P, Lincoln S, Manning J, Heckman M, Skipper L, et al. 2004. alpha-Synuclein promoter confers susceptibility to Parkinson's disease. *Ann Neurol* 56: 591-5
- Pan X, Gong N, Zhao J, Yu Z, Gu F, et al. 2010. Powerful beneficial effects of benfotiamine on cognitive impairment and beta-amyloid deposition in amyloid precursor protein/presenilin-1 transgenic mice. *Brain* 133: 1342-51
- Papp MI, Kahn JE, Lantos PL. 1989. Glial cytoplasmic inclusions in the CNS of patients with multiple system atrophy (striatonigral degeneration, olivopontocerebellar atrophy and Shy-Drager syndrome). *J Neurol Sci* 94: 79-100
- Papp MI, Lantos PL. 1992. Accumulation of tubular structures in oligodendroglial and neuronal cells as the basic alteration in multiple system atrophy. *J Neurol Sci* 107: 172-82
- Park JS, Blair NF, Sue CM. 2015. The role of ATP13A2 in Parkinson's disease: Clinical phenotypes and molecular mechanisms. *Movement disorders : official journal of the Movement Disorder Society* 30: 770-9



- Parkinson J. 2002. An essay on the shaking palsy. 1817. *J Neuropsychiatry Clin Neurosci* 14: 223-36; discussion 22
- Parkkinen L, Kauppinen T, Pirttila T, Autere JM, Alafuzoff I. 2005. Alpha-synuclein pathology does not predict extrapyramidal symptoms or dementia. *Ann Neurol* 57: 82-91
- Parkkinen L, Pirttila T, Alafuzoff I. 2008. Applicability of current staging/categorization of alpha-synuclein pathology and their clinical relevance. *Acta Neuropathol* 115: 399-407
- Pasanen P, Myllykangas L, Siitonen M, Raunio A, Kaakkola S, et al. 2014. Novel alpha-synuclein mutation A53E associated with atypical multiple system atrophy and Parkinson's disease-type pathology. *Neurobiol Aging* 35: 2180 e1-5
- Patterson GH, Lippincott-Schwartz J. 2002. A photoactivatable GFP for selective photolabeling of proteins and cells. *Science* 297: 1873-7
- Paumier KL, Luk KC, Manfredsson FP, Kanaan NM, Lipton JW, et al. 2015. Intrastriatal injection of pre-formed mouse alpha-synuclein fibrils into rats triggers alpha-synuclein pathology and bilateral nigrostriatal degeneration. *Neurobiol Dis* 82: 185-99
- Pennuto M, Palazzolo I, Poletti A. 2009. Post-translational modifications of expanded polyglutamine proteins: impact on neurotoxicity. *Human molecular genetics* 18: R40-7
- Perrin RJ, Woods WS, Clayton DF, George JM. 2000. Interaction of human alpha-Synuclein and Parkinson's disease variants with phospholipids. Structural analysis using site-directed mutagenesis. *J Biol Chem* 275: 34393-8
- Petersen K, Olesen OF, Mikkelsen JD. 1999. Developmental expression of alpha-synuclein in rat hippocampus and cerebral cortex. *Neuroscience* 91: 651-9
- Petersen NO, Hoddellius PL, Wiseman PW, Seger O, Magnusson KE. 1993. Quantitation of membrane receptor distributions by image correlation spectroscopy: concept and application. *Biophys J* 65: 1135-46
- Pfeiffer RF. 2016. Non-motor symptoms in Parkinson's disease. *Parkinsonism Relat Disord* 22 Suppl 1: S119-22
- Platt NJ, Gispert S, Auburger G, Cragg SJ. 2012. Striatal dopamine transmission is subtly modified in human A53Talpha-synuclein overexpressing mice. *PLoS One* 7: e36397
- Polymeropoulos MH, Lavedan C, Leroy E, Ide SE, Dehejia A, et al. 1997. Mutation in the alpha-synuclein gene identified in families with Parkinson's disease. *Science* 276: 2045-7
- Pronin AN, Morris AJ, Surguchov A, Benovic JL. 2000. Synucleins are a novel class of substrates for G protein-coupled receptor kinases. *J Biol Chem* 275: 26515-22
- Proukakis C, Dudzik CG, Brier T, MacKay DS, Cooper JM, et al. 2013. A novel alpha-synuclein missense mutation in Parkinson disease. *Neurology* 80: 1062-4

- Prydz K, Tveit H, Vedeler A, Saraste J. 2013. Arrivals and departures at the plasma membrane: direct and indirect transport routes. *Cell Tissue Res* 352: 5-20
- Qing H, Wong W, McGeer EG, McGeer PL. 2009. Lrrk2 phosphorylates alpha synuclein at serine 129: Parkinson disease implications. *Biochem Biophys Res Commun* 387: 149-52
- Quadri M, Fang M, Picillo M, Olgiati S, Breedveld GJ, et al. 2013. Mutation in the SYNJ1 gene associated with autosomal recessive, early-onset Parkinsonism. *Hum Mutat* 34: 1208-15
- Rajput A, Vilarino-Guell C, Rajput ML, Ross OA, Soto-Ortolaza AI, et al. 2009. Alpha-synuclein polymorphisms are associated with Parkinson's disease in a Saskatchewan population. *Movement disorders : official journal of the Movement Disorder Society* 24: 2411-4
- Ramirez A, Heimbach A, Grundemann J, Stiller B, Hampshire D, et al. 2006. Hereditary parkinsonism with dementia is caused by mutations in ATP13A2, encoding a lysosomal type 5 P-type ATPase. *Nat Genet* 38: 1184-91
- Ramsey CP, Giasson BI. 2008. The E163K DJ-1 mutant shows specific antioxidant deficiency. *Brain Res* 1239: 1-11
- Raposo G, Stoorvogel W. 2013. Extracellular vesicles: exosomes, microvesicles, and friends. *J Cell Biol* 200: 373-83
- Remy I, Michnick SW. 1999. Clonal selection and in vivo quantitation of protein interactions with protein-fragment complementation assays. *Proc Natl Acad Sci U S A* 96: 5394-9
- Remy I, Michnick SW. 2004. A cDNA library functional screening strategy based on fluorescent protein complementation assays to identify novel components of signaling pathways. *Methods* 32: 381-8
- Rendon WO, Martinez-Alonso E, Tomas M, Martinez-Martinez N, Martinez-Menarguez JA. 2013. Golgi fragmentation is Rab and SNARE dependent in cellular models of Parkinson's disease. *Histochem Cell Biol* 139: 671-84
- Reyes JF, Rey NL, Bousset L, Melki R, Brundin P, Angot E. 2014. Alpha-synuclein transfers from neurons to oligodendrocytes. *Glia* 62: 387-98
- Ribeiro JA, Sebastiao AM. 2010. Caffeine and adenosine. *J Alzheimers Dis* 20 Suppl 1: S3-15
- Richards P, Didszun C, Campesan S, Simpson A, Horley B, et al. 2011. Dendritic spine loss and neurodegeneration is rescued by Rab11 in models of Huntington's disease. *Cell Death Differ* 18: 191-200
- Rino J, Braga J, Henriques R, Carmo-Fonseca M. 2009. Frontiers in fluorescence microscopy. *Int J Dev Biol* 53: 1569-79
- Rizzo MA, Springer GH, Granada B, Piston DW. 2004. An improved cyan fluorescent protein variant useful for FRET. *Nature biotechnology* 22: 445-9
- Rodriguez MS, Dargemont C, Hay RT. 2001. SUMO-1 conjugation in vivo requires both a consensus modification motif and nuclear targeting. *J Biol Chem* 276: 12654-9

- Roodveldt C, Bertocini CW, Andersson A, van der Goot AT, Hsu ST, et al. 2009. Chaperone proteostasis in Parkinson's disease: stabilization of the Hsp70/alpha-synuclein complex by Hip. *EMBO J* 28: 3758-70
- Ross CA, Poirier MA. 2004. Protein aggregation and neurodegenerative disease. *Nat Med* 10 Suppl: S10-7
- Ross OA, Braithwaite AT, Skipper LM, Kachergus J, Hulihan MM, et al. 2008. Genomic investigation of alpha-synuclein multiplication and parkinsonism. *Ann Neurol* 63: 743-50
- Ross OA, Vilarino-Guell C, Wszolek ZK, Farrer MJ, Dickson DW. 2010. Reply to: SNCA variants are associated with increased risk of multiple system atrophy. *Ann Neurol* 67: 414-5
- Rott R, Szargel R, Haskin J, Shani V, Shainskaya A, et al. 2008. Monoubiquitylation of alpha-synuclein by seven in absentia homolog (SIAH) promotes its aggregation in dopaminergic cells. *J Biol Chem* 283: 3316-28
- Roy B, Jackson GR. 2014. Interactions between Tau and alpha-synuclein augment neurotoxicity in a Drosophila model of Parkinson's disease. *Hum Mol Genet* 23: 3008-23
- Roy S, Yang G, Tang Y, Scott DA. 2012. A simple photoactivation and image analysis module for visualizing and analyzing axonal transport with high temporal resolution. *Nat Protoc* 7: 62-8
- Sakamoto M, Arawaka S, Hara S, Sato H, Cui C, et al. 2009. Contribution of endogenous G-protein-coupled receptor kinases to Ser129 phosphorylation of alpha-synuclein in HEK293 cells. *Biochem Biophys Res Commun* 384: 378-82
- Salazar C, Hofer T. 2009. Multisite protein phosphorylation--from molecular mechanisms to kinetic models. *FEBS J* 276: 3177-98
- Sancenon V, Lee SA, Patrick C, Griffith J, Paulino A, et al. 2012. Suppression of alpha-synuclein toxicity and vesicle trafficking defects by phosphorylation at S129 in yeast depends on genetic context. *Hum Mol Genet* 21: 2432-49
- Sato K, Kaji R, Matsumoto S, Nagahiro S, Goto S. 2007. Compartmental loss of striatal medium spiny neurons in multiple system atrophy of parkinsonian type. *Movement disorders : official journal of the Movement Disorder Society* 22: 2365-70
- Savina A, Vidal M, Colombo MI. 2002. The exosome pathway in K562 cells is regulated by Rab11. *J Cell Sci* 115: 2505-15
- Saxena SK, Kaur S. 2006. Rab27a negatively regulates CFTR chloride channel function in colonic epithelia: involvement of the effector proteins in the regulatory mechanism. *Biochemical and biophysical research communications* 346: 259-67
- Schaffar G, Breuer P, Boteva R, Behrends C, Tzvetkov N, et al. 2004. Cellular toxicity of polyglutamine expansion proteins: mechanism of transcription factor deactivation. *Molecular cell* 15: 95-105
- Schenk D, Barbour R, Dunn W, Gordon G, Grajeda H, et al. 1999. Immunization with amyloid-beta attenuates Alzheimer-disease-like pathology in the PDAPP mouse. *Nature* 400: 173-7

- Schneider BL, Seehus CR, Capowski EE, Aebischer P, Zhang SC, Svendsen CN. 2007. Over-expression of alpha-synuclein in human neural progenitors leads to specific changes in fate and differentiation. *Hum Mol Genet* 16: 651-66
- Scott D, Roy S. 2012. alpha-Synuclein inhibits intersynaptic vesicle mobility and maintains recycling-pool homeostasis. *J Neurosci* 32: 10129-35
- Seabra MC, Wasmeier C. 2004. Controlling the location and activation of Rab GTPases. *Curr Opin Cell Biol* 16: 451-7
- Seixas E, Barros M, Seabra MC, Barral DC. 2013. Rab and Arf proteins in genetic diseases. *Traffic* 14: 871-85
- Seixas E, Ramalho JS, Mota LJ, Barral DC, Seabra MC. 2012. Bacteria and protozoa differentially modulate the expression of Rab proteins. *PLoS one* 7: e39858
- Seo JH, Rah JC, Choi SH, Shin JK, Min K, et al. 2002. Alpha-synuclein regulates neuronal survival via Bcl-2 family expression and PI3/Akt kinase pathway. *FASEB J* 16: 1826-8
- Shen J, Du T, Wang X, Duan C, Gao G, et al. 2014. alpha-Synuclein amino terminus regulates mitochondrial membrane permeability. *Brain Res* 1591: 14-26
- Shin N, Jeong H, Kwon J, Heo HY, Kwon JJ, et al. 2008. LRRK2 regulates synaptic vesicle endocytosis. *Exp Cell Res* 314: 2055-65
- Shinbo Y, Niki T, Taira T, Ooe H, Takahashi-Niki K, et al. 2006. Proper SUMO-1 conjugation is essential to DJ-1 to exert its full activities. *Cell Death Differ* 13: 96-108
- Shyu YJ, Suarez CD, Hu CD. 2008. Visualization of AP-1 NF-kappaB ternary complexes in living cells by using a BiFC-based FRET. *Proc Natl Acad Sci U S A* 105: 151-6
- Siddiqui A, Chinta SJ, Mallajosyula JK, Rajagopalan S, Hanson I, et al. 2012. Selective binding of nuclear alpha-synuclein to the PGC1alpha promoter under conditions of oxidative stress may contribute to losses in mitochondrial function: implications for Parkinson's disease. *Free Radic Biol Med*
- Singleton AB, Farrer M, Johnson J, Singleton A, Hague S, et al. 2003. alpha-Synuclein locus triplication causes Parkinson's disease. *Science* 302: 841
- Slepek TI, Salay LD, Lemmon VP, Bixby JL. 2012. Dyrk kinases regulate phosphorylation of doublecortin, cytoskeletal organization, and neuronal morphology. *Cytoskeleton (Hoboken)* 69: 514-27
- Smith WW, Liu Z, Liang Y, Masuda N, Swing DA, et al. 2010. Synphilin-1 attenuates neuronal degeneration in the A53T alpha-synuclein transgenic mouse model. *Hum Mol Genet* 19: 2087-98
- Smith WW, Margolis RL, Li X, Troncoso JC, Lee MK, et al. 2005. Alpha-synuclein phosphorylation enhances eosinophilic cytoplasmic inclusion formation in SH-SY5Y cells. *J Neurosci* 25: 5544-52
- Soma H, Yabe I, Takei A, Fujiki N, Yanagihara T, Sasaki H. 2006. Heredity in multiple system atrophy. *J Neurol Sci* 240: 107-10

- Soper JH, Kehm V, Burd CG, Bankaitis VA, Lee VM. 2011. Aggregation of alpha-synuclein in *S. cerevisiae* is associated with defects in endosomal trafficking and phospholipid biosynthesis. *J Mol Neurosci* 43: 391-405
- Sotiriou S, Gibney G, Baxevanis AD, Nussbaum RL. 2009. A single nucleotide polymorphism in the 3'UTR of the SNCA gene encoding alpha-synuclein is a new potential susceptibility locus for Parkinson disease. *Neurosci Lett* 461: 196-201
- Sousa VL, Bellani S, Giannandrea M, Yousuf M, Valtorta F, et al. 2009. {alpha}-synuclein and its A30P mutant affect actin cytoskeletal structure and dynamics. *Mol Biol Cell* 20: 3725-39
- Souza JM, Giasson BI, Chen Q, Lee VM, Ischiropoulos H. 2000a. Dityrosine cross-linking promotes formation of stable alpha -synuclein polymers. Implication of nitrative and oxidative stress in the pathogenesis of neurodegenerative synucleinopathies. *J Biol Chem* 275: 18344-9
- Souza JM, Giasson BI, Lee VM, Ischiropoulos H. 2000b. Chaperone-like activity of synucleins. *FEBS Lett* 474: 116-9
- Specht CG, Tigaret CM, Rast GF, Thalhammer A, Rudhard Y, Schoepfer R. 2005. Subcellular localisation of recombinant alpha- and gamma-synuclein. *Mol Cell Neurosci* 28: 326-34
- Spillantini MG, Crowther RA, Jakes R, Cairns NJ, Lantos PL, Goedert M. 1998a. Filamentous alpha-synuclein inclusions link multiple system atrophy with Parkinson's disease and dementia with Lewy bodies. *Neurosci Lett* 251: 205-8
- Spillantini MG, Crowther RA, Jakes R, Hasegawa M, Goedert M. 1998b. alpha-Synuclein in filamentous inclusions of Lewy bodies from Parkinson's disease and dementia with lewy bodies. *Proc Natl Acad Sci U S A* 95: 6469-73
- Spillantini MG, Schmidt ML, Lee VM, Trojanowski JQ, Jakes R, Goedert M. 1997. Alpha-synuclein in Lewy bodies. *Nature* 388: 839-40
- Stefanis L, Kholodilov N, Rideout HJ, Burke RE, Greene LA. 2001. Synuclein-1 is selectively up-regulated in response to nerve growth factor treatment in PC12 cells. *J Neurochem* 76: 1165-76
- Steinert JR, Campesan S, Richards P, Kyriacou CP, Forsythe ID, Giorgini F. 2012. Rab11 rescues synaptic dysfunction and behavioural deficits in a *Drosophila* model of Huntington's disease. *Hum Mol Genet* 21: 2912-22
- Stenmark H. 2009. Rab GTPases as coordinators of vesicle traffic. *Nat Rev Mol Cell Biol* 10: 513-25
- Streit WJ, Mrak RE, Griffin WS. 2004. Microglia and neuroinflammation: a pathological perspective. *J Neuroinflammation* 1: 14
- Su HL, Li SS. 2002. Molecular features of human ubiquitin-like SUMO genes and their encoded proteins. *Gene* 296: 65-73
- Sugawara K, Shibasaki T, Mizoguchi A, Saito T, Seino S. 2009. Rab11 and its effector Rip11 participate in regulation of insulin granule exocytosis. *Genes Cells* 14: 445-56

- Sung JY, Kim J, Paik SR, Park JH, Ahn YS, Chung KC. 2001. Induction of neuronal cell death by Rab5A-dependent endocytosis of alpha-synuclein. *J Biol Chem* 276: 27441-8
- Sung JY, Park SM, Lee CH, Um JW, Lee HJ, et al. 2005. Proteolytic cleavage of extracellular secreted {alpha}-synuclein via matrix metalloproteinases. *J Biol Chem* 280: 25216-24
- Surgucheva I, Ninkina N, Buchman VL, Grasing K, Surguchov A. 2005. Protein aggregation in retinal cells and approaches to cell protection. *Cell Mol Neurobiol* 25: 1051-66
- Surguchov A. 2015. Intracellular Dynamics of Synucleins: "Here, There and Everywhere". *Int Rev Cell Mol Biol* 320: 103-69
- Takahashi M, Kanuka H, Fujiwara H, Koyama A, Hasegawa M, et al. 2003. Phosphorylation of alpha-synuclein characteristic of synucleinopathy lesions is recapitulated in alpha-synuclein transgenic *Drosophila*. *Neurosci Lett* 336: 155-8
- Takahashi Y, Okamoto Y, Popiel HA, Fujikake N, Toda T, et al. 2007. Detection of polyglutamine protein oligomers in cells by fluorescence correlation spectroscopy. *The Journal of biological chemistry* 282: 24039-48
- Tambasco N, Simoni S, Marsili E, Sacchini E, Murasecco D, et al. 2012. Clinical aspects and management of levodopa-induced dyskinesia. *Parkinsons Dis* 2012: 745947
- Tampellini D, Magrane J, Takahashi RH, Li F, Lin MT, et al. 2007. Internalized antibodies to the Abeta domain of APP reduce neuronal Abeta and protect against synaptic alterations. *J Biol Chem* 282: 18895-906
- Taschenberger G, Toloe J, Tereshchenko J, Akerboom J, Wales P, et al. 2013. beta-synuclein aggregates and induces neurodegeneration in dopaminergic neurons. *Ann Neurol* 74: 109-18
- Tatham MH, Jaffray E, Vaughan OA, Desterro JM, Botting CH, et al. 2001. Polymeric chains of SUMO-2 and SUMO-3 are conjugated to protein substrates by SAE1/SAE2 and Ubc9. *J Biol Chem* 276: 35368-74
- Taylor JP, Hardy J, Fischbeck KH. 2002. Toxic proteins in neurodegenerative disease. *Science (New York, N.Y)* 296: 1991-5
- Taylor TN, Potgieter D, Anwar S, Senior SL, Janezic S, et al. 2014. Region-specific deficits in dopamine, but not norepinephrine, signaling in a novel A30P alpha-synuclein BAC transgenic mouse. *Neurobiol Dis* 62: 193-207
- Tenreiro S, Reimao-Pinto MM, Antas P, Rino J, Wawrzycka D, et al. 2014. Phosphorylation modulates clearance of alpha-synuclein inclusions in a yeast model of Parkinson's disease. *PLoS genetics* 10: e1004302
- Tetzlaff JE, Putcha P, Outeiro TF, Ivanov A, Berezovska O, et al. 2008. CHIP targets toxic alpha-Synuclein oligomers for degradation. *J Biol Chem* 283: 17962-8
- Thayanidhi N, Helm JR, Nycz DC, Bentley M, Liang Y, Hay JC. 2010. Alpha-synuclein delays endoplasmic reticulum (ER)-to-Golgi transport in mammalian cells by antagonizing ER/Golgi SNAREs. *Mol Biol Cell* 21: 1850-63

- Thornalley PJ. 1998. Glutathione-dependent detoxification of alpha-oxoaldehydes by the glyoxalase system: involvement in disease mechanisms and antiproliferative activity of glyoxalase I inhibitors. *Chem Biol Interact* 111-112: 137-51
- Trinh J, Farrer M. 2013. Advances in the genetics of Parkinson disease. *Nat Rev Neurol* 9: 445-54
- Trojanowski JQ, Revesz T, Neuropathology Working Group on MSA. 2007. Proposed neuropathological criteria for the post mortem diagnosis of multiple system atrophy. *Neuropathol Appl Neurobiol* 33: 615-20
- Tsika E, Moysidou M, Guo J, Cushman M, Gannon P, et al. 2010. Distinct region-specific alpha-synuclein oligomers in A53T transgenic mice: implications for neurodegeneration. *J Neurosci* 30: 3409-18
- Tsuang D, Leverenz JB, Lopez OL, Hamilton RL, Bennett DA, et al. 2013. APOE epsilon4 increases risk for dementia in pure synucleinopathies. *JAMA Neurol* 70: 223-8
- Tyson T, Steiner JA, Brundin P. 2015. Sorting Out Release, Uptake and Processing of Alpha-Synuclein During Prion-Like Spread of Pathology. *J Neurochem*
- Uchikado H, Lin WL, DeLucia MW, Dickson DW. 2006. Alzheimer disease with amygdala Lewy bodies: a distinct form of alpha-synucleinopathy. *J Neuropathol Exp Neurol* 65: 685-97
- Ueda K, Fukushima H, Masliah E, Xia Y, Iwai A, et al. 1993. Molecular cloning of cDNA encoding an unrecognized component of amyloid in Alzheimer disease. *Proc Natl Acad Sci U S A* 90: 11282-6
- Ueda K, Saitoh T, Mori H. 1994. Tissue-dependent alternative splicing of mRNA for NACP, the precursor of non-A beta component of Alzheimer's disease amyloid. *Biochem Biophys Res Commun* 205: 1366-72
- Ullrich O, Reinsch S, Urbe S, Zerial M, Parton RG. 1996. Rab11 regulates recycling through the pericentriolar recycling endosome. *J Cell Biol* 135: 913-24
- Ulmer TS, Bax A. 2005. Comparison of structure and dynamics of micelle-bound human alpha-synuclein and Parkinson disease variants. *J Biol Chem* 280: 43179-87
- Ulmer TS, Bax A, Cole NB, Nussbaum RL. 2005. Structure and dynamics of micelle-bound human alpha-synuclein. *J Biol Chem* 280: 9595-603
- Um JW, Chung KC. 2006. Functional modulation of parkin through physical interaction with SUMO-1. *J Neurosci Res* 84: 1543-54
- Unni VK, Weissman TA, Rockenstein E, Masliah E, McLean PJ, Hyman BT. 2010. In vivo imaging of alpha-synuclein in mouse cortex demonstrates stable expression and differential subcellular compartment mobility. *PLoS One* 5: e10589
- Urbe S, Huber LA, Zerial M, Tooze SA, Parton RG. 1993. Rab11, a small GTPase associated with both constitutive and regulated secretory pathways in PC12 cells. *FEBS Lett* 334: 175-82
- Uversky VN, Li J, Fink AL. 2001. Evidence for a partially folded intermediate in alpha-synuclein fibril formation. *J Biol Chem* 276: 10737-44

- Valente EM, Abou-Sleiman PM, Caputo V, Muqit MM, Harvey K, et al. 2004. Hereditary early-onset Parkinson's disease caused by mutations in PINK1. *Science* 304: 1158-60
- Vamvaca K, Volles MJ, Lansbury PT, Jr. 2009. The first N-terminal amino acids of alpha-synuclein are essential for alpha-helical structure formation in vitro and membrane binding in yeast. *J Mol Biol* 389: 413-24
- van de Warrenburg BP, Lammens M, Lucking CB, Deneffe P, Wesseling P, et al. 2001. Clinical and pathologic abnormalities in a family with parkinsonism and parkin gene mutations. *Neurology* 56: 555-7
- Vandrovцова J, Anaya F, Kay V, Lees A, Hardy J, de Silva R. 2010. Disentangling the role of the tau gene locus in sporadic tauopathies. *Curr Alzheimer Res* 7: 726-34
- Vekrellis K, Xilouri M, Emmanouilidou E, Stefanis L. 2009. Inducible over-expression of wild type alpha-synuclein in human neuronal cells leads to caspase-dependent non-apoptotic death. *J Neurochem* 109: 1348-62
- Verhoeven K, De Jonghe P, Coen K, Verpoorten N, Auer-Grumbach M, et al. 2003. Mutations in the small GTP-ase late endosomal protein RAB7 cause Charcot-Marie-Tooth type 2B neuropathy. *Am J Hum Genet* 72: 722-7
- Vicente Miranda H, Outeiro TF. 2010. The sour side of neurodegenerative disorders: the effects of protein glycation. *J Pathol* 221: 13-25
- Vidi PA, Chemel BR, Hu CD, Watts VJ. 2008. Ligand-dependent oligomerization of dopamine D(2) and adenosine A(2A) receptors in living neuronal cells. *Mol Pharmacol* 74: 544-51
- Vilarino-Guell C, Soto-Ortolaza AI, Rajput A, Mash DC, Papapetropoulos S, et al. 2011a. MAPT H1 haplotype is a risk factor for essential tremor and multiple system atrophy. *Neurology* 76: 670-2
- Vilarino-Guell C, Wider C, Ross OA, Dachsel JC, Kachergus JM, et al. 2011b. VPS35 mutations in Parkinson disease. *Am J Hum Genet* 89: 162-7
- Villarroel-Campos D, Gastaldi L, Conde C, Caceres A, Gonzalez-Billault C. 2014. Rab-mediated trafficking role in neurite formation. *J Neurochem* 129: 240-8
- Visanji NP, Brooks PL, Hazrati LN, Lang AE. 2013. The prion hypothesis in Parkinson's disease: Braak to the future. *Acta Neuropathol Commun* 1: 2
- Vivacqua G, Casini A, Vaccaro R, Fornai F, Yu S, D'Este L. 2011. Different sub-cellular localization of alpha-synuclein in the C57BL/6J mouse's central nervous system by two novel monoclonal antibodies. *J Chem Neuroanat* 41: 97-110
- Volles MJ, Lansbury PT, Jr. 2007. Relationships between the sequence of alpha-synuclein and its membrane affinity, fibrillization propensity, and yeast toxicity. *J Mol Biol* 366: 1510-22
- Volpicelli-Daley LA, Luk KC, Lee VM. 2014. Addition of exogenous alpha-synuclein preformed fibrils to primary neuronal cultures to seed recruitment of endogenous alpha-synuclein to Lewy body and Lewy neurite-like aggregates. *Nature protocols* 9: 2135-46



- Wakabayashi K, Engelender S, Yoshimoto M, Tsuji S, Ross CA, Takahashi H. 2000. Synphilin-1 is present in Lewy bodies in Parkinson's disease. *Ann Neurol* 47: 521-3
- Wakabayashi K, Yoshimoto M, Tsuji S, Takahashi H. 1998. Alpha-synuclein immunoreactivity in glial cytoplasmic inclusions in multiple system atrophy. *Neurosci Lett* 249: 180-2
- Wang D, Chan CC, Cherry S, Hiesinger PR. 2013. Membrane trafficking in neuronal maintenance and degeneration. *Cellular and molecular life sciences : CMLS* 70: 2919-34
- Wang D, Hiesinger PR. 2012. Autophagy, neuron-specific degradation and neurodegeneration. *Autophagy* 8: 711-3
- Wang W, Perovic I, Chittuluru J, Kaganovich A, Nguyen LT, et al. 2011. A soluble alpha-synuclein construct forms a dynamic tetramer. *Proc Natl Acad Sci U S A* 108: 17797-802
- Waxman EA, Giasson BI. 2010. A novel, high-efficiency cellular model of fibrillar alpha-synuclein inclusions and the examination of mutations that inhibit amyloid formation. *J Neurochem* 113: 374-88
- Waxman EA, Giasson BI. 2011. Characterization of kinases involved in the phosphorylation of aggregated alpha-synuclein. *J Neurosci Res* 89: 231-47
- Weihofen A, Thomas KJ, Ostaszewski BL, Cookson MR, Selkoe DJ. 2009. Pink1 forms a multiprotein complex with Miro and Milton, linking Pink1 function to mitochondrial trafficking. *Biochemistry* 48: 2045-52
- Weinreb PH, Zhen W, Poon AW, Conway KA, Lansbury PT, Jr. 1996. NACP, a protein implicated in Alzheimer's disease and learning, is natively unfolded. *Biochemistry* 35: 13709-15
- Wilcke M, Johannes L, Galli T, Mayau V, Goud B, Salamero J. 2000. Rab11 regulates the compartmentalization of early endosomes required for efficient transport from early endosomes to the trans-golgi network. *J Cell Biol* 151: 1207-20
- Williams A, Gill S, Varma T, Jenkinson C, Quinn N, et al. 2010. Deep brain stimulation plus best medical therapy versus best medical therapy alone for advanced Parkinson's disease (PD SURG trial): a randomised, open-label trial. *Lancet Neurol* 9: 581-91
- Williamson WR, Yang T, Terman JR, Hiesinger PR. 2010. Guidance receptor degradation is required for neuronal connectivity in the Drosophila nervous system. *PLoS biology* 8: e1000553
- Wilson GR, Sim JC, McLean C, Giannandrea M, Galea CA, et al. 2014. Mutations in RAB39B cause X-linked intellectual disability and early-onset Parkinson disease with alpha-synuclein pathology. *Am J Hum Genet* 95: 729-35
- Winkler S, Hagenah J, Lincoln S, Heckman M, Haugarvoll K, et al. 2007. alpha-Synuclein and Parkinson disease susceptibility. *Neurology* 69: 1745-50
- Winner B, Jappelli R, Maji SK, Desplats PA, Boyer L, et al. 2011. In vivo demonstration that alpha-synuclein oligomers are toxic. *Proc Natl Acad Sci U S A* 108: 4194-9
- Wirawan E, Vanden Berghe T, Lippens S, Agostinis P, Vandenabeele P. 2012. Autophagy: for better or for worse. *Cell research* 22: 43-61

- Witt SN. 2010. Hsp70 molecular chaperones and Parkinson's disease. *Biopolymers* 93: 218-28
- Wong SL, Chan WM, Chan HY. 2008. Sodium dodecyl sulfate-insoluble oligomers are involved in polyglutamine degeneration. *Faseb J* 22: 3348-57
- Wood SJ, Wypych J, Steavenson S, Louis JC, Citron M, Biere AL. 1999. alpha-synuclein fibrillogenesis is nucleation-dependent. Implications for the pathogenesis of Parkinson's disease. *J Biol Chem* 274: 19509-12
- Wu B, Liu Q, Duan C, Li Y, Yu S, et al. 2011a. Phosphorylation of alpha-synuclein upregulates tyrosine hydroxylase activity in MN9D cells. *Acta Histochem* 113: 32-5
- Wu C, Agrawal S, VasANJI A, Drazba J, Sarkaria S, et al. 2011b. Rab13-dependent trafficking of RhoA is required for directional migration and angiogenesis. *J Biol Chem* 286: 23511-20
- Wu T, Hallett M, Chan P. 2015. Motor automaticity in Parkinson's disease. *Neurobiol Dis* 82: 226-34
- Wullner U, Schmitt I, Kammal M, Kretschmar HA, Neumann M. 2009. Definite multiple system atrophy in a German family. *J Neurol Neurosurg Psychiatry* 80: 449-50
- Xu J, Kao SY, Lee FJ, Song W, Jin LW, Yankner BA. 2002. Dopamine-dependent neurotoxicity of alpha-synuclein: a mechanism for selective neurodegeneration in Parkinson disease. *Nat Med* 8: 600-6
- Xu S, Zhou M, Yu S, Cai Y, Zhang A, et al. 2006. Oxidative stress induces nuclear translocation of C-terminus of alpha-synuclein in dopaminergic cells. *Biochem Biophys Res Commun* 342: 330-5
- Yang ML, Hasadsri L, Woods WS, George JM. 2010. Dynamic transport and localization of alpha-synuclein in primary hippocampal neurons. *Mol Neurodegener* 5: 9
- Yang Z, Klionsky DJ. 2010. Eaten alive: a history of macroautophagy. *Nature cell biology* 12: 814-22
- Yao Y, Cui X, Al-Ramahi I, Sun X, Li B, et al. 2015. A striatal-enriched intronic GPCR modulates huntingtin levels and toxicity. *Elife* 4
- Yin G, Lopes da Fonseca T, Eisbach SE, Anduaga AM, Breda C, et al. 2014. alpha-Synuclein interacts with the switch region of Rab8a in a Ser129 phosphorylation-dependent manner. *Neurobiol Dis* 70: 149-61
- Yonetani M, Nonaka T, Masuda M, Inukai Y, Oikawa T, et al. 2009. Conversion of wild-type alpha-synuclein into mutant-type fibrils and its propagation in the presence of A30P mutant. *J Biol Chem* 284: 7940-50
- Yoshimoto M, Iwai A, Kang D, Otero DA, Xia Y, Saitoh T. 1995. NACP, the precursor protein of the non-amyloid beta/A4 protein (A beta) component of Alzheimer disease amyloid, binds A beta and stimulates A beta aggregation. *Proc Natl Acad Sci U S A* 92: 9141-5
- Yu YJ, Watts RJ. 2013. Developing therapeutic antibodies for neurodegenerative disease. *Neurotherapeutics* 10: 459-72

- Zaccai J, McCracken C, Brayne C. 2005. A systematic review of prevalence and incidence studies of dementia with Lewy bodies. *Age Ageing* 34: 561-6
- Zarranz JJ, Alegre J, Gomez-Esteban JC, Lezcano E, Ros R, et al. 2004. The new mutation, E46K, of alpha-synuclein causes Parkinson and Lewy body dementia. *Ann Neurol* 55: 164-73
- Zerial M, McBride H. 2001. Rab proteins as membrane organizers. *Nat Rev Mol Cell Biol* 2: 107-17
- Zhang F, Shi JS, Zhou H, Wilson B, Hong JS, Gao HM. 2010. Resveratrol protects dopamine neurons against lipopolysaccharide-induced neurotoxicity through its anti-inflammatory actions. *Mol Pharmacol* 78: 466-77
- Zhou C, Emadi S, Sierks MR, Messer A. 2004a. A human single-chain Fv intrabody blocks aberrant cellular effects of overexpressed alpha-synuclein. *Mol Ther* 10: 1023-31
- Zhou Y, Gu G, Goodlett DR, Zhang T, Pan C, et al. 2004b. Analysis of alpha-synuclein-associated proteins by quantitative proteomics. *J Biol Chem* 279: 39155-64
- Zhu M, Fink AL. 2003. Lipid binding inhibits alpha-synuclein fibril formation. *J Biol Chem* 278: 16873-7
- Zimprich A, Biskup S, Leitner P, Lichtner P, Farrer M, et al. 2004. Mutations in LRRK2 cause autosomal-dominant parkinsonism with pleomorphic pathology. *Neuron* 44: 601-7

